

AD-A160 378

DEVELOPMENT OF FATIGUE AND CRACK PROPAGATION DESIGN AND  
ANALYSIS METHODOLOGY (U) GENERAL DYNAMICS FORT WORTH TX  
FORT WORTH DIV S D MANNING ET AL OCT 84

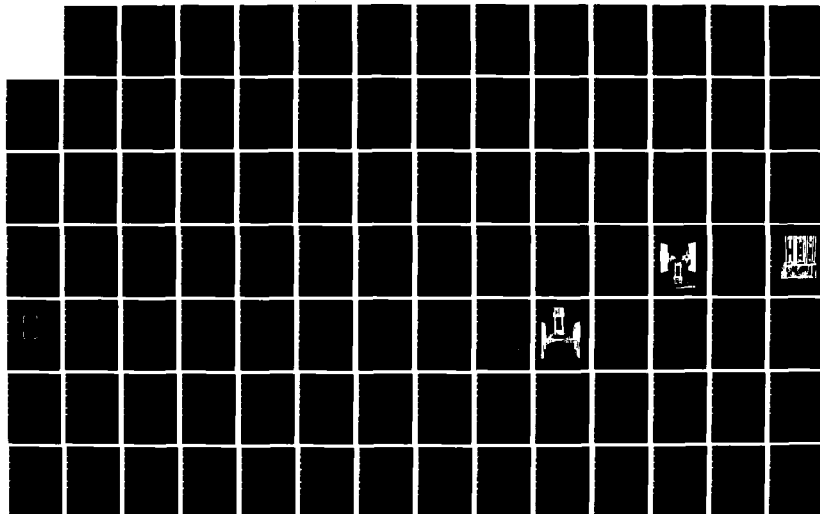
1/4

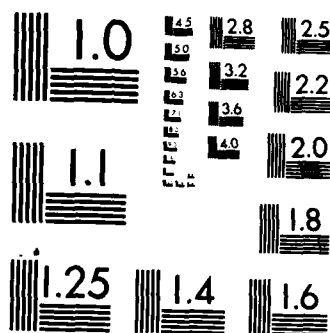
UNCLASSIFIED

NADC-83126-60-VOL-3 N62269-81-C-0268

F/G 11/6

NL





MICROCOPY RESOLUTION TEST CHART  
NATIONAL BUREAU OF STANDARDS-1963-A



**DEVELOPMENT OF FATIGUE AND CRACK PROPAGATION  
DESIGN & ANALYSIS METHODOLOGY IN A CORROSIVE  
ENVIRONMENT FOR TYPICAL MECHANICALLY-FASTENED JOINTS**

**VOLUME III — PHASE II DOCUMENTATION**

**AD-A160 378**

S.D. Manning and D.E. Gordon  
General Dynamics Corporation  
P.O. Box 748, Ft. Worth, TX 76101

and

R.P. Wei  
Lehigh University  
Bethlehem, PA 18015

**30 OCTOBER 1984**

**FINAL REPORT  
FOR PERIOD SEPTEMBER 1982 - OCTOBER 1984**

**APPROVED FOR PUBLIC RELEASE; DISTRIBUTION UNLIMITED**

Prepared for  
NAVAL AIR DEVELOPMENT CENTER (604)  
DEPARTMENT OF THE NAVY  
Warminster, PA 18974

85 10 11 029

## NOTICES

**REPORT NUMBERING SYSTEM** – The numbering of technical project reports issued by the Naval Air Development Center is arranged for specific identification purposes. Each number consists of the Center acronym, the calendar year in which the number was assigned, the sequence number of the report within the specific calendar year, and the official 2-digit correspondence code of the Command Office or the Functional Directorate responsible for the report. For example: Report No. NADC-78015-20 indicates the fifteenth Center report for the year 1978, and prepared by the Systems Directorate. The numerical codes are as follows:

CODE	OFFICE OR DIRECTORATE
00	Commander, Naval Air Development Center
01	Technical Director, Naval Air Development Center
02	Comptroller
10	Directorate Command Projects
20	Systems Directorate
30	Sensors & Avionics Technology Directorate
40	Communication & Navigation Technology Directorate
50	Software Computer Directorate
60	Aircraft & Crew Systems Technology Directorate
70	Planning Assessment Resources
80	Engineering Support Group

**PRODUCT ENDORSEMENT** – The discussion or instructions concerning commercial products herein do not constitute an endorsement by the Government nor do they convey or imply the license or right to use such products.

1  
 2  
 3  
 4  
 5  
 6  
 7  
 8  
 9  
 10  
 11  
 12  
 13  
 14  
 15  
 16  
 17  
 18  
 19  
 20  
 21  
 22  
 23  
 24  
 25  
 26  
 27  
 28  
 29  
 30  
 31  
 32  
 33  
 34  
 35  
 36  
 37  
 38  
 39  
 40  
 41  
 42  
 43  
 44  
 45  
 46  
 47  
 48  
 49  
 50  
 51  
 52  
 53  
 54  
 55  
 56  
 57  
 58  
 59  
 60  
 61  
 62  
 63  
 64  
 65  
 66  
 67  
 68  
 69  
 70  
 71  
 72  
 73  
 74  
 75  
 76  
 77  
 78  
 79  
 80  
 81  
 82  
 83  
 84  
 85  
 86  
 87  
 88  
 89  
 90  
 91  
 92  
 93  
 94  
 95  
 96  
 97  
 98  
 99  
 100  
 101  
 102  
 103  
 104  
 105  
 106  
 107  
 108  
 109  
 110  
 111  
 112  
 113  
 114  
 115  
 116  
 117  
 118  
 119  
 120  
 121  
 122  
 123  
 124  
 125  
 126  
 127  
 128  
 129  
 130  
 131  
 132  
 133  
 134  
 135  
 136  
 137  
 138  
 139  
 140  
 141  
 142  
 143  
 144  
 145  
 146  
 147  
 148  
 149  
 150  
 151  
 152  
 153  
 154  
 155  
 156  
 157  
 158  
 159  
 160  
 161  
 162  
 163  
 164  
 165  
 166  
 167  
 168  
 169  
 170  
 171  
 172  
 173  
 174  
 175  
 176  
 177  
 178  
 179  
 180  
 181  
 182  
 183  
 184  
 185  
 186  
 187  
 188  
 189  
 190  
 191  
 192  
 193  
 194  
 195  
 196  
 197  
 198  
 199  
 200  
 201  
 202  
 203  
 204  
 205  
 206  
 207  
 208  
 209  
 210  
 211  
 212  
 213  
 214  
 215  
 216  
 217  
 218  
 219  
 220  
 221  
 222  
 223  
 224  
 225  
 226  
 227  
 228  
 229  
 230  
 231  
 232  
 233  
 234  
 235  
 236  
 237  
 238  
 239  
 240  
 241  
 242  
 243  
 244  
 245  
 246  
 247  
 248  
 249  
 250  
 251  
 252  
 253  
 254  
 255  
 256  
 257  
 258  
 259  
 260  
 261  
 262  
 263  
 264  
 265  
 266  
 267  
 268  
 269  
 270  
 271  
 272  
 273  
 274  
 275  
 276  
 277  
 278  
 279  
 280  
 281  
 282  
 283  
 284  
 285  
 286  
 287  
 288  
 289  
 290  
 291  
 292  
 293  
 294  
 295  
 296  
 297  
 298  
 299  
 300  
 301  
 302  
 303  
 304  
 305  
 306  
 307  
 308  
 309  
 310  
 311  
 312  
 313  
 314  
 315  
 316  
 317  
 318  
 319  
 320  
 321  
 322  
 323  
 324  
 325  
 326  
 327  
 328  
 329  
 330  
 331  
 332  
 333  
 334  
 335  
 336  
 337  
 338  
 339  
 340  
 341  
 342  
 343  
 344  
 345  
 346  
 347  
 348  
 349  
 350  
 351  
 352  
 353  
 354  
 355  
 356  
 357  
 358  
 359  
 360  
 361  
 362  
 363  
 364  
 365  
 366  
 367  
 368  
 369  
 370  
 371  
 372  
 373  
 374  
 375  
 376  
 377  
 378  
 379  
 380  
 381  
 382  
 383  
 384  
 385  
 386  
 387  
 388  
 389  
 390  
 391  
 392  
 393  
 394  
 395  
 396  
 397  
 398  
 399  
 400  
 401  
 402  
 403  
 404  
 405  
 406  
 407  
 408  
 409  
 410  
 411  
 412  
 413  
 414  
 415  
 416  
 417  
 418  
 419  
 420  
 421  
 422  
 423  
 424  
 425  
 426  
 427  
 428  
 429  
 430  
 431  
 432  
 433  
 434  
 435  
 436  
 437  
 438  
 439  
 440  
 441  
 442  
 443  
 444  
 445  
 446  
 447  
 448  
 449  
 450  
 451  
 452  
 453  
 454  
 455  
 456  
 457  
 458  
 459  
 460  
 461  
 462  
 463  
 464  
 465  
 466  
 467  
 468  
 469  
 470  
 471  
 472  
 473  
 474  
 475  
 476  
 477  
 478  
 479  
 480  
 481  
 482  
 483  
 484  
 485  
 486  
 487  
 488  
 489  
 490  
 491  
 492  
 493  
 494  
 495  
 496  
 497  
 498  
 499  
 500  
 501  
 502  
 503  
 504  
 505  
 506  
 507  
 508  
 509  
 510  
 511  
 512  
 513  
 514  
 515  
 516  
 517  
 518  
 519  
 520  
 521  
 522  
 523  
 524  
 525

Distribution Statement: Approved for  
Public Release per Ms. Mary Hellings,  
Naval Air Development Center.

DTIC-FDAC-16 Oct 85



Unclassified

SECURITY CLASSIFICATION OF THIS PAGE (When Data Entered)

REPORT DOCUMENTATION PAGE		READ INSTRUCTIONS BEFORE COMPLETING FORM
1. REPORT NUMBER NADC-83126-60-Vol. III	2. GOVT ACCESSION NO.	3. RECIPIENT'S CATALOG NUMBER AD-A160 378
4. TITLE (and Subtitle) Development of Fatigue & Crack Propagation Design & Analysis Methodology in a Corrosive Environment for Typical Mechanically-Fastened Joints - Vol III - Phase II Documentation		5. TYPE OF REPORT & PERIOD COVERED
7. AUTHOR(S) S. D. Manning, R. P. Wei and D. E. Gordon		6. PERFORMING ORG REPORT NUMBER
9. PERFORMING ORGANIZATION NAME AND ADDRESS General Dynamics P.O. Box 748 Fort Worth, Texas 76101		8. CONTRACT OR GRANT NUMBER: N62269-81-C-0268
11. CONTROLLING OFFICE NAME AND ADDRESS Naval Air Development Center (NADC) Warminster, PA 18974		10. PROGRAM ELEMENT PROJ. ECT. TASK AREA & WORK UNIT NUMBERS 62241N WF 41400, ZA-61A
14. MONITORING AGENCY NAME & ADDRESS (if different from Controlling Office)		12. REPORT DATE October 1984
<p style="text-align: center;">This document has been approved for public release and sale; its distribution is unlimited.</p>		13. NUMBER OF PAGES 369
		15. SECURITY CLASS. of this report Unclassified
16. DISTRIBUTION STATEMENT of this Report Distribution limited to U.S. Government Agencies and their contractors (Critical Technology) (October 1984). All other requests for this document must be referred to COMNAVAIRDEVCON.		
17. DISTRIBUTION STATEMENT of the abstract entered in Block 20, if different from Report		
18. SUPPLEMENTARY NOTES The subcontractor/consultant for this report was R. P. Wei, Lehigh University, Bethlehem, PA 19015.		
19. KEY WORDS (Continue on reverse side if necessary and identify by block number) Corrosion fatigue, crack initiation, crack propagation, environment (dry air, 3.5% NaCl), loading (constant amplitude & spectrum), percent bolt load transfer, effect loading frequency, strain controlled tests, preconditioning, long term exposure testing.-		
20. ABSTRACT (Continue on reverse side if necessary and identify by block number) -A workable corrosion fatigue (CF) analysis methodology has been developed for mechanically-fastened joints. The methodology includes the strain-life approach for predicting time-to-crack-initiation (TTCI) and the deterministic crack growth approach for predicting crack propagation. Guidelines are presented for acquiring the experimental data and for implementing the CF analysis. The CF analysis methodology was evaluated for 7075-T7651 aluminum, three load spectra, two environments (i.e., dry air and 3.5% NaCl), and three different bolt load transfer levels (i.e., 0%, 20% and 40%).		

For the 7000 series aluminum alloys in the over-aged condition it was concluded that: (1) the CF methodology is adequate for both crack initiation and crack propagation, (2) no significant synergistic effect between loading and environment was observed; hence, strain-controlled data and  $da/dN$  versus  $\Delta K$  data required to implement the methodology can be acquired at a fast frequency, (3) the effect of environment on both CF crack initiation and CF crack propagation can be "scaled", (4) no special crack growth models are required to account for the effect of environment on  $da/dN$  versus  $\Delta K$ , (5) existing load-interaction models do not apply to all load spectra irrespective of the loading sequences, multiple overloads, number of loading cycles, (6) the load retardation is independent of the environment, and (7) the effect of specimen preconditioning (pretesting and presoaking in 3.5% NaCl solution) was more pronounced for CF crack initiation than for crack propagation.

CF crack propagation predictions correctly predicted the trends in the experimental data and correctly ranked the predictions in order of spectrum severity. Predictions in general did not agree with the average test results. This lack of correlation is attributed mainly to an inadequate load-retardation model rather than a problem with the CF analysis methodology. The CF methodology should also apply to 7000 series alloys in the peak-aged condition providing the strain-life data and the  $da/dN$  versus  $\Delta K$  data are acquired at the lowest frequency expected in service.

The effect of frequency on fatigue crack growth in a beta annealed Ti-6Al-4V alloy in a 3.5% NaCl solution at room temperature was investigated. Details are documented in Volume V and highlights are summarized in this Volume (III). It was concluded that: (1) crack growth rates strongly depend on frequency and K level, (2) crack growth enhancement appeared to result from the formation and rupture of a hydride phase, (3) the environment can also interact with the applied load to influence the crack growth retardation, (4) the spectrum load fatigue life is expected to be a complex function of frequency, load level and load sequence, (5) a prohibitively large amount of data would be required to make life predictions using one of the available cycle-by-cycle procedures and (6) novel procedures should be developed which incorporates the combined load/environment interaction effect on CF crack propagation predictions.

## FOREWORD

This program was conducted by General Dynamics, Fort Worth Division (under NADC Contract N62269-81-C-0268) with Lehigh University (Dr. R. P. Wei) as a subcontractor/consultant. The program was sponsored by the Naval Air Development Center, Warminster, PA, with Mr. P. Kozel as the project engineer. Dr. S. D. Manning of General Dynamics, Fort Worth Division, was the Program Manager/Principal Investigator and Dr. R. P. Wei of Lehigh University was a co-investigator.

Several General Dynamics personnel supported the Phase II effort as follows. D. E. Gordon coordinated the overall testing effort, procured specimens, performed the strain-controlled and the constant amplitude tests, eddy current inspections, fractographic evaluations, data analyses, and documentation. S. B. Kirschner coordinated the dog-bone specimen spectrum tests and performed fractographic evaluations and data analyses. Dog-bone specimen spectrum tests and specimen dimensional checks were performed by R. O. Nay. Corrosion fatigue testing support was provided by F. C. Nordquist, J. W. Hagemayer and H. C. Hoffman. S. D. Forness developed the test tapes for the F-18 load spectra, performed preliminary strain life analyses and contributed to the strain life computer program implementation. The strain life computer software was implemented by J. W. Norris and the final strain life analyses were performed by W. W. Robbins.

Crack growth analyses were performed by J. B. Heckel, R. Roach and L. E. Brubaker. Technical support was also provided by J. W. Morrow, Dr. J. H. Chung, B. J. Pendley and P. D. Hudson.

This report (Volume III) documents the Phase II technical effort and includes the final summary, conclusions and recommendations for the program. The following reports (NADC-83126-60) were also prepared under the Phase II effort:

- o Volume IV - Phase II Test and Fractographic  
Results
- o Volume V - Corrosion Fatigue Cracking Response of  
Beta-Annealed Ti-6AL-4V Alloy in 3%  
NaCl Solution

## TABLE OF CONTENTS

<u>Section</u>		<u>Page</u>
I	INTRODUCTION	1
II	PHASE II TEST PROGRAM	9
	2.1 Introduction	9
	2.2 Phase II Test Objectives	9
	2.3 Specimen and Test Matrices	10
	2.4 Test Setups and Procedures	19
	2.4.1 Strain-Controlled Tests	19
	2.4.2 No-Load Transfer Dog-Bone Specimen Tests	23
	2.4.3 Load Transfer Dog-Bone Specimen Tests	23
	2.5 Specimen Preconditioning	28
	2.6 Load Spectra	29
III	EXPERIMENTAL METHODOLOGY DEVELOPMENT AND EVALUATION	31
	3.1 Introduction	31
	3.2 Strain-Controlled Tests	31
	3.2.1 Calibration of Strain-Controlled Specimen	32
	3.2.2 Environmental Simulation	36
	3.2.3 Establishing TCI Acquisition Methods	37
	3.3 Dog-Bone Specimens	38
	3.3.1 Test Procedures	39
	3.3.2 Evaluation of Environmental Simulation Methods	40
	3.3.3 Establishing Crack Growth Monitoring Methods	40
	3.3.3.1 Eddy Current Techniques	40
	3.3.3.2 Fractography	41
	3.4 Corrosion Fatigue Testing Guidelines	42
	3.4.1 Acquisition of Strain Life Initiation Data	43
	3.4.2 Acquisition of Crack Propagation Data	44
	3.4.3 Spectrum Testing	44

## TABLE OF CONTENTS (CONT'D)

<u>Section</u>		<u>Page</u>
IV	EVALUATION OF CORROSION FATIGUE TEST RESULTS	47
4.1	Introduction	47
4.2	Strain Controlled Test Results	47
4.3	Compact Tension Test Results	51
4.4	Dog-Bone Specimen Test Results	52
4.4.1	Constant Amplitude Test Results	62
4.4.2	Spectrum Fatigue Test Results	62
4.5	Evaluate Effects of Test Variables on TTCI, TFCG, and TTF	63
V	CORROSION FATIGUE ANALYSIS METHODOLOGY FOR MECHANICALLY-FASTENED JOINTS	
5.1	Introduction	67
5.2	Corrosion Fatigue Analysis Approach and Rationale	68
5.3	Corrosion Fatigue Crack Initiation Methodology	74
5.3.1	General Procedure	74
5.3.2	Strain Life Analysis	77
5.3.3	Effective $K_t$ Versus TTCI Relationship	78
5.3.4	Baseline Effective $K_t(0)$	79
5.3.5	Accounting for Bolt Load Transfer	80
5.3.5.1	Superposition Model for Estimating $\sigma_{max}$ at Edge of Hole	80
5.3.5.2	Modification of Strain Life Analysis Scaling Factor for Effect of Bolt Load Transfer	84
5.4	Corrosion Fatigue Crack Propagation Methodology	88
5.4.1	General Procedure	88
5.4.2	Crack Growth Analysis Program	92
5.4.3	Crack Growth Model	93
5.4.4	Load-Interaction Model	94
5.4.5	Cycle Counting	96
5.4.6	Stress Intensity Factor for Loaded Bolt Holes	97

## TABLE OF CONTENTS (CONT'D)

<u>Section</u>	<u>Page</u>
5.5 Experimental Requirements/Guidelines	99
5.5.1 Strain-Controlled Data	99
5.5.2 da/dN Versus $\Delta K$ Data	102
5.5.3 Dog-Bone Specimen Data	103
5.5.3.1 Crack Initiation Data	103
5.5.3.2 Crack Propagation Data	105
5.6 Applicability of Corrosion Fatigue Methodology to Other Alloys	106
5.7 Evaluation of Corrosion Fatigue Analysis Methodology	111
5.7.1 Evaluation Approach	111
5.7.1.1 CF Crack Initiation	111
5.7.1.2 CF Crack Propagation	112
5.7.2 CF Crack Initiation Analysis/Results	114
5.7.2.1 TCI Predictions and Correlations	114
5.7.2.2 Scaling of Environmental Effects	120
5.7.3 CF Crack Propagation Analysis/Results	123
5.7.3.1 TFCG Predictions and Correlations	123
5.7.3.2 Sensitivity of Willenborg Retardation Model Parameters	126
5.7.3.3 Scaling of Environmental Effects	127
5.7.4 Conclusions and Recommendations	130
5.7.4.1 CF Crack Initiation Methodology	130
5.7.4.2 CF Crack Propagation Methodology	134

## TABLE OF CONTENTS (CONT'D)

<u>Section</u>		<u>Page</u>
VI	SUMMARY OF CORROSION FATIGUE RESEARCH FOR BETA ANNEALED TI-6AL-4V ALLOY	141
	6.1 Introduction	141
	6.2 Effect of Frequency on Fatigue Crack Growth	142
	6.3 Implications of Titanium Alloy Response on Corrosion Fatigue Life Predictions	144
VII	CONCLUSIONS AND RECOMMENDATIONS	147
	7.1 Conclusions	147
	7.1.1 CF Methodology/Aluminum Research	147
	7.1.2 Titanium Research	152
	7.2 Recommendations	153
APPENDICES		
A	Material Constants for Implementing the Strain Life Approach for Crack Initiation	A-1
B	Evaluation of $da/dN$ versus $\Delta K$ Experimental Data for 7075-T7651 Aluminum	B-1
C	Evaluation of Corrosion Fatigue Test Results for 7075-T7651 Aluminum Dog-Bone Specimens	C-1
D	Normalized Crack Growth Results for 7075-T7651 Aluminum Dog-Bone Specimens Tested Under Spectrum Loading	D-1
E	Description of Local Strain Computer Program (BROSE)	E-1
F	Corrosion Fatigue Crack Initiation Analysis Details	F-1
G	Description of Analytical Crack Growth Computer Program RXN	G-1
H	Load Spectra Descriptions and Comparisons	H-1
REFERENCES		R-1

## LIST OF FIGURES

<u>Figure</u>		<u>Page</u>
1	Strain-Controlled Specimen	12
2	Compact Tension Specimen for Beta-Annealed Ti-6Al-4V Alloy	13
3	Dog-Bone Specimen	14
4	Environmental Chamber and Test Setup for Strain-Controlled Tests	22
5	Test Setup for No-Bolt-Load Transfer Dog-Bone Specimen Tests	24
6	Environmental Chamber Used for No-Load-Transfer Dog-Bone Tests	25
7	Test Setup for Bolt Load Transfer Dog-Bone Specimen Tests	26
8	Details of Integral Environmental Chamber Used in Loading Bar for Bolt Load Transfer Tests	27
9	Elements of Strain-Controlled Experimental Methodology Development	33
10	Setup for Strain Surveys Using Strain-Controlled Specimen	34
11	Strain Gage Locations for Strain-Controlled Specimen	35
12	Total Strain Amplitude Versus Reversals to Crack Initiation for 7075-T7651 Aluminum in Both Dry Air and 3.5% NaCl Environments	49
13	Total Strain Amplitude Versus 2N <sub>i</sub> Reversals to Initiation for Beta-Annealed Ti-6Al-4V in Both Dry Air and 3.5% NaCl Environments	50
14	Corrosion Fatigue Analysis Approach	71
15	Essential Elements of the CF Crack Initiation Methodology	75
16	Superposition Model for Estimating Geometric Stress Concentration Factor ( $K_T$ )	81

## LIST OF FIGURES (CONT'D)

<u>Figure</u>		<u>Page</u>
17	Concept of Determining Notch Stress Due to Maximum Linear Stress at Edge of Hole Based on Stress-Strain Relationship	87
18	Essential Elements of the CF Crack Propagation Methodology	89
19	Superposition Concept for Determining Stress Intensity Factor for Through Stress and Bearing Stress	98
20	Effect of Frequency on Crack Growth Rates for 7075-T7651 Aluminum Alloy in Dry Air at Room Temperature (R = 0.3; f = 0.1 HZ, 1 HZ, and 6 HZ)	107
21	Effect of Frequency on Crack Growth Rates for 7075-T7651 Aluminum Alloy Exposed to 3.5% NaCl Solution at Room Temperature (R = 0.3; f = 0.1 HZ, 0.3 HZ, 1 HZ, 3 HZ, and 6 HZ)	108
22	Effect of Environment on Crack Growth Rates for 7075-T7651 Aluminum Alloy at Room Temperature (R = 0.05, f = 6 HZ)	109
23	Overload Shut-Off Ratio Versus Time-for-Crack Growth for Load Spectra A, B, and C for Both Dry Air and 3.5% NaCl Environments and $\Delta K_{th} = 1.5 \text{ ksi } \sqrt{\text{in.}}$	129
24	The influence of frequency on fatigue crack growth rate of beta-annealed Ti-6Al-4V alloy in 3.5% NaCl solution at room temperature (R = 0.05).	143

(This page intentionally left blank)

## LIST OF TABLES (CONT'D)

<u>Table</u>		<u>Page</u>
F-10	Summary of Scaling Factors for Scaling Strain Life Predictions to Dog-Bone Specimen Test Results for 7075-T7651 Aluminum	F-24
F-11	Summary of $K_{\sigma}$ (LT) values for 7075-T7651 Aluminum ( $W = 2.00"$ , $d = 0.4375"$ )	F-27
F-12	Summary of $\bar{K}_{\sigma}$ (LT) Scaling Factors for Strain Life Analysis Predictions for T7651	F-28
F-13	Summary of Results for (Ave. Ni) (Ave. Ni) <sub>Wet</sub> Ratios for 7075-T7651 <sup>Dry</sup> Aluminum	F-32
G-1	Description of Standard Geometry Types	G-4
G-2	Description of Standard Stress Intensity Factors	G-5
G-3	Typical Output for RXN Computer Run	G-6
H-1	Load Summary for the F-16 400 Hour Spectrum "A"	H-2
H-2	Load Summary for the NADC F-16 Spectrum ("NADC")	H-3
H-3	Load Summary for the F-18 300 Hour Spectrum ("B")	H-5
H-4	Load Summary for the F-18 300 Hour Spectrum ("C")	H-6
H-5	Comparison of Exceedances per 300 Flight Hours for Selected & Maximum Load for Load Spectra "A", "B", "C" and "NADC"	H-7

## LIST OF TABLES (CONT'D)

<u>Table</u>		<u>Page</u>
E-1	Typical Input/Output for Local Strain Analysis Computer Program (BROSE)	E-4
F-1	Summary of Local Strain Analysis Results for 7075-T7651 Aluminum: TTCI ( $a_i = 0.01"$ ) Predictions for Selected Effective $K_t$ Value, $\sigma_{Gross} = 28$ ksi and F-16 400 Hour (Block) Spectrum	F-5
F-2	Example Output from Strain-Life Computer Program (Neuber's Rule Option)	F-6
F-3	Example Output from Strain-Life Computer Program (Generalized Neuber Rule Option)	F-9
F-4	Summary of Constants in $K_t = A(TTCI)^B$ for TTCI ( $a_i = 0.01"$ ) Predictions for 7075-T7651 Aluminum Based on: Local Strain Analysis, F-16 400 Hour (Block) Spectrum and $\sigma_{Gross} = 28$ ksi	F-12
F-5	Summary of Constants in $K_t = A(TTCI)^B$ for TTCI ( $a_i = 0.01"$ ) Predictions for 7075-T7651 Aluminum Based on: Local Strain Analysis, F-18 300 Hour (Random) Spectrum ("B") and $\sigma_{gross} = 28$ ksi	F-13
F-6	Summary of Constants in $K_t = A(TTCI)^B$ for ( $a_i = 0.01"$ ) Predictions for 7075-T7651 Aluminum Based on: Local Strain Analysis, F-18 300 Hour (Block) Spectrum ("C") and $\sigma_{gross} = 28$ ksi	F-14
F-7	Summary of TTCI Results ( $a_i = 0.01"$ ) for 7075-T7651 Aluminum Dog-Bone Specimens Tested Using the F-16 400 Hour Spectrum	F-21
F-8	Summary of TTCI Results ( $a_i = 0.01"$ ) for 7075-T7651 Aluminum Dog-Bone Specimens Tested Using the F-18 300 Hour (Random) Spectrum ("B")	F-22
F-9	Summary of TTCI Results ( $a_i = 0.01"$ ) for 7075-T7651 Aluminum Dog-Bone Specimens Tested Using the F-18 300 Hour (Block) Spectrum ("C")	F-23

## LIST OF TABLES (CONT'D)

<u>Table</u>		<u>Page</u>
B-4	da/dN Versus $\Delta K$ Results for 7075-T7651 Aluminum in 3.5% NaCl Solution at Room Temperature ( $R = 0.3$ ; $f = 0.1$ HZ, 0.3 HZ, 1 HZ, 3 HZ, 6 HZ)	B-8
B-5	Summary of Paris Law Parameters ( $m$ and $C$ ) for 7075-T7651 Aluminum for Both Dry Air and 3.5% NaCl Solution	B-16
B-6	Effect of Environment and R-Ratio on da/dN Based on Paris Model Constants	B-18
B-7	Least Squares Fit Results for Two-Segment Superposition Crack Growth Model for 7075-T7651 Aluminum in 3.5% NaCl Solution at Room Temperature ( $R = .05$ )	B-21
B-8	Least Squares Fit Results for Two-Segment Superposition Crack Growth Model for 7075-T7651 Aluminum in 3.5% NaCl Solution at Room Temperature ( $R = .30$ )	B-22
B-9	Summary of Forman Equation Parameters for 7075-T7651 Aluminum for Both Dry Air and 3.5% NaCl Environments	B-28
C-1	Summary of 7075-T7651 Aluminum Dog-Bone Test Results for Task 5	C-3
C-2	Summary of 7075-T7651 Aluminum Dog-Bone Specimens for Task 6	C-6
C-3	Summary of Statistics for T <sub>TCI</sub> /T <sub>TF</sub> Ratio for 7075-T7651 Aluminum Dog-Bone Specimens, F-16 400 Hour (Block) Spectrum and Dry Air/3.5% NaCl Environments	C-29
C-4	Summary of Statistics for T <sub>TCI</sub> /T <sub>TF</sub> Ratio for 7075-T7651 Aluminum Dog-Bone Specimens, F-18 300 Hour (Random) Spectrum and Dry Air/3.5% NaCl Environments	C-30
C-5	Summary of Statistics for T <sub>TCI</sub> /T <sub>TF</sub> Ratio for 7075-T7651 Aluminum Dog-Bone Specimens, F-18 300 Hour (Block Spectrum and Dry Air/3.5% NaCl Environments	C-31

## LIST OF TABLES (CONT'D)

<u>Table</u>		<u>Page</u>
16	Comparison of TTCI Predictions and Test Results (7075-T7651 Aluminum) for Loading Spectrum "C" for Various Cases	117
17	Summary of TTCI Predictions for Load Spectra A, B and C Based on Spectrum A Baseline with Dry/Wet Ratios	121
18	Summary of TTCI Predictions for Load Spectra A, B and C Based on Spectrum B Baseline with Dry/Wet Ratios	122
19	Corrosion Fatigue Analysis Matrix for Crack Growth Predictions for 7075-T7651 Aluminum	124
20	Summary of TFCG Predictions and Correlations with Dog-Bone Specimen Test Results for 7075-T7651 Aluminum	125
21	Summary of TFCG Predictions (Dry & Wet) for Various $\Delta K_{th}$ and Overload Shut-Off Ratios ( $R_{os}$ )	128

## APPENDICES

A-1	Summary of Strain-Life Results for 7075-T7651 Aluminum in Dry Air and Lab Air	A-7
A-2	Summary of Strain-Life Results for 7075-T7651 Aluminum in 3.5% NaCl Solution at Room Temperature	A-8
A-3	Summary of Strain-Life Constants for Both Dry Air and 3.5% NaCl Solution	A-15
B-1	da/dN Versus $\Delta K$ Results for 7075-T7651 Aluminum in Dry Air ( $R = 0.05$ ; $f = 0.1$ HZ, 1 HZ, 6 HZ)	B-5
B-2	da/dN Versus $\Delta K$ Results for 7075-T7651 Aluminum in 3.5% NaCl Solution at Room Temperature ( $R = 0.05$ , $f = 1$ HZ, 3 HZ, 6 HZ)	B-6
B-3	da/dN Versus $\Delta K$ Results for 7075-T7651 Aluminum in Dry Air ( $R = .30$ , $f = 0.1$ HZ, 1 HZ, 6 HZ)	B-7

## LIST OF TABLES

<u>Table</u>		<u>Page</u>
1	Test Specimen Matrix for Phase II	11
2	Phase II Test Variables	15
3	Experimental Methodology Development and Evaluation Tests (Task 4)	16
4	Strain-Controlled Tests for Task 5	17
5	Ti-6Al-4V Alloy Crack Growth Tests for Task 5	17
6	Dog-Bone Specimen Tests for Task 5	18
7	Dog-Bone Specimen Tests for Task 6	20
8	Coding System For Describing Tests	21
9	Constant Amplitude Stress-Controlled Test Results for Preconditioned Dog-Bone Specimens in Both Dry Air and 3.5% NaCl Environments (7075-T7651 Aluminum; R = 0.05; Freq. = 6 HZ; Open Hole)	53
10	Constant Amplitude Stress-Controlled Test Results for Dog-Bone Specimens Tested for 20% LT and 40% LT in Both Dry Air and 3.5% NaCl Environments (7075-T7651 Aluminum)	54
11	Summary of Dog-Bone Specimen Spectrum Fatigue Test Results for Task 4 (7075-T7651 Aluminum; F-16 400 Hour Spectrum)	55
12	Summary of Dog-Bone Specimen Spectrum Fatigue Test Results for Task 5 (7075-T7651 Aluminum)	57
13	Summary of Dog-Bone Specimen Fatigue Test Results for Task 6 (7075-T7651 Aluminum)	60
14	Comparison of TTCI Predictions and Test Results (7075-T7651) Aluminum for Loading Spectrum "A" for Various Cases	115
15	Comparison of TTCI Predictions and Test Results (7075-T7651 Aluminum) for Loading Spectrum "B" for Various Cases	116

LIST OF FIGURES (CONT'D)

<u>Figure</u>		<u>Page</u>
G-1	Deterministic Crack Growth Concept	G-2
G-2	Superposition Concept for Determining Stress Intensity Factor for Through Stress and Bearing Stress	G-6
H-1	Samples of the Load History for the F-16 400 Hr. Spectrum	H-10
H-2	Strip Chart Trace of Load History for F-18 300 Hour (Random) Spectrum ("B")	H-11
H-3	Strip Chart Trace of Load History for F-18 300 Hour (Block) Spectrum ("C")	H-11

## LIST OF FIGURES (CONT'D)

<u>Figure</u>		<u>Page</u>
D-15	Normalized Crack Growth Results ( $a_i = 0.01"$ ) for 7075-T7651 Aluminum Dog-Bone Specimens (Open Hole; Dia. = 0.4375") Tested Using: F-18 300-Hour (Block) Spectrum ( $\sigma_{GROSS} = 28$ ksi Max.), Dry Air Environment, and Fast Loading Frequency	D-16
D-16	Normalized Crack Growth Results ( $a_i = 0.01"$ ) for 7075-T7651 Aluminum Dog-Bone Specimens (Open Hole; Dia. = 0.4375") Tested Using: F-18 300-Hour (Block) Spectrum ( $\sigma_{GROSS} = 28$ ksi Max.), 3.5% NaCl Environment and Fast Loading Frequency	D-17
D-17	Normalized Crack Growth Results ( $a_i = 0.01"$ ) for 7075-T7651 Aluminum Dog-Bone Specimens (Open Hole; Dia. = 0.500") Tested Using: F-18 300-Hour (Block) Spectrum ( $\sigma_{GROSS} = 28$ ksi Max.), 3.5% NaCl Environment and Fast Loading Frequency	D-18
D-18	Normalized Crack Growth Results ( $a_i = 0.01"$ ) for 7075-T7651 Aluminum Dog-Bone Specimens (40% Load Transfer) Tested Using: F-18 300 Hour (Block) Spectrum ( $\sigma_{GROSS} = 28$ ksi Max.), Dry Air Environment and Fast Loading Frequency	D-19
E-1	Typical Problem for Predicting the TTCI in Fastener Hole Using the Local Strain Analysis Approach	E-3
F-1	Effective $K_t$ Versus TTCI ( $a_i = 0.01"$ ) for 7075-T7651 Aluminum Based on: Strain-Life Analysis, F-16 400-Hour Spectrum, $\sigma_{Gross} = 28$ ksi (Max.), and Dry Air Environment	F-17
F-2	Effective $K_t$ Versus TTCI ( $a_i = 0.01"$ ) for 7075-T7651 Aluminum Based on: Strain Life Analysis, F-16 400-Hour Spectrum, $\sigma_{Gross} = 28$ ksi (Max.), and 3.5% NaCl Environment	F-18

## LIST OF FIGURES (CONT'D)

<u>Figure</u>		<u>Page</u>
D-8	Comparison of Normalized Crack Growth Results ( $a_i = 0.035"$ , Fast Versus Slow Loading Frequency) for 7075-T7651 Aluminum Dog-Bone Specimens (Open Hole) Tested Using: F-18 300-Hour (Random) Spectrum ( $\sigma_{GROSS} = 28$ ksi Max.) and Dry Air Environment	D-9
D-9	Comparison of Normalized Crack Growth Results ( $a_i = 0.01"$ ; Fast Versus Slow Loading Frequency) for 7075-T7651 Aluminum Dog-Bone Specimens (Open Hole) Tested Using: F-18 300-Hour (Random) Spectrum ( $\sigma_{GROSS} = 28$ ksi Max.) and 3.5% NaCl Environment	D-10
D-10	Comparison of Normalized Crack Growth Results ( $a_i = 0.035"$ ; Fast Versus Slow Loading Frequency) for 7075-T7651 Aluminum Dog-Bone Specimens (Open Hole) Tested Using: F-18 300-Hour (Random) Spectrum ( $\sigma_{GROSS} = 28$ ksi Max.) and 3.5% NaCl Environment	D-11
D-11	Normalized Crack Growth Results ( $a_i = 0.01"$ ) for 7075-T7651 Aluminum Dog-Bone Specimens (20% Load Transfer) Tested Using: F-18 300 Hour (Random) Spectrum ( $\sigma_{GROSS} = 28$ ksi Max.), Dry Air Environment and Fast Loading Frequency	D-12
D-12	Normalized Crack Growth Results ( $a_i = 0.01"$ ) for 7075-T7651 Aluminum Dog-Bone Specimens (20% Load Transfer) Tested Using: F-18 300 Hour (Random) Spectrum ( $\sigma_{GROSS} = 28$ ksi Max.), 3.5% NaCl Environment and Fast Loading Frequency	D-13
D-13	Normalized Crack Growth Results ( $a_i = 0.01"$ ) for 7075-T7651 Aluminum Dog-Bone Specimens (40% Load Transfer) Tested Using: F-18 300 Hour (Random) Spectrum, Dry Air Environment and Fast Loading Frequency	D-14
D-14	Normalized Crack Growth Results ( $a_i = 0.01"$ ) for 7075-T7651 Aluminum Dog-Bone Specimens (40% Load Transfer) Tested Using: F-18 300 Hour (Random) Spectrum, 3.5% NaCl Environment and Fast Loading Frequency	D-15

## LIST OF FIGURES (CONT'D)

<u>Figure</u>		<u>Page</u>
D-2	Normalized Crack Growth results ( $a_i = 0.01"$ ) for 7075-T7651 Aluminum Dog-Bone Specimens (Open Hole) Tested Using: F-16 400-Hour Block Spectrum ( $\sigma_{GROSS} = 28$ ksi Max.), 3.5% NaCl Environment and Three Loading Frequencies (Fast, Slow, Extra Slow)	D-3
D-3	Comparison of Normalized Crack Growth Results ( $a_i = 0.01"$ , Dry Air Versus 3.5% NaCl) for 7075-T7651 Aluminum Dog-Bone Specimens (Bolt-in-Hole) Tested Using F-16 400-Hour Block Spectrum ( $\sigma_{GROSS} = 28$ ksi Max.) and Two Loading Frequencies (Fast, Slow)	D-4
D-4	Normalized Crack Growth Results ( $a_i = 0.01"$ ) for 7075-T7651 Aluminum Dog-Bone Specimens (20% Load Transfer) Tested Using: F-16 400-Hour Block Spectrum ( $\sigma_{GROSS} = 28$ ksi Max.), Dry Air Environment and Two Loading Frequencies (Fast, Slow)	D-5
D-5	Normalized Crack Growth Results ( $a_i = 0.01"$ ) for 7075-T7651 Aluminum Dog-Bone Specimens (20% Load Transfer) Tested Using: F-16 400-Hour Block Spectrum ( $\sigma_{GROSS} = 28$ ksi Max.), 3.5% NaCl Environments and Fast Frequency	D-6
D-6	Comparison of Normalized Crack Growth Results ( $a_i = 0.01"$ , Dry Air Versus 3.5% NaCl) for 7075-T7651 Aluminum Dog-Bone Specimens (40% Load Transfer) Tested Using: F-16 400-Hour Block Spectrum ( $\sigma_{GROSS} = 28$ ksi Max.) and Fast Loading Frequency	D-7
D-7	Comparison of Normalized Crack Growth Results ( $a_i = 0.01"$ ); Fast Versus Slow Loading Frequency) for 7075-T7651 Aluminum Dog-Bone Specimens (Open Hole) Tested Using: F-18 300-Hour (Random) Spectrum ( $\sigma_{GROSS} = 28$ ksi Max.) and Dry Air Environment	D-8

## LIST OF FIGURES (CONT'D)

<u>Figure</u>		<u>Page</u>
C-12	Comparison of Crack Growth Test Results for 7075-T7651 Aluminum Dog-Bone Specimens (Open Hole) for F-16 400 Hour Spectrum ("A") and Dry Air/3.5% NaCl Environments	C-19
C-13	Comparison of Crack Growth Test Results for 7075-T7651 Aluminum Dog-Bone Specimens (Open Hole; Bolt-In-hole) Based on F-16 400 Hour Spectrum ("A"), Dry Air/3.5% NaCl Environments and Specimen Preconditioning	C-20
C-14	Comparison of Crack Growth Test Results for 7075-T7651 Aluminum Dog Bone Specimens (Open Hole; 20% LT; 40% LT) Based on F-18 300 Hour (Random) Spectrum ("B") and Dry Air/3.5% NaCl Environments	C-21
C-15	Comparison of Crack Growth Test Results for 7075-T7651 Aluminum Dog-Bone Specimens (Open Hole; 40% LT) Based on F-18 300 Hour (Block) Spectrum ("C") and Dry Air/3.5% NaCl Environments	C-22
C-16	Comparison of Crack Growth Test Results for 7075-T7651 Aluminum Dog-Bone Specimens (Open Hole) Based on F-16 400 Hour (Block) Spectrum ("A"), Different Stress Levels and Dry Air/3.5% NaCl Environments	C-23
C-17	Summary of Dry/Wet Ratios for 7075-T7651 Aluminum Dog-Bone Specimens for F-16 400 Hour Spectrum ("A") and Dry Air/3.5% NaCl Environments	C-26
C-18	Summary of Dry/Wet Ratios for 7075-T7651 Aluminum Dog-Bone Specimens for F-18 300 Hour (Spectra "B" and "C") and Dry Air/3.5% NaCl Environments	C-27
D-1	Normalized Crack Growth Results ( $a_i = 0.01"$ ) for 7075-T7651 Aluminum Dog-Bone Specimens (Open Hole) Tested Using: F-16 400-Hour Block Spectrum ( $\sigma_{GROSS} = 28$ ksi Max.), Dry Air Environment and Two Loading Frequencies (Fast, Slow)	D-2

## LIST OF FIGURES (CONT'D)

<u>Figure</u>		<u>Page</u>
C-4	Comparison of TTCI Test Results for 7075-T7651 Aluminum Dog-Bone Specimens (20% LT; 40% LT) Based on F-16 400 Hour Spectrum ("A") and Dry Air/3.5% NaCl Environments	C-11
C-5	Comparison of TTCI Test Results for 7075-T7651 Aluminum Dog-Bone Specimens (Open Hole) Based on F-18 300 Hour (Random) Spectrum ("B"), Specimen Preconditioning and Dry Air/3.5% NaCl Environments	C-12
C-6	Comparison of TTCI Test Results for 7075-T7651 Aluminum Dog-Bone Specimens (20% LT; 40% LT) Based on F-18 300 Hour (Random) Spectrum ("B") and Dry Air/3.5% NaCl Environments	C-13
C-7	Comparison of TTCI Test Results for 7075-T7651 Aluminum Dog-Bone Specimens (Open Hole; 40% LT) Based on F-18 300 Hour (Block) Spectrum ("C") and Dry Air/3.5% NaCl Environments	C-14
C-8	Comparison of TTF Test Results for 7075-T7651 Aluminum Dog-Bone Specimens (Open Hole) for F-16 400 Hour Spectrum ("A") and Dry Air/3.5% NaCl Environments	C-15
C-9	Comparison of TTF Test Results for 7075-T7651 Aluminum Dog-Bone Specimens (Open Hole; Bolt-In-Hole) Based on F-16 400 Hour Spectrum ("A"), Dry Air/3.5% NaCl Environments and Specimen Preconditioning	C-16
C-10	Comparison of TTF Test Results for 7075-T7651 Aluminum Dog-Bone Specimens (Open Hole; 20% LT; 40% LT) Based on F-18 300 Hour (Random) Spectrum ("B") and Dry Air/3.5% NaCl Environments	C-17
C-11	Comparison of TTF Test Results for 7075-T7651 Aluminum Dog-Bone Specimens (Open Hole; 40% LT) Based on F-18 300 Hour (Block) Spectrum ("C") and Dry Air/3.5% NaCl Environments	C-18

## LIST OF FIGURES (Cont'd)

<u>Figure</u>		<u>Page</u>
B-4	da/dN Versus $\Delta K$ Results for 7075-T7651 Aluminum Alloy Exposed to 3.5% NaCl at Room Temperature (R = 0.3; f = 0.1 Hz, 0.3 Hz, 1 Hz, 3 Hz and 6 Hz)	B-14
B-5	Two-Segment Crack Growth Model Fitted to da/dN Versus $\Delta K$ Data for 7075-T7651 Aluminum in 3.5% NaCl at Room Temperature (R = 0.05)	B-23
B-6	Two-Segment Crack Growth Model Fitted to da/dN Versus $\Delta K$ Data for 7075-T7651 Aluminum in 3.5% NaCl at Room Temperature (R = 0.30)	B-24
B-7	Forman Model Goodness-of-Fit Plots for da/dN Versus $\Delta K$ (7075-T7651 Aluminum, R = 0.05, Dry Air Environment)	B-29
B-8	Forman Model Goodness-of-Fit Plots for da/dN Versus $\Delta K$ (7075-T7651 Aluminum, R = 0.3, Dry Air Environment)	B-30
B-9	Forman Model Goodness-of-Fit Plots for da/dN Versus $\Delta K$ (7075-T7651 Aluminum, R = 0.05, 3.5% NaCl Environment)	B-31
B-10	Forman Model Goodness-of-Fit Plots for da/dN Versus $\Delta K$ (7075-T7651 Aluminum, R = 0.3, 3.5% NaCl Environment)	B-32
C-1	Comparison of TTCI Test Results for 7075-T7651 Aluminum Dog-Bone Specimens (Open Hole) Based on F-16 400 Hour Spectrum ("A") and Dry Air/3.5% NaCl Environments	C-8
C-2	Comparison of TTCI Test Results for 7075-T7651 Aluminum Dog-Bone Specimens (Open Hole) Based on F-16 400 Hour Spectrum ("A"), Specimen Preconditioning and Dry Air/3.5% NaCl Environments	C-9
C-3	Comparison of TTCI Test Results for 7075-T7651 Aluminum Dog-Bone Specimens (Bolt-In-Hole) Based on F-16 400 Hour Spectrum ("A"), Specimen Preconditioning Dry Air/3.5% NaCl Environments	C-10

## LIST OF FIGURES (CONT'D)

<u>Figure</u>		<u>Page</u>
A-1	Cyclic Stress-Strain Curve for 7075-T7651 Aluminum	A-3
A-2	True Stress Versus Plastic Strain for Cyclic Response (log-log scale)	A-5
A-3	Strain Amplitude Versus $2N_i$ (Reversals) for 7075-T7651 Aluminum in <sup>i</sup> Dry Air	A-11
A-4	Strain Amplitude Versus $2N_i$ (Reversals) for 7075-T7651 Aluminum in <sup>i</sup> 3.5% NaCl Solution at Room Temperature	A-12
A-5	Total Strain Amplitude Versus $2N_i$ (Reversals) for 7075-T7651 Aluminum in <sup>i</sup> Dry Air	A-13
A-6	Total Strain Amplitude Versus $2N_i$ (Reversals) for 7075-T7651 Aluminum in <sup>i</sup> 3.5% NaCl Solution at Room Temperature	A-14
B-1	$da/dN$ Versus $\Delta K$ Results for 7075-T7651 Aluminum Alloy Exposed to Dry Air at Room Temperature ( $R = 0.05$ ; $f = 0.1$ Hz, 1 Hz and 6 Hz)	B-11
B-2	$da/dN$ Versus $\Delta K$ Results for 7075-T7651 Aluminum Alloy Exposed to 3.5% NaCl at Room Temperature ( $R = 0.05$ ; $f = 1$ Hz, 3 Hz and 6 Hz)	B-12
B-3	$da/dN$ Versus $\Delta K$ Results for 7075-T7651 Aluminum Alloy Exposed to Dry Air at Room Temperature ( $R = 0.3$ ; $f = 0.1$ Hz, 1 Hz and 6 Hz)	B-13

LIST OF SYMBOLS

"A"	=	F-16 400 hour (hi-lo block) spectrum
$a_{cr}$	=	Critical crack size
$a_i$	=	Initial flaw depth
$a_o$	=	Reference crack depth for TICI
$a(t)$	=	Crack size at time, t
"B"	=	F-18 300 hour (random) spectrum
b	=	Empirical constant in strain amplitude relationship
C,m	=	Paris crack growth model parameters in the eq. $da/dN = C(\Delta K)^m$
"C"	=	F-18 300 hour (hi-lo block) spectrum
c	=	Empirical constant in strain amplitude relationship
		Plastic: $\Delta\epsilon_p/2 = (\epsilon'_f)(2N_i)^c$
CF	=	Corrosion fatigue
CT	=	Compact tension
CCT	=	Center-cracked-tension
d	=	Hole or bolt diameter
$da/dN$	=	Crack growth rate
$(da/dN)_{cf}$	=	Cycle-dependent corrosion fatigue crack growth rate
$(da/dN)_{cf}$	=	$[(da/dN)_{cf,s}^* - (da/dN)_r]\phi$
$(da/dN)_{cf,s}^*$	=	Cycle-dependent rate of "pure" corrosion fatigue crack growth
$(da/dN)_{cf,s}$	=	Saturation fatigue crack growth rate for the transport and surface reaction controlled case
$(da/dN)_e$	=	Rate of fatigue crack growth in an aggressive environment
$(da/dN)_r$	=	Rate of fatigue crack growth in an inert environment

LIST OF SYMBOLS (CONT'D)

$(da/dN)_{scc}$	= Contribution of sustained load crack growth (i.e., by stress corrosion cracking) at K levels above $K_{ISCC}$
$da/dt$	= Crack growth rate as a function of time
E	= Elastic modulus
ESF	= Environmental scaling factor (e.g., $ESF = CF \text{ Life (Dry)} / CF \text{ Life (Wet)}$ $ESF = (da/dN)_{wet} / (da/dN)_{dry}$ )
f	= Loading frequency
$K'$	= Cyclic strength coefficient
$K_b$	= Stress concentration factor at the edge of a fastener hole due to the bearing stress in the hole
$K_C$	= Fracture toughness
$K_{IC}$	= Critical stress intensity factor for static loading and plane strain conditions or plane strain fracture toughness
$K_{ISCC}$	= Plane strain stress intensity threshold below which subcritical cracks will not propagate under static loading
$K_Q$	= Tentative value of plane strain fracture toughness
$K_t$	= Stress concentration factor
$\bar{K}_t(o)$	= Baseline effective $K_t$ value for the open hole/dry air environment case after scaling the strain life analysis using spectrum fatigue test results
$\bar{K}_t(LT)$	= Effective stress concentration factor for a given % bolt load transfer = $\bar{K}_t(o) * K_{\sigma}(LT) / K_{\sigma}(o)$ (Note: $\bar{K}_t(LT=0) = \bar{K}_t(o)$ )
$K_T$	= Total stress concentration factor at the edge of a fastener hole based on the combined effect of the through-stress and bearing stress

## LIST OF SYMBOLS (CONT'D)

$K_{\sigma}(c), K_{\sigma}(LT)$	= Elastic or plastic stress concentration factor for an open hole and hole with a given amount of bolt load transfer, respectively.
LT	= Load transfer (through the fastener)
$n'$	= Cyclic strain hardening exponent
$N_f$	= Number of cycles to failure
$N_i$	= Number of cycles to initiate crack depth of $a_o$
NLT	= No load transfer (through the fastener)
P	= Load or probability
$P_b$	= Bolt load
R	= $\sigma_{min}/\sigma_{max}$ = R-ratio
$R_{os}$	= Overload shut-off ratio
RXN	= Analytical crack growth computer program developed by General Dynamics/Fort Worth Division
S-C	= Strain-controlled
t	= Time or thickness
TFCG	= Time-for-crack-growth
TTCI	= Time-to-crack-initiation
TTF	= Time-to-failure
W	= Width
$\Delta\epsilon$	= Total strain range
$\epsilon_e$	= Elastic strain range
$\Delta\epsilon_e/2$	= Total elastic strain amplitude
$\Delta\epsilon_p$	= Plastic strain range
$\Delta\epsilon_p/2$	= Total plastic strain amplitude
$\Delta\epsilon_T/2$	= Total strain amplitude

LIST OF SYMBOLS (CONT'D)

$\Delta K$	= Range of stress intensity factor
$\Delta\sigma$	= Stress range
$\delta_T$	= Total axial deformation over specified gage length
$\epsilon, \epsilon_1, \epsilon_2$	= Strain
$\epsilon_f'$	= Fatigue-ductility coefficient
$\sigma$	= Local stress
$\epsilon_f'$	= Fatigue strength coefficient
$\sigma_{brg}$	= Bearing stress in fastener hole
$\sigma_I$	= Input gross stress
$\sigma_{max}$	= Maximum stress
$\sigma_{min}$	= Minimum stress
$\sigma_{net}$	= Net section stress
$\sigma_{net_T}$	= Net section stress due to the through-stress
$\sigma_T$	= Through stress
$\sigma_o'$	= Cyclic yield stress
$\sigma(\bar{x})$	= Standard deviation for $\bar{x}$
$\sigma_{ys}$	= Yield strength of material

S E C T I O N     I

I N T R O D U C T I O N

Metallic airframes must be designed to resist "corrosion fatigue" (CF) in service, to assure, with a high degree of confidence, that the airframe will have a useful service life and can be economically maintained. Carrier-based aircraft are particularly susceptible to corrosion fatigue due to the wide range and severity of operating loads and environments (e.g., 3.5% NaCl, stack gases, acid rain, etc.).

Airframes contain literally thousands of fastener holes and service experience has shown that mechanically-fastened joints are very susceptible to fatigue cracking in service [1-6]. Furthermore, mechanically-fastened joints are particularly prone to corrosive attack as skin protective coatings and fastener plating break down from the fretting action due to relative motion occurring in the loaded fasteners and holes. Removing fasteners for airframe maintenance and repairs can also lead to surface scratches around fastener holes which may break through the protective coating and expose the surface of the metal to corrosive attack. Also, fasteners may loosen in service.

Foreign material and moisture can enter a mechanically-fastened joint between the fastener and hole surface by

capillary action. This can ultimately cause galvanic corrosion. After prolonged operation, severe pitting and extensive exfoliation can also occur in mechanically-fastened joints. Corrosion preventative maintenance is required to minimize the deteriorating effects of the environment on the airframe during its service life. Such maintenance is not only costly and time consuming but it also effects the operational readiness of the fleet.

Reliable methods are required to design mechanically-fastened joints in metallic airframes to resist corrosion fatigue and to analytically assure, with a high degree of confidence, that a specified service life can be attained in service. The Navy has design requirements for airframe strength and life [7-15]. Various methods have been developed to acquire corrosion fatigue design data for mechanically fastened joints [e.g., 16]. Analytical tools for predicting the time-to-crack-initiation (TTCI) and time to failure (TTF) in mechanically-fastened joints have also been developed. However, further improvements in the testing and predictive methodology are needed to unify the corrosion fatigue methodology and to increase confidence in its application.

The corrosion fatigue of mechanically-fastened joints is a complex problem for several reasons. Various aspects are discussed below:

1. Corrosion fatigue behavior involves the synergistic effects of mechanical, metallurgical and environmental factors. Such factors must be accounted for when characterizing the corrosion fatigue behavior of mechanically-fastened joints and in the corrosion fatigue predictive methodology.

2. It is very difficult to realistically define the expected service loads, environments and their extremes for carrier-based aircraft during the design stage. Also, there are an infinite number of possible loading and environment combinations that could be encountered in service. A more realistic definition of actual service loads and environments may be possible only after considerable in-service experience.

3. Even if the service loads and environments could be accurately defined during the design stage, such information must ultimately be translated into suitable corrosion fatigue test requirements. Real-time tests of expected service load/environment combinations are not practical due to the prohibitive test costs and test times. Therefore, simplified corrosion fatigue tests are required to cover different mechanically-fastened joint variables and configurations that may be encountered at different airframe locations.

4. There are many variables to consider when setting up

the test plan for acquiring corrosion fatigue design data [e.g., 17-21]. For example, such variables include load spectra, environment (e.g., dry air, 3.5% NaCl, etc.), stress level, loading frequency, stress ratio, hold-time, fastener type/fit, amount of fastener load transfer, temperature, material, specimen geometries, specimen preconditioning, protective coatings, duration of environmental exposure, etc. The number of test variables need to be minimized to reduce test costs and to focus attention on those variables with the most significant effect on the corrosion fatigue behavior of mechanically-fastened joints.

5. Corrosion fatigue test results for the TCI and crack propagation typically exhibit considerable scatter. A suitable number of tests must be selected to acquire statistically valid data. Also, the scatter in the corrosion fatigue design data must be accounted for when making fatigue life predictions for mechanically-fastened joints.

6. Corrosion fatigue behavior may vary for different materials and for different combinations of variables. For example, the corrosion fatigue behavior of the 7075-T7651 aluminum alloy is considerably different than the beta annealed 6Al-4V Ti alloy. Moreover, the corrosion behavior of different aluminum alloys may vary. This complicates the selection and ranking of the most appropriate combination of material, fastener system and protective coating for mechan-

ically-fastened joint design.

7. Corrosion fatigue tests and testing methods have not been standardized for acquiring design data. Hence, much of the existing corrosion fatigue data currently available from various aircraft development programs are not compatible. As a result, a new series of corrosion fatigue tests are required for each aircraft procurement. This is costly and time-consuming. Standardized corrosion fatigue tests, methods and data are needed to provide applicable data for different aircraft systems and to minimize the number of additional corrosion fatigue tests required.

8. Mechanically-fastened joints are usually designed for corrosion fatigue using the expected operating service loads and environments, suitable corrosion fatigue design data/test results, appropriate corrosion fatigue analysis methods and engineering judgement/experience. Elaborate corrosion fatigue tests and strict manufacturing/quality controls can be used to produce the best airframe possible. However, the real test of structural performance and fatigue life can be obtained only from actual service experience. Hopefully, corrosion fatigue problems that are "hell-to-fix" can be minimized.

The main objectives of this program are to:

1. Develop and verify an analytical methodology for predicting the TTCI and crack propagation life of mechanically-fastened joints in a corrosive environment.

2. Develop corrosion fatigue test/data-acquisition methods and guidelines for acquiring statistically-valid data needed to implement the analytical methodology.

3. Study the effects of various factors on the corrosion fatigue behavior of mechanically-fastened joints.

The Phase I effort, documented in Volumes I and II [6, 22], was concerned with three tasks as follows:

- o Task 1 - Methodology and Data State-of-the-Art  
Assessment
- o Task 2 - Methodology Development
- o Task 3 - Test Plan Development

In Phase I, the existing corrosion fatigue analysis methods were reviewed, the effects of various variables (i.e., stress level, R-ratio, loading frequency, environment hold-time, etc.) on TTCI and crack growth were experimentally investigated and evaluated for two different materials (7075-T7651 aluminum alloy and beta-annealed 6Al-4V Ti

alloy), and a test plan was developed for the Phase II effort. The most suitable corrosion fatigue analysis methods for predicting the TTCI and crack propagation for mechanically-fastened joints were recommended in Phase I for evaluation in Phase II. Constant amplitude corrosion fatigue data was acquired under the Phase I effort.

The objectives of the Phase II effort were to: (1) develop and evaluate suitable experimental methods and specimens for acquiring corrosion fatigue data for mechanically-fastened joints, (2) acquire corrosion fatigue data needed to implement the predictive methods recommended under Phase I, (3) evaluate the effectiveness of the CF analysis methodology for predicting the fatigue life of mechanically-fastened joints under the spectrum loading, and (4) evaluate the effects of various factors (e.g., loading frequency, R-ratio, stress level, load transfer, load spectra) on the TTCI and crack propagation in mechanically-fastened joints. This report (Volume III) documents the Phase II effort.

In Phase I, it was found that the corrosion fatigue behavior of the beta-annealed 6Al-4V titanium alloy was very complex [22]. For this reason, the Phase II effort was mainly concerned with the demonstration and evaluation of the corrosion fatigue methodology for 7075-T7651 aluminum. In Phase II, the beta-annealed 6Al-4V titanium alloy investigations were limited to the development of a better understand-

ing of the corrosion fatigue crack growth mechanisms and the effects of loading frequency were emphasized [23].

Since corrosion fatigue is a complex problem, continuing research is necessary to advance the CF test and analysis methodology state-of-the-art. This program provides one of the steps in this development process.

S E C T I O N     I I

P H A S E     I I     T E S T     P R O G R A M

2.1 INTRODUCTION

Essential elements of the Phase II test program are described in this section, including the test objectives, test variables considered, specimen geometries, test matrices, test setup and procedures, etc. A more complete description of the Phase II experimental work and test results are presented in Volume IV [24].

2.2 PHASE II TEST OBJECTIVES

The main objectives of the Phase II test program were to:

1. Develop and evaluate suitable experimental methods and specimens for acquiring corrosion fatigue data for mechanically fastened joints (Task 4).
2. Acquire statistically-valid corrosion fatigue data needed to implement and "tune" the corrosion fatigue analysis methodology for spectrum loading applications (Task 5).
3. Provide statistically-valid experimental data for

evaluating the effects of various factors (e.g., loading frequency, R-ratio, stress level, load spectra, and percent bolt load transfer) on the time-to-crack-initiation (TTCI) and time-to-failure (TTF) in fastener holes (Task 5).

4. Provide key experimental results for Ti-6Al-4V alloy for developing a better understanding of basic mechanism and the effects of loading frequency on fatigue crack growth (Task 5).

5. Provide corrosion fatigue test results for crack initiation and crack growth in fastener holes that can be used to evaluate the accuracy of analytical methodology described in Volume I [3] (Task 6).

### 2.3 SPECIMEN AND TEST MATRICES

The corrosion fatigue test program for Phase II included 253 test specimens as shown in Table 1. Three basic specimen geometries were used (ref. Figs. 1-3). A summary of the test variables used in Phase II are summarized in Table 2.

The test matrix for the experimental methodology development effort is shown in Table 3. Tests performed under Task 5 are presented in Tables 4, 5 and 6 for strain-controlled tests, for Ti-6Al-4V compact tension tests, and

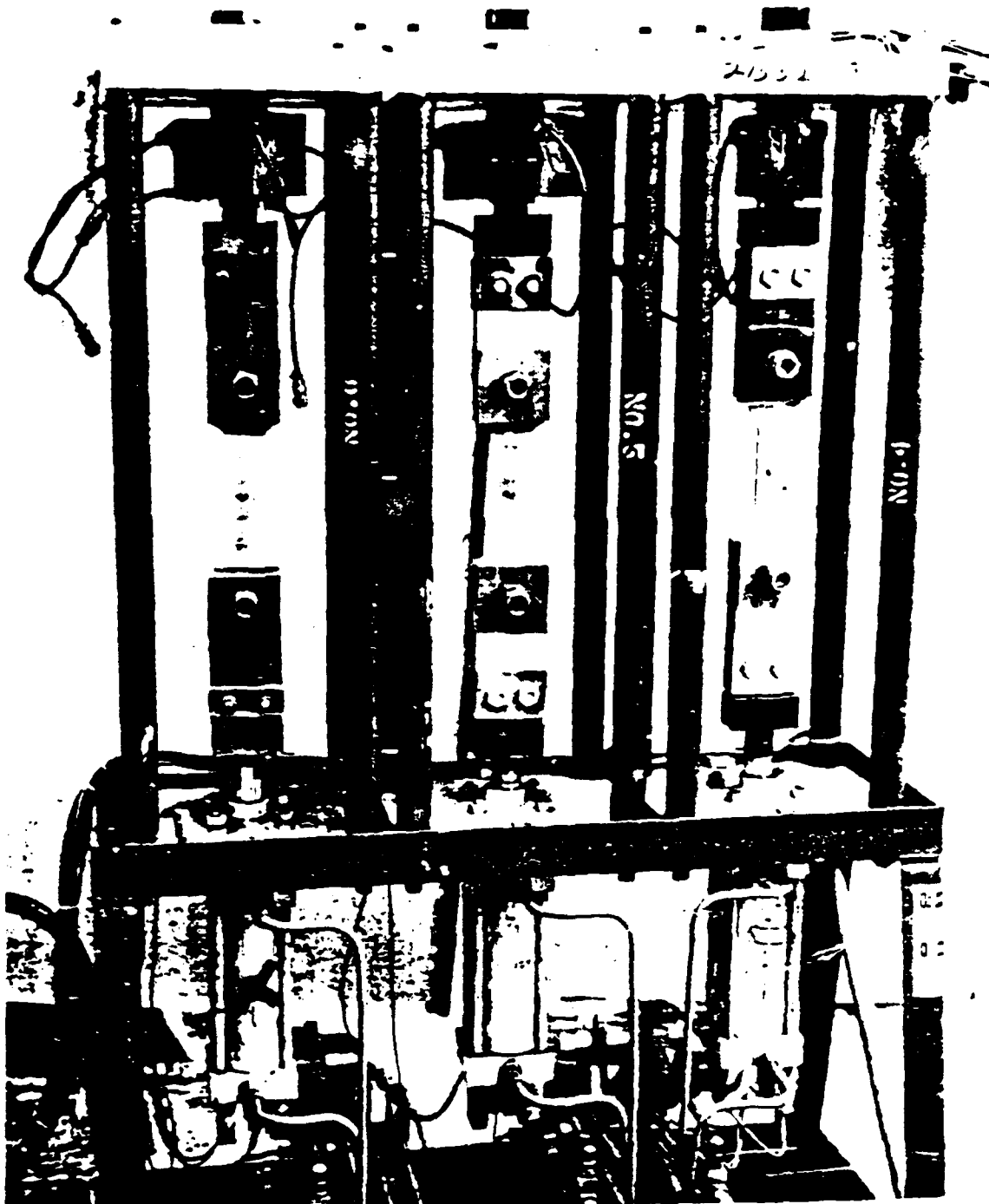


Fig. 5 Test Setup for No-Bolt Load Transfer  
Dog-Bone Specimen Tests

tension specimens (Fig. 2). The strain-controlled and the compact tension tests for the titanium alloy are documented in Volume IV, Appendix A [24] and Volume V [23], respectively.

#### 2.4.2 No-Load Transfer Dog-Bone Specimen Tests

Dog one specimens (Fig. 3) of 7075-T7651 aluminum were fatigue tested. The test setup for the no-load transfer specimen tests is shown in Fig. 5. Details of the environmental chamber used for the no-load transfer tests are shown in Fig. 6. Both desiccant (for dry air environment) and 3.5% NaCl solution could be placed in these chambers. The environment chamber system shown was used for both constant amplitude and spectrum fatigue tests in Phase II.

#### 2.4.3 Load Transfer Dog-Bone Specimen Tests

The test setup for the load transfer tests are shown in Figure 7. The environmental chamber was an integral part of the loading bar used to transmit load directly from the ram to the bolt. Details of the chamber are shown in Figure 8. Either desiccant crystals (dry air) or 3.5% NaCl solution could be added to the chambers.

Test spectrum loads were simulated using a haversine wave form for positive-to-zero loads and for zero-to-negative loads. This provided a short dwell time at zero load for

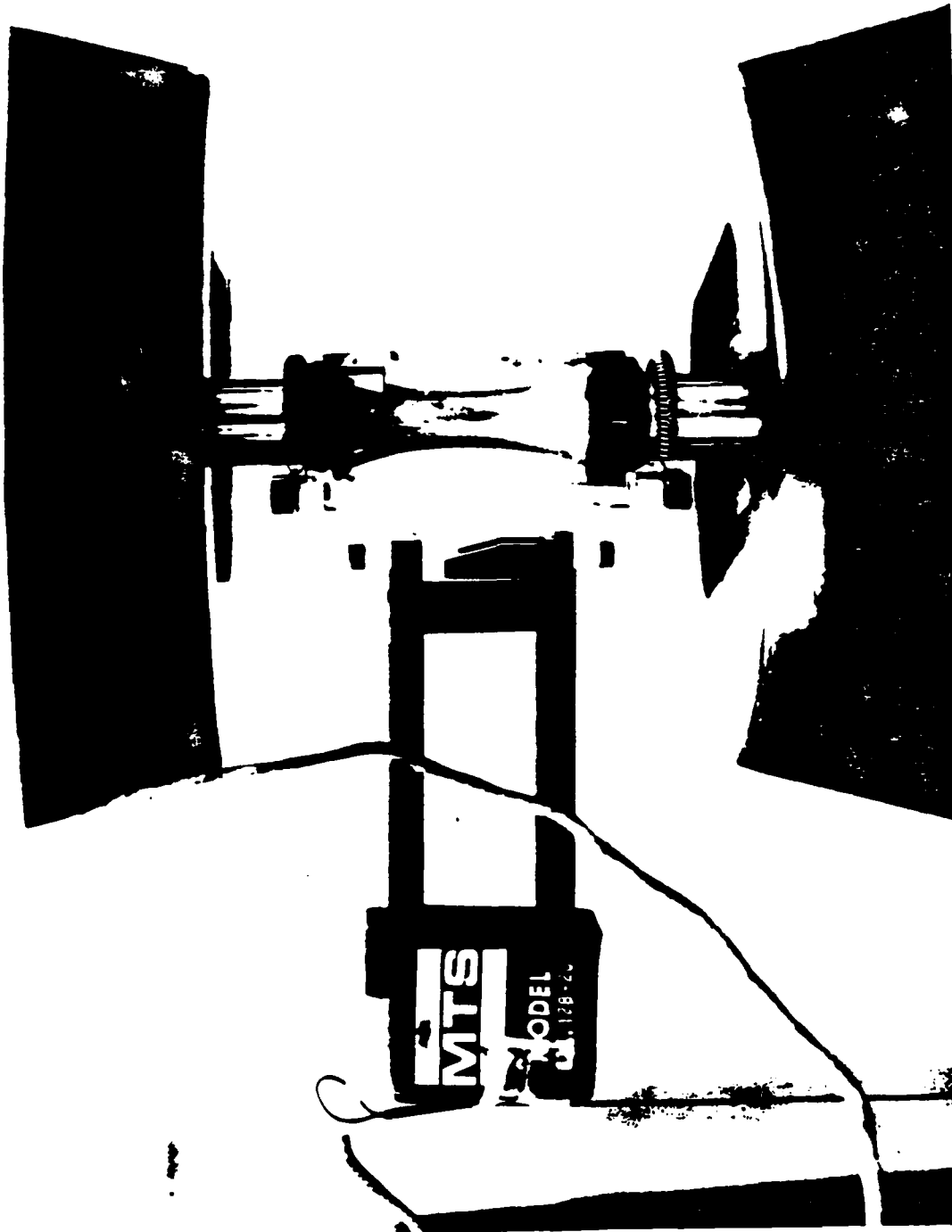


Fig. 4 Environmental Chamber and Test Setup for Strain-Controlled Tests

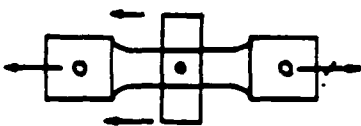
TABLE 8 CODING SYSTEM FOR DESCRIBING TESTS

ITEM	CODE
Type Test or Spectrum	<ul style="list-style-type: none"> <li>o CA = Constant Amplitude Test</li> <li>o SC = Strain-Controlled Test</li> <li>o A = F-16 400 Hr. (Hi-Lo Block)</li> <li>o B = F-18 300 Hr. (Random)</li> <li>o C = F-18 300 Hr. (Hi-Lo Block)</li> </ul>
Stress Level (ksi, gross)	<ul style="list-style-type: none"> <li>o 28, 30, 32, 34 ksi</li> </ul>
% Bolt Load Transfer	<ul style="list-style-type: none"> <li>o 20 or 40 (Follows stress level if applicable)</li> </ul>
Spectrum Loading Frequency	<ul style="list-style-type: none"> <li>o F = Fast (8000 flt hrs/2 days)</li> <li>o S = Slow (8000 flt hrs/16 days)</li> <li>o X = XSlow (8000 flt hrs/90 days)</li> </ul>
Environment	<ul style="list-style-type: none"> <li>o D = Dry Air @ R.T.</li> <li>o W = 3.5% NaCl Solution @ R.T.</li> </ul>
Bolt in Hole	<ul style="list-style-type: none"> <li>o B = Bolt in Hole (Noted for 0% LT Tests)</li> </ul>
Preconditioning	<ul style="list-style-type: none"> <li>o PC = Specimen Preconditioned (Pretested and Soaked in 3.5% NaCl Solution)</li> </ul>

Examples:

- (1) A-28/F/W = F-16 400 Hr. Spectrum; 28 ksi  
(gross) stress on test section;  
fast loading frequency; 3.5%  
NaCl environment
- (2) A-28/20/S/D/B/PC = F-16 400 Hr. Spectrum; 28 ksi  
(gross) stress on test section;  
20% bolt load transfer; slow  
loading frequency; dry air; bolt  
in hole; specimen preconditioned

TABLE 7 DOG-BONE SPECIMEN TESTS FOR TASK 6

SPECIMEN	SPECTRUM	MATERIAL	TEST I.D.	DATA SET NO.	SPECIMEN DETAILS		ENVIRONMENT		FREQUENCY		NO. SPECIMENS TESTED
					Z LT	PC?	DRY	3.5Z NaCl	FAST	SLOW	
 (Fig. 3)	CONSTANT AMPLITUDE ↓	7075-T7651 ↓	CA-23/20/F/D	63	20	NO	X	-	6 Hz	-	1
			CA-17/20/F/D	64	20	NO	X	-	↑	-	3
			CA-17/20/F/W	65	20	-	X	-	-	-	3
		7075-T7651 ↓	CA-17/40/F/D	66	40	NO	X	-	↓	-	2
			CA-17/40/F/W	67	40	NO	-	X	-	-	3
	F-16 400 HR. (BLOCK) ↓	7075-T7651 ↓	A-28/20/F/D	15	20	NO	X	-	X	-	3
			A-28/20/F/W	16	20	NO	-	X	X	-	2
			A-28/20/S/D	17	20	NO	X	-	-	X	1
		7075-T7651 ↓	A-28/20/S/W	18	20	NO	-	X	-	X	2
			A-28/40/F/D	19	40	NO	X	-	X	-	3
			A-28/40/F/W	20	40	NO	-	X	X	-	3
	F-18 300 HR. (RANDOM) ↓	7075-T7651 ↓	B-28/20/F/D	29	20	NO	X	-	X	-	4
			B-28/20/F/W	30	20	NO	-	X	X	-	4
		7075-T7651 ↓	B-28/40/F/D	31	40	NO	X	-	X	-	3
			B-28/40/F/W	32	40	NO	-	X	X	-	3
	F-18 300 HR. (BLOCK)	7075-T7651 ↓	C-28/40/F/D	35	40	NO	X	-	X	-	3
			C-28/40/F/W	36	40	NO	-	X	X	-	3
											46

for dog-bone specimen tests, respectively. Forty-six dog-bone specimens were tested under Task 6 as indicated in Table 7. Test conditions were described in a coded format to concisely define the test variables (Table 8).

## 2.4 TEST SETUPS AND PROCEDURES

Test setups for the different types of tests performed under Phase II are described in this section, including a brief summary of experimental procedures. Details are given in Volume IV [24] and V [23].

### 2.4.1 Strain-Controlled Tests

The test setup for the strain-controlled tests is shown in Fig. 4. Essential elements of the test include: specimen (Fig. 1), MTS machine with hydraulic grips, environmental chamber, environment (dry air simulated by desiccant; 3.5% NaCl solution), two-inch modified MTS extensometer, and instrumentation.

Beta-annealed Ti-6Al-4V was also tested but tests were limited to smooth un-notched specimens (Fig. 1) and compact

TABLE 6 DOG-BONE SPECIMEN TESTS FOR TASK 5


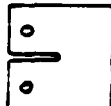
SPECIMEN	SPECTRUM	MATERIAL	TEST I.D.	DATA SET NO.	SPECIMEN DETAILS			ENVIRONMENT		FREQUENCY			NO. SPECIMENS TESTED
					Z LT	BOLT?	PC?	DRY	3.5% NaCl	FAST	SLOW	XSLOW	
 (Fig. 3)	CONSTANT AMPLITUDE	7075-T7651 7075-T7651	CA/F/D/PC CA/F/W/PC	61 62	0 0	NO NO	YES YES	X X	- -	X X	- -	3 4	
	P-16 400 HR. (BLOCK)	7075-T7651	A-28/F/D A-28/S/D A-28/F/W A-28/S/W A-28/F/W A-28/F/D/PC A-28/S/D/PC A-28/F/W/PC A-28/S/W/PC A-28/F/D/B A-28/F/W/B A-28/S/W/B A-28/F/D/B/PC A-28/F/W/B/PC	1 2 3 4 5 6 7 8 9 10 11 12 13 14	0 0 0 0 0 0 0 0 0 0 0 0 0 0 0	NO NO NO NO NO YES YES NO YES YES YES YES YES YES YES	NO NO NO NO NO YES YES NO YES YES YES YES YES YES YES	X X - - - X X - - X X - - X X - X					

TABLE 4 STRAIN-CONTROLLED TESTS FOR TASK 5

LOADING	MATERIAL	TEST I.D.	DATA SET NO.	ENVIRONMENT		FREQUENCY	NO. SPECIMENS TESTED
				DRY	3.5% NaCl		
Constant Amplitude (R=-1)	7075-T7651	SC/D/A	72	X	-	VARIABLE	22
	7075-T7651	SC/W/A	73	-	X	VARIABLE	23
	Ti-6Al-4V	SC/D/T	82	X	-	VARIABLE	18
	Ti-6Al-4V	SC/D/T	83	-	X	VARIABLE	11
							74

TABLE 5 Ti-6Al-4V ALLOY CRACK GROWTH TESTS FOR TASK 5

SPECIMEN	MATERIAL	ENVIRONMENT	K LEVEL			NO. SPECIMEN TESTED
			LOW	MED	HIGH	
	Ti-6Al-4V	Oxygen (Ref.)	X	-	-	2
	↓		-	X	-	2
	↓		-	-	X	2
	Ti-6Al-4V	3.5% NaCl	X	-	-	1
	↓		-	X	-	1
	↓		-	-	X	1
						9

Notes: 1. Ref. Volume I [22] for tests in vacuum.

2. Ref. Volume V [24] for testing details and results.

TABLE 3 EXPERIMENTAL METHODOLOGY DEVELOPMENT AND EVALUATION TESTS (TASK 4)



SPECIMEN	SPECTRUM	MATERIAL	TEST I.D.	DATA SET NO.	SPECIMEN DETAILS			ENVIRONMENT		FREQUENCY		NO. SPECIMENS TESTED
					Z LT	BOLT?	PC?	DRY	3.5%NaCl	FAST	SLOW	
 (Fig. 3)	F-16 400 NR	7075-T7651	A-34/S/D	41	0	No	No	X	-	-	X	1
			A-34/F/W	42				-	X	X	-	1
			A-34/S/W	43				-	X	-	X	3
			A-32/S/D	44				X	-	-	X	3
			A-32/F/W	45				-	X	X	-	1
			A-32/S/W	46				-	X	-	X	3
			A-30/F/D	47				X	-	-	-	2
			A-30/S/D	48				X	-	-	-	1
			A-30/F/W	49				-	-	-	-	3
			A-30/20/S/W	50	20	Yes		-	X	-	-	1
			A-30/20/F/W	54	20	Yes		-	X	-	-	1
			A-28/F/W/B	51	0	Yes		-	X	X	-	1
			A-28/F/W/B/PC	52	0	Yes		-	X	X	-	2
			A-28/S/W/B/PC	53	0		Yes	-	X	-	X	2
 (Fig. 1)	CONSTANT AMPLITUDE (R = -1) (STRAIN CONTROLLED)	T1-6A1-4V	SC 1A	71	<div style="border: 1px solid black; padding: 5px; text-align: center;">STRAIN SURVEY TESTS</div>							5
			SC 1T	81								1
												31

TABLE 2 PHASE II TEST VARIABLES

MATERIAL	<ul style="list-style-type: none"> <li>o 7075-T7651 ALUMINUM ALLOY</li> <li>o T1-6Al-4V ALLOY</li> </ul>
ENVIRONMENT	<ul style="list-style-type: none"> <li>o DRY AIR</li> <li>o 3.5% NaCl SOLUTION</li> </ul>
TYPE LOADING	<ul style="list-style-type: none"> <li>o STRAIN-CONTROLLED</li> <li>o CONSTANT AMPLITUDE</li> <li>o SPECTRUM</li> </ul>
LOAD SPECTRA	<ul style="list-style-type: none"> <li>o F-16 400 HR. (HI-LO BLOCKS)</li> <li>o F-18 300 HR. (RANDOMIZED)</li> <li>o F-18 300 HR. (HI-LO BLOCKS)</li> </ul>
LOADING FREQUENCY AND HOLD TIME	<ul style="list-style-type: none"> <li>o CONSTANT AMPLITUDE (0.3 Hz TO 20 Hz)</li> <li>o SPECTRUM (FAST, SLOW, X-SLOW)</li> <li>o HOLD TIME (0 s TO 2.33 s)</li> </ul>
TEST SPECIMENS	<ul style="list-style-type: none"> <li>o UN-NOTCHED AXIAL (STRAIN-CONTROL)</li> <li>o COMPACT TENSION</li> <li>o DOG-BONE WITH CENTER HOLE</li> </ul>
FASTENER HOLE	<ul style="list-style-type: none"> <li>o OPEN (W/O BOLT)</li> <li>o WITH BOLT</li> </ul>
BOLT HOLE FINISH	<ul style="list-style-type: none"> <li>o POLISHED</li> </ul>
BOLT TYPE	<ul style="list-style-type: none"> <li>o STEEL PROTRUDING HEAD (CAD-PLATED) (e.g., NAS 6207)</li> </ul>
BOLT LOAD TRANSFER	<ul style="list-style-type: none"> <li>o 0% LT</li> <li>o 20% LT</li> <li>o 40% LT</li> </ul>
STRESS LEVEL	<ul style="list-style-type: none"> <li>o BASELINE STRESS</li> <li>o OTHER</li> </ul>
SPECIMEN PRECONDITIONING	<ul style="list-style-type: none"> <li>o NONE</li> <li>o PRETEST AND PRESOAK IN 3.5% NaCl</li> </ul>

Fig. 3 Dog-Bone Specimen



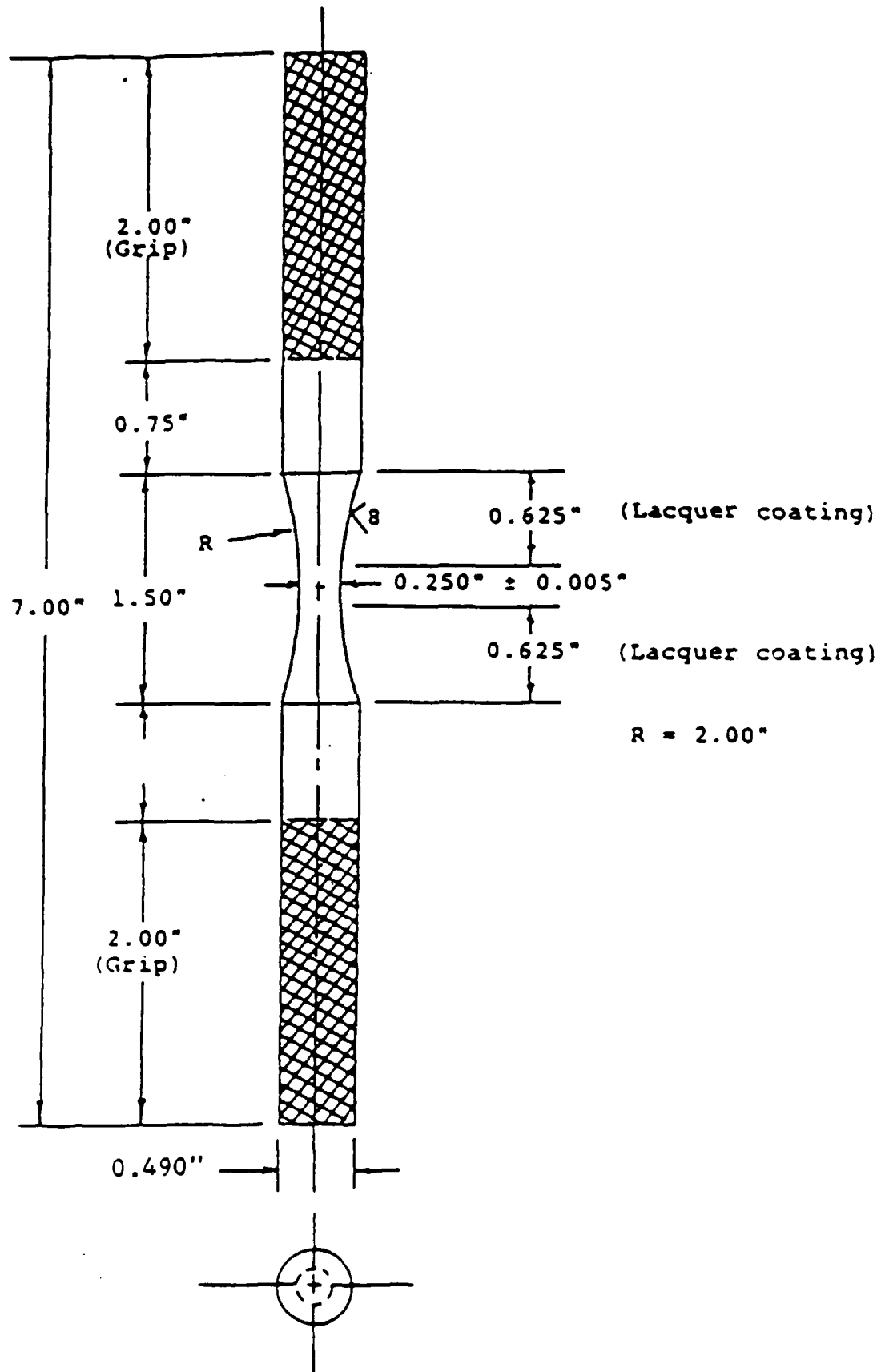






Fig. 1 Strain-Controlled Specimen

TABLE 1 TEST SPECIMEN MATRIX FOR PHASE II

SPECIMEN		MATERIAL	NO. OF SPECIMEN			
CONFIGURATION	TYPE		TASK 4	TASK 5	TASK 6	$\Sigma$
 (Fig. 1)	S-C	7075-T7651	5	45	0	50
		Ti-6Al-4V	1	29	0	30
 (Fig. 2)	CT	Ti-6Al-4V	0	9*	0	9*
 (Fig. 3)	NLT	7075-T7651	23	90	0	113
 (Fig. 3)	LT	7075-T7651	2	3	46	51
$\Sigma$			31	176	46	253

NOTES:

Task 4 - Experimental Methodology Development &amp; Evaluation

Task 5 - Acquisition of Data for Prediction of Environmentally-Assisted Crack Growth in Aircraft Joints

Task 6 - Prediction Methodology Evaluation and Verification

S-C - Strain-controlled

CT - Compact Tension

NLT - No Load Transfer (through the fastener)

LT - Load Transfer (through the fastener)

\* Results are documented and evaluated in Volume V [23].

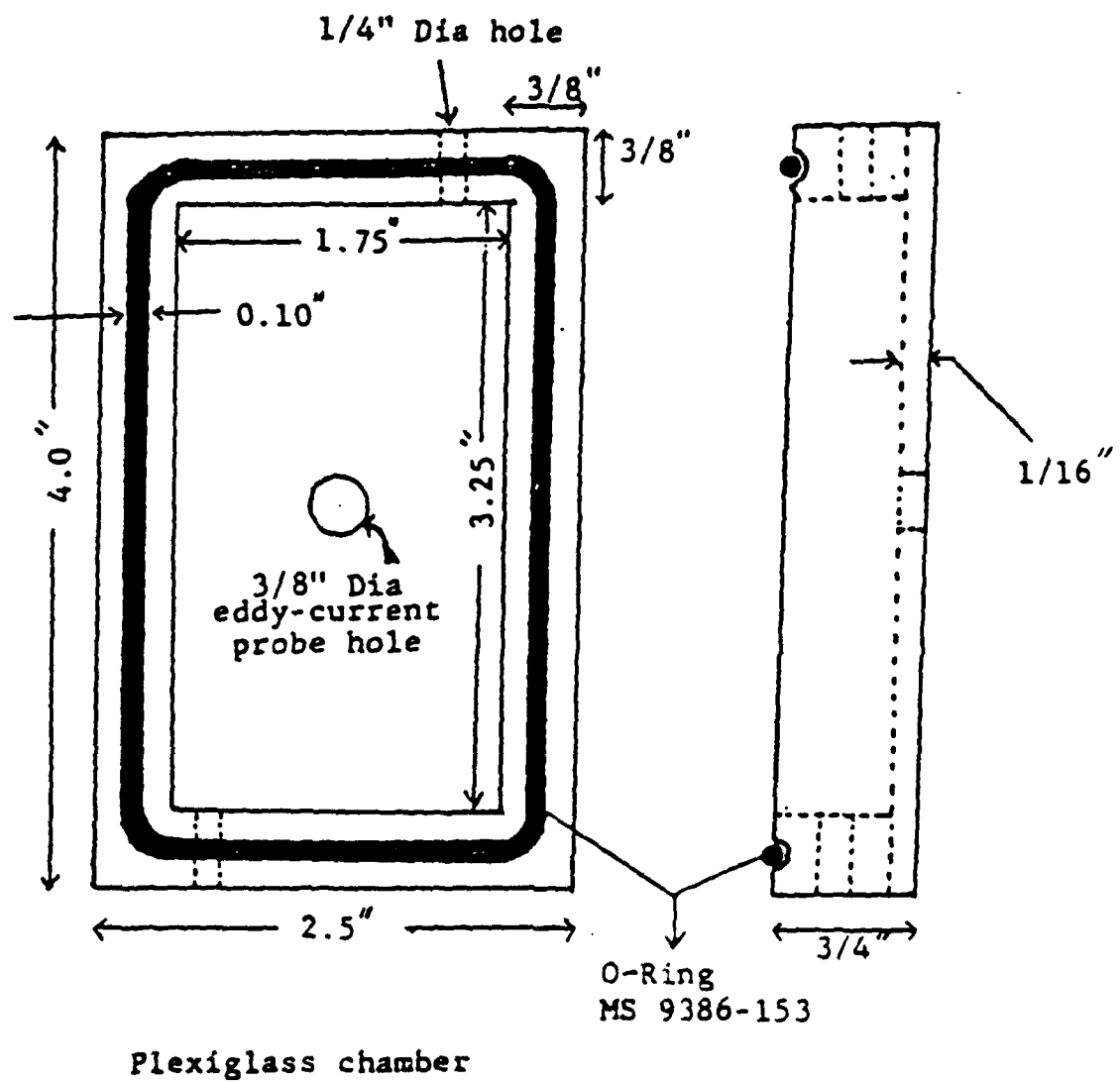


Fig. 6 Environmental Chamber Used for NO - Load Transfer Dog-Bone Tests

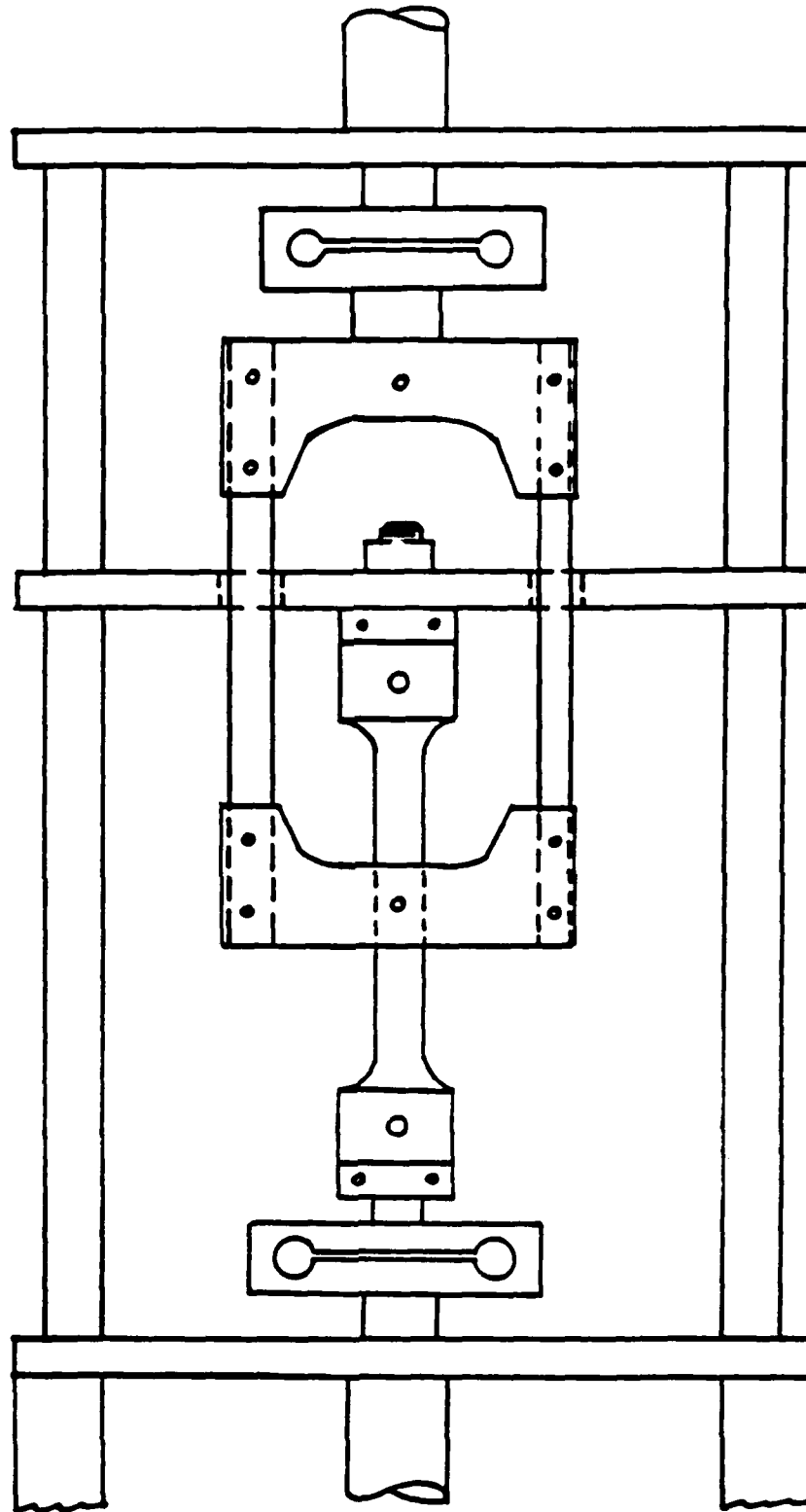


Fig. 7 Test Setup for Bolt Load Transfer Dog-Bone Specimen Tests

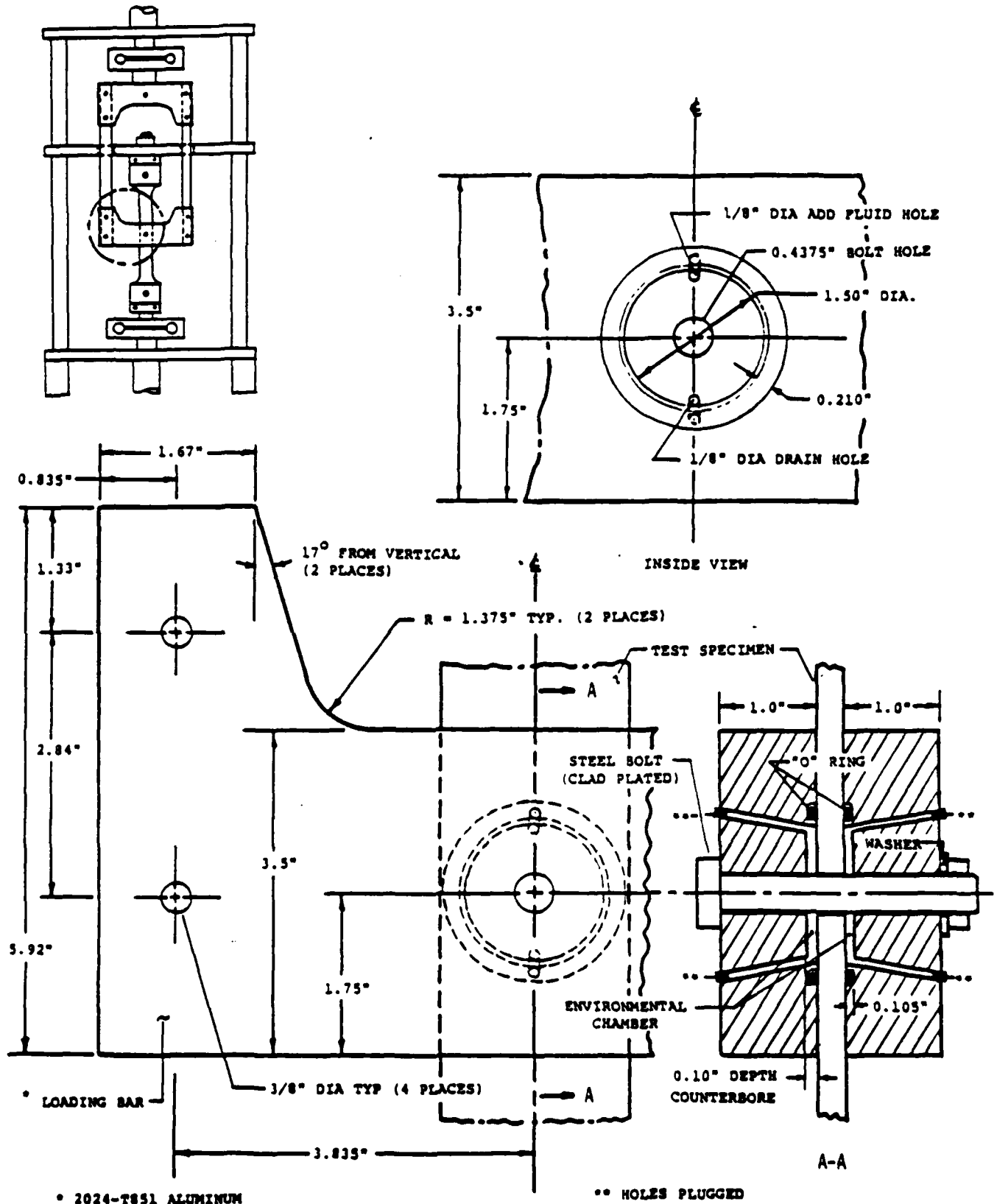


Fig. 8 Details of Integral Environmental Chamber Used In Loading Bar for Bolt Load Transfer Tests

those cases where the load was changing from positive to negative. The dwell time duration decreased as the loading frequency was increased. This simulation method for the spectrum loading was used to minimize the "hammering" action between the clearance-fit bolt and the fastener hole.

## 2.5 SPECIMEN PRECONDITIONING

Specimen preconditioning was used to complement the AGARD program effort [16] and to further evaluate the effects of preconditioning on the time-to-crack-initiation and crack growth in fastener holes.

Selected dog-bone specimens from Tasks 4 and 5 were preconditioned as follows:

1. One block of the F-16 400 hour block spectrum was applied to the test specimen in lab air at a maximum spectrum stress of 28 ksi (i.e., peak load in spectrum produces 28 ksi stress on gross section of test specimen).

2. The specimen was then soaked in a 3.5% NaCl solution at room temperature for 72 hours.

3. Specimens were then cleaned and dried using the procedure described in AGARD report 695 [16].

## 2.6 LOAD SPECTRA

Three test spectra were used in the Phase II testing of 7075-T7651 aluminum alloy dog-bone specimens: (1) F-16 400 hour (hi-lo block), (2) F-18 300 (random) and (3) F-18 300 hour (hi-lo block). Details of these spectra are discussed in Appendix H of this report (Vol. III) and Volume IV [24]. The three load spectra are compared in Appendix H, including maximum-minimum percent loads versus number of load points or load cycles and load exceedances for selected % maximum load.

NADC-83126-60-Vol. III

(This page intentionally left blank)

## SECTION III

### EXPERIMENTAL METHODOLOGY DEVELOPMENT AND EVALUATION

#### 3.1 INTRODUCTION

Experimental procedures were developed and verified under Task 4 for acquiring data used in Tasks 5 and 6. Test specimen, environmental simulation chambers, test procedures, stress and strain levels and methods for acquiring the time-to-crack-initiation and crack growth data were verified under this task. Procedures were established for: (a) strain controlled tests, (b) no-load transfer (dog-bone specimen) tests, and (c) load transfer (dog-bone specimen) tests. These separate procedures will be discussed in this section.

#### 3.2 STRAIN CONTROLLED TESTS

Experimental procedures were established for obtaining strain-controlled data in both dry air and 3.5% NaCl environments. The strain-controlled data was needed to implement the strain life approach for making time-to-crack-initiation (TTCI) predictions for mechanically-fastened joints.

Strain controlled experimental procedures were developed in three stages: (1) calibrate strain-controlled specimen and ram loading; (2) evaluate environmental simulation methods; and (3) verify the time-to-crack initiation (TTCI) acquisition method. Elements of the experimental methodology development are described in Fig. 9. Experimental procedures are described in Vol. IV [24]. Since the same experimental procedures developed for the aluminum alloy worked equally well for the titanium alloy, only one titanium specimen was needed for Task 4 and it was used to conduct a strain survey.

#### 3.2.1 Calibration of Strain-controlled Specimen

Strain surveys and strain-controlled specimen calibration tests were conducted to experimentally determine the relationship between ram load, axial strain and axial deformations (over 2.00" gage length). The test setup is shown in Fig. 10. Four axial strain gages and an extensometer were mounted on the calibration specimen as shown in Fig. 11.

The instrumented specimen shown in Fig. 10 was statically loaded in tension and compression using a selected range of loads. Strain and extensometer measurements were taken at selected load levels. Typical results are presented in Appendix A, Vol. IV, for the 7075-T7651 aluminum alloy.

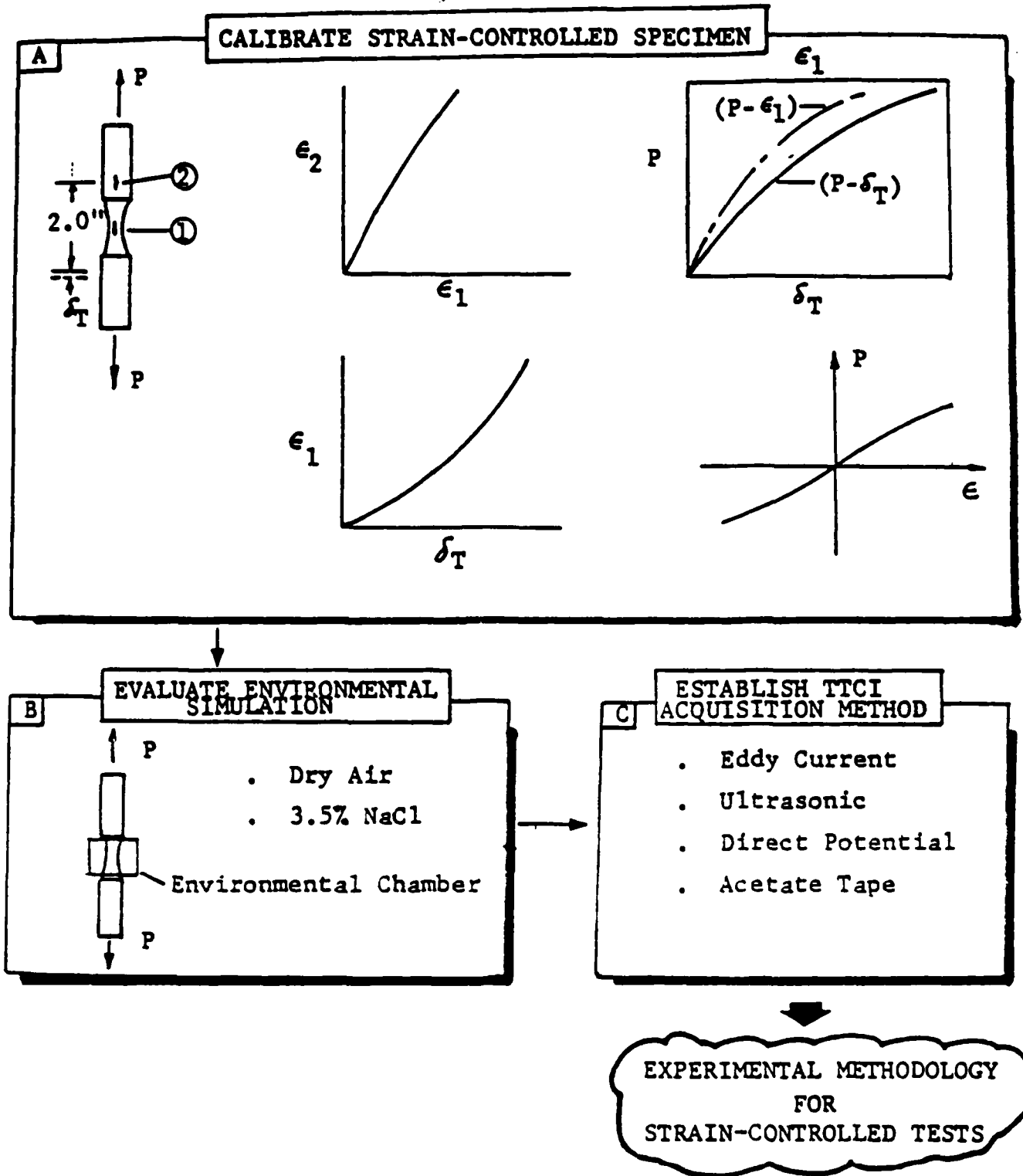


Fig. 9 Elements of Strain-Controlled Experimental Methodology Development

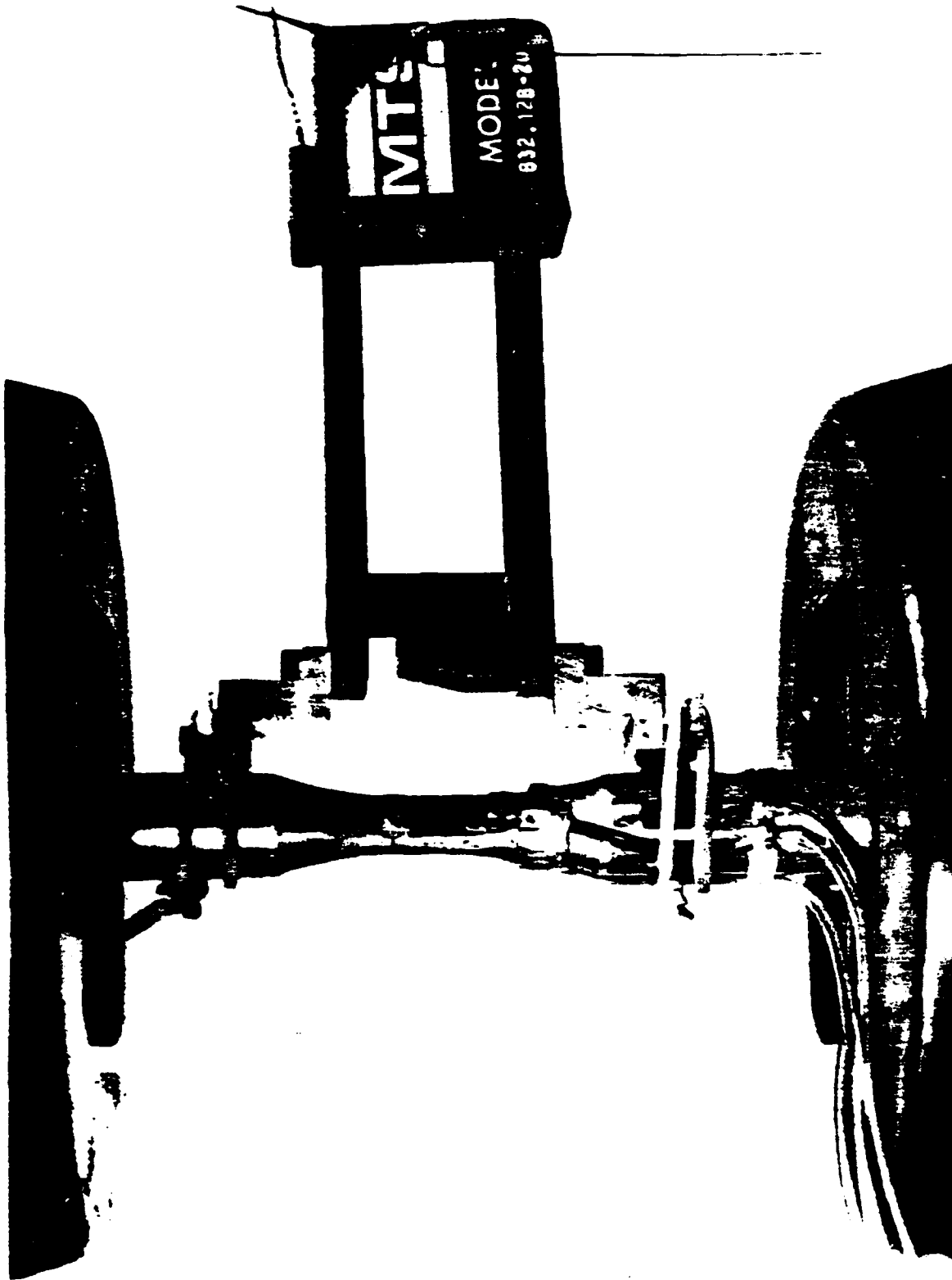


Fig. 10 Setup for Strain Surveys Using Strain-Controlled Specimen

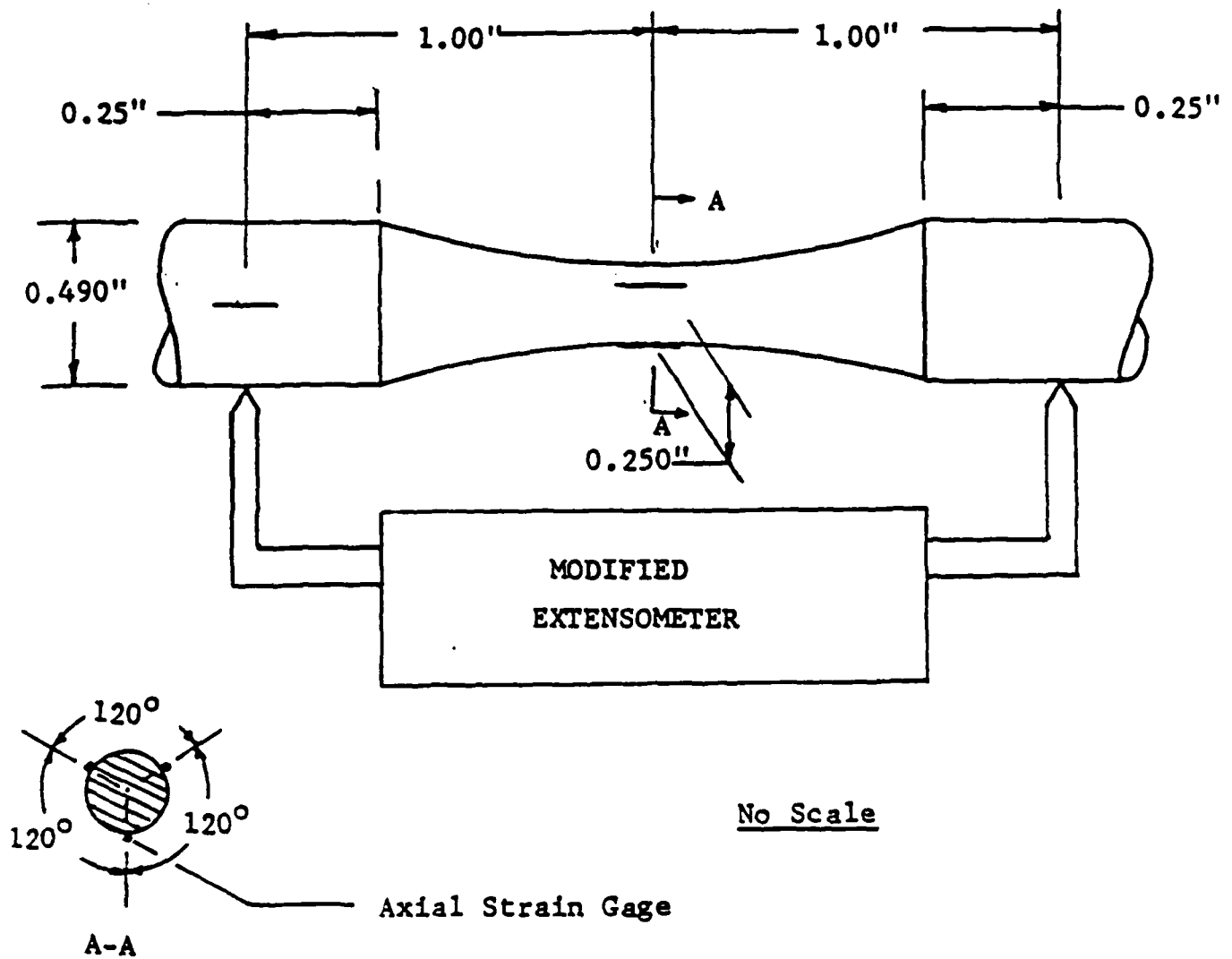


Fig. 11 Strain Gage Locations for Strain-Controlled Specimen

Calibration curves for 7075-T7651 aluminum alloy and Ti-6Al-4V alloy, respectively, were used to select extensometer voltages to obtain a specified strain value in the Task 5 experiments. The shape of the calibration curves were similar for both beta-annealed Ti-6Al-4V and 7075-T7651 aluminum alloys.

### 3.2.2 Environmental Simulation

Two different environments were considered in the Phase II testing: dry air and 3.5% NaCl solution, both at room temperature. Dry air conditions were simulated by placing desiccant crystals in the environmental chambers before testing. The salt water solution for the Phase II tests was prepared by dissolving reagent grade NaCl in triply-distilled water. The average solution pH was about 6.5 over the duration of each test. All Phase II salt water tests were performed in a constant immersion environment with periodic changing of the 3.5% NaCl solution to keep the solution fresh. The environmental chamber used for both dry air and 3.5% NaCl solution is shown in Fig. 4, and further details are given in Volume IV [24].

### 3.2.3 Establishing TTCI Acquisition Methods

Early monitoring of experimental methodology specimens was accomplished with eddy current techniques. These techniques, used in fastener hole inspections, are described in Volume I [22]. For surface inspection, an eddy current pencil probe (NDT Product Engineering, MP-20 micro-probe) was used to inspect for early fatigue cracks in the reduced section of the specimen. Since scanning had to be performed manually instead of automatically, there was some loss of sensitivity. This monitoring was compared to crack detection as observed from the decrease in maximum tensile load with cycling. The decrease in the maximum tensile load, due to load shedding, was found to be more sensitive than eddy current techniques for determining macroscopic crack initiation. Therefore, the load shedding technique was used to determine the TTCI for Tests under Task 5 (Ref. Table 4) for both 7075-T7651 aluminum alloy and beta-annealed Ti-6Al-4V.

In the 7075-T7651 aluminum alloy material, after the first few cycles, the maximum tensile stress remained relatively constant until a fatigue crack was initiated. A calibration curve was established between the decrease in maximum tensile stress and crack depth. After tensile stress decreases of different percentages were observed during fatigue testing, specimens were then overloaded in tension to

failure. Fatigue crack sizes were then measured. Detailed test results are shown in Appendix A of Volume IV [24] and these results are evaluated in Appendix A of this Volume (III) for strain-life analysis applications. Cycles to crack initiation for test specimens in Task 5 were defined in terms of cycles completed before a 2% drop in maximum tensile stress occurred.

Cyclic softening occurred in the beta-annealed Ti-6Al-4V alloy at higher strain amplitudes. Both the maximum tensile stress and compressive stress decreased as a function of cycling. The percentage decrease in maximum compressive stress was used to measure cyclic softening occurrence and thus allows the effects of "load shedding" and cyclic softening to be separated in the measurements of maximum tensile stress. The onset of a 0.010" deep fatigue crack was defined as the number of cycles when the maximum tensile stress showed a 2% greater decrease than the maximum compressive stress.

### 3.3 DOG-BONE SPECIMENS

Experimental procedures were established for obtaining TTCI, TTF-TTCI, and TTF data in both dry air and 3.5% NaCl environments. Procedures were developed in three stages: (1) develop test methods that could be used in spectrum and constant amplitude testing in Tasks 5 and 6, (2) evaluate envir-

predictions under Phase II of this program.

2. Study the influence of various factors (e.g., R ratio, loading frequency and environment) on the Paris and Forman crack growth model parameters.

3. Determine if  $(da/dN)_{cf}$  in the superposition model proposed by Wei et al [27], Eq. B-3 in Appendix B of this Volume (III), depends on  $(\Delta K)^2$  or not.

4. Details of the studies described above, including conclusions and recommendations are given in Appendix B.

#### 4.4 DOG BONE SPECIMEN TEST RESULTS

Test results for 7075-T7651 aluminum dog bone specimens (Ref. Fig. 3) from Phase II are summarized in Tables 9-13. Phase II test results are documented in Volume IV [24]. A comprehensive evaluation of the dog bone specimen test results is presented in Appendices C and D of this Volume (III). The purpose of this section is to summarize the dog bone test results acquired under Phase II and to evaluate the implications of these results for this program.

is observed in the 3.5% NaCl environment. However, the difference between the 3.5% NaCl and dry air data is quite small. The effect of the 3.5% NaCl environment on crack initiation is considerably less in this alloy than in the 7075-T7651 aluminum alloy.

The effect of test frequency on crack initiation in both dry air and 3.5% NaCl environment were examined. Frequencies ranging from .5 Hz to 5.0 Hz were used. Results indicated that both the dry air and 3.5% NaCl environment data was strain rate dependent. Accelerated crack initiation was observed at lower test frequencies in most cases.

#### 4.3 COMPACT TENSION TEST RESULTS

Compact tension tests for 7075-T7651 aluminum specimens were performed under Phase I of this program. These results, documented in Volume I [22] provide the data base needed to make crack growth predictions under Phase II.

A comprehensive evaluation of the  $da/dN$  versus  $\Delta K$  results from Volume I [22] is documented in Appendix B of this Volume (III). Objectives of this evaluation were to:

1. Study both the Paris and Forman crack growth models using the applicable  $da/dN$  versus  $\Delta K$  data and to provide appropriate results needed to implement the crack growth

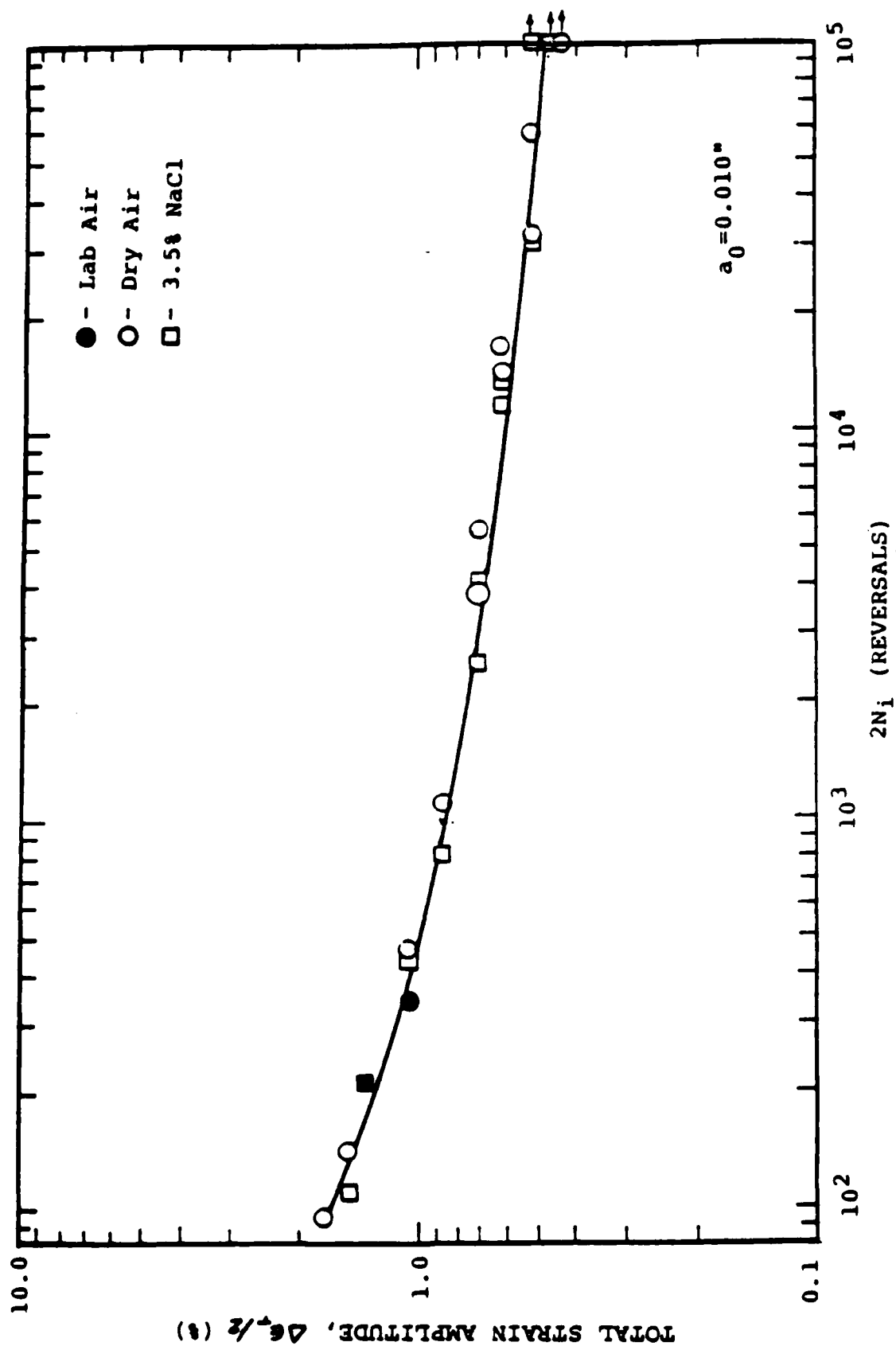


Fig. 13 Total Strain Amplitude Versus  $2N_i$  Reversals to Initiation for Beta-Annealed Ti-6Al-4V in Both Dry Air and 3.5% NaCl Environments

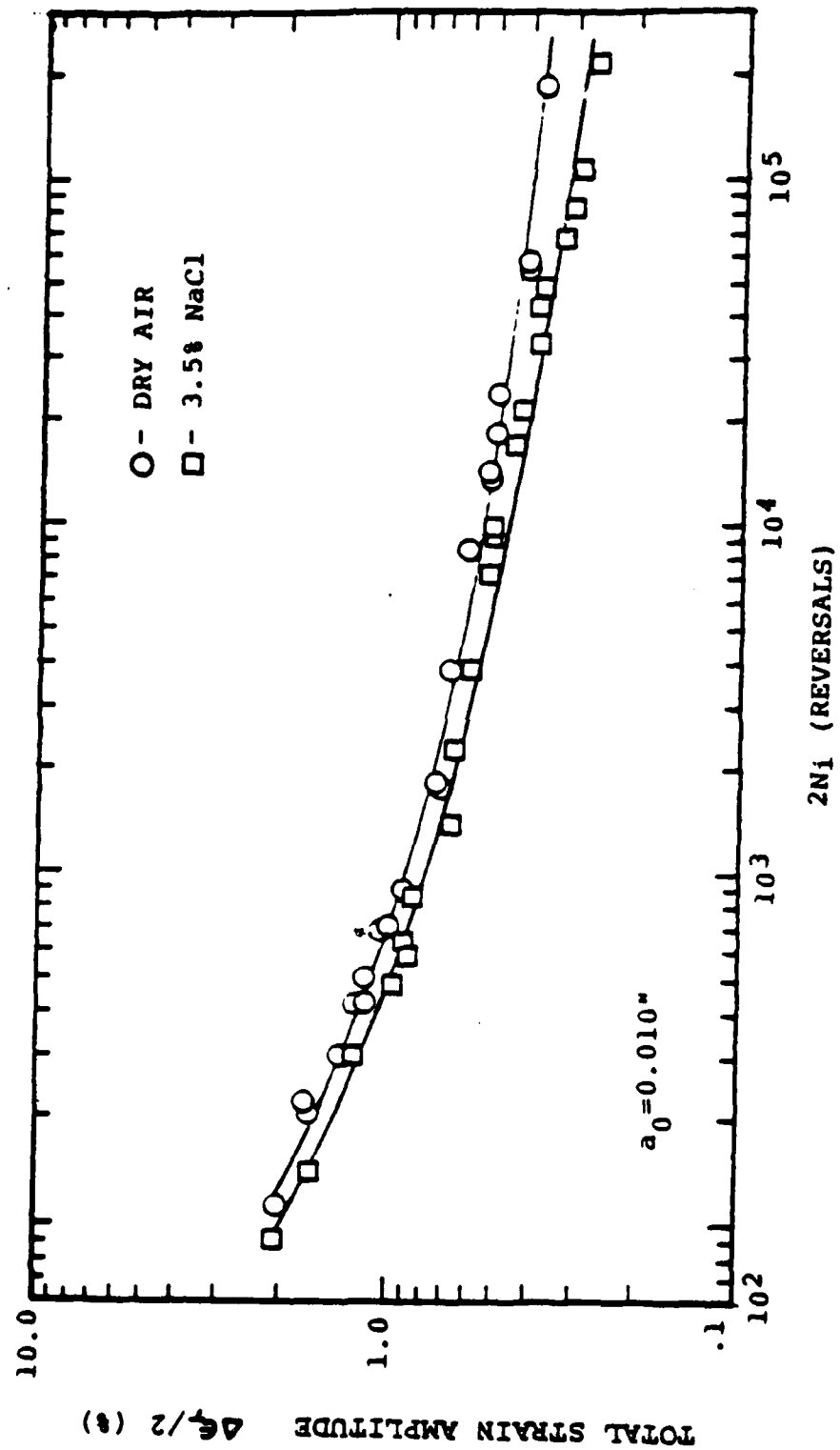


Fig. 12 Total Strain Amplitude Versus Reversals to Crack Initiation for 7075-T7651 Aluminum in Both Dry Air and 3.5% NaCl Environments

crack-initiation predictions for mechanically-fastened joints under Task 6.

Strain-controlled results for 7075-T7651 aluminum alloy are presented in Appendix A for dry air/lab air and for 3.5% NaCl environments, respectively. Detailed results are presented for: strain amplitude (total, elastic and plastic), area under the hysteresis loop, load frequency, and  $2N_i$  cycles to initiate a crack depth of 0.010" in Appendix A of Volume IV [24]. A plot of the total strain amplitude versus  $2N_i$  reversals to crack initiation ( $a_0 = 0.010"$ ) for 7075-T7651 aluminum is shown in Figure 12 for dry air and 3.5% NaCl environment. Accelerated fatigue crack initiation was observed in the 3.5% NaCl environment at both high and low strain amplitudes. Curves for both dry air and 3.5% NaCl have the same general shape. No appreciable effect of frequency on crack initiation was observed in this alloy. All of the data could be fitted to one general curve.

Strain-controlled results for beta-annealed Ti-6Al-4V are shown in Appendix B of Volume IV [24] for lab air, dry air, and 3.5% NaCl solution environments. Values of total strain amplitude, load frequency, and  $2N_i$  cycles to initiate a crack depth of 0.010" are given. The total strain amplitude versus  $2N_i$  reversals to crack initiation ( $a_0 = 0.010"$ ) is plotted in Fig. 13 for lab air, dry air, and 3.5% NaCl environments. Slightly accelerated fatigue crack initiation

S E C T I O N     I V

E V A L U A T I O N     O F     C O R R O S I O N  
F A T I G U E     T E S T     R E S U L T S

4.1 INTRODUCTION

Tasks 5 and 6 were concerned with acquiring an experimental data base and conducting Corrosion Fatigue Methodology Verification tests. Test results for 7075-T7651 aluminum for: strain-controlled specimens, and dog-bone specimens are presented in this section. A comprehensive evaluation of the 7075-T7651 aluminum test results is presented in Appendices A-D. The effects and significance of different test variables on TTCI, TTF, and crack propagation are also discussed.

Titanium (Beta-annealed Ti-6Al-4V alloy) strain-controlled specimen test results are presented in this section and further documented in Volume IV [24].

4.2 STRAIN CONTROLLED TEST RESULTS

Using the experimental procedures developed and evaluated under Task 4, the required strain-controlled data for Task 5 was obtained. The experimental data acquired under Task 5 provided the information needed to make time-to-

4. Obtaining Crack Growth Data - In order for fractographic data to be obtained from spectrum testing, distinguishable markings must be resolved on the fracture surfaces. For all three spectra used (Spectra "A", "B", and "C"), we were able to rely on fractographic readings to obtain both TTCI (time to obtain a crack 0.010 inch depth) and crack growth rate.

5. Initial Hole Quality - A sufficient number of fatigue tests (e.g., ten or more) should be performed to account for the initial quality variation of fastener holes on fatigue life. The initial hole quality variation is an important factor which influences the scatter in crack initiation test results for fastener holes [25, 26, 63, 76, 77]. To minimize these problems, fastener holes in this program were polished.

case, the maximum compression load in the three spectra considered was approximately 30% of the maximum positive load in the spectrum. If significantly larger compression loads are encountered, the present design might require lateral support or have to be redesigned to prevent specimen buckling in the fixture.

2. Environmental Chambers - The plexi-glas sealed chambers used for the no load transfer testing were fairly simple and caused no problems. The loading bar with the integral environmental chamber was found to insure the proper load transfer desired in the Task 6 tests.

3. Bolt-Load-Transfer Loading System - The bolt load transfer loading system shown in Fig. 7 worked very well for this program. Since this system introduces the load directly to the bolt, the actual percentage of bolt load transfer can be controlled. If the effects of the bolt load transfer on corrosion fatigue is to be investigated, the percentage of bolt load transfer should be carefully controlled. Reverse double dog-bone specimens have been previously used to simulate desired percentages of bolt load transfer and to acquire crack initiation data in fastener holes [25,26]. Such specimens are fine for simulating variable bolt load transfer conditions. However, the actual percentage of bolt load transfer can vary depending on the fastener type/fit and applied load level.

### 3.4.2 Acquisition of Crack Propagation Data

1. Specimen Design - Compact tension specimens used in these investigations have been in common use at General Dynamics Fort Worth Division. If possible, the specimen should be thick enough to assure plane strain conditions.

2. Environmental Chamber - The plexi-glass sealed chamber has been used extensively for environmental studies at the General Dynamics Fort Worth Division for several years. Such chambers have worked very well for environmental simulations.

3. Effects of Different Parameters on Crack Growth Rate - Normally the effects of environment, R-ratio, loading frequency, hold time, etc., on crack growth need to be investigated.

### 3.4.3 Spectrum Testing

1. Specimen Design - The dog-bone specimen design shown in Fig. 3 worked very well for the tests performed under this program. The same specimen geometry was used for open hole, bolt-in-hole (without load transfer) and bolt load transfer configurations. No specimen buckling problems were encountered with any of the three load spectra considered. In our

3.4.1 Acquisition of Strain Life Initiation Data

1. Specimen Design - Hourglass specimen were successfully used in this program considering both high and low strain amplitudes.

2. Environmental Chamber - Tygon tubing sealed to the specimen worked well. This tubing is inexpensive and easy to use.

3. Determination of Crack Initiation - The load shedding technique is fairly sensitive to detecting 0.010 inch deep fatigue crack. Whether material is cyclic softening, hardening or stable is important when using this technique.

4. Testing Reliability of Data - Whether test data is frequency dependent or not needs to be established in obtaining a strain-life curve. Strain amplitudes need to be selected in both the high and low strain amplitudes region where more than one specimen can be tested in order to determine experimental scatter.

5. Material Constants Needed - The material constants required in order to use strain-life data are listed in Appendix A.

### 3.4 CORROSION FATIGUE TESTING GUIDELINES

General guidelines are given in this section for acquiring statistically-valid corrosion fatigue data needed to implement the corrosion fatigue analysis methodology evaluated under this program. As such, the guidelines reflect the understandings reached under this program. Since further research is required to resolve some of the questions raised under this program, the following recommendations should be used in the context under which they were developed.

The number of test replications needed to acquire the data base for implementing the CF analysis methodology depends on several factors. For example, one should consider: (1) the desired confidence level, (2) whether-or-not the main interest is in the mean value, the extreme values or both, (3) whether-or-not the distribution of values is desired, (4) the complexity of the test conditions and how well the controlling factors are understood, (5) initial hole quality variations and specimen replications, and (6) the material to be used.

the bolt through the loading bar and environmental chamber was removed to make eddy current measurements.

The eddy current technique, described in Volume I [22] provided backup information on the TCI for the spectrum fatigue tests. This technique was used to complement the fractography - particularly for those tests when the 3.5% NaCl environment might affect the fatigue markings on the fracture surface.

#### 3.3.3.2 Fractography

Fractographic measurements were made on all coupons exposed to spectrum tests. Readings were made to as small a crack size as possible. In some cases, fractographic measurements could not be traced to the desired minimum crack size due to poor surface markings for the smaller crack sizes. Crack sizes versus time measurements and other pertinent details were recorded on fractographic data sheets. This included, in most cases, a photograph of the fracture surface, specimen dimensions, crack origins, peculiarities, number of load points at failure, etc. These fractographic data sheets are contained in the Vol. IV report, Appendices D, E and F.

ered: (1) F = fast (8000 flight hours/2 days), (2) S = slow (8000 flight hours/16 days), and (3) M = medium (8000 flight hours/8 days), and (4) s = extra slow (8000 flight hours/90 days).

### 3.3.2 Evaluation of Environmental Simulation Methods

Environmental chambers used for the dog-bone tests are shown in Figs. 6 and 8. Both dry air and 3.5% NaCl solution environments were used. Methods used in obtaining these conditions were identical to those used in the strain-controlled experiments.

### 3.3.3 Establishing Crack Growth Monitoring Methods

#### 3.3.3.1 Eddy Current Techniques

Eddy current measurements were periodically made in the center hole of the test specimen for all constant amplitude tests. Spot check measurements were also made during the spectrum fatigue tests to determine the time to initiate a crack size of 0.01" in the fastener hole. The eddy current probe was inserted directly into the fastener hole without disassembling the environmental chamber. For the no-load transfer tests the cork in the hole at the side of the environmental chamber was removed to make eddy current measurements. In the case of the bolt load transfer tests,

onmental simulation methods, and (3) verify crack growth measurement techniques for both constant amplitude and spectrum testing. Task 4 corrosion fatigue test results for dog-bone specimens are documented in Appendix D of Volume IV [24].

### 3.3.1 Test Procedures

Testing procedures established in Task IV included stress levels and test frequency. Maximum stress levels using Spectrum "A" (F-16 400 hr. block spectrum) varied from 28 ksi to 34 ksi. From these studies a maximum stress level of 28 ksi was selected for all spectrum tests conducted in Tasks 5 and 6. This stress level achieved crack initiation and time-to-failure in desired test time ranges.

The maximum positive load in spectrum "A" (F-16 400 hour block spectrum), 100% load level, was scaled to a test load that would produce the desired gross stress on the specimen cross section. All other loads, positive and negative, were "scaled" to the 100% load level.

Fatigue loading frequencies for spectrum "A" were selected such that the spectrum loads corresponding to 8000 equivalent flight hours could be applied to the respective tests specimen in a selected number of days (24 hours a day continuous testing). Four loading frequencies were consid-

Table 9 Constant Amplitude Stress-Controlled Test Results  
for Preconditioned Dog-Bone Specimens in Both Dry  
Air and 3.5% NaCl Environments (7075-T7651 Aluminum;  
R=0.05; Freq. = 6HZ; Open Hole)

SPECIMEN NO.	$\Delta\sigma$ (ksi)	$N_f$ (cycles)	$N_i$ (cycles)	ENVIRONMENT
200	16.5	92,827	70,000	Dry Air
204	15.0	85,720	52,000	Dry Air
202	14.0	99,389	70,000	Dry Air
199	14.0	38,202	25,000	3.5% NaCl
203	13.0	44,409	26,000	3.5% NaCl
205	12.0	167,539	95,000	3.5% NaCl
206	12.0	80,887	40,000	3.5% NaCl

Table 10 Constant Amplitude Stress-Controlled Test Results for Dog-Bone Specimens Tested for 20% LT and 40% LT in Both Dry Air and 3.5% NaCl Environments (7075-T7651 Aluminum)

ENVIRONMENT	SPECIMEN NUMBER	DATA SET NO.	$\Delta\sigma$ - (KSI)	PERCENT LOAD TRANSFER	NUMBER OF CYCLES TO INITIATION ( $a_o = 0.010"$ ) $N_i$	NUMBER OF CYCLES TO FAILURE $N_f$
Dry Air	401	63	23	20	17,000	22,623
	400	64	17	"	49,000	61,958
	402			"	48,000	58,715
	403			"	35,000	40,000
3.5% NaCl	407	66	17	40	41,000	53,059
	408			"	25,000	32,881
	404	65	17	20	41,000	44,766
	405			"	41,000	44,951
	406			"	20,000	22,000
	410	67	17	40	12,000	14,515
	412			"	18,000	21,888
	413			"	13,000	15,100

Table 11 Summary of Dog-Bone Specimen Spectrum  
Fatigue Test Results for Task 4 (7075-T7651  
Aluminum; F-16 400 Hour Spectrum)

SPECIMEN NO.	TEST I.D. (b)	DATA SET NO.	TEST DATE	SPECIMEN DETAILS				FATIGUE CRACK ORIGIN (f)	TTCI (FLT. HRS.) (g)	TTF (FLT. HRS.) (h)	TTF-TTCI (FLT. HRS.) (i)	TTCI/TTF
				WIDTH (IN.)	THICK (IN.)	HOLE DIA (IN.)	CROSS AREA (IN <sup>2</sup> )					
41	A-34/S/W	43	3-3-83	1.9980	.3000	.2502	.5994	B	4657	6640	1983	.70
42	A-34/S/D	41	3-22-83	1.9985	.2990	.4404	.5976		4207	8408	4201	.50
43	A-32/F/W	45	3-24-83	2.00	.3060	.4415	.6120		5147(a)	7606	2459	.68
47	A-30/F/D	47	6-6-83	2.0100	.3010	.4452	.6050		4777	12432	7655	.38
48(a)	A-30/F/D	47	6-10-83	2.0100	.3010	.4422	.6050		(e)	13680	-	-
49	A-32/S/D	44	5-12-83	2.0115	.3010	.4495	.6055		5441	9606	4165	.57
50	A-32/S/D	44	5-16-83	2.0090	.3010	.4426	.6047		2200	9635	7435	.23
51	A-32/S/D	44	5-19-83	2.0100	.3010	.4426	.6050		1000(c)	8835	7835	.11
52(a)	A-30/S/D	48	5-31-83	2.0115	.3020	.4452	.6075		6143	12035	5892	.51
53	A-34/F/W	42	5-6-83	2.0140	.3000	.4450	.6042		433	3235	2802	.13
54	A-30/F/W	49	6-7-83	2.0135	.3015	.4455	.6071		(e)	7606	-	-
55	A-30/F/W	49	6-8-83	2.0145	.3020	.4504	.6084		3067	6678	3611	.46
56	A-30/F/W	49	6-6-83	2.0110	.3005	.4500	.6043	C	(e)	6407	-	-
57	A-34/S/W	43	5-6-83	2.0120	.3000	.4460	.6036	B	133(d)	2348	2215	.06
58	A-34/S/W	43	5-6-83	2.0115	.3010	.4457	.6055		1200	3206	2006	.37
59	A-32/S/W	46	5-16-83	2.0110	.3010	.4475	.6053		3289	5235	1946	.63
60	A-32/S/W	46	5-11-83	2.0120	.3015	.4465	.6066		4037	6348	2311	.64
61	A-32/M/W	46	5-11-83	2.0120	.3010	.4470	.6056		2451	4835	2384	.51
64	A-30/20/F/W	54	6-21-83	2.0080	.3045	.4392	.6114		(e)	6759	-	-
65	A-30/20/S/W	50	6-29-83	2.0090	.3040	.4408	.6107		(e)	5946	-	-
111(a)	A-28/F/W/B/PC	52	10-14-83	2.002	.301	.4395	.6026	S	(e)	(a)	-	-
121(a)	A-28/F/W/B	51	10-6-83	2.002	.303	.4415	.6066	S	(e)	39120	-	-
129	A-28/S/W/B/PC	53	12-13-83	2.0065	.3025	.4415	.6069	B	6916	11864	4948	.58
143(a)	A-28/F/W/B/PC	52	12-14-83	2.0090	.3030	.4420	.6067	B	6750(d)	11600	4850	.58
144	A-28/S/W/B/PC	53	1-9-84	2.0095	.3030	.4440	.6088	B	10500	16800	6300	.62

Notes for Table 11

- (a) Testing anomaly
- (b) Ref. Table 8 for description code
- (c) Linear extrapolation from two smallest consecutive crack sizes from fractographic data sheet
- (d) Extrapolation based on power law (Eqs. 1 and 3)
- (e) Fractography not read for this specimen for various reasons (e.g., testing anomaly, not 28 ksi baseline stress surface crack away from hole).
- (f) Fatigue crack origins: B = bore of hole, C = corner of hole and S = surface crack away from hole.
- (g) Time to initiate crack depth of 0.010" in fastener hole (determined from fractographic results).
- (h) Time-to-failure
- (i) Time spent in crack growth

Table 12 Summary of Dog-Bone Specimen Spectrum Fatigue Test Results  
for Task 5 (7075-T7651 Aluminum)

SPECIMEN NO.	TEST I.D. (a)	DATA SET NO.	TEST DATE	SPECIMEN DETAILS				FATIGUE CRACK ORIGIN (b)	TTCI (FLT. HRS.) (c)	TTP (FLT. HRS.) (d)	TTP-TTCI (FLT. HRS.) (e)	TTCI/TTP
				WIDTH (IN.)	THICK (IN.)	HOLE DIA (IN.)	GROSS AREA (IN <sup>2</sup> )					
45	A-28/F/D	1	5-31-83	2.0170	.3010	.4412	.6071	B	14000	22000	8000	.64
46	A-28/F/D	1	6-5-83	2.0100	.3005	.4434	.6040	B	6600	16035	9435	.41
62	A-28/F/W	3	6-22-83	2.0110	.3025	.4380	.6083	B	5872	12035	6163	.49
67	A-28/S/W	4	7-1-83	2.012	.3050	.4427	.6137	C	7531(f)	14835	7304	.51
71	A-28/S/W	4	7-13-83	2.005	.3040	.4455	.6095	C	1600	7606	6006	.21
72	A-28/S/D	2	7-21-83	1.9980	.2915	.4440	.5824	B	8471	16435	7964	.52
76	A-28/F/W	3	7-5-83	1.9990	.3045	.4395	.6087	B	8000	13999	5999	.57
77	A-28/F/W	3	8-1-83	2.0105	.3030	.4395	.6092	B	16400	21949	5549	.75
79	A-28/F/D	1	8-11-83	2.0065	.3045	.4435	.6110	B	10600	17558	6958	.60
81	A-28/S/W	4	8-17-83	2.0095	.3025	.4395	.6079	B	3434	6749	3315	.51
82	A-28/F/W	3	8-18-83	2.0120	.3020	.4395	.6076	C	6700	12035	5335	.56
83	A-28/S/D	2	8-22-83	2.0030	.3030	.4395	.6069	B	25200	33677	8477	.75
84	A-28/W/W	5	9-12-83	2.002	.3020	.4440	.6046	B	8063(f)	10228	2165	.79
85	A-28/W/W	5	9-20-83	2.0025	.2880	.4430	.5767	B	8160(f)	10430	2270	.78
86	A-28/W/W	5	9-20-83	2.0085	.3010	.4443	.6045	B	8178(f)	12406	4228	.66
87	A-28/S/D	2	10-6-83	2.0005	.3025	.4410	.6052	B	16800	24835	8035	.68
88	A-28/S/W	4	11-8-83	2.000	.3010	.440	.6020	B	12554(f)	15074	2520	.83
89	A-28/F/D	1	11-3-83	2.006	.3045	---	.6108	B	21600	32806	11206	.66
90	A-28/S/W	4	11-3-83	2.013	.3040	---	.6119	C	15226(f)	21635	6409	.70
91	A-28/S/W	4	11-3-83	2.006	.303	---	.6078	B	9400	18276	8876	.51
92	A-28/S/D	2	12-5-83	2.009	.301	.4435	.6047	B	13249(f)	24279	11030	.54
101	A-28/20/F/W/PC	37	8-23-83	2.0065	.2990	.4380	.5999	B	3775	6007	2232	.63
102	A-28/F/W/PC	8	8-16-83	2.0065	.3010	.4370	.6039	C	1622	4835	3213	.34
103	A-28/F/D/PC	6	8-17-83	2.0090	.3025	.4395	.6077	C	10800	27235	16435	.40
104(h)	A-28/20/F/W/PC	37	8-24-81	2.0045	.2990	.4380	.5993	B	2812	5550	2738	.51
105	A-28/F/D/PC	6	8-24-81	2.0125	.3040	.4395	.6118	B	6651	20007	13356	.33
106	A-28/F/D/PC	6	8-24-83	2.0025	.3030	.4395	.6077	B	2800	10806	8006	.26
107	A-28/F/W/PC	8	8-25-83	2.0045	.3035	.4395	.6083	B	1600	6806	5206	.24
108	A-28/F/W/PC	8	8-26-83	2.0045	.3030	.4395	.6074	B	1097	4192	3095	.26

Table 12 Summary of Dog-Bone Specimen Spectrum Fatigue Test Results  
for Task 5 (7075-T7651 Aluminum) (Continued)

SPECIMEN NO.	TEST I.D. (a)	DATA SET NO.	TEST DATE	SPECIMEN DETAILS				FATIGUE CRACK ORIGIN (b)	TTC1 (FLT. HRS.) (c)	TTF (FLT. HRS.) (d)	TTF-TTC1 (FLT. HRS.) (e)	TTC1/TTF
				WIDTH (IN.)	THICK (IN.)	HOLE DIA (IN.)	GROSS AREA (IN <sup>2</sup> )					
109	A-28/S/D/PC	7	8-26-83	2.0055	.3030	.4395	.6076	C	28000	43596	15596	.64
110	A-28/S/D/PC	7	8-30-83	2.012	.3045	.4395	.6126	B	18400	31325	12925	.59
112	A-28/R/N/D/PC	14	10-28-83	2.003	.303	.4415	.6089	B	3120	9635	6515	.32
113	A-28/S/N/PC	9	9-2-83	2.002	.3045	.4400	.6096	B	875	2806	1931	.31
114	A-28/R/N/D/PC	14	10-31-83	2.004	.3015	.4390	.6042	B	2323(f)	10000	7677	.23
115	A-28/S/N/PC	9	9-12-83	2.0110	.3035	.4395	.6103	B	4440	7245	2805	.61
116	A-28/R/N/D/PC	14	10-31-83	2.0095	.3015	.4395	.6059	C	4549	10835	6286	.42
117	A-28/S/D/PC	7	12-9-83	2.0090	.3010	----	.6047	B	23600	32000	8400	.74
122	A-28/R/N/D	11	10-18-83	1.9983	.304	.4415	.6075	B	3200	16006	12806	.20
123	A-28/R/N/D	11	10-21-83	2.0090	.3040	.4410	.6107	B	13668	18902	5034	.73
124	A-28/R/N/D	11	10-25-83	2.0080	.3015	.4435	.6054	B	11600	16806	5206	.69
125	A-28/R/N/D	11	10-28-83	2.0030	.303	.4405	.6089	C	5777	10358	4581	.56
126	A-28/R/D/D	10	11-28-83	2.009	.304	.4435	.6099	B	23600	36035	12435	.65
127	A-28/R/D/D	10	11-18-83	2.00	.3005	.4415	.6010	B	14800	24748	9948	.60
128	A-28/R/D/D	10	11-29-83	2.0030	.3045	.4430	.6099	B	35600	42835	7235	.83
131	A-28/S/N/D	12	12-14-83	2.0035	.3045	.4420	.6100	C	8359(f)	14007	5648	.59
132	A-28/S/N/D	12	12-16-83	2.003	.3035	.4485	.6079	C	9300(g)	20435	11135	.46
140	A-28/R/D/D/PC	13	12-1-83	2.002	.3035	----	.6076	B	3857(g)	17440	13583	.22
141	A-28/R/D/D/PC	13	12-5-83	2.0115	.3010	.4415	.6055	B	9200	22000	12800	.42
142	A-28/R/D/D/PC	13	12-7-83	2.0035	.3010	.4415	.6031	B	12400	24400	12000	.51
300	B-28/R/N	23	2-1-84	2.0740	.3030	.4460	.6133	B	13002(f)	16646	3644	.78
301	B-28/R/N	23	2-1-84	2.0030	.3038	.4470	.6085	B	9077	12152	3075	.75
302	B-28/R/N	23	2-2-84	2.001	.3030	.4450	.6063	B	8267	11737	3470	.70
303	B-28/R/N	23	2-2-84	2.003	.302	.4415	.6049	B	17323(f)	21452	4129	.81
304	B-28/R/N/PC	27	2-1-84	2.0	.3025	.4400	.6050	B	7310(f)	10716	3406	.68
305	B-28/R/N/PC	27	2-1-84	2.0045	.3010	.4405	.6034	B	5548(f)	8163	2615	.68
306	B-28/R/N/PC	27	2-2-84	2.003	.3045	.4410	.6099	B	3141(f)	5916	2775	.53
307	B-28/R/N/PC	27	2-2-84	2.002	.302	.4435	.6046	B	6161(f)	9558	3197	.64
312	B-28/R/D/PC	25	2-2-84	2.0040	.2900	.4415	.5841	B	9650	15693	6043	.61
313	B-28/R/D/PC	25	2-3-84	2.0030	.3070	.4455	.6149	B	7176(f)	14916	7740	.48
314	B-28/R/D/PC	25	2-3-84	2.0065	.3030	.4435	.6079	B	4733	11493	6760	.41
315	B-28/R/D	21	2-6-84	2.0015	.2960	.4435	.5924	B	15752(f)	20853	5101	.76
316	B-28/R/D	21	2-6-84	2.0035	.3010	.4405	.6031	B	22608(f)	26595	3987	.85
317	B-28/R/D	21	2-6-84	2.0015	.2990	.4435	.5985	B	10824(f)	25053	14229	.43
318	B-28/S/N	24	2-6-84	2.0010	.3020	.4415	.6043	B	12038	14676	2638	.82
319	B-28/S/N	24	2-7-84	2.0010	.3050	.4435	.6103	B	6517	10707	4190	.61
320	B-28/S/N	24	2-7-84	1.9985	.3020	.4425	.6035	B	8447	11916	3469	.71
321	B-28/S/N	24	2-7-84	1.9995	.2980	.4435	.5959	B	7140	9975	2835	.72
322	B-28/S/N/PC	28	2-3-84	2.0045	.3030	.4405	.6074	B	6076	8358	2282	.73
323B	B-28/S/N/PC	28	2-24-84	2.0000	.3020	.4415	.6040	B	6097(f)	9451	3156	.64
324	B-28/S/N/PC	28	2-20-84	2.0000	.3035	.4425	.6070	B	2172	24969	1197	.87

Table 12 Summary of Dog-Bone Specimen Spectrum Fatigue Test Results  
for Task 5 (7075-T7651 Aluminum) (Continued)

SPECIMEN NO.	TEST I.D. (a)	DATA SET NO.	TEST DATE	SPECIMEN DETAILS				FATIGUE CRACK ORIGIN (b)	TTCI (FLT. HRS.) (c)	TTF (FLT. HRS.) (d)	TTF-TTCI (FLT. HRS.) (e)	TTCI/TTF
				WIDTH (IN.)	THICK (IN.)	HOLE DIA (IN.)	GROSS AREA (IN <sup>2</sup> )					
325	B-28/S/W/PC	28	2-14-84	2.0010	.3015	.4425	.6033	B	5368(f)	7863	2495	.68
326	B-28/S/D	22	2-13-84	2.0010	.3010	.4425	.6023	B	20143	22716	2573	.89
327	B-28/S/D	22	2-13-84	2.0015	.3010	.4415	.6025	B	21824	24516	2692	.89
328	B-28/S/D	22	2-13-84	2.0000	.3025	.4415	.6050	B	19800	22446	2646	.88
329	B-28/S/D/PC	26	2-21-84	2.0005	.3015	.4465	.6032	B	12797(f)	16116	3319	.79
330	B-28/S/D/PC	26	2-17-84	1.9990	.2950	.4470	.5897	B	15650	18753	3103	.83
331	B-28/S/D/PC	26	2-14-84	1.9990	.2990	.4430	.5977	B	12175(f)	15693	3518	.78
334	A-28/S/W/PC	9	3-1-84	2.0040	.3010	.4415	.6032	B	851	3200	2349	.27
337	A-28/S/W/PC	9	3-9-84	2.001	.3005	.4415	.6013	B	4456	5792	1336	.77
338	A-28/20/S/W/PC	38	3-15-84	1.9990	.2950	.4425	.5897	B	2000	3959	1959	.51
515	C-28/F/D	33	5-10-84	1.9955	.3050	.5030	.6086	B	27709	50100	22391	.55
516	C-28/F/D	33	5-16-84	2.0050	.2955	.5065	.5924	B	10789	31596	20807	.34
517	C-28/F/D	33	5-16-84	1.9935	.2970	.5050	.5920	B	40500(g)	64916	24416	.62
518	C-28/F/W	34	5-17-84	1.9955	.2960	.5030	.5906	C	15300	20400	5100	.75
519	C-28/F/W	34	5-18-84	2.0020	.2945	.5030	.5895	C	4500	19500	15000	.23
520	C-28/F/W	34	5-18-84	2.0045	.3010	.5050	.6033	B	11100	19200	8100	.58

Notes: (a) Ref. Table 8 for description code.

(b) Fatigue crack origins: B = bore of hole, C = corner of hole and S = surface crack away from hole.

(c) Time to initiate crack depth of 0.010" in fastener hole (determined from fractographic results).

(d) Time-to-Failure (TTF)

(e) Time spent in crack growth.

(f) Extrapolation based on power law

(g) Linear extrapolation.

(h) Testing anomaly

Table 13 Summary of Dog-Bone Specimen Fatigue Test  
Results for Task 6 (7075-T7651 Aluminum)

SPECIMEN NO.	TEST I.D. (a)	DATA SET NO.	TEST DATE	SPECIMEN DETAILS				FATIGUE CRACK ORIGIN (b)	TTCI (FLT. HRS.) (c)	TTF (FLT. HRS.) (d)	TTF-TTCI (FLT. HRS.) (e)	TTCI/TTF
				WIDTH (IN)	THICK (IN)	HOLE DIA (IN.)	CROSS AREA (IN <sup>2</sup> )					
66	A-28/20/F/W	16	6-30-83	2.0	.2975	.4444	.5950	B	3400	8904	5504	.38
68	A-28/20/F/W	16	7-6-83	2.0139	.3079	.4450	.6201	B	4508	7600	3092	.59
69	A-28/20/S/W	18	7-11-83	2.0800	.3040	.4450	.6323	B	1662	5607	3945	.29
70	A-28/20/S/W	18	7-11-83	2.0065	.3040	.447	.6099	B	3665	7068	3403	.52
73	A-28/20/S/W	17	7-20-83	2.0450	.3040	.4455	.6217	B	14100	24800	10700	.57
74	A-28/20/F/W	15	7-21-83	2.0350	.3030	.446	.6166	B	8800	18000	9200	.49
75	A-28/20/F/W	15	8-1-83	2.010	.3025	.4405	.6080	B	10203	20000	9797	.51
80	A-28/20/F/W	15	8-9-83	1.9995	.3035	.4410	.6068	B	16800	28000	11200	.600
308	B-28/20/F/D	30	2-6-84	2.0010	.3030	.4405	.6063	B	7228	11163	3935	.65
309	B-28/20/F/D	30	2-7-84	2.0035	.3010	.4415	.6031	B	8100	12037	3937	.67
310	B-28/20/F/D	30	2-8-84	1.9990	.3020	.4435	.6037	B	17115	21037	3922	.81
311	B-28/20/F/D	30	2-9-84	1.9995	.3020	.4435	.6039	B	8764	11916	3152	.74
332	B-28/20/F/D	29	2-17-84	2.0000	.3010	.4465	.6020	B	6343	11358	5015	.56
333	B-28/20/F/D	29	2-20-84	2.0005	.3030	.4415	.6062	B	11311(f)	14253	2942	.79
334	B-28/20/F/D	29	2-21-84	2.0000	.3020	.4430	.6040	B	6712	9258	2546	.72
335	B-28/20/F/D	29	2-23-84	2.0020	.3015	.4435	.6036	B	7799(f)	9858	2059	.79
500	B-28/40/F/D	31	5-2-84	2.0025	.3065	.4455	.6138	B	16800	19653	2853	.85
501	B-28/40/F/D	31	5-3-84	1.9995	.3020	.4460	.6039	B	21522	25236	3714	.85
502	B-28/40/F/D	31	5-3-84	2.0000	.3035	.4445	.6070	B	16064	19716	3652	.81
503	B-28/40/F/W	32	5-7-84	2.0010	.3020	.4435	.6043	B	6633	8916	2283	.74
504	B-28/40/F/W	32	5-7-84	2.0010	.3030	.4440	.6063	B	8218	11446	3228	.72
505	B-28/40/F/W	32	5-9-84	2.0000	.3030	.4435	.6060	B	5127	7836	2709	.65
506	A-28/40/F/D	19	4-16-84	2.0025	.3020	.4450	.6048	B	11736	24835	13099	.47
507	A-28/40/F/D	19	4-17-84	2.0030	.3020	.4450	.6049	B	16000	30006	14006	.53
508	A-28/40/F/D	19	4-23-84	2.0015	.3030	.4440	.6065	B	22218	36006	13788	.62
509	A-28/40/F/W	20	4-23-84	2.0010	.3015	.4450	.6033	B	6048	11206	5158	.54
510	A-28/40/F/W	20	4-25-84	2.0030	.3030	.4455	.6069	B	5149	8400	3251	.61
511	A-28/40/F/W	20	4-27-84	2.0015	.3000	.4455	.6005	B	6821	9635	2814	.71
521	C-28/40/F/D	35	5-10-84	2.0030	.3015	.4455	.6039	B	9591(f)	30600	21009	.31
522	C-28/40/F/D	35	5-10-84	2.0010	.3015	.4470	.6033	B	16200	33300	17100	.49
523	C-28/40/F/D	35	5-14-84	2.0020	.3020	.4465	.6046	B	21278	40200	18922	.53
524	C-28/F/W	36	5-14-84	2.0000	.2995	.5030	.5990	B	6900	13500	6600	.51
525	C-28/F/W	36	5-16-84	1.9965	.3005	.5030	.5999	B	6600	13800	7200	.48
526	C-28/F/W	36	5-17-84	2.0025	.3005	.5045	.6017	B	955(g)	9900	8945	.09

Notes For Table 13

- (a) Ref. Table 8 for description code
- (b) Fatigue Crack Origins: B = bore of hole, C = Corner of hole and S = surface crack away from hole
- (c) Time to initiate crack depth of 0.010" in fastener hole (determined from fractographic results)
- (d) Time-to-failure
- (e) Time spent in crack growth
- (f) Extrapolation based on power law
- (g) Linear extrapolation from two smallest consecutive crack sizes from fractographic data sheet
- (h) Diameter measurement not recorded

#### 4.4.1 Constant Amplitude Test Results

Constant amplitude test results for open hole dog bone specimens are shown in Table 9. Specimens were preconditioned as described in Section III and both dry air and 3.5% NaCl environments were considered. In Table 9, the number of cycles to initiate a crack depth of 0.010" ( $N_i$ ) and the number of cycles to failure ( $N_f$ ) are shown.

Twenty and 40% bolt load transfer specimen configurations (Ref. Fig. 3) were also fatigue tested using a constant amplitude loading. The amount of load transferred through the bolt is expressed as a percentage of the total applied load to the dog bone specimen. Test results are shown in Table 10 for both dry air and 3.5% NaCl environments.

#### 4.4.2 Spectrum Fatigue Test Results

Spectrum fatigue test results are shown in Table 11, 12 and 13 for Tasks 4, 5 and 6, respectively. Test results are evaluated in Appendices C and D and the effects of related test variables on TTCI, TTF and crack propagation are discussed in Section 4.5.

#### 4.5 EVALUATE EFFECTS OF TEST VARIABLES ON TTCI, TFCG AND TTF

The effects of key test variables on TTCI, TFCG and TTF for 7075-T7651 aluminum dog-bone specimens were evaluated in Appendices C and D. A summary of this evaluation is given below for seven (7) different test variables. These conclusions should be considered in the context of the test results acquired under the present program for 7075-T7651 aluminum.

1. Test Frequency - There was no significant influence of test frequency on TTCI, ( $a_0 = 0.01"$ ), TFCG or TTF attributable to the dry air or 3.5% NaCl environments for either load spectra "A" OR "B". These conclusions are based on tests results for dog-bone specimens with and without a bolt in the hole and small sample significance tests for differences in the mean. Three test frequencies were considered: (1) F = fast = 8000 flight hours/2 days, (2) S = slow = 8000 flight hours/16 days, and (3) s = extra slow = 8000 flight hours/90 days. The extra slow frequency (s) was considered only for the 3.5% NaCl environment.

2. Environment - The presence of a wet environment (3.5% NaCl solution) reduced TTCI, TFCG and TTF for all three load spectra (i.e., "A", "B" and "C"). The amount of reduction is consistent with the influence of environment on these

quantities under constant amplitude conditions. The dry/wet ratios for TTCI ( $a_0 = 0.01"$ ), TFCG and TTF lives indicate that the effects of environment on these quantities can be "scaled" for the 7075-T7651 aluminum alloy.

3. Load Spectra - The type and severity of the load spectra can have a significant effect on the TTCI, TFCG and TTF in mechanically-fastened joints. For example, the corrosion fatigue test results for the two block-type spectra (i.e., spectra "A" and "C") exhibited noticeable crack retardation behavior; whereas, the random-type spectrum (i.e., "B") had a much smaller effect on crack retardation. For ductile material, such as 7075-T7651 aluminum used in this program, fatigue cracks tend to close under compression loading. With crack closure the material doesn't recognize the presence of a crack. Current state-of-the-art load retardation models are inadequate for handling the effects of compressive loads on spectrum crack growth analyses for all load spectra. This issue remains and needs to be resolved. As far as the environment effect is concerned there is no additional enhancement in crack growth as a result of compressive loading cycles.

4. Bolt-In-Hole - A clearance-fit bolt in the fastener hole improved the crack initiation life (TTCI;  $a_0 = 0.01"$ ) for the dry air environment, and produced no net effect on TTCI for the wet environment (3.5% NaCl solution). There was no significant influence on the TFCG. The absence of a signi-

ficant influence on TCI in the wet environment is believed to result from the combined effects of the presence of the bolt (which improved life) and the environment (which reduced life). The latter effect may be further enhanced by galvanic action between the steel bolt and the aluminum specimen. The amount of hole restraint provided by the bolt in the hole varies depending on the fastener-hole clearances, the magnitude of the load applied to the specimen and the degree of bolt torque.

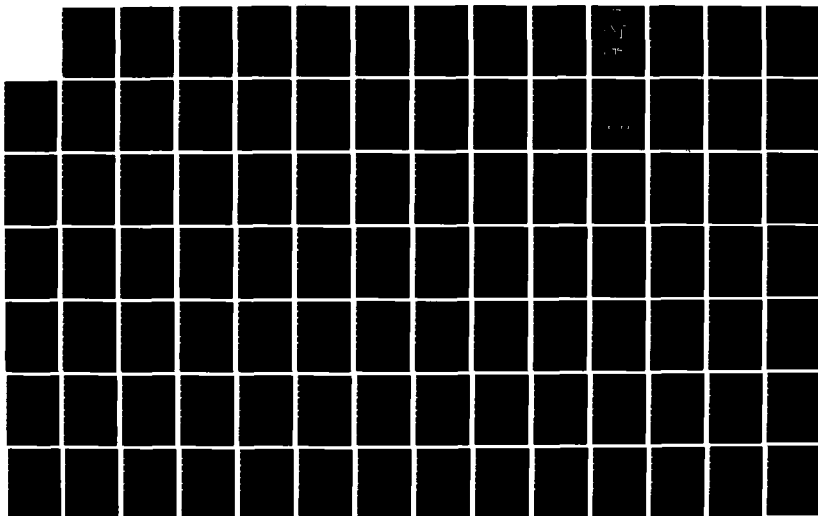
5. Bolt Load Transfer - Test specimens with 20% and 40% bolt load transfer typically had shorter fatigue lives than those with no load transfer for both spectra "A" and "B". Load transfer is one of several competing factors (e.g., fastener-hole clearance, surface residual stress variation in bore of hole, fretting, bolt torque, etc.) influencing the fatigue life of a mechanically fastened joint. Because the effects of such competing factors are buried in the test results, the individual contributions to fatigue life could not be properly resolved within the context of this program.

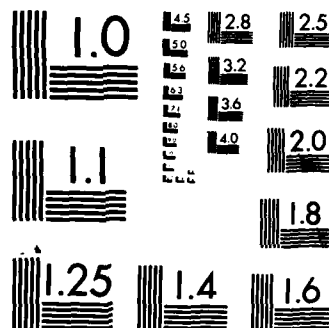
6. Preconditioning - Specimen preconditioning (i.e., exposure to the 3.5% NaCl environment for 72 hours following one 300 or 400 hour block of fatigue loading) significantly reduced the TCI ( $a_0 = 0.01"$ ) but it had a negligible effect on the crack propagation (TFCG). The deleterious effect is believed to result from surface damage produced by fatigue

assisted corrosion (e.g., pitting). The irregular nature of this damage is reflected in the considerable scatter in TTCI and the overall fatigue lives (TTF) of preconditioned specimens.

7. Stress Level - A limited number of corrosion fatigue tests were performed using different stress levels (i.e., 28, 30, 32 and 34 ksi) and spectrum "A" under Task 4 (Ref. Table 11) to establish a baseline stress level for Tasks 5 and 6 (i.e., 28 ksi). Bar graph plots for selected data sets are shown in Fig. C-16 of Appendix C. Based on these limited results, it is concluded that: (1) increasing the stress level reduces the fatigue life (TTF) and (2) there was no significant effect of loading frequency on the average TTF for applicable data sets with the same stress levels.

AD-A160 378 DEVELOPMENT OF FATIGUE AND CRACK PROPAGATION DESIGN AND 2/4  
ANALYSIS METHODOLOGY (U) GENERAL DYNAMICS FORT WORTH TX  
FORT WORTH DIV S D MANNING ET AL OCT 84  
UNCLASSIFIED NADC-83126-60-VOL-3 N62269-81-C-0268 F/G 11/6 NL





MICROCOPY RESOLUTION TEST CHART  
NATIONAL BUREAU OF STANDARDS-1963-A

## SECTION V

### CORROSION FATIGUE ANALYSIS METHODOLOGY FOR MECHANICALLY - FASTENED JOINTS AND EVALUATIONS

#### 5.1 INTRODUCTION

The purpose of this section is to: (1) describe a corrosion fatigue (CF) analysis methodology, rationale, and procedures for applications to mechanically - fastened joints, (2) describe recommended experimental test/data requirements and guidelines for implementing the methodology, (3) evaluate and discuss CF analysis predictions and correlations for 7075-T7651 aluminum and (4) discuss the applicability of the CF methodology to other aluminum alloys.

The "CF Methodology" includes the strain life approach [e.g., 28 - 51] for predicting crack initiation and the fracture mechanics approach [e.g., 93] for predicting crack propagation. Since these approaches and practices are documented elsewhere, only the essential features will be considered herein. References will be cited where further details are given. The recommended framework and guidelines for performing CF analysis and requisite tests will be emphasized. The "CF Analysis Methodology" is divided into modules or basic building blocks

(e.g., crack growth and load - interaction models) in the overall framework.

## 5.2 CORROSION FATIGUE ANALYSIS APPROACH AND RATIONALE

The CF analysis methodology described and discussed herein is recommended for 7000 series aluminum alloys in the over - aged condition. Special considerations are needed in applying this methodology for these alloys in the peak-aged condition. There are many aspects of the CF analysis methodology. One of the most important considerations is: there is no significant synergistic effect between the mechanical loading and the environment on CF crack initiation and CF crack propagation for 7000 series aluminum alloys in the over - aged condition. This conclusion has several important implications for the CF analysis methodology recommended herein. Both the mechanical-loading and the environment affect the crack initiation and crack growth rates of 7075-T7651 aluminum. Although they both contribute to the CF behaviour, each contribution can be treated separately. Thus, the effects of the environment on CF crack initiation and crack propagation can be "scaled" in the CF analysis. This means that the effects of the environment on crack initiation can be accounted for in the strain life allowables used in the strain life analysis. By the same token, the effects of the environment on crack propagation, can be accounted for in the  $da/dN$  versus  $\Delta K$

data used in the crack growth computer program [e.g., 66,67]. This greatly simplifies the CF analysis methodology because special models are not required for crack growth, load-interaction or bolt load transfer to account for the effects of environment on CF crack initiation and CF crack propagation.

There is no additional enhancement in crack growth due to the environment effect as a result of compression loading cycles. For a ductile aluminum alloy, such as we considered under this program (i.e., 7075-T7651), the fatigue crack tends to close under compressive loading. Because of this phenomena, there is uncertainty about handling the effects of compressive loads in spectrum crack growth analyses.

This program was not charged with developing new crack growth or load-interaction models for CF analysis applications. Several different models have been proposed and an appropriate model is required to implement the CF analysis methodology. Unfortunately, state-of-the-art load interaction models need to be further advanced to: (1) properly handle both tension and compression load cycles and (2) obtain a model applicable to different load spectra and ideally a model that can be calibrated using basic material data.

A conceptual description of the CF analysis approach is described in Fig. 14. The total corrosion fatigue life of mechanically fastened joints is divided into two parts: (1) time-to-crack-initiation(TTCI) and (2) time-for-crack-growth (TFCG). Each part is briefly discribed below and further details are given later. A general procedure is emphasized.

Essential elements of the approach for predicting corrosion fatigue crack initiation in fastener holes includes: (1) strain life approach [e.g., 28 -51], (2) strain-controlled tests for acquiring strain life crack initiation data for the baseline and selected environment, (3) dog-bone specimen tests for baseline geometry, environment, stress level and loading spectrum, (4) relationship for effective stress concentration factor versus TTCI based on the strain life analysis results for a given load spectrum and stress level, (5) determine a baseline effective stress concentration factor by calibrating the strain life analysis to dog bone specimen test results for a baseline geometry, environment, load spectrum and stress level, (6) modify the baseline effective stress concentration factor to account for the effects of hole geometry, & bolt load transfer and stress level, and (7) predict TTCI using the effective stress concentration factor versus TTCI relationship.

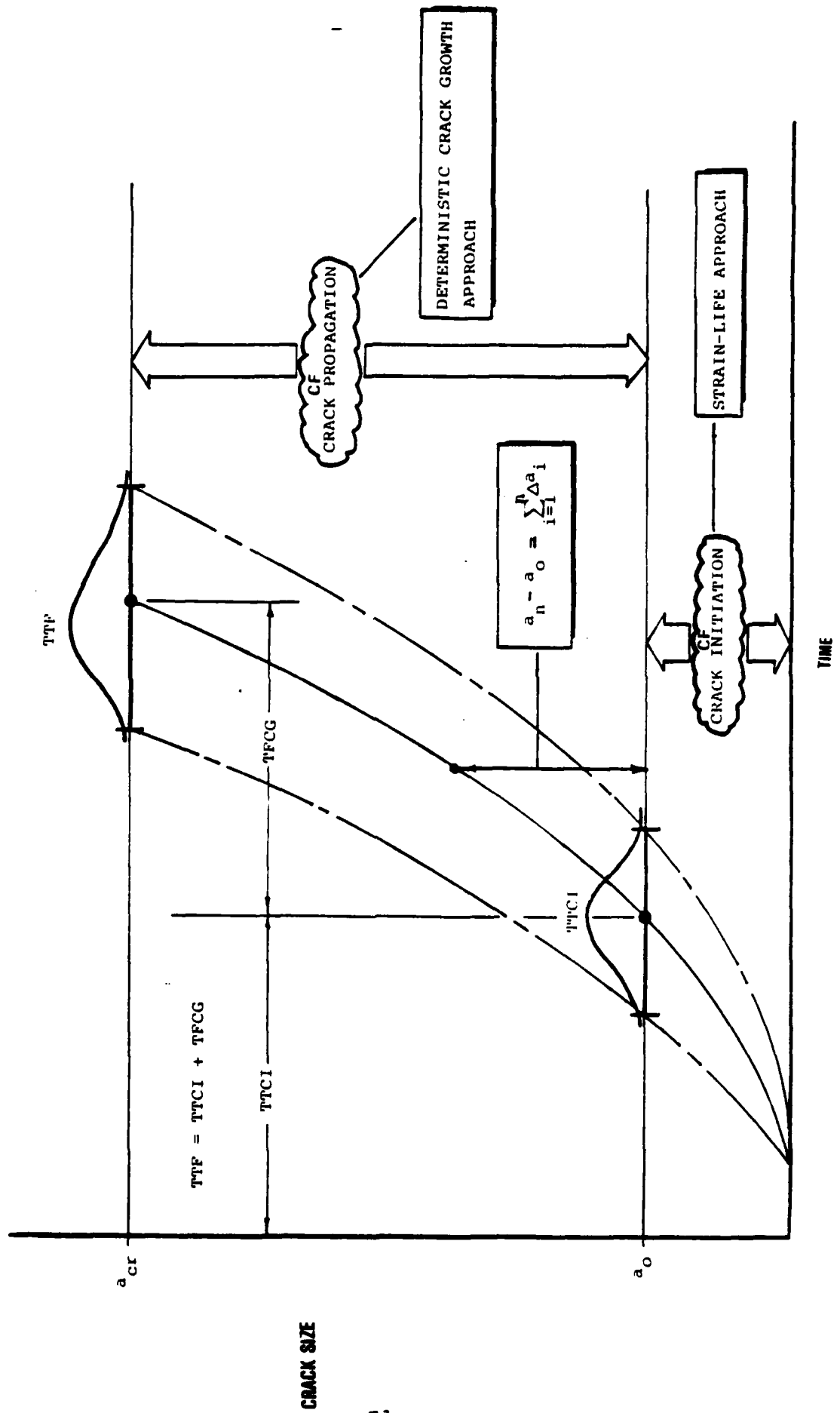


Fig. 14 Corrosion Fatigue Analysis Approach

Strain controlled tests for smooth, un-notched hour-glass specimens (e.g., Fig.1) for both dry air and 3.5% NaCl environments are performed to obtain strain life allowables.  $a_0$  is the reference crack size for TTCI and the initial flaw size for the CF crack propagation analysis. Hence, the  $a_0$  value selected should be large enough to justify using linear elastic fracture mechanics (LEFM) principles. A universally accepted limiting flaw size for LEFM has not been established. However,  $a_0 \geq 0.01"$  is considered reasonable.

Strain life allowable curves are developed based on average test results. Upper and lower bound strain life allowables can be estimated for selected probabilities (ref. Appendix A). Extreme value predictions for TTCI can be estimated using the strain life analysis and upper and lower bound allowables.

Results of the CF crack initiation analysis (i.e., TTCI) provide the starting point for the CF crack growth analysis (i.e., TFCG). The predicted time-to-failure (TTF) is equal to TTCI + TFCG. Predictions for TTCI, TFCG and TTF can be obtained for the average or estimated for selected probabilities.

Essential elements of the CF methodology for predicting the time-for-crack-growth (TFCG) are: (1) a suitable deterministic crack growth analysis computer program based on state-of-the-art

fracture mechanics principles [e.g., 66,67], (2)  $da/dN$  versus  $\Delta K$  data for the desired material for the baseline (e.g., dry air) and selected environment (e.g., 3.5% NaCl), (3) suitable crack growth and load-interaction models and spectrum load cycle counting scheme, and (4) means for accounting for the effects of % bolt load transfer in the crack growth analysis. Also, it is recommended that dog bone specimens with a preflawed center hole be fatigue tested under spectrum loading to acquire "baseline data" for calibrating the applicable load-interaction model parameters for a baseline environment (i.e., dry air), load spectrum and stress levels. Ideally, the load-interaction model parameters should be basic material properties which are independent of the environment, load spectrum, stress level, hole geometry, % bolt load transfer, etc.

### 5.3 CORROSION FATIGUE CRACK INITIATION METHODOLOGY

Essential elements of the CF crack initiation methodology are described in Fig. 15. Details of the methodology are documented in this section.

#### 5.3.1 General Procedure

The general procedure for implementing the CF crack initiation methodology is described and discussed below.

1. Use the strain life analysis computer program (BROSE) and applicable strain life materials data to make TICI ( $a_0 = 0.01"$ ) predictions for a given load spectrum. Do analysis for different assumed effective  $K_t$  values.

2. Determine suitable relationships for effective  $K_t$  as a function of TICI for both dry air and 3.5% NaCl environments using results from step 1. Such relationships can be determined graphically or empirically. A simple power law, such as Eq. 1, may be suitable.

$$\text{Effective } K_t = A(\text{TICI})^B \quad (1)$$

In Eq. 1, A and B are empirical constants. The effective  $K_t$  versus TICI can also be determined directly by plotting the results of the strain life analysis.

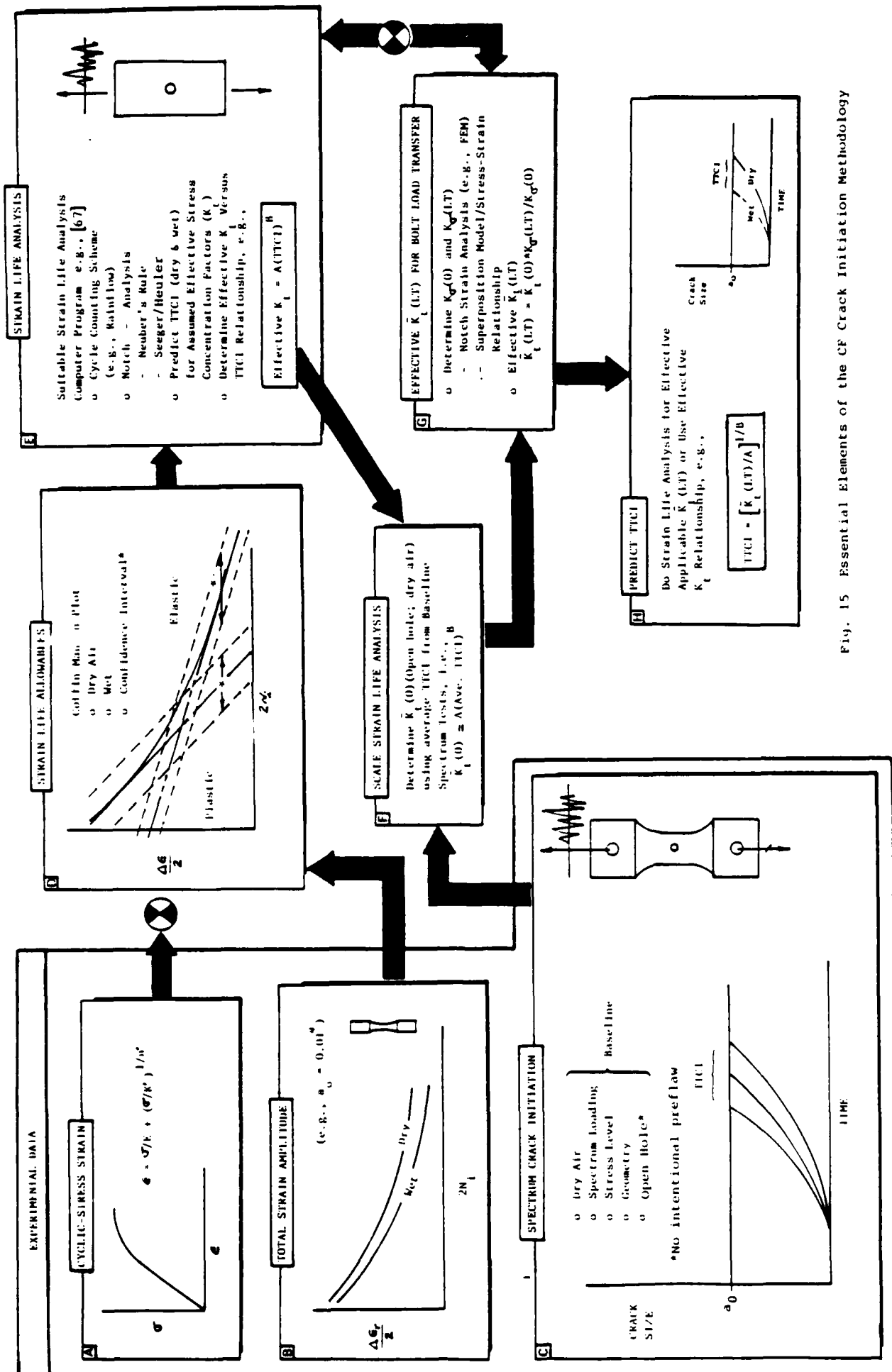


Fig. 15 Essential Elements of the CF Crack Initiation Methodology

3. Scale the strain life analysis in step 1 using dog-bone specimen tests results for the open hole configuration. This involves determining an effective  $K_t$ , denoted as  $\bar{K}_t(0)$ , by scaling the strain life analysis and average TTCI ( $a_0 = 0.01"$ ) test results for the open hole case.  $\bar{K}_t(0)$  is the baseline for making TTCI predictions for other design conditions (e.g., bolt load transfer, load spectra and stress level).

4. To account for the effects of bolt load transfer in the strain life analysis predictions for TTCI, the baseline effective  $\bar{K}_t(0)$  is modified using the applicable elastic or plastic stress concentration factor [74] for an open hole ( $K_\sigma(0)$ ) and for a hole with a given amount of bolt load transfer ( $K_\sigma(LT)$ ). A rigorous notch strain analysis can be performed to determine  $K_\sigma(0)$  and  $K_\sigma(LT)$  (e.g., finite element approach). A simple superposition model, based on the total maximum stress (elastic) at the edge of the hole and the applicable stress-strain relationship, was used in this report to estimate both  $K_\sigma(0)$  and  $K_\sigma(LT)$  values. Whatever method is used to determine  $K_\sigma(0)$  and  $K_\sigma(LT)$ , the effective  $K_t$  for a given bolt load transfer, denoted by  $\bar{K}_t(LT)$ , can be estimated using Eq. 2.

$$\text{Effective } \bar{K}_t(LT) = \bar{K}_t(0) * K_\sigma(LT)/K_\sigma(0) \quad (2)$$

5. TTCI predictions for different stress levels, % bolt load transfer and load spectra are obtained as follows.  $K_{\sigma}(0)$  and  $K_{\sigma}(LT)$  are determined for the applicable peak stress in the load spectrum. These results and  $\bar{K}_t(0)$  are used in Eq. 2 to estimate the effective  $\bar{K}_t(LT)$ . Finally, the TTCI prediction is obtained using the applicable effective  $\bar{K}_t(LT)$  and the strain life analysis program.

6. Once the  $\bar{K}_t(0)$  and  $\bar{K}_t(LT)$  values have been determined, the TTCI predictions for a given load spectra, % bolt load transfer and stress level can be determined in one of two ways: (1) Use the strain life analysis computer program and the applicable  $\bar{K}_t(0)$  and  $\bar{K}_t(LT)$  values to predict TTCI directly, or (2) use the effective  $K_t$  relationship (e.g., Eq. 1 where  $\bar{K}_t(0)$  or  $\bar{K}_t(LT)$  equals  $K_t$ ) based on the strain life analysis results for different assumed  $K_t$  values to predict TTCI values.

### 5.3.2 Strain Life Analysis

A strain life analysis computer program is needed to implement the strain life approach [e.g., 28-51]. Strain life allowables (dry and wet) for a given crack initiation reference crack size ( $a_0$ ) are developed from total strain amplitude versus  $2N_f$  plots (Ref. Fig. 15; Frame B and D). A cycle counting method (e.g., rainflow) is needed to transform a random spectrum into fatigue-equivalent constant amplitude load

cycles. The cumulative damage is determined using a notch strain analysis (e.g., Neuber's rule, Seeger/Heuler), the equivalent constant amplitude load cycles and the applicable strain life allowables for a given  $a_0$ . The predicted time-to-crack-initiation (TTCI) is determined from the cumulative damage.

A computer program has been developed for implementing the strain life analysis described above. This program, referred to as "BROSE", is briefly described in Appendix E and details are given in Ref. 45.

The procedures for determining the cyclic stress-strain relationship and the strain life allowables (i.e., Coffin-Manson plots) are described and illustrated in Appendix A.

Strain life analysis details, including results for TTCI predictions, and typical computer output from Program "BROSE" are given in Appendix F.

### 5.3.3 Effective $K_t$ Versus TTCI Relationship

An effective  $K_t$  versus TTCI relationship for a given load spectrum and maximum stress level provides a convenient means for "scaling" the strain life analysis using dog bone specimen test results. A relationship between the effective stress concentration factor,  $K_t$ , at the edge of a fastener

data (dry air) for replicate dog bone specimens with a preflawed center hole may not be available to tune the crack growth analysis. In this case the following options are reasonable:

- (1) tune the load interaction model parameters using spectrum crack propagation data (dry air) based on replicate dog-bone specimens with no intentional preflaw in the center hole (i.e., Normalize the crack propagation results to the same initial flaw size) or
- (2) use available or suitable retardation model parameters in the CF crack growth analysis. Use  $da/dN$  versus  $\Delta K$  data for the applicable environment and a suitable crack growth model which accounts for the effect of R-ratio.

#### 5.4.2 Crack Growth Analysis Program

A general purpose analytical crack growth computer program is needed to implement the CF crack propagation methodology for mechanically-fastened joints. Essential features of the required computer program are described in step 4 of Section 5.4.1 and in Fig. 18, Frame C.

5. Acquire spectrum crack growth data using replicate dog-bone specimens with an open center hole (ref. Fig. 18, Frame B). Each hole in the test specimen should have a preflawed corner crack on one side of the hole (e.g.,  $a_0 = 0.01$ "). Tests should be performed using a baseline geometry, environment (e.g., dry air), loading spectrum, and stress level. The main purpose of these tests is to acquire spectrum crack growth data that can be used to "tune on scale" the crack growth analysis. Tuning is a practical way to calibrate the load-interaction model parameters until general-purpose mechanistic-based models have been developed which apply to any load spectrum.

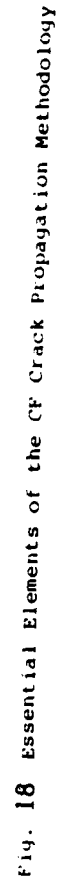
6. Tune or scale the crack growth analysis or load-interaction model using the spectrum crack growth data (ref. Fig. 18, Frame B). Suitable load-interaction model parameters can be determined for a baseline geometry (open hole), environment (dry air), load spectrum and stress level using a trail and error procedure. A suitable analytical crack growth program (e.g., "RXN", Ref. 67) is used to match the average crack growth test results for dog-bone specimens.

7. Make CF crack growth predictions for selected geometry, stress level, load spectrum, environment and % bolt load transfer using the calibrated load-interaction model parameters determined in step 6 for the baseline case (i.e.g open hold, dry air, corner flaw). Spectrum crack propagation

3. Select a suitable load-interaction model to use. Principal yield-zone and crack closure models are listed in Fig. 18, Frame C and details for each model are given elsewhere [96 - 114]. Whatever load-interaction model is used, it should account for the effects of tension and compression loads, and load sequence, on crack growth. Ideally, the calibrated model should apply to any load spectra, geometry, stress level or bolt load transfer and should be independent of the environment. There is no additional enhancement in crack growth due to the environment effect as a result of compression loading cycles for the 7075-T7651 aluminum alloy considered under this program.

4. Select an analytical crack growth computer program for performing the crack growth predictions. The general-purpose program should incorporate the following feature and options:

- (1) Crack growth model(s) which account for R-ratio,
- (2) Cycle counting methods,
- (3) load-interaction model,
- (4) stress intensity factor which accounts for different flaw shapes/geometries and bolt load transfers,
- (5) a procedure that accounts for part-through crack growth, through-the-thickness crack growth and crack growth transition, and
- (6) a damage accumulation procedure.



#### 5.4 CORROSION FATIGUE CRACK PROPOGATION METHODOLOGY

Essential elements of the corrosion fatigue (CF) crack propogation methodology are given in Fig.18. Further details are given in this section.

##### 5.4.1 General Procedure

The general procedure for making CF crack propogation predictions is described and discussed below.

1. Acquire suitable  $da/dN$  versus  $\Delta K$  data (ref. Fig.18 , Frame A) using either compact-tension (CT) or center-cracked-tension (CCT) in dry air and applicable environment (c.g., 3.5% NaCl solution). Test requirements and procedures are described in Section 5.5.2 and elsewhere [24,80].

2. Select a crack growth model for the CF crack growth analysis which accounts for the effects of R-ratio [e.g., 87,90,91]. Best fit the selected model parameters using the  $da/dN$  versus  $\Delta K$  data for both dry air and applicable environment (e.g., 3.5% NaCl). Justify using the calibrated crack growth model for a range of R-ratios covered by the applicable loading spectrum.

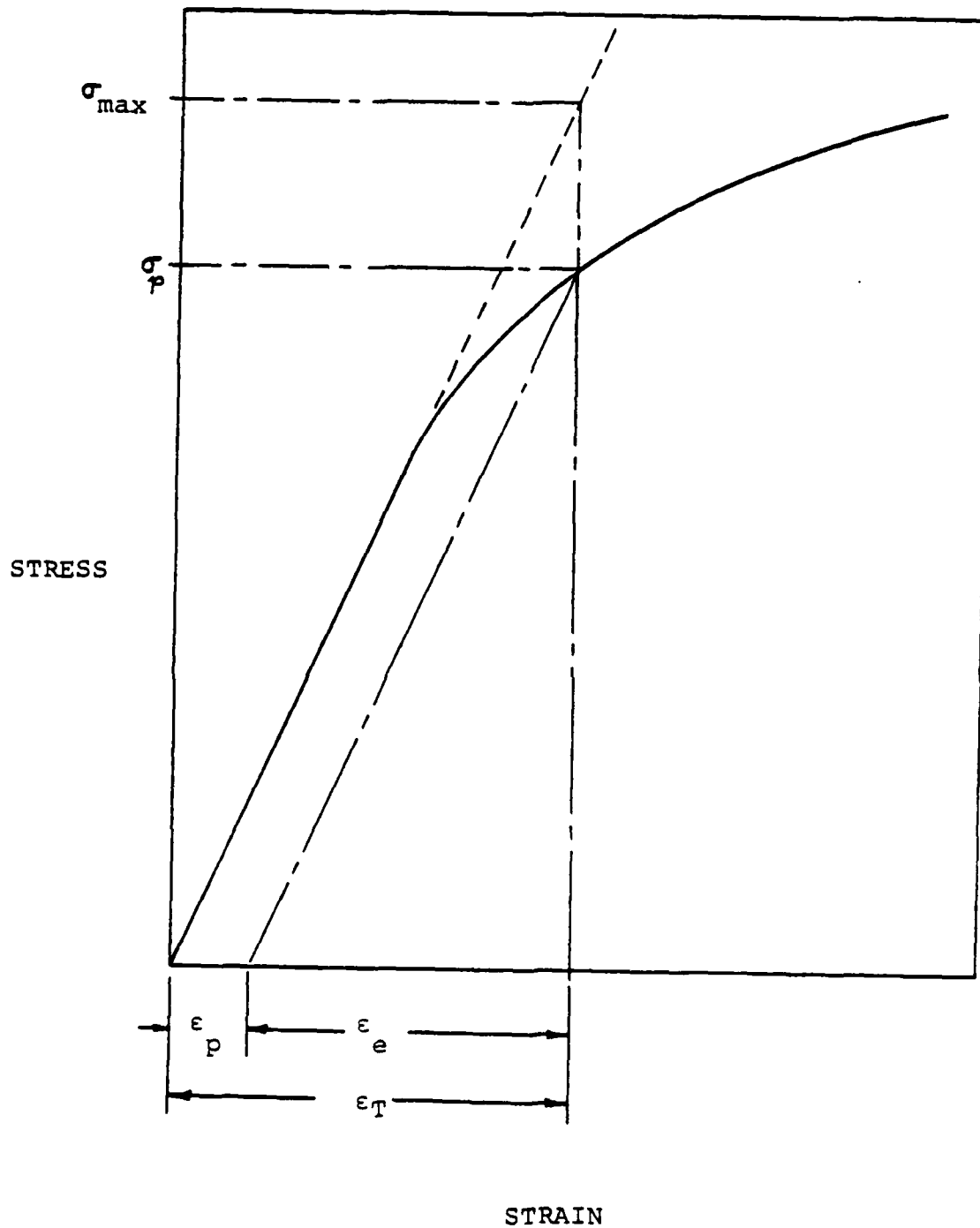


Fig. 17 Concept of Determining Notch Stress Due to Maximum Linear Stress at Edge of Hole Based on Stress Strain Relationship

3. Use the stress-strain curve or applicable relationship, such as Eq. 12, to determine the plastic stress corresponding to the total strain  $\epsilon_T$  (see Fig. 17). In Eq. 13,  $\epsilon$  = total strain,  $\sigma$  = stress level,  $E$  = elastic modulus of elasticity,  $n'$  = cyclic strain hardening exponent and  $K'$  = cyclic strength coefficient. The plastic stress,  $\sigma_p$ , corresponding to the total strain,  $\epsilon_T$ , can be estimated by setting the right hand side of Eq. 13 equal to  $\epsilon_T$  (Eq. 12) and solving for  $\sigma$  by trial and error.

$$\epsilon = \sigma/E + (\sigma/K')^{1/n'} \quad (13)$$

$$= K_{\sigma}(LT = 0)).$$

There are different ways to determine  $K_{\sigma}(0)$  and  $K_{\sigma}(LT)$  in Eq. 11. For example, a detailed notch strain analysis could be performed using the finite element approach. The following procedure is suggested for estimating  $K_{\sigma}(0)$  and  $K_{\sigma}(LT)$  for corrosion fatigue crack initiation analysis. Once  $\bar{K}_t(LT)$  has been determined, TTCI predictions can then be made for particular point conditions using the strain life analysis results.

$\sigma_{\max} < \text{Elastic Limit of Material}$

If the maximum stress at the edge of the hole is elastic, then  $K_{\sigma}(0) = K_t$  (see Eq. 4) and  $K_{\sigma}(LT) = K_T$  (see Eq. 9).

$\sigma_{\max} > \text{Elastic Limit of Material}$

1. Compute the maximum elastic stress at the edge of the hole,  $\sigma_{\max}$ , based on the maximum stress in the loading spectrum and Eq. 10.

2. Compute the total strain,  $\epsilon_T$ , based on  $\sigma_{\max}$  and Eq. 12, where  $E$  = elastic modulus of elasticity.

$$\epsilon_T = \sigma_{\max}/E \quad (12)$$

$$K_T = \left\{ \frac{3(1 - LT)}{(1 - d/W)} + [1 + (d/W)^2](LT)(W/d) \right\} ; (LT \leq 1) \quad (9)$$

$$\sigma_{\max} = K_T \sigma_{\text{Net}} \quad (10)$$

#### 5.3.5.2 Modification of Strain Life Analysis Scaling Factor for Effect of Bolt Load Transfer

In the corrosion fatigue crack initiation analysis, the effects of bolt load transfer are accounted for by modifying the strain life analysis scaling factor for the open hole case (denoted by  $\bar{K}_t(0)$ ). It is assumed that the baseline scaling factor  $\bar{K}_t(0)$  for the open hole case can be ratioed up using Eq. 11 to obtain the scaling factor for the desired amount of bolt load transfer, denoted by  $\bar{K}_t(LT)$ . In Eq. 11,  $K_\sigma(0)$  and  $K_\sigma(LT)$

$$\bar{K}_t(LT) = \bar{K}_t(0) \frac{K_\sigma(LT)}{K_\sigma(0)} \quad (11)$$

are the stress concentration factors for the open hole case and the bolt load transfer case, respectively. (Note:  $K_\sigma(0)$

The bolt bearing load,  $P_b$ , depends on the degree of load transfer and it is determined from the input gross stress,  $\sigma_I$ , as follows. In Eq. 6,

$$P_b = (LT) \underbrace{\sigma_I}_{P_I} Wt = (LT) Wt(1 - d/W) \sigma_{Net}; 0 \leq LT \leq 1.0 \quad (6)$$

$LT = P_b/P_I$ ,  $W$  = plate width,  $t$  = plate thickness and  $P_I$  = total input load to joint. The average bolt bearing stress,  $\sigma_{brg}$ , is determined using Eq. 6 and Eq. 7.

$$\sigma_{brg} = P_b/dt = (LT)(W/d)(1 - d/W) \sigma_{Net} \quad (7)$$

Equation 8 for the net section through stress, denoted as  $\sigma_{Net_T}$ , can be determined from equilibrium considerations,

$$\sigma_{Net_T} = \frac{\sigma_I Wt - P_b}{Wt(1 - d/W)} = (1 - LT) \sigma_{Net} \quad (8)$$

The following expression for the geometric stress concentration factor, denoted by  $K_T$ , can be obtained by substituting Eqs. 4, 5, 7 and 8 into Eq. 3 and simplifying. Equation 9 expresses  $K_T$  as a function of the geometry and the amount of bolt load transfer (i.e.,  $LT = 1.0$ ). Hence, the total maximum elastic stress at the edge of a fastener hole, given by Eq. 10, can be estimated using Eq. 9 and the applicable net section stress.

fastener hole (Fig. 16(a)) can be estimated considering the contribution of the through stress (Fig. 16(b)) and the bolt bearing stress (Fig. 16(c)) on  $\sigma_{\max}$  separately.

The general equation for the geometric stress concentration factor, for  $K_t$ , is given by Eq. 3, where:  $\sigma_{\text{net}}$  = net section stress based on

$$K_T = (1/\sigma_{\text{net}})(K_t \sigma_{\text{net}} + K_b \sigma_{\text{brg}}) \quad (3)$$

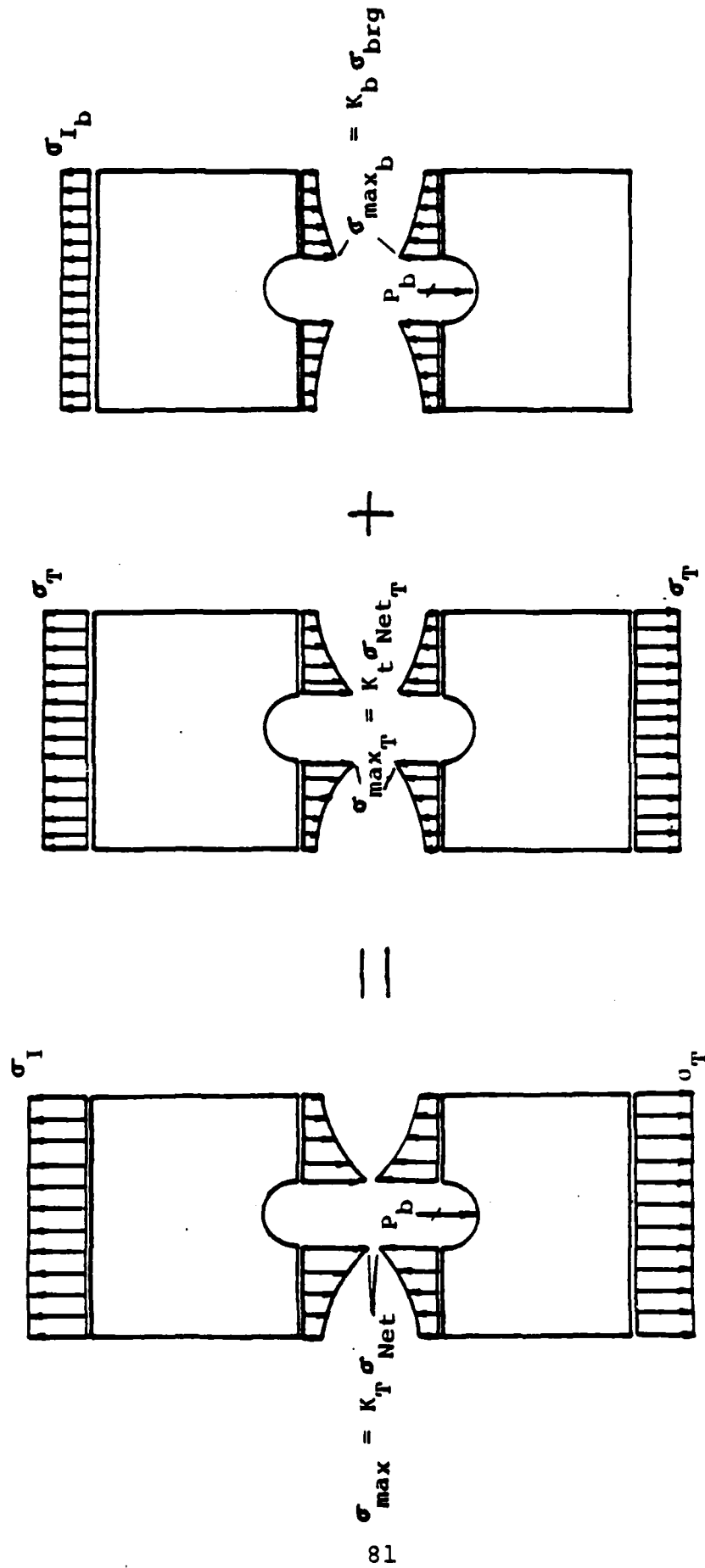
the far field total gross stress,  $K_t$  = geometric stress concentration factor for an open hole,  $\sigma_{\text{net}_T}$  = net section stress due to the through stress,  $K_b$  = stress concentration factor due to bearing and  $\sigma_{\text{brg}}$  = bolt bearing stress. Heywood's approximation [61] for the stress concentration factor ( $K_t$ ) for an open hole is given in Eq. 4.

$$K_t = \sigma_{\max}/\sigma_{\text{net}} = 3/(1 + d/W); (d/W \leq 0.3) \quad (4)$$

where:  $d$  = hole diameter and  $W$  = plate width. Barrios [61] has developed an approximate relationship, Eq. 4, for the bearing stress concentration factor ( $K_b$ ) based on results from Theocaris [57].

$$K_b = [1 + (d/W)^2]/(1 - d/W) \quad (5)$$

In Eq. 5,  $d$  and  $W$  have the same meaning as given in Eq. 4.



- (a) Combined Effect of through Stress and Bolt Bearing on  $\sigma_{\text{max}}$  at Edge of Hole
- (b) Effect of through Stress on  $\sigma_{\text{max}_T}$  at Edge of Hole
- (c) Effect of Bolt Bearing on  $\sigma_{\text{max}_b}$  at Edge Hole

Fig. 16 Superposition Model for Estimating Geometric Stress Concentration Factor ( $K_T$ )

### 5.3.5 Accounting for Bolt Load Transfer

A reasonable method is described in this section for accounting for the effects of bolt load transfer on corrosion fatigue crack initiation predictions. The method includes: (1) a superposition model for estimating the total maximum elastic stress at the edge of a fastener hole due to the through stress and the bearing stress, (2) a technique for estimating the elastic or plastic stress concentration factor for an open hole ( $K_{\sigma}(0)$ ) and for a hole with a given amount of bolt load transfer ( $K_{\sigma}(LT)$ ) based on the stress-strain relationship, and (3) a means for scaling the baseline effective  $\bar{K}_t(0)$  for an open hole to the desired % bolt load transfer level.

The method described in this section is illustrated in Appendix F.

#### 5.3.5.1 Superposition Model for Estimating $\sigma_{\max}$ at Edge of Hole

A simple superposition model is proposed for estimating the total maximum elastic stress at the edge of the fastener hole. This idea has been used before by other researchers [e.g., 57,61] to estimate  $K_t$ . The proposed superposition model is shown in Fig. 16. The basic idea of the model is that the total maximum elastic stress,  $\sigma_{\max}$ , at the edge of a

hole and TTCI can be determined using the strain life analysis computer program as follows. Assume different  $K_t$  values to cover the possible range of values expected for the particular geometry (e.g.,  $K_t = 1.5, 2.0, 2.5, 3.0, 3.5, 4.0, \dots$ ). Using the strain life analysis program, determine the TTCIs corresponding to a given  $K_t$ . A relationship can then be established for the effective  $K_t$  in terms of TTCI - either empirically or graphically. For example, the simple power law of Eq. 1 has been successfully used in this program and it is promising for future applications. The constants A and B in Eq. 1 can be determined using a linear least squares fit form of Eq. 1 and using the predicted TTCIs for given  $K_t$ s as input.

#### 5.3.4 Baseline Effective $\bar{K}_t(0)$

An effective stress concentration factor for the open hole (dry air environment case), denoted as  $\bar{K}_t(0)$ , can be used to make predictions for other geometries, environments, % bolt load transfer, load spectrum and stress level. This factor can be determined using the effective  $K_t$  versus TTCI relationship and the average test results for dog-bone specimen tests (see Fig. 15, Frame C). The procedures for determining  $\bar{K}_t(0)$  are further described and illustrated in Appendix F.

Various analytical crack growth computer programs have been developed [e.g., 67]. The General Dynamics/Fort Worth Division has developed a state-of-the-art analytical crack growth computer program, referred to as "RXN" [66,67]. This program can be used to implement the recommended CF crack propagation methodology proposed. Other computer programs could also be used. Essential details and features of the "RXN" computer program are described in Appendix G and further details are given elsewhere [66,67].

#### 5.4.3 Crack Growth Model

A suitable crack growth model is needed to define  $da/dN$  versus  $\Delta K$  for a given environment (e.g., dry air and 3.5% NaCl) for any given spectrum. Since it would be impractical to acquire  $da/dN$  versus  $\Delta K$  data for every possible R-ratio in the load spectrum, a crack growth model is needed. Several crack growth models have been proposed [e.g., 85-91]. The following features of a crack growth model are needed to implement the CF crack propagation analysis:

- (1) accounts for R-ratio,
- (2) accounts for the effects of  $\Delta K$  extremes on  $da/dN$  (i.e.,  $\Delta K$  threshold below which  $da/dN = 0$  and  $\Delta K = K_c$  where  $da/dN = \infty$  (failure)), and

- (3) models reasonably well  $da/dN$  versus  $\Delta K$  over the  $\Delta K$  and R-ratio ranges of most interest for the corrosion fatigue crack growth analysis.

Procedures are described and discussed in Appendix B, including a data pooling method, for determining crack growth model parameters from experimental  $da/dN$  versus  $\Delta K$  data. The procedures for calibrating the crack growth model parameters for the Forman model [87] are illustrated in Appendix B. Goodness-of-fit plots are shown for  $da/dN$  versus  $\Delta K$  for both dry air and 3.5% NaCl environment for two different R-ratios (i.e.,  $R = 0.05$  and  $0.3$ ).

#### 5.4.4 Load-Interaction Model

A load-interaction or retardation model is needed to account for the effects of tension and compression loads, multiple overloads, load sequence and number of load cycles in the loading spectrum on crack propagation. Several retardation models have been proposed [96-113]. These models can be divided into two groups: (1) yield zone models and (2) crack closure models. Saff [114] has recently reviewed the capabilities and limitations of the yield zone and the crack closure models.

Since the effects of the environment on CF crack propagation can be "scaled" for the 7000 series alloys in the

over-aged condition, it is not necessary for the retardation model to account for the effects of the environment. The effect of the environment on CF crack propagation in fastener holes is accounted for in the  $da/dN$  versus  $\Delta K$  basic data used in the CF crack growth analysis.

There is no significant synergistic effect between the frequency of the mechanical loading and the environment for the 7000 series alloy in the over-aged condition. Moreover, the environment produces no additional enhancement in crack growth as a result of the compressive loading cycles.

None of the existing retardation models can adequately handle the effects of multiple overloads, compression loads, loading sequence and any number of load cycles on spectrum crack propagation. Ideally, the retardation model should apply to any load spectra and the model parameters should be definable using basic data.

Advanced retardation models are needed which apply to any load spectrum. Until such models are developed and proven, it is recommended that replicate dog-bone specimens (a minimum of 3 specimens) be spectrum fatigue tested to acquire baseline crack propagation data for the dry air, open hole case. These data can then be used to calibrate the retardation model parameters and to justify the use of the retardation model for

different fastener hold geometries, stress levels, % bolt load transfer and load spectra.

The following retardation model philosophy is recommended. First, calibrate the applicable retardation model parameters for the open hole configuration using baseline spectrum crack growth data for a dry air environment and a selected maximum stress level. Then use the resulting retardation model parameters to make CF crack propagation predictions for other geometries, environments (e.g., 3.5% NaCl), % bolt load transfers and stress levels.

In any case, improved retardation models are needed. However, this is a separate problem from the CF crack propagation methodology.

#### 5.4.5 Cycle Counting

A suitable cycle counting method is needed for transforming the load spectrum into equivalent load cycles. This step is essential to make the constant amplitude  $da/dN$  versus  $\Delta K$  data apply to CF crack propagation predictions for a given environment and load spectrum.

Several cycle counting methods have been developed, including rainflow and range-pair counting methods [e.g., 74]. The analytical crack growth computer program used

should provide the cycle counting option best suited to the user's needs.

#### 5.4.6 Stress Intensity Factor for Loaded Bolt Holes

A superposition method has been developed [92,93] for determining the stress intensity factor for a loaded bolt hole. The stress intensity factor is based on the through-stress and bearing stress (ref. Fig. 19) for both part-through and through-the-thickness cracks in a fastener hole.

The stress intensity factor  $K_I$ , due to the through stress and the bearing stress is given in Eq. 14.

$$K_I = \sigma_T \sqrt{\pi a/Q} [\beta_{TENS} + (\sigma_{br}/\sigma_T) \beta_{BR}] \quad (14)$$

where:  $\sigma_T$  = through stress,  $\sigma_{br}$  = bearing stress ( $P_b/dt$ ),  $Q$  = shape factor,  $\beta_{TENS}$  and  $\beta_{BR}$  are tabulated factors for through stress and bearing based on Ref. 92. A close tolerance fit of the bolt in the hole is assumed.

The method described above is included in the "RXN" computer program [67] for predicating crack propagation. A brief description of "RXN" is given in Appendix G.

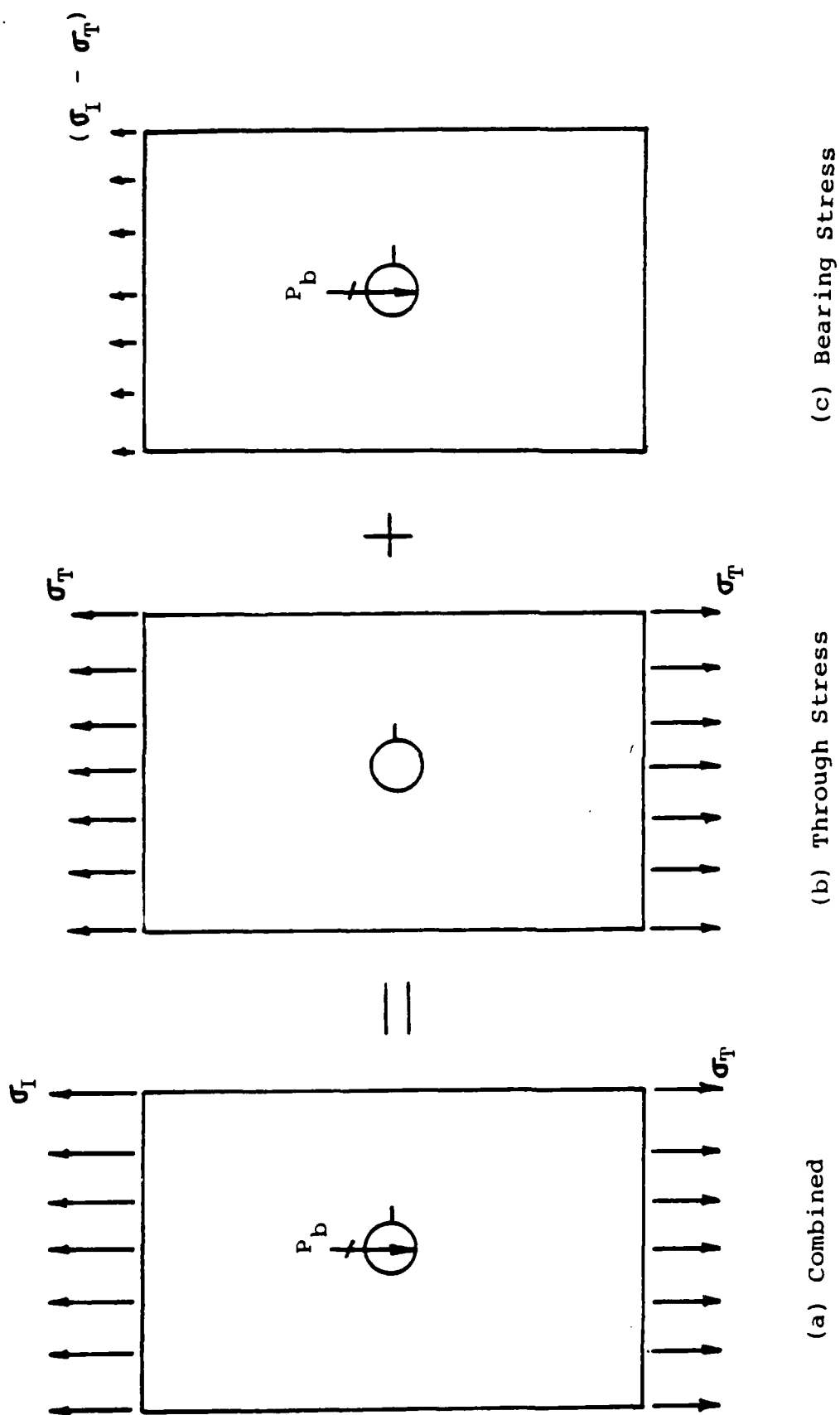


Fig. 19 Superposition Concept for Determining Stress Intensity Factor for Through Stress and Bearing Stress

## 5.5 EXPERIMENTAL DATA REQUIREMENTS/GUIDELINES

Experimental data requirements and guidelines for implementing the recommended CF analysis methodology are described and discussed in this section. Testing details are discussed (e.g., type of specimen, number of specimens, specimen geometries, loading frequency, test environments, environmental simulation procedures, stress levels, R-ratio, etc.), including testing rationale.

### 5.5.1 Strain-Controlled DATA

Strain-controlled tests are needed for a given material to acquire allowable strain life data. (i.e., allowable strain amplitude versus  $2N_1$  cycles to initiate a specified crack size). These data are needed to implement the strain life analysis described in Appendix E and elsewhere [28-51].

Tests should be conducted using smooth un-notched (hour-glass type) specimens. The specimen geometry shown in Fig. 1 worked very well for this program. Other geometries could be used e.g., (ref. ASTM Standard E606-80; Ref. 133). Essential specimen requirements are: (1) long enough in the test section to obtain reasonable axial deformation, (2) short enough to be

stable under compressive loading and (3) compatible with selected environmental simulation method.

Strain-controlled tests, test set-up, and suitable test procedures are described in Volume IV [24] and elsewhere. Recommended environmental simulation procedures/chambers are also described in Volume IV.

A reference crack size  $a_0$  for crack initiation must be selected.  $a_0 = 0.01"$  was used for this program and it seemed to work well. Whatever  $a_0$  is used, it should be large enough to justify the use of LEFM for crack growth from an initial flaw size of  $a_0$ . Also,  $a_0$  should be consistent with the experimental detection capability and desired confidence level.

Strain levels, environment, and reference crack size are the main variables. A minimum of three strain levels should be used (e.g., high, low and intermediate). The low strain level should be selected to provide crack initiation data in a reasonable test time.

Strain life data should be acquired for two environments: (1) baseline (e.g., dry air at room temperature) and (2) 3.5% NaCl solution at room temperature. It is possible to estimate

the strain life allowables for a 3.5% NaCl environment using a knockdown factor (based on strain life results for similar alloys) and the dry air environment result. However, we recommend that strain life allowables also be acquired for the 3.5% NaCl environment to cover the different exposure times associated with the high and low strain extremes.

Specimens can be tested at a fairly fast frequency for both dry air and 3.5% NaCl environments. The loading frequency should be consistent with the user's experimental facilities and capabilities.

The number of test specimens required for each strain level depends on the main goals of the strain life analysis. For example, if the analysis is concerned with the accuracy of the central tendency prediction for CF crack initiation, then a minimum of three specimens per strain level will probably be adequate. However, if the strain life analysis is concerned with the distribution of TTCIs for a given  $a_0$ , the accuracy of extreme value predictions, and a high confidence level, thirty or more specimens per strain level may be required. In any case, the user must decide what tests and how many are needed to meet his requirements.

### 5.5.2 $da/dN$ Versus $\Delta K$ Data

Constant amplitude tests are required to acquire  $da/dN$  versus  $\Delta K$  data for the desired material. Compact tension (CT) or center crack tension (CCT) type specimens can be used. Standard specimen geometries and testing procedures are described in ASTM standard E647-81 [80].

Consider two environments: (1) baseline (e.g., dry air at room temperature) and (2) 3.5% NaCl solution (at room temperature). A suitable environmental chamber and test procedure are described in Volume IV [24]. Use a constant immersion condition for the 3.5% NaCl environment.

A minimum of three specimens (CT or CCT type) is recommended for each environment. This is consistent with the recommendation of Fong and Dowling [123].

Consider a minimum of two different R-ratios (e.g.,  $R = 0.05$  and  $0.5$ ). for each environment. Also, the user should select R-ratios that are typical for his applicable load spectrum. Since CT and CCT tests are relatively inexpensive, the user is advised to test as many different R-ratios as he can because the  $da/dN$  versus  $\Delta K$  results will be invaluable for evaluating the

effectiveness of the crack growth model used for a wide range of R-ratios.

### 5.5.3 Dog-Bone Specimen Data

Dog-bone specimen fatigue tests are recommended to acquire data for "scaling" the CF crack initiation analysis and for calibrating the load-interaction model used. These tests should be performed using a baseline environment (e.g., dry air), load spectrum and stress level.

#### 5.5.3.1 Crack Initiation Data

Test specimens should be tested using as high a loading frequency as possible to minimize testing costs. For example, 10 Hz to 20 Hz is recommended. We typically used a maximum of 6 Hz for the constant amplitude tests under this program.

Dog-bone specimens with a center hole (open) should be fatigue tested using a baseline environment, load spectrum and stress level. A suitable specimen and hole geometry should be used. The specimen shown in Fig. 3 worked very well for this program. Whatever specimen geometry is used, the specimen should be stable in compression without special lateral support in the middle.

The fastener hole in the test section should be prepared using the applicable manufacturing methods. We recommend that test specimens be fatigue tested to failure with the center hole open (in the as drilled condition). No intentional preflaws should be implanted in the center hole so that natural fatigue cracks can be obtained.

A fastener in the hole tends to constrain the deformation on each side of the hole. The amount of hole constraint provided by the fastener varies depending on the fastener type and fit. Constraining the hole deformation can reduce the effective stress concentration at the edge of the hole and result in a longer crack initiation life. However, due to the variable nature of the fastener - hole fit and the typically large scatter in CF test results, we recommend that the dog-bone specimens be tested without a bolt in the center hole.

The largest fatigue crack in the center hole for each specimen should be evaluated fractographically. From the fractography, the time to initiate a crack size of  $a_0$  can be determined. The average TTCI results from the fatigue tests provide the basis for "scaling" the strain life analysis.

A minimum of three specimens should be fatigue tested.

Three specimens should be adequate to estimate the central tendency behavior of the TTCIs.

#### 5.5.3.2 Crack Propagation Data

Crack propagation tests are recommended to acquire fatigue data that can be used to "tune" the crack growth analysis; i.e., calibrate the load-retardation model parameters. We recommend that three dog-bone specimens with a preflawed center hole (open) be fatigue tested to failure using a baseline environment (e.g., dry air), load spectrum and stress level. The center hole in each specimen should be preflawed (e.g., 0.01" corner crack) on one side of the hole - perpendicular to the applied axial loading. The same specimen type, geometry and hole preparation details described in Section 5.5.3.1 apply. We recommend that the fastener holes be preflawed so that the fatigue crack growth starts from the same initial flaw size and geometry. If the fastener holes are not preflawed and the fatigue cracks are allowed to occur naturally, there will typically be more scatter in the crack growth results.

After the test specimens have been fatigue tested to failure, the fatigue crack growing from the preflaw should be evaluated fractographically. The crack growth results, obtained from the fractographic evaluations, provide a practical means for

calibrating the load - interaction model used. This approach could be used until more advanced load - interaction models have been developed which apply to a wide range of load spectra.

#### 5.6 APPLICABILITY OF CORROSION FATIGUE METHODOLOGY TO OTHER ALUMINUM ALLOYS

The observed independence of fatigue crack growth rate on frequency (see Fig. 20 and 21) and the essential agreement between growth rates in moist air and in the aqueous solutions (see Fig. 22) for the 7075-T7651 aluminum alloy indicate that the crack growth rates are at their "saturation" level [117,118]. These results are consistent with available data on other 7000 series (Al-Mg-Zn and Al-Mg-Zn-Cu) alloys in the overaged conditions [119] and on a 2219-T851 (Al-Cu) alloy [120]. They are also in agreement with a model for corrosion fatigue crack growth proposed by Weir et al. [117] and Wei and Simmons [118], where the enhancement in crack growth rate is determined by the extent of surface reaction at the crack tip, which is limited.

Because the reactions of water/water vapor with aluminum is very rapid, these reactions are essentially completed at very low exposures or equivalent exposures (pressure x time) [120]. For example, at a water vapor pressure of 1.3kPa (corresponding to about 40% relative humidity at room temperature), the reactions

5.7.2.2 Scaling of Environmental Effects

If there is no significant synergistic effect between the mechanical-loading and environment on TTCI for the 7075-T7651 aluminum alloy, the "effect of the environment" on TTCI can be "scaled". In this section, dry/wet ratios for TTCI predictions are compared with test results to evaluate the feasibility of scaling.

TTCI predictions for load spectra A, B, and C including dry/wet ratios, are summarized in Tables 17 and 18 for spectra A and B baselines, respectively. The corresponding average test results for dog-one specimens [24] are shown in parenthesis. Test results reflect the fast (F) loading frequency (ref. Tables C-1 and C-2 in Appendix C).

Dry/wet ratios shown in Tables 17 and 18 are based on predicted and test TTCI values. The dry/wet ratio statistics (average value, N=no. of samples,  $\sigma(x)$ =standard deviation and c.o.v) are noted in Tables 17 and 18. The 95% confidence intervals for the dry/wet ratios, based on the results of Table 17 are:

- o Predicted ave. dry/wet ratio: 1.47 to 1.91
- o Test ave. dry/wet ratio: 1.38 to 2.78

air). Once the strain life analysis has been scaled, the resulting  $\bar{K}_t(0)$  can then be used to make TSCI predictions for other load spectra, geometries, % bolt load transfer, stress levels and environments. The effect of the environment on the TSCI prediction is reflected in the strain life allowables used in the strain life analysis.

4. A simple superposition model was used, along with the stress-strain relationship, to estimate the effective  $\bar{K}_t(LT)$  for a given % bolt load transfer (ref. Appendix F).  $\bar{K}_t(LT) = \bar{K}_t(0) * K_\sigma(LT)/K_\sigma(0)$  was used, where  $\bar{K}_t(0)$  = effective stress concentration factor for the baseline case ("scaled");  $K_\sigma(LT)$  and  $K_\sigma(0)$  = elastic stress concentration factor for the given % load transfer and the open hole configuration, respectively. The effective  $\bar{K}_t(0)$  value was ratioed up to account for the effect of the % bolt load transfer on the stress concentration at the edge of the hole.

5. Once the effective  $\bar{K}_t(LT)$  stress concentration factor has been defined for a given hole geometry and % bolt load transfer, the strain life analysis can be used to make TSCI predictions for other load spectra, stress levels, % bolt load transfer. The strain life analysis can be performed for each  $\bar{K}_t(LT)$  value separately to predict TSCI or the effective  $K_t$  versus TSCI relationship described in step 2 above can be used.

Essential details of the CF crack initiation analysis are given below and further details are given in Appendix F.

1. Baseline data was used to define the stress strain relationship. Elastic/plastic strain life allowables for both dry air and 3.5% NaCl environments were developed using the modified Coffin Manson approach. Average and upper/lower bound extremes (strain life allowables) were estimated.

2. Strain life analyses were performed using the strain life approach and the computer program "BROSE" [45] described in Appendix E. TTCI predictions were made for three load spectra ("A", "B", "C") using assumed effective  $K_t$  values. A simple powerlaw was used to determine an effective  $K_t$  relationship; i.e.  $K_t = A(TTCI)^B$ . Other functional forms could also be used.

3. The strain life analysis for spectrum "A" was scaled using the average TTCI test results for the open hole specimen, load spectrum "A", dry air environment and applicable stress level. The analysis was "scaled" by determining the effective  $\bar{K}_t(0)$ , based on the strain life analysis results, corresponding to the average TTCI test result for the baseline case (i.e., open hole, dry air, spectrum "A"). The basic idea used was this: The strain life analysis for a given load spectrum and stress level can be "scaled" using dog-bone specimen test results for a baseline specimen/hole geometry and environment (e.g., dry

Table 16 Comparison of TTCl Predictions and Test Results (7075-T7651 Aluminum) for Loading Spectrum "C" for Various Cases

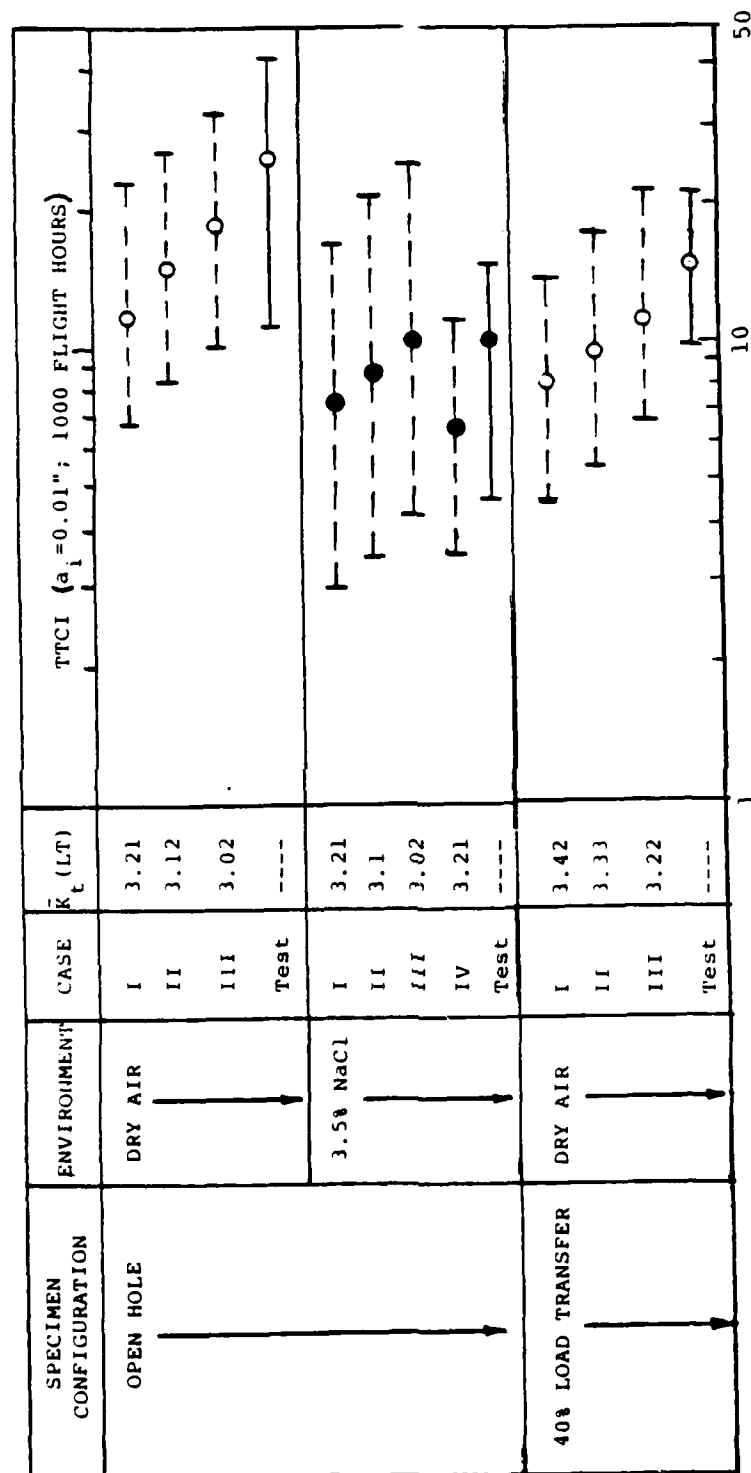


Table 15 Comparison of TTCI Predictions and Test Results (7075-T7651 Aluminum) for Loading Spectrum "B" for Various Cases

SPECIMEN CONFIGURATION	ENVIRONMENT	CASE	$\bar{K}_t$ (LT)	TTCI ( $a_i=0.01"$ ; 1000 FLIGHT HOURS)
OPEN HOLE ↓	DRY AIR ↓	I	3.21	
		II	3.12	
		III	3.02	
		Test	----	
	3.5% NaCl ↓	I	3.21	
		II	3.12	
		III	3.02	
		IV	3.21	
20% LOAD TRANSFER ↓	DRY AIR ↓	I	3.33	
		II	3.24	
		III	3.14	
		Test	----	
	3.5% NaCl ↓	I	3.33	
		II	3.24	
		III	3.14	
		IV	3.33	
40% LOAD TRANSFER ↓	DRY AIR ↓	I	3.42	
		II	3.33	
		III	3.22	
		Test	----	
	3.5% NaCl ↓	I	3.42	
		II	3.33	
		III	3.22	
		IV	3.42	

TABLE 14 Comparison of TTCI Predictions and Test Results (7075-T7651 Aluminum)  
for Loading Spectrum "A" for Various Cases

SPECIMEN CONFIGURATION	ENVIRONMENT	CASE	$\bar{K}_t$ (LT)	TTCI ( $a_1=0.01"$ ; 1000 FLIGHT HOURS)
OPEN HOLE ↓	DRY AIR ↓	I	3.21	
		II	3.12	
		III	3.02	
		Test	----	
	3.5% NaCl ↓	I	3.21	
		II	3.12	
		III	3.02	
		IV	3.21	
		Test	----	
20% LOAD TRANSFER ↓	DRY AIR ↓	I	3.33	
		II	3.24	
		III	3.14	
		Test	----	
	3.5% NaCl ↓	I	3.33	
		II	3.24	
		III	3.14	
		IV	3.33	
		Test	----	
40% LOAD TRANSFER ↓	DRY AIR ↓	I	3.42	
		II	3.33	
		III	3.22	
		Test	----	
	3.5% NaCl ↓	I	3.42	
		II	3.33	
		III	3.22	
		IV	3.42	
		Test	----	

## 5.7.2 CF Crack Initiation Analysis/Results

### 5.7.2.1 TTCI Predictions and Correlations

TTCI predictions and correlations for the following four cases are summarized in Tables 14, 15 and 16 for load spectra "A", "B" and "C", respectively:

- o Case I - Strain life analysis calibrated for baseline spectrum "A" and  $\bar{K}_t(LT=0)=3.21$  (based on dry air environment)
- o Case II - Strain life analysis calibrated for baseline spectrum "A" and  $\bar{K}_t(LT=0)=3.12$  (average based on dry air and 3.5% NaCl environments)
- o Case III - Strain life analysis calibrated for baseline spectrum "B" and  $\bar{K}_t(LT=0)=3.12$  (average based on dry air and 3.5% NaCl environments)
- o Case IV - Strain life analysis calibrated for baseline spectrum "A" with  $\bar{K}_t(LT=0)=3.21$  (based on dry air environment) and an environmental scaling factor (ESF) = 2.11 (see Appendix F)

3.5% NaCl environments, (2) Forman crack growth model, (3) generalized Willenborg retardation modes, (4) rainflow cycle counting, (5) an initial flaw size of  $a_0=0.01$ " (corner crack), (6) "RXN" crack growth computer program [66, 67], and (7) a superposition model for determining the stress intensity factor for through-stress and bolt hole bearing stress combinations. Generalized Willenborg model parameters were based on published values for  $\Delta K_{th}$  (threshold) and  $R_{OS}$  (overload shut-off ratio) for 7075-T7651 aluminum [122].

2. Basic issues considered in the evaluation of the CF crack propagation methodology were: (1) accuracy of TFCG predictions compared with dog-bone specimen test results?, (2) does the CF methodology track the trends and order of spectrum severity?, and (3) can the effects of the environment TFCG be "scaled"?

3. The affect and sensitivity of the generalized Willenborg model parameters (  $\Delta K_{th}$  and  $R_{OS}$  ) on TFCG predictions were studied for the open hole configuration. Both dry air and 3.5% NaCl environments were considered as well as three load spectra (i.e., "A", "B" and "C").

and results are compared with test result for dog-bone specimens from Volume IV [24].

2. An environmental scaling factor (ESF) and dry air TTCI predictions are used to make TTCI predictions for the 3.5 NaCl environment for three specimen configurations (i.e., open hole, 20% LT and 40% LT). TTCI predictions are made for load spectra "A", "B" and "C", and the results are compared with dog-bone specimen tests from Volume IV [24].

3. Can the effects of the environment on TTCI be "scaled" (i.e., are the dry/wet ratios independent of load spectra and load transfer)? To address this question, dry/wet ratios based on TTCI predictions were compared with those based on actual test results. The dry/wet ratios provide the basis for defining the environmental scaling factor (ESF).

4. The effectiveness of the CF crack initiation methodology is based on the results for the studies described above. This also provides a basis for generalizing the methodology.

#### 5.7.1.2 CF Crack Propagation

1. Time-for-crack-growth (TFCG) predictions were made for three configurations (i.e., open hole, 20% LT and 40% LT), three load spectra (i.e., "A", "B" and "C"), and for both dry air and 3.5% NaCl environments. Predictions were based on: (1)  $da/dN$  versus  $\Delta K$  data for both dry air and

## 5.7 EVALUATION OF CORROSION FATIGUE ANALYSIS METHODOLOGY

The corrosion fatigue (CF) analysis methodology for mechanically-fractured joints was evaluated in two parts: (1) Crack initiation and (2) crack propagation. Details of the evaluation, including approach, studies, results and conclusions are given in this section and selected appendices. The evaluation is based on dog-bone specimen test results for 7075-T7651 aluminum from Volume IV [24].

## 5.7.1 Evaluation Approach

5.7.1.1 CF Crack Initiation

1. The strain life analysis is "scaled" to a baseline configuration geometry (i.e., open hole), environment (i.e., dry air) and peak load stress level (i.e., 28 ksi) using the average time-to-crack-initiation (TTCI) test results for spectrum "A". These results are then used to predict the TTCI for different configurations (i.e., open hole, 20% LT and 40% LT), load spectrum ("A", "B" and "C") and environments (i.e., dry air and 3.5% NaCl). In a similar manner, the strain life analysis is scaled using TTCI results for spectrum "B" and TTCI predictions are made for other load spectra and configurations. TTCI predictions for the average and extreme values (upper and lower bound estimates) are made

would be completed in about 1 microsecond. Consequently, for environmental conditions and loading frequencies that are of practical interest, it is adequate to use the crack growth rate in water for design and the influence of frequency can be essentially ignored.

Recent results on 7000 series alloys in the peak-age condition (specifically 7075-T651) indicated that there could be a strong effect of water vapor pressure and frequency [119,121]. The additional enhancement in crack growth rate has been attributed to the further reactions of water with the segregated magnesium in these alloys [121]. As such, special attention should be given in applying the recommended methodology to all magnesium containing alloys in the peak-aged condition. For these alloys, the growth rates or environmental scaling factors to be used should be derived from data that have been obtained at the lowest frequency that may be encountered during service.

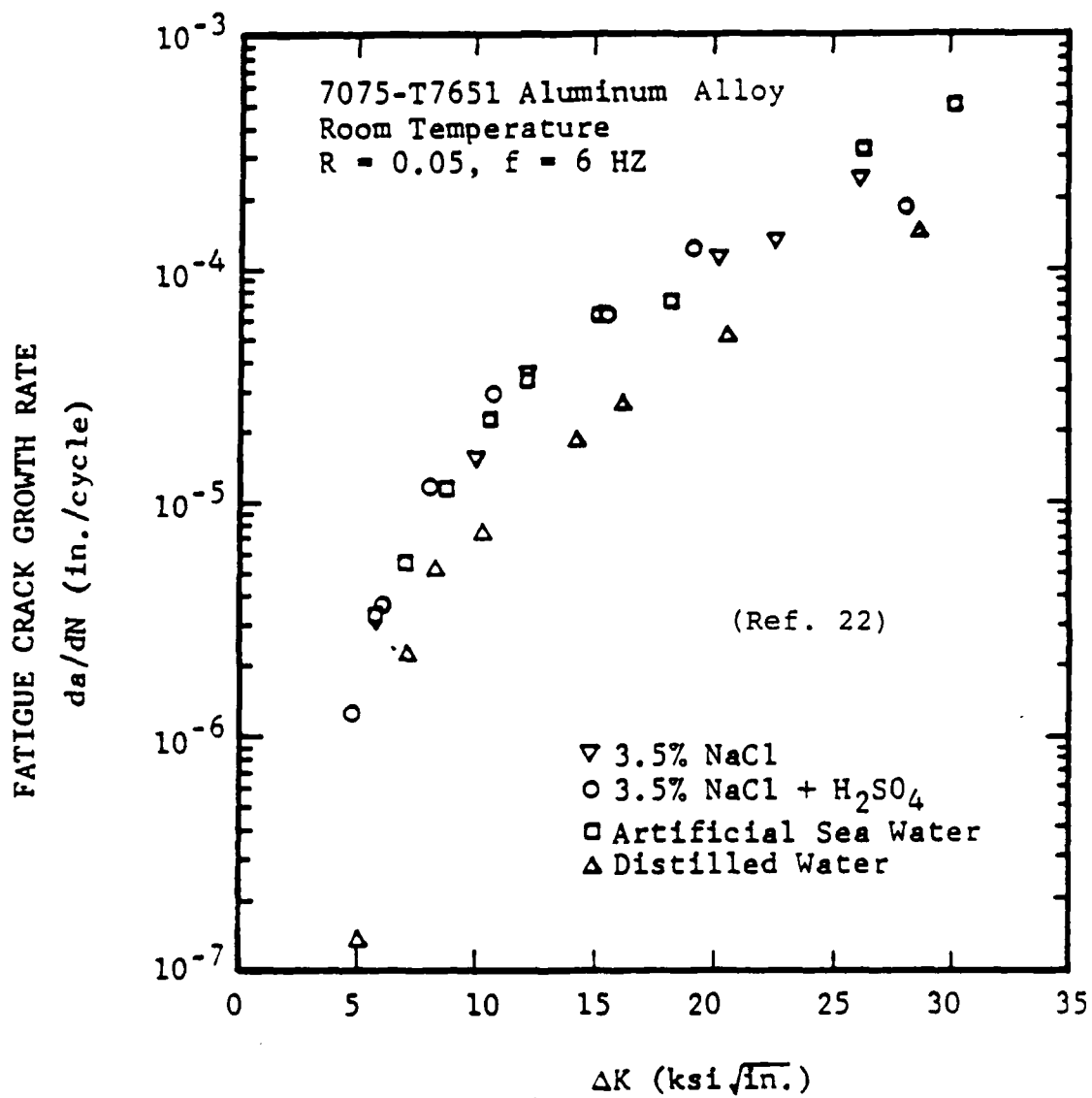


Fig. 22 Effect of Environment on Crack Growth Rates for 7075-T7651 Aluminum Alloy at Room Temperature ( $R=0.05$ ,  $f = 6 \text{ Hz}$ )

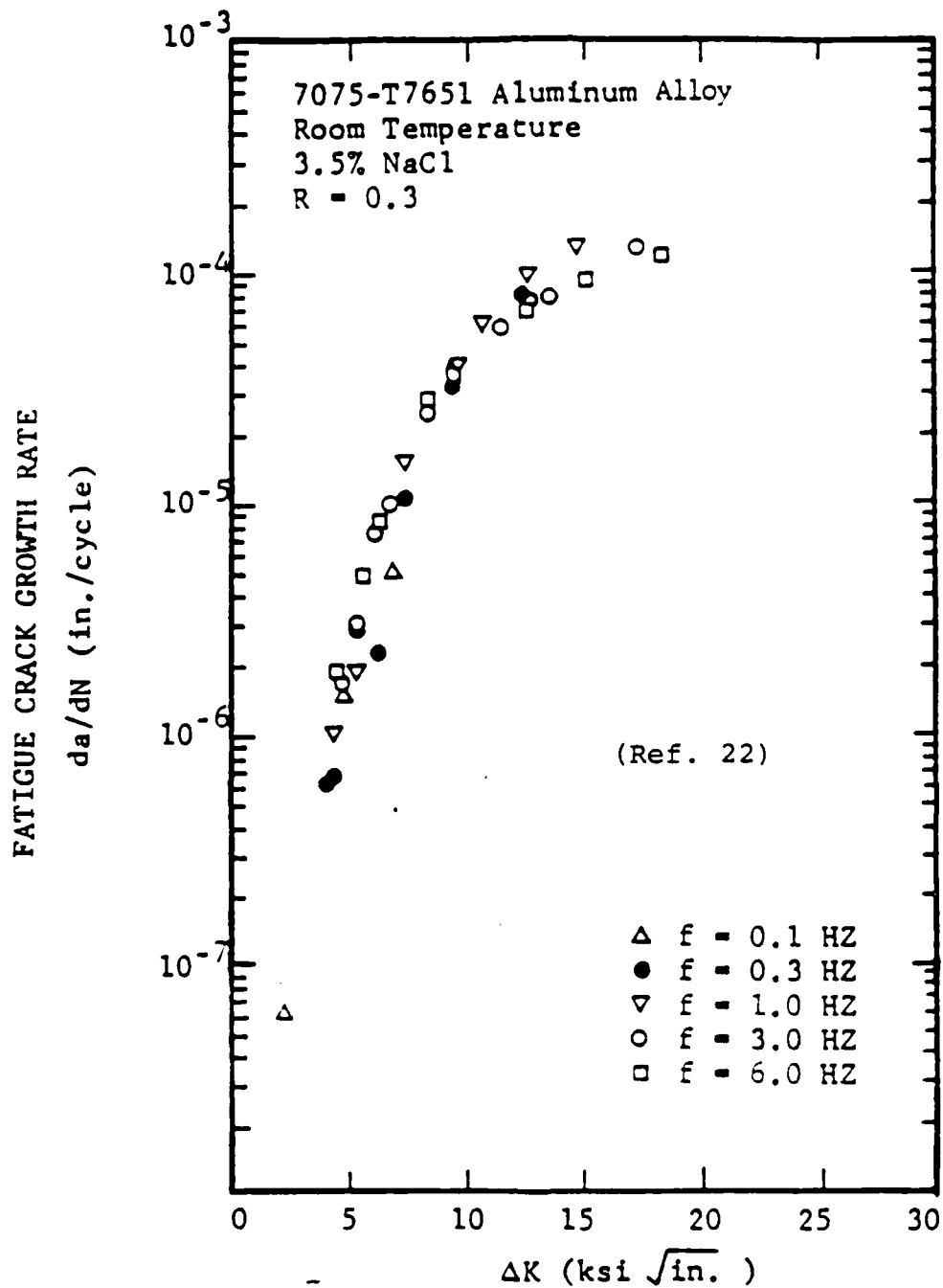


Fig. 21 Effect of Frequency on Crack Growth Rates for 7075-T7651 Aluminum Alloy Exposed to 3.5% NaCl Solution at Room Temperature ( $R = 0.3$ ;  $f = 0.1\text{HZ}$ ,  $0.3\text{HZ}$ ,  $1\text{HZ}$ ,  $3\text{HZ}$ , and  $6\text{HZ}$ )

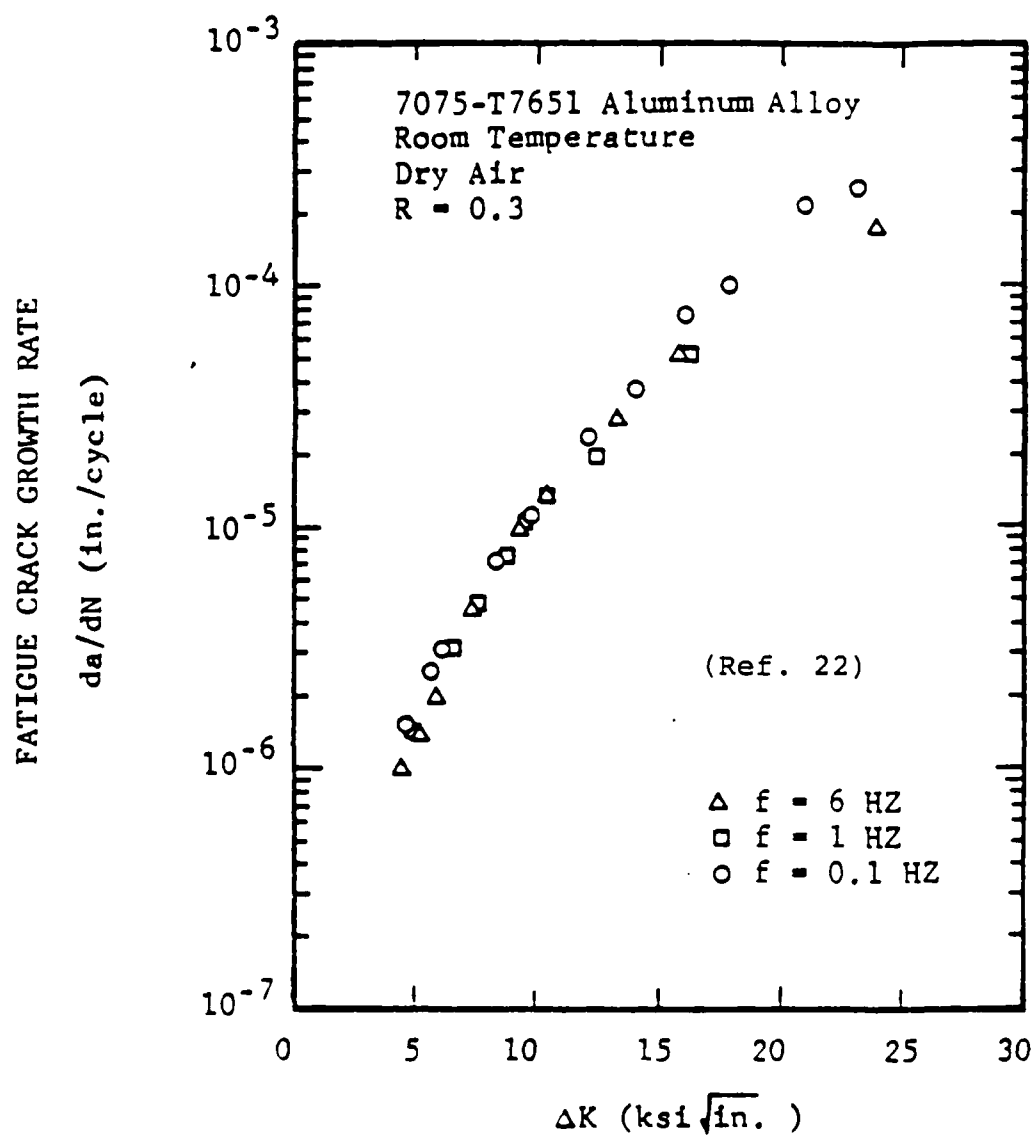


Fig. 20 Effect of Frequency on Crack Growth Rates for 7075-T7651 Aluminum Alloy in Dry Air at Room Temperature (R = 0.3; f = 0.1 HZ, 1 HZ, and 6 HZ)

TABLE 17 Summary of TTCI Predictions for Load Spectra A, B and C  
Based on Spectrum A Baseline with Dry/Wet Ratios

Specimen Configuration	Spectrum	Effective $\bar{K}_t$ (LT)	AVE. TTCI (FLT. HRS.; $a_0=0.01"$		Dry/Wet Ratio
			Dry Air	3.5% NaCl	
Open Hole	"A"	3.21	13200 (13200)	6560 (9243)	2.01 (1.43)
	"B"		11210 (16395)	7580 (11917)	1.48 (1.38)
	"C"		12210 (26333)	7260 (10300)	1.68 (2.56)
20% LT	"A"	3.33	10530 (12476)	5330 (3954)	1.98 (3.16)
	"B"		8560 (10302)	6010 (8041)	1.42 (1.28)
40% LT	"A"	3.42	8900 (16651)	4590 (6006)	1.94 (2.77)
	"B"		7033 (13050)	5080 (6659)	1.38 (1.96)
	"C"		8000 (15689)	5030 (---) *	1.59 (---) *

NOTES: (xxx) = average test results

\* Test results not available for this case.

Predicted: Ave. dry/wet ratio = 1.69; N=8;  $\sigma(\bar{x})=0.259$ ; C.O.V.=15.4%

Test: Ave. dry/wet ratio = 2.08; N=7;  $\sigma(\bar{x})=0.757$ ; C.O.V.=36.4%

TABLE 18 SUMMARY OF TTCl PREDICTIONS FOR LOAD SPECTRA A, B AND C  
BASED ON SPECTRUM B BASELINE WITH DRY/WET RATIOS

Specimen Configuration	Spectrum	Effective $K_t$ (LT)	AVE. TTCl (FLT. HRS.; $a_0=0.01"$ )		Dry/Wet Ratio
			Dry Air	3.5% NaCl	
Open Hole ↓	"A"	3.02 ↓	19470 (13200)	9240 (9243)	2.11 (1.43)
	"B"		17550 (16395)	11160 (11917)	1.57 (1.38)
	"C"		18340 (26333)	10330 (10300)	1.78 (2.56)
20% LT ↓	"A"	3.14 ↓	15240 (12476)	7420 (3954)	2.05 (3.16)
	"B"		13180 (10302)	8720 (8041)	1.51 (1.28)
40% LT ↓	"A"	3.22 ↓	13000 (16651)	6440 (6006)	2.02 (2.77)
	"B"		10950 (13050)	7440 (6659)	1.47 (1.96)
	"C"		11960 (15689)	7130 (---) *	1.68 (---) *

NOTES: (xxx) = Average test result

\* Test results not available for this case

o Predicted: Ave. Dry/Wet Ratio = 1.77; N=8;  $\sigma(\bar{x})=0.257$ ; C.O.V. = 14.5%

o Test: Ave. Dry/Wet Ratio = 2.08; N=7;  $\sigma(\bar{x}) = 0.757$ ; C.O.V. = 36.4%

## 5.7.3 CF Crack Propagation Analysis/Results

5.7.3.1 TFGC Predictions and Correlations

Time-for-crack-growth (TFGC) predictions were made for three load spectra (i.e., "A", "B" and "C") and for three specimen configurations (i.e., open hole, 20% LT and 40% LT). The analysis matrix is shown in Table 19. Predictions and average test results are summarized in Table 20. Average test results are shown in parenthesis in Table 20. Essential details of the analysis are described in Section 5.7.1.2 and below.

The Forman crack growth model parameters (i.e.,  $n$  and  $C$ ) were determined using a data pooling procedure described in Appendix B. The following values were used in the Forman model:  $n = 2.913$ ,  $C(\text{dry air}) = 4.722 \times 10^{-7} \text{ (in/cycle) (ksi } \sqrt{\text{in.}})^{-n}$ ,  $C(3.5\% \text{ NaCl}) = 8.551 \times 10^{-7} \text{ (in/cycle) (ksi } \sqrt{\text{in.}})^{-n}$ , and  $K_c = 62.5 \text{ ksi } \sqrt{\text{in.}}$ . The Forman crack growth model accounts for R-ratio. It was found that the Forman model fit the  $da/dN$  versus  $\Delta K$  data rather well for different R-ratios and for both the dry air and 3.5% NaCl environments (ref. Fig. B7 through B10).

Several load-interaction models were considered [96-114]. However the generalized Willenborg was selected for two reasons: (1) the model parameters are independent of the load spectra and (2) there are published values for the

Table 19 Corrosion Fatigue Analysis Matrix for Crack Growth Predictions  
for 7075-T7651 Aluminum

SPECIMEN CONFIGURATION (c)	ENVIRONMENT	LOAD SPECTRUM			FORMAN CRACK GROWTH PARAMETERS		GENERALIZED WILLENBORG PARAMETERS		PEAK STRESS (ksi) (d)	
		"A"	"B"	"C"	n(a)	C x 10 <sup>7</sup> (a)	$\Delta K_{th}$ (b)	R <sub>os</sub> (b)		
Open Hole	Dry Air	X	X	X	2.913	4.722 8.551	1.5	2.65	28	
	3.5% NaCl	X	X	X						4.722 8.551
20% Load Transfer	Dry Air	X	X	X						
	3.5% NaCl	X	X	-	4.722 8.551					
40% Load Transfer	Dry Air	X	X	X		4.722 8.551				
	3.5% NaCl	X	X	-						

Notes: (a) Ref. Appendix B (Section B.5) for details, including goodness-of-fit plots (Fig. B-7 through B-10)

(b)  $\Delta K_{th}$  (threshold) and R<sub>os</sub> (overload shut-off ratio) values from Ref. 122

(c) Ref. Fig. 3 for geometry (D = 0.4375")

(d) Gross section

Table 20 Summary of TFCG Predictions and Correlations  
with Dog-Bone Specimen Test Results for  
7075-T7651 Aluminum

Specimen Type (b)	(a), (d) Time-For-Crack-Growth (Flight Hours)					
	Spectrum "A"		Spectrum "B"		Spectrum "C"	
	Dry Air	3.5% NaCl	Dry Air	3.5% NaCl	Dry Air	3.5% NaCl
Open Hole	3200 (8899)	1600 (5762)	7200 (7772)	3000 (3579)	11400 (22538)	6000 (9400)
20% LT	1200 (10066)	400 (4298)	2100 (3737)	900 (3140)	3900 (c) (---)	1800 (c) (---)
40% LT	<400 (13631)	<400 (3741)	300 (7622)	<300 (2740)	600 (19010)	300 (c) (---)

- Notes: (a) XXXX = predicted TFCG; (XXXX) = average test result  
 (b) Ref. Fig. 3 for specimen geometry ( $D = 0.4375"$ )  
 (c) No test results available  
 (d) TFCG predictions based on the "RXN" crack growth program [67] and the following models and parameters:

- o Crack growth model (Forman Equation)

$$da/dN = \frac{C(\Delta K)^n}{(1-R)K_C - \Delta K}$$

$$C(\text{dry air}) = 4.722 \times 10^{-7}; C(3.5\% \text{ NaCl}) = 8.551 \times 10^{-7}$$

$$n = 2.913$$

$$K_C = 62.5 \text{ ksi} - \sqrt{\text{in}}$$

- o Load-Interaction Model (Generalized Willenborg)

$$\Delta K_{th} = 1.5 \text{ ksi} - \sqrt{\text{in}}$$

$$R_{os} = 2.65 \text{ (overload shut-off ratio)}$$

} Ref. 122

- o  $a_0 = 0.01"$  (corner crack)
- o Cycle counting by Rainflow method

two key parameters in the model for 7075-T7651 aluminum. The following parameter values were used in the CF crack growth analysis:  $\Delta K_{th} = 1.5 \text{ ksi } \sqrt{\text{in}}$  and overload shut-off ratio =  $R_{Os} = 2.65$  [122].

A state-of-the-art analytical crack growth computer program ("RXN") [66, 67] was used to make the TFCG predictions. This proven computer program has been used extensively by the General Dynamics/Fort Worth Division for the durability and damage tolerance analysis of metallic aircraft structures [e.g., 64, 65]. Essential features of the "RXN" program are described in Appendix G. Typical output from "RXN" for the TFCG predictions herein is also shown in Appendix G. Details about the load spectra, including exceedance comparisons are given in Appendix H.

#### 5.7.3.2 Sensitivity of Willenborg Retardation Model Parameters

A study was made to determine the effects and sensitivity of the generalized Willenborg retardation model parameters ( $\Delta K_{th}$  and  $R_{Os}$ ) on the CF crack propagation predictions for the open hole configuration. The study was performed as follows. CF crack growth predictions were made for the open hole case using the "RXN" computer program [67]. Predictions were made using selected values for  $\Delta K_{th}$  and overload shut-off ratio for load spectra "A", "B" and "C" and for both dry air and 3.5% NaCl environments. Results of the

sensitivity study are summarized in Table 21. Plots of the overload shut-off ratio versus time-for-crack-growth (TFCG) are shown in Fig. 23 for load spectra "A", "B" and "C".

#### 5.7.3.3 Scaling of Environmental Effects

If there is no significant synergistic effect between the mechanical-loading and the environment on crack propagation for the 7075-T7651 aluminum alloy, the "effect of the environment" on crack propagation can be "scaled". Dry/wet ratios for TFCG predictions are compared with test results to evaluate the feasibility of scaling the environmental effect.

TFCG predictions for 7075-T7651 aluminum dog-bone specimens and average test results are summarized in Table 20 for both dry air and 3.5% NaCl environments, load spectra "A", "B" and "C" and three specimen configurations (i.e., open hole, 20% LT and 40% LT).

The following statistics for the dry/wet ratio are based on the results shown in Table 20:

- o Predicted: ave. dry/wet ratio = 2.26 (N=7;  $\sigma(x)=0.375$ ;  
C.O.V.=16.6%)
- o Test: ave. dry/wet ratio = 2.29 (N=7;  $\sigma(x)=0.802$ ;  
C.O.V.=34.9%)

Table 21 Summary of TFCG Predictions (Dry & Wet) for Various  $\Delta K_{th}$  and Overload Shut-Off Ratios ( $R_{os}$ )

SPECIMEN	(e) $\Delta K_{th}$ (a)	(f) $R_{os}$ (a)	TFCG (Flt Hours) (d)					
			SPECTRUM "A"		SPECTRUM "B"		SPECTRUM "C"	
			DRY AIR	WET (c)	DRY AIR	WET (c)	DRY AIR	WET (c)
OPEN HOLE W = 2.00" t = 0.300" D = 0.4375" 7075-T7651 Al	1.50	2.00	8400	2800	11400	3600	20700	10500
	↑	2.39	4000	1600	8100	3300	13800	7200
	↑	2.65	3200	1600	7200	3000	11400	6000
	↑	2.92	2800	1200	6600	3000	10200	5400
	1.50	3.30	2400	1200	6300	3000	8700	4500
	1.0	2.65	3600	1600	7500	3300	12000	6300
	1.35	↑	2800	1200	6900	3000	10800	5700
	1.65	↑	3200	1600	6900	3000	11400	6000
(b) AVE. TEST RESULT	2.0	2.65	2800	1200	6900	3000	10800	5700
			(8899)	(5762)	(7772)	(3579)	(22538)	(9400)

- Notes:
- (a) Generalized Willenborg Model parameter
  - (b) Based on fast frequency (Ref. Table C-1 (Appendix C))
  - (c) 3.5% NaCl solution at room temperature
  - (d) RXN crack growth program [67]; Forman crack growth model  
( $n = 2.913$ ;  $C(\text{dry}) = 4.722 \times 10^{-7}$ ;  $C(\text{wet}) = 8.557 \times 10^{-7}$ ;  
Generalized Willenborg Model; Rainflow Cycle Counting.
  - (e) Stress Intensity Range Threshold ( $\text{ksi} \sqrt{\text{in.}}$ )
  - (f) Overload Shut-off Ratio

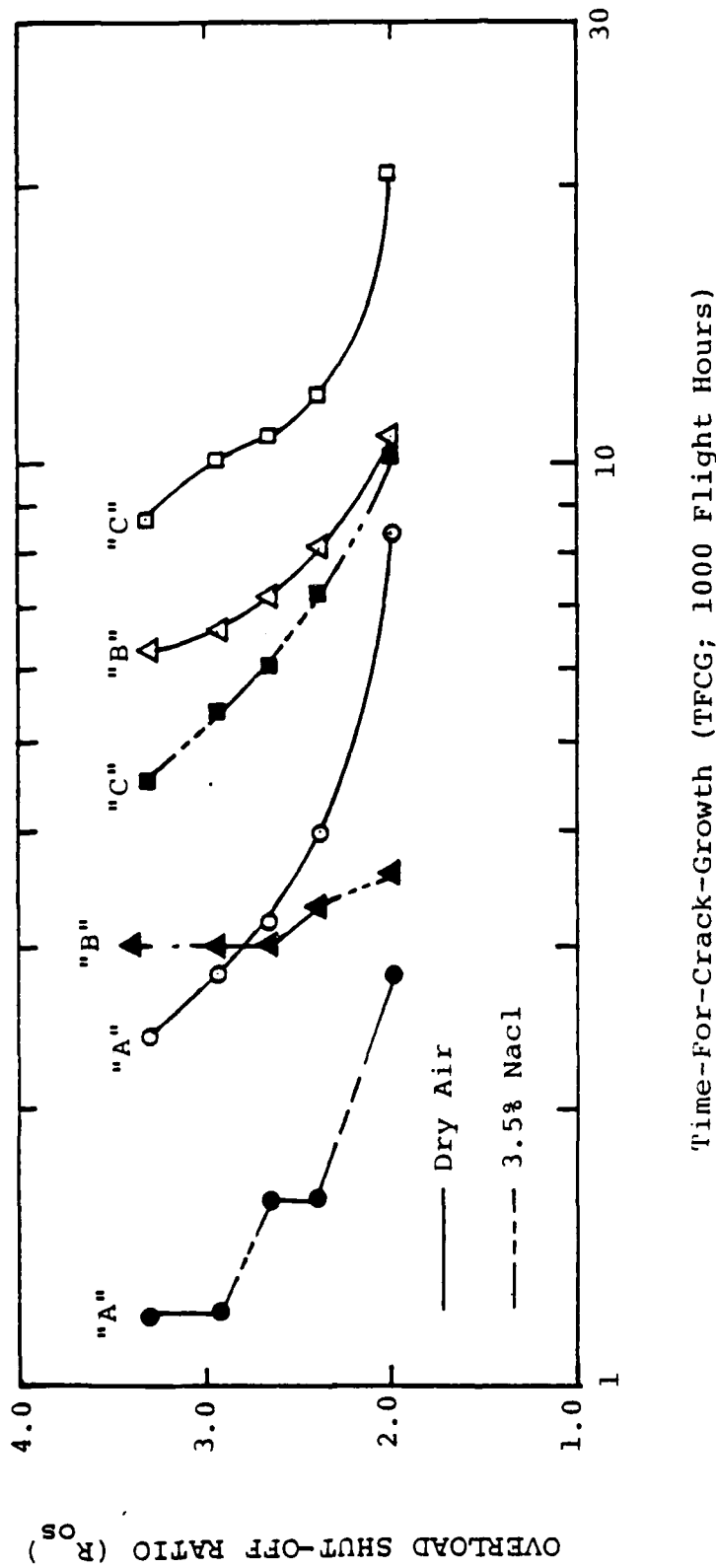


Fig. 23 Overload Shut-Off Ratio Versus Time-For-Crack Growth For Load Spectra A, B, and C For Both Dry Air and 3.5% NaCl Environments and  $\Delta K_{th} = 1.5 \text{ ksi} \sqrt{\text{in.}}$

The 95% confidence interval for the (dry/wet) ratio, based on seven results each from Table 20, was found to be 1.91 and 2.61 and 1.55 and 3.03 for the predicted and experimental results, respectively.

#### 5.7.4 Conclusions and Recommendations

The CF analysis methodology for crack initiation and for crack propagation described in this report is recommended for application to 7000 series aluminum alloys in the over-aged condition. Special attention should be given to the application of the CF methodology to magnesium containing alloys in the peak-aged condition. For these alloys, the crack growth rates or environmental scaling factors (ESF) used should be based on data acquired at the lowest frequency that may be encountered in service.

Specific conclusions and observations about the CF crack initiation and CF crack propagation methodology, including problems requiring further research are discussed in the following subsections. CF crack initiation and CF crack propagation discussions are treated separately.

##### 5.7.4.1 CF Crack Initiation Methodology

The following conclusions, discussions and recommendations are based on the results presented in Section 5.7.2, Appendix F and other results obtained under this program:

1. The TTCI predictions for load spectra "A", "B" and "C" respectively, shown in Tables 14-16 compare reasonably well with applicable average test results. In general, the TTCI predictions are smaller than the average test results. Also, the range of the predicted TTCI extreme values (estimated) are typically larger than the comparable range based on the low/high test results (see Tables 14-16).

2. The strain life analysis can be "scaled" to the open hole configuration (dry air environment) for a given load spectrum and the results can be used to make reasonable TTCI predictions for different configurations (i.e., open hole, 20% LT and 40% LT), environment (i.e., 3.5% NaCl) and load spectra. Reference Table 14-16.

3. The CF crack initiation predictions for the three load spectra considered were correctly ranked in the order of severity. Thus, the CF crack initiation methodology is promising for screening and ranking different load spectra.

4. Reasonable TTCI predictions for the 3.5% NaCl environment were obtained using TTCI predictions for dry air and an environmental scaling factor (ESF). Reference Appendix F for further details .

5. The effects of environment on TTCI can be "scaled". This is based on the fact that the average dry/wet ratio based on TTCI predictions compared very well with the average

dry/wet ratio based on actual test results. For example, the average dry/wet ratio based on predicted TTCIs was 1.69 (spectrum A baseline; ref. Table 17). The average dry/wet ratio based on test results was 2.08.

6. It was interesting to note that the coefficient of variation (C.O.V.) for the average dry/wet ratio, based on predictions, was virtually the same for both TTCI and TFCG. For example the C.O.V. for the average dry/wet ratio was 15.4% (Table 17) and 16.6% (Table 20) for TTCI and TFCG predictions, respectively.

7. The C.O.V. for the average dry/wet ratio based on test results was virtually the same for both TTCI and TFCG test results. For example, the C.O.V. for the average dry/wet ratio was 36.4% (Table 17) and 34.9% (Table 20) for TTCI and TFCG test results, respectively. Also, the C.O.V. for the average dry/wet ratio based on TTCI or TFCG predictions was approximately one-half of the C.O.V. based on test results.

8. Strain life allowables (see Fig. 15, Frame D) should be acquired for both dry air and 3.5% NaCl environments to implement the CF crack initiation methodology until further experience and understanding is acquired on the effects of the environment on the strain life allowables over the high and low strain regimes. For preliminary CF analysis purposes, the TTCI prediction for a 3.5% NaCl environment can

be estimated from the dry air environment prediction as follows:  $TTCI (wet) = TTCI (Dry Air) / ESF$ . The environmental scaling factor based on test results for similar alloys. The ESF is independent of load spectra and configuration (e.g. open hole, bolt-in-hole or  $\frac{1}{2}$  bolt load transfer). Furthermore, no significant differences in the environmental scaling factors for either constant amplitude or spectrum loading test results were found. This is very encouraging and suggests that the ESF is a practical means for making wet environment predictions based on dry air predictions.

9. The effects of both load transfer on CF crack initiation in fastener holes need to be investigated further to better understand the effects of fastener type/fit and bearing stress in the hole on the determination of the effective stress concentration factor,  $\bar{K}_t(LT)$  (see Fig. 15, Frame G and Section 5.3.1). Also, the effects of initial hole quality on CF crack initiation should be accounted for.

10. A minimum of three dog-bone specimens with an open hole (without intentional preflaws) should be fatigue tested in dry air using a baseline spectrum and maximum stress level to acquire TTCI data. Such tests are relatively inexpensive and the results are invaluable for scaling the strain life analysis. The open hole, rather than a bolt-in-hole configuration is recommended because: (1) it's generally more conservative to ignore the possible restraint provided by the bolt in the hole and (2) some degree of conservatism is

justified in view of the typically large scatter exhibited in corrosion fatigue test results in a 3.5% NaCl environment.

#### 5.7.4.2 CF Crack Propagation Methodology

Conclusions, recommendations and discussions on the CF crack propagation methodology are as follows:

1. The CF crack propagation predictions for 7075-T7651 aluminum dog-bone specimens correctly predicted the " trends " and "ranking" of the experimental test results very well for three different load spectra (see Table 20). However, there was a general lack of correlation between the TFCG predictions and the average test results. This lack of correlation is attributed to the retardation model used (generalized Willenborg) rather than the basic CF crack propagation methodology. Unfortunately, none of the retardation models currently available can be calibrated using basic material data and the results be applied, with a high degree of confidence, to any load spectra irrespective of the loading sequence, multiple overloads (tension and compression) and number of loading cycles.

2. Since the effect of loading frequency on  $da/dN$  versus  $\Delta K$  data is not significant for the 7000 series aluminum alloy in the over-aged condition, the  $da/dN$  versus  $\Delta K$  experimental data can be acquired using a fast loading frequency (e.g., 10 Hz-20Hz). However, for all magnesium

Recent results for 7000 series alloys in the peak-aged condition (specifically 7075-T651) indicated that there could be a strong effect of water vapor pressure and frequency [119, 121]. The additional enhancement in crack growth rate has been attributed to the further reactions of water with the segregated magnesium in these alloys [121]. Therefore, special attention should be given in applying the recommended CF methodology to all magnesium containing alloys in the peak-aged condition. For these alloys, the growth rates or environmental scaling factors to be used should be derived from data that have been obtained at the lowest frequency that may be encountered during service.

#### 7.1.2 Titanium Research

The effect of frequency on fatigue crack growth in a beta annealed Ti-6Al-4V alloy in 3.5% NaCl solution at room temperature was investigated (see Vol. V [23]). It was found that: (1) crack growth rates are a complex function of frequency and K level, (2) crack growth enhancement appeared to result from the formation and rupture of a hydride phase, (3) the effect of hold-time at maximum load is compatible with the observed frequency dependence, and (4) the environment can interact with the applied load to influence the so-called delay in fatigue crack growth following a high load excursion. Due to the complex dependency of the corrosion fatigue crack growth rates on both frequency and K

Whatever crack growth model is used, it should account for R-ratio and it should be justified for a range of R-ratios applicable to the given load spectrum. The effect of environment is reflected in the  $da/dN$  versus  $\Delta K$  data and a suitable crack growth model is "best fitted" to the applicable data. Data pooling procedures are recommended for calibrating the crack growth model parameters (see Appendix B) to put the parameters on a comparable baseline and to drive the variance in the  $da/dN$  versus  $\Delta K$  data into a single parameter.

There is no additional enhancement in crack growth due to the environment effect as a result of compression loading cycles. For a ductile aluminum alloy, such as we considered under this program (i.e., 7075-T7651), the fatigue crack tends to close under compressive loading. Because of this phenomena, there is uncertainty about handling the effects of compressive loads in spectrum crack growth analyses.

The effect of specimen preconditioning (preloading and presoaking in 3.5% NaCl solution at room temperature) was more pronounced for CF crack initiation than for crack propagation. After a certain pre-exposure time, a saturation point may be reached at which there is no further effect of pre-exposure on the resulting CF fatigue life. This aspect needs to be further investigated.

(5) a superposition method for determining the stress intensity factor for the combined through stress and bolt hole bearing stress case.

It is concluded that the CF analysis methodology is adequate for the 7000 series aluminum alloys in the over-aged condition. Since no significant synergistic effect between loading and environment was observed for this alloy, strain life allowables for CF crack initiation analysis and  $da/dN$  versus  $\Delta K$  data for the CF crack propagation analysis can be acquired using a fast loading frequency. This simplifies things considerably because the crack growth model used can be independent of the environment. Furthermore, the load retardation model for this alloy can be independent of the environment. It has been shown, based on both constant amplitude and spectrum fatigue test results, that the effect of the environment in CF crack initiation and CF crack propagation can be "scaled". The environmental scaling factor (ESF) was found to be very consistent for both CF crack initiation and crack propagation. An average ESF of approximately 2.0 was typically observed with the 95% confidence interval ranging from approximately 1.5 to 3.0. It is promising and reasonable to make CF crack initiation and crack propagation predictions based on a dry air environment and a suitable ESF. This aspect needs to be further investigated.

acquired using a minimum of three specimens each for crack initiation and for crack propagation. Spectrum fatigue data can also be used to justify the CF analysis for other load spectra, stress levels, environments, geometries, etc. Dog-bone specimen spectrum data are recommended for scaling the CF crack propagation analysis until suitable load-retardation models have been developed and verified for applications to any load spectra.

The CF analysis methodology has been evaluated for 7075-T7651 aluminum, two environments (i.e., dry air and 3.5% NaCl), three load spectra, and three different % bolt load transfers (i.e., 0%, 20% and 40%). The CF crack initiation predictions compared reasonably well with dog-bone specimen fatigue test results for three load spectra and two environments (dry air and 3.5% NaCl). CF crack propagation predictions correctly predicted the trends in the dog-bone specimen test results and correctly ranked the three load spectra. However, the CF crack propagation predictions did not, in general, agree with average test results. This lack of agreement is attributed mainly to an inadequate load-retardation model.

The CF crack propagation predictions were based on: (1) the RXN crack growth program [66, 67], (2) the Forman crack growth model, (3) the generalized Willenborg load-retardation model, (4) an initial crack size of 0.01" (corner flaw) and

To implement the methodology, the following experimental data is required: (1) cyclic stress-strain, (2) strain life allowables for both dry air and 3.5% NaCl environments based on smooth un-notched strain-controlled specimens, (3) constant amplitude  $da/dn$  versus  $\Delta K$  data based on compact tension or center-cracked-tension specimens for both dry air and 3.5% NaCl environments, and (4) spectrum fatigue data for a baseline specimen configuration/geometry, load spectra, stress level and environment (e.g., dry air) acquired using dog-bone specimens with a center hole.

Spectrum fatigue data should be acquired using dog-bone specimens with an open hole. An "open hole" specimen is recommended because: (1) the effect of a fastener in the hole on CF life varies depending on the fastener/hole fit, and (2) there is typically large scatter in CF test results. Therefore, a degree of conservatism is justified in view of the above and other uncertainties.

Crack initiation dog-bone specimens should be spectrum fatigue tested with no intentional preflaw in the center hole so that cracks can originate naturally. For crack propagation tests, the specimens should be spectrum fatigue tested using a corner flaw in the fastener hole (e.g., 0.01"). Spectrum fatigue test data provides the basis for "scaling" or "tuning" the CF crack initiation and crack propagation analyses. These data can be economically

## SECTION VII

### CONCLUSIONS AND RECOMMENDATIONS

#### 7.1 CONCLUSIONS

The major conclusions of this investigation for both 7075-T7651 aluminum alloy and beta annealed Ti-6Al-4V alloy are summarized below. Further conclusions about the effects of specific test variables on corrosion fatigue for the aluminum alloy are given in Section IV and Appendices A - D in this volume (III) and in volume I [22]. The titanium research is documented in volume V [23]; highlights are discussed in Section VI (Vol. III) and overall conclusions are summarized in this section.

##### 7.1.1 CF Methodology/Aluminum Research

A reasonable corrosion fatigue (CF) analysis methodology has been developed for mechanically-fastened joints and it has been evaluated for 7000 series aluminum alloy applications. The methodology includes the strain-life approach for predicting the time-to-crack-initiation (TTCI) and the deterministic crack growth approach for predicting crack propagation.

following a high load excursion [116]. Specifically delay, defined as the number of cycles of loading before the rate of fatigue crack growth recovers to its steady-state value, is a complex function of K level, overload ratio, the number of overload cycles and the duration of each overload. The spectrum-load fatigue life, therefore, is expected to be a complex function of frequency, load level and load sequence. The amount of data that would be required to make life predictions, using one of the available cycle-by-cycle procedures, is prohibitively large. Development of novel procedures that can incorporate the combined load/environment interactions on an integrated or an average basis must be considered, and is recommended for future research.

rupture of a hydride phase. The formation of hydrides is known to a function of strain, and is apparently a strong function of strain rate.

Based on these experimental observations, the corrosion fatigue crack growth response of beta annealed Ti-6Al-4V alloy in 3.5% NaCl solution, at room temperature, is interpreted in terms of control by hydrogen diffusion to the "fracture process zone" at frequencies below that for the maximum rate at each K level and of a critical strain rate required for hydride formation in the crack tip region. Reductions in frequency below that required to produce a maximum in crack growth rate lowered the effective crack tip strain rate below an apparent "critical" value, whereby hydrides could not be formed and embrittlement ceased.

### 6.3 IMPLICATIONS OF TITANIUM ALLOY RESPONSE ON CORROSION FATIGUE LIFE PREDICTION METHODS

The observed complex dependency of corrosion fatigue crack growth rates on both frequency and K level makes it nearly impossible to formulate an effective life prediction procedure for the titanium alloys at this time. Furthermore, the environment can also interact with the applied load to influence the so-called delay in fatigue crack growth

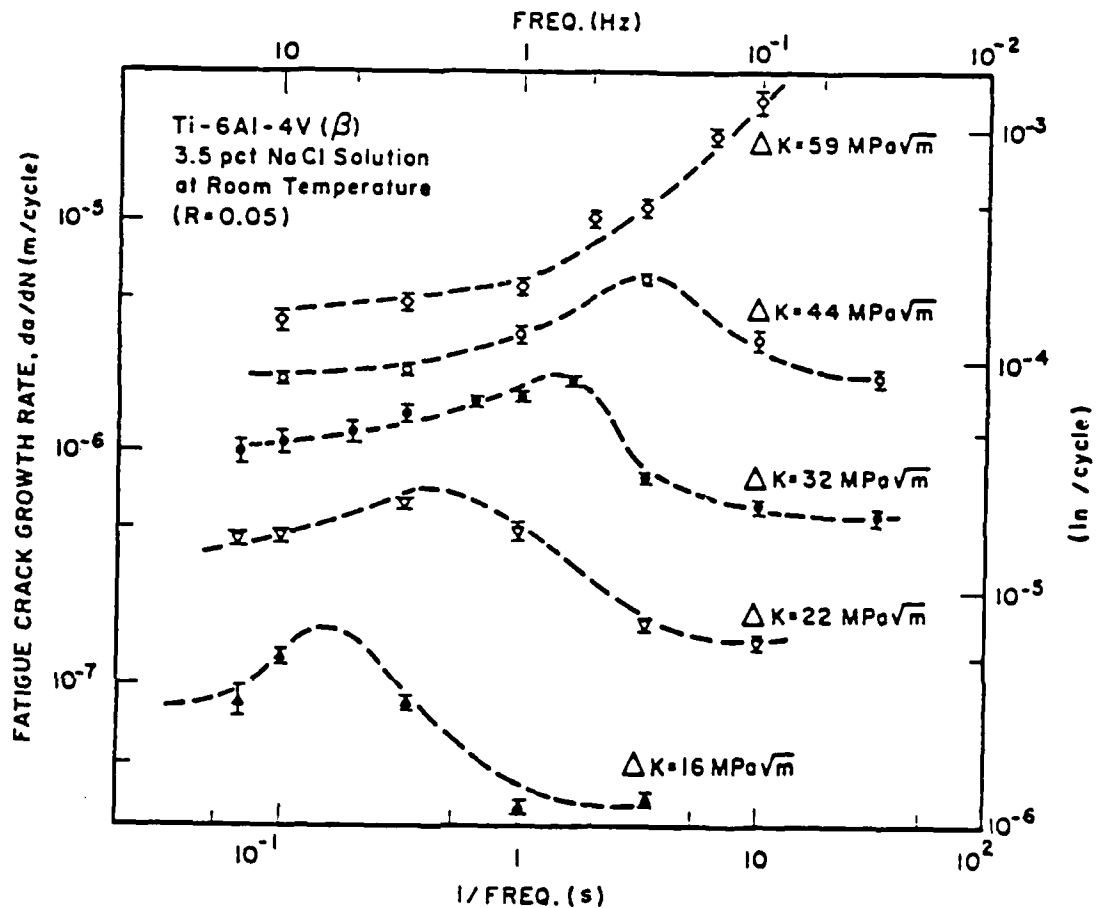


Fig. 24 The influence of frequency on fatigue crack growth rate of beta-annealed Ti-6Al-4V alloy in 3.5% NaCl solution at room temperature (R = 0.05).

## 6.2 EFFECT OF FREQUENCY ON FATIGUE CRACK GROWTH

The results showed that fatigue crack growth rates in the beta annealed Ti-6Al-4V alloy increased with decreasing frequency, and then decreased rapidly with further decreases in frequency, reaching rates that are commensurate with those in an inert reference environment (for example, in vacuum). The frequency at which the crack growth rates reached a maximum depended on the K level, and was found to be proportional to  $(\Delta K)^3$ .

For example, at  $\Delta K = 22 \text{ MPa}\sqrt{\text{m}}$  (or  $20 \text{ ksi}\sqrt{\text{in}}$ ) and  $R = 0.05$ , the crack growth rate increased from about  $5 \times 10^{-7} \text{ m/cycle}$  (or  $2 \times 10^{-5} \text{ in./cycle}$ ) at 10 Hz to its maximum of about  $8 \times 10^{-7} \text{ m/cycle}$  (or  $3.2 \times 10^{-5} \text{ in./cycle}$ ) at about 2 Hz, and then decreasing to about  $1.3 \times 10^{-7} \text{ m/cycle}$  (or  $5 \times 10^{-6} \text{ in./cycle}$ ) at 0.1 Hz (Ref. Fig. 15). At  $\Delta K = 44 \text{ MPa}\sqrt{\text{m}}$  (or  $40 \text{ ksi}\sqrt{\text{in}}$ ), the frequency for the maximum in growth rate was shifted to about 0.4 Hz, and that for the minimum rate was shifted to below 0.03 Hz. The effect of hold-time at maximum load is compatible with the observed frequency dependence.

The fracture surface morphology also showed strong dependence on frequency and K level, and suggested that the enhancement of crack growth resulted from the formation and

CF crack propagation (TFCG) life. The deleterious effect of preconditioning is believed to be the result of surface damage produced by fatigue assisted corrosion (e.g., pitting) the irregular nature of the damage is reflected in the considerable scatter observed in the experimental results for preconditioned specimens.

Further research is required to resolve the following issues on preconditioning: (1) how long should test specimens be pre-exposed to a 3.5% NaCl environment to reach a saturation point where pre-exposure no longer reduces CF life? (2) how can specimen preconditioning be directly related to actual in-service conditions?, and (3) realistic accelerated corrosion fatigue testing procedures are needed.

TFCG predictions correctly rank the three load spectra considered according to severity.

8. Preconditioning - Fastener holes in exterior surfaces of in-service aircraft are particularly susceptible to corrosion-related problems when the paint or protective coating is broken. The protective coating may be broken by a combination of service loading, wear, temperature, etc. Once the protective barrier has been broken, the metal surfaces are exposed to corrosive attack. Specimens can be preconditioned to simulate a break in the protective coating and the subsequent effect of surface exposure to a corrosive environment (e.g., 3.5% NaCl).

Methods have been developed and evaluated for preconditioning test specimens by Wanhill and LeLuccia [16, 19]. Selected dog-bone specimens were preconditioned and then fatigue tested under this program using the general procedure described in Ref. 16. Dog-bone specimens were preconditioned by exposing them to 72 hours of 3.5% NaCl solution (constant immersion) following one 300 or 400 hour block of fatigue loading. Only dog-bone specimens were preconditioned. After preconditioning the specimens, they were fatigue tested the same way as un-preconditioned specimens (see Vol. IV [24]).

The dog-bone specimen test results showed that preconditioning significantly reduced the CF time-to-crack-initiation (TTCI) life but it had a negligible effect on the

used.

6. It has been shown herein, that the effects of the environment on the CF crack propagation can be "scaled" for the 7000 series aluminum alloys in the over-aged condition. For example, in Table 20 the average dry/wet ratio for TFCG predictions and test results was 2.26 and 2.29, respectively. This strongly suggests that the effect of the environment on CF crack propagation can be accounted for in the baseline  $da/dN$  versus  $\Delta K$  data for the applicable environment. It is interesting to note that the average dry/wet ratio for TICI predictions was 1.69 (see Table 17) and that for TFCG predictions was 2.26. Similarly, the average dry/wet ratio for TICI test results was 2.09 (see Table 17) and that for TFCG test results was 2.29. Although corrosion fatigue test results typically exhibit considerable scatter, the "scaling" factors for accounting for the environmental effect are very comparable for both CF crack initiation and CF crack propagation.

7. The modified Willenborg retardation model was used to make TFCG predictions in this report. A study was made to determine the effect and sensitivity of the  $\Delta K_{th}$  (threshold) and overload a shut-off ratio ( $R_{os}$ ) on the TFCG predictions. The results shown in Table 20 show that: (1) the effects of the environment on TFCG predictions correctly scale as borne out by the dry/wet test results and (2) the

containing alloys in the peak-aged condition, the crack growth data should be acquired at the lowest loading frequency expected in service.

3. Further research is needed to develop a mechanistic-based retardation model that generally applies to widely different load spectra. Ideally, the applicable model parameters should be definable using basic material data rather than spectrum data. Until an improved retardation model is developed and proven it is recommended that a minimum of three dog-bone specimens with a center hole (0.01" corner preflaw) be fatigue tested using a baseline spectrum to acquire data that can be used to calibrate the retardation model used. Such tests are relatively inexpensive and the payoff is increased confidence in the CF crack propagation predictions.

4. The retardation model and the crack growth model used to implement the CF crack propagation methodology should be independent of the environment. Edwalds et al [130] found that crack closure behavior was independent of environment for 2024-T3 aluminum. The crack growth model can be calibrated using  $da/dN$  versus  $\Delta K$  data for a dry air environment and for other environments (e.g., 3.5% NaCl).

5. In any case, the crack growth model used to implement the CF crack propagation methodology should account for R-ratio. Also, the calibrated model should apply to a range of R-ratios that are applicable to the load spectrum

level, it is nearly impossible to formulate an effective life prediction procedure for the titanium alloys at this time.

## 7.2 RECOMMENDATIONS

The following research is recommended:

1. Develop an improved load-retardation model which applies to any load spectra. The model should account for load sequence, both tension and compression overloads, multiple overloads, and the number of loading cycles. Ideally, the model parameters can be calibrated using basic material data independent of load spectra and the model can be applied to any load spectra without having to generate a new data base for each load spectrum.

2. This program was concerned with straight bore fastener holes with clearance-fit steel bolts with protruding heads. The CF behavior of countersunk fastener holes should also be investigated and the CF analysis methodology described in Section V should be evaluated for application to countersunk fastener holes.

3. The CF analysis methodology described in Section V has been evaluated considering the most fundamental elements of a mechanically-fastened joint (i.e., hole, bolt and bolt load transfer. An evaluation of the CF analysis methodology

for applications to more complex mechanically-fastened joints should be investigated.

4. In practice, the amount of bolt load transfer in metallic aircraft joints usually depends on factors, such as the fastener type and fit, the stiffness of the mating elements and the applied load level. Under this program spectrum fatigue tests were performed using dog-bone specimens with a fixed amount of bolt load transfer (i.e. ram load introduced directly into bolt to control the amount of load transfer). The effect of a variable % bolt load transfer in a mechanically-fastened joint on CF crack initiation and crack propagation life should be investigated and the CF analysis methodology refined (if necessary) to account for this effect.

5. Investigate the environmental pre-exposure time required to reach a saturation point where the effect of the pre-exposure (i.e., 3.5% NaCl solution at room temperature) no longer has a significant effect on crack initiation and crack propagation life. This investigation should be performed using an over-aged and peak-aged aluminum alloy such as 7075-T7651 and 7075-T651, respectively. General guidelines for specimen preconditioning need to be further developed and evaluated for implementing the recommended CF analysis methodology.

6. The effect of strain-controlled specimen precondi-

tioning (i.e., precycling and pre-exposure to a 3.5% NaCl solution at room temperature) on strain life allowables and CF crack initiation life should be investigated.

7. Since the crack growth rate for the beta annealed Ti-6Al-4V alloy depends on both frequency and K level, an effective CF life prediction procedure cannot be formulated at this time. Novel procedures should be developed that can incorporate the combined load/environment interactions on an integrated or average basis into the CF crack propagation prediction method for the beta annealed Ti-6Al-4V alloy.

(This page intentionally left blank)

APPENDIX A

MATERIAL CONSTANTS FOR IMPLEMENTING  
THE STRAIN-LIFE APPROACH  
FOR CRACK INITIATION

A.1 INTRODUCTION

Material constants for 7075-T7651 aluminum that are needed to implement the strain-life analysis for predicting the time-to-crack-initiation are presented herein. Procedures are described for computing the material constants from the experimental data. Constants are presented for the cyclic stress-strain relationship and for the modified Coffin-Manson strain-life equation.

A.2 CYCLIC STRESS-STRAIN RELATIONSHIP

A cyclic stress-strain relationship is needed to determine the local stress and strain at the notch using Neuber's rule [48]. The empirical expression, given in Eq. A-1, provides the relationship between local stresses and strains. In Eq. A-1:  $\sigma$  = local stress (ksi),  $E$  = modulus of elasticity (ksi),  $n'$  = cyclic strain hardening exponent and  $K'$  = cyclic strength coefficient (ksi).

$$\epsilon = \frac{\sigma}{E} + \left( \frac{\sigma}{K'} \right)^{1/n'} \quad (A-1)$$

The constants  $n'$  and  $K'$  in Eq. A-1 can be determined from the applicable cyclic stress-strain curve. Such a curve is shown in Fig. A-1 for 7075-T7651 aluminum [28]. The first term in Eq. A-1,  $\sigma/E$ , is the elastic strain relationship and the second term,  $(\sigma/K')^{1/n'}$ , is the relationship for plastic strain.

The plastic strain can be determined from the cyclic stress-strain curve (Fig. A-1) by subtracting the elastic strain from the total strain. The resulting plastic strain results can then be used to determine the constants  $n'$  and  $K'$  in Eq. A-1 using the expression for plastic strain,  $\epsilon_p$ .

$$\epsilon_p = \left( \sigma/K' \right)^{1/n'} \quad (A-2)$$

Equation A-2 can be transformed into a linear least squares fit form by taking the log of both sides of the equation as follows

$$\log \epsilon_p = 1/n' \log(\sigma/K') = \frac{1}{n'} \log \sigma - \frac{1}{n'} \log K' \quad (A-3)$$

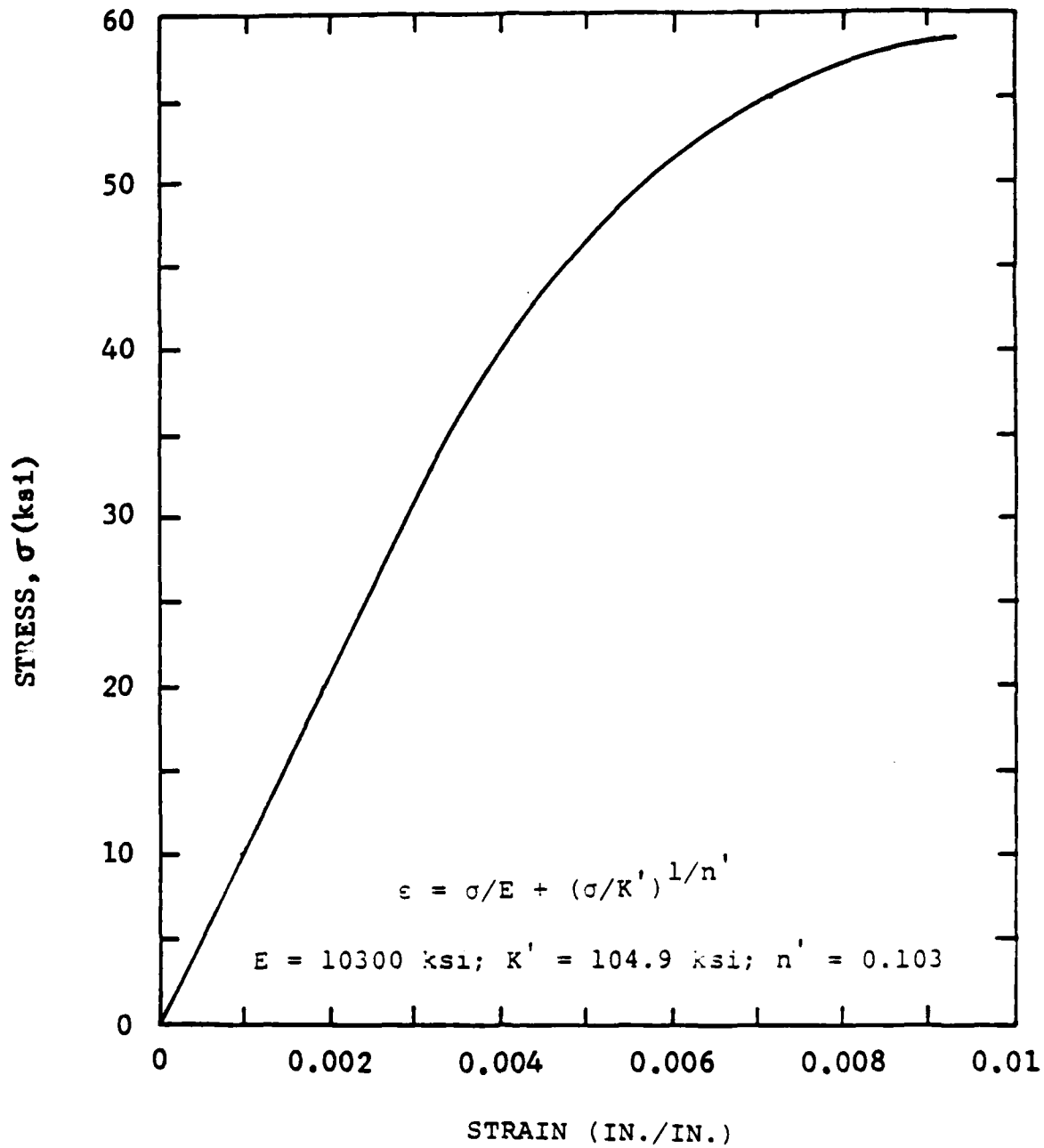


Fig. A-1 Cyclic Stress-Strain Curve for 7075-T7651 Aluminum

Using the cyclic stress-strain curve of Fig. A-1 and Eq. A-3, the following results were obtained using a least squares fit:  $n' = 0.103$ ,  $K' = 104.9$  ksi. The meaning of the constants  $n'$  and  $K'$  is illustrated in Fig. A-2.

### A.3 CONSTANTS FOR MODIFIED COFFIN-MANSON EQUATION

The constants  $b$ ,  $c$ ,  $(\sigma'_f/E)$  and  $\epsilon'_f$  in the modified Coffin-Manson expression, Eq. A-4, are determined in this section for 7075-T7651 aluminum for both dry air and 3.5% NaCl environment.

$$\begin{aligned} \epsilon &= \epsilon_e + \epsilon_p \\ \epsilon &= \underbrace{(\sigma'_f/E)(2N_i)^b}_{\text{Elastic}} + \underbrace{\epsilon'_f(2N_i)^c}_{\text{Plastic}} \end{aligned} \quad \left. \vphantom{\begin{aligned} \epsilon &= \epsilon_e + \epsilon_p \\ \epsilon &= \underbrace{(\sigma'_f/E)(2N_i)^b}_{\text{Elastic}} + \underbrace{\epsilon'_f(2N_i)^c}_{\text{Plastic}} \end{aligned}} \right\} \quad (\text{A-4})$$

In Eq. A-4,  $\epsilon_e$  = elastic strain amplitude (in/in),  $\epsilon_p$  = plastic strain amplitude (in/in),  $\sigma'_f$  = fatigue strength coefficient (ksi),  $E$  = modulus of elasticity (ksi),  $2N_i$  = number of reversals to crack initiation,  $b$  = fatigue strength exponent,  $\epsilon'_f$  = fatigue ductility coefficient (in/in) and  $c$  = fatigue ductility exponent.

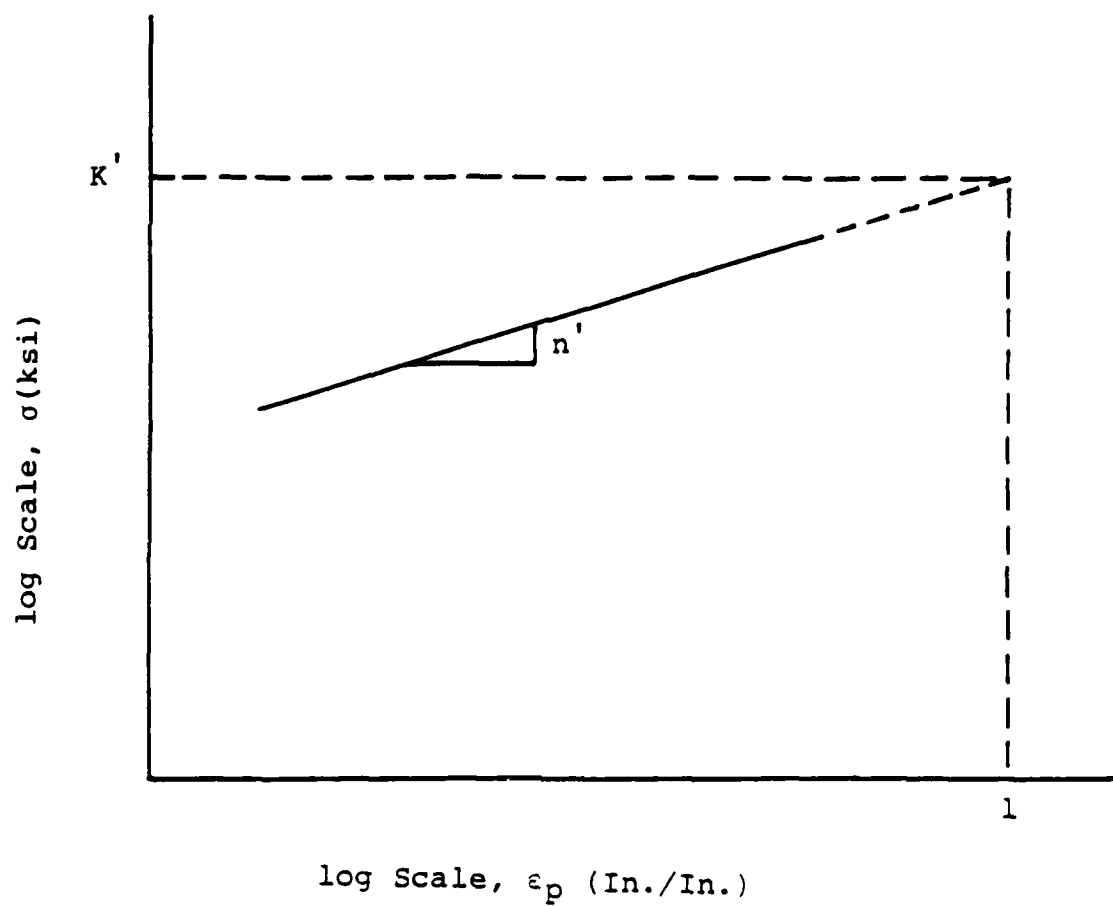


Fig. A-2 True Stress Versus Plastic Strain  
for Cyclic Response (log-log Scale)

The strain-life results from the strain-controlled tests performed in Phase II are presented in Tables A-1 and A-2 for dry air/lab air and 3.5% NaCl solution, respectively. The total strain amplitude is approximated by elastic and plastic segments as follows, where  $\Delta\epsilon_{T/2} = \Delta\epsilon_{e/2} + \Delta\epsilon_{p/2}$ .

$$\Delta\epsilon_{e/2} = (\sigma'_{f/E}) (2N_i)^b \quad (A-5)$$

$$\Delta\epsilon_{p/2} = \epsilon'_f (2N_i)^c \quad (A-6)$$

Equations A-5 and A-6 can be transformed into a linear least squares fit form as follows:

$$\log \Delta\epsilon_{e/2} = \log(\sigma'_{f/E}) + b \log(2N_i) \quad (A-7)$$

$$\log \Delta\epsilon_{p/2} = \log \epsilon'_f + c \log(2N_i) \quad (A-8)$$

The constants  $b$ ,  $c$ ,  $(\sigma'_{f/E})$  and  $\epsilon'_f$  in Eqs. A-5 and A-6 were determined using Eqs. A-7 and A-8 and the applicable strain life results from Tables A-1 and A-2.

TABLE A-1 SUMMARY OF STRAIN-LIFE RESULTS FOR  
7075-T7651 ALUMINUM IN DRY AIR AND LAB AIR

SPECIMEN NO.	FREQ. (HZ)	ENVIRONMENT	$\Delta\epsilon_e/2$ (IN/IN)	$\Delta\epsilon_p/2$ (IN/IN)	$\Delta\epsilon_T/2$ (IN/IN)	$2N_i$ (REVERSALS)
40CS	5	DRY AIR	.00370	--	.0037	183200
12CS	2	DRY AIR	.00420	--	.0042	57660
6CS	2	LAB AIR	.00420	--	.0042	55400
39CS	5	DRY AIR	.00496	--	.0050	23600
29CS	0.5	↑	.00510	--	.0051	18800
31CS	2		.00530	--	.0053	14000
20CS	2		.00520	--	.0052	13600
7CS	0.5		.00594	.00006	.0060	8380
37CS	↑		.00658	.00012	.0067	3820
43CS	↑		.00680	.00030	.0071	1760
17CS	↓		.00690	.00050	.0074	1800
21CS	↓		.00786	.00104	.0089	920
46CS	0.5		.00803	.00097	.0090	860
51CS	0.1		.00788	.00112	.0090	860
28CS	5	↓	.00802	.00178	.0098	700
13CS	0.5		.00860	.00180	.0104	680
18CS	↑		.01003	.00277	.0128	420
8CS	↑		.00907	.00233	.0114	420
4CS	↑		.00955	.00395	.0135	300
24CS	↓		.01117	.00513	.0163	200
19CS	↓		.01164	.00596	.0170	220
52CS	0.5		.01210	.00810	.0202	110

NOTES:  $\Delta\epsilon_{e/2}$  = Total elastic strain amplitude

$\Delta\epsilon_{p/2}$  = Total elastic strain amplitude

$\Delta\epsilon_{T/2}$  = Total strain amplitude

$2N_i$  = Number of reversals to initiate  
a crack depth of  $a_0 = 0.010"$

Ref. Vol. IV [24] Test Results

TABLE A-2 SUMMARY OF STRAIN-LIFE RESULTS FOR 7075-T7651 ALUMINUM  
IN 3.5% NaCl SOLUTION AT ROOM TEMPERATURE

SPECIMEN NO.	FREQ. (HZ)	ENVIRONMENT	$\Delta\epsilon_e/2$ (IN/IN)	$\Delta\epsilon_p/2$ (IN/IN)	$\Delta\epsilon_T/2$ (IN/IN)	$2N_i$ (REVERSALS)
49CS	5	3.5% NaCl ↑	.00270	--	.0027	213000
48CS	5		.00290	--	.0029	109060
42CS	5		.00310	--	.0031	81120
38CS	2		.00330	--	.0033	66700
47CS	5		.00370	--	.0037	49260
34CS	2		.00380	--	.0038	43680
30CS	2		.00370	--	.0037	33660
11CS	2		.00430	--	.0043	38100
15CS	0.5		.00430	--	.0043	22080
35CS	2		.00450	--	.0045	16740
22CS	2		.00520	--	.0052	9740
32CS	0.5		.00519	.00001	.00520	9160
33CS	5		.00527	.00003	.00530	7020
9CS	0.5		.00583	.00007	.00590	3820
16CS	2		.00635	.00015	.00650	2280
44CS	0.5		.00631	.00029	.00660	1380
36CS	0.5		.00792	.00068	.00860	850
45CS	0.1		.00795	.00105	.00900	640
23CS	0.5		.00786	.00104	.00890	580
14CS	↑		.00818	.00162	.00980	480
10CS	↓		.00950	.00300	.01250	300
26CS	↓		.01136	.00490	.01630	140
41CS	0.5	3.5% NaCl	.01220	.00800	.02020	88

NOTES:  $\Delta\epsilon_{e/2}$  = Total elastic strain amplitude

$\Delta\epsilon_{p/2}$  = Total plastic strain amplitude

$\Delta\epsilon_{T/2}$  = Total strain amplitude

$2N_i$  = Number of reversals to initiate a crack  
depth of  $a_0 = 0.010"$

Ref. Vol IV [24] Test Results

The strain life-results for dry air and 3.5% NaCl solution are plotted in Figs. A-3 and A-4, respectively. Applicable constants are also shown for 50% confidence for both elastic and plastic strain amplitudes.

A 95% scatter band was also estimated for the elastic and plastic strain amplitude segments using correlation theory [e.g., 78]. The scatter band was determined assuming the applicable "b" and "c" constants in Eqs. A-7 and A-8 were fixed for any percentile and the strain amplitude variance was fixed for both the elastic and plastic strain segments. The standard error of estimate of the population of applicable sample strain amplitudes was determined using Eq. A-9.

$$\hat{S}_{y.x} = \sqrt{\frac{\sum (y - y_{EST})^2}{N-2}} \quad (A-9)$$

In Eq. A-9,  $y = \log \Delta \epsilon_{e/2}$  (elastic) or  $\log \Delta \epsilon_{p/2}$  (plastic),  $y_{EST} = \log (\sigma'_f/E) + b \log (2N_i)$  (elastic) or  $\log \epsilon'_f + c \log (2N_i)$  (Plastic),  $N$  = strain amplitude sample size. Strain amplitude for selected probabilities (i.e.,  $P = .025$  and  $P = 0.975$ ) were determined using Eqs. A-10 through A-12.

$$X = \mu \pm Z \hat{S}_{y.x} \quad (A-10)$$

$$\log \Delta \epsilon_{e/2} = \{ \log(\sigma'_{f/E}) + b \log(2N_i) \pm Z \hat{S}_{y.x} \} \quad (A-11)$$

$$\log \Delta \epsilon_{p/2} = \{ \log(\epsilon'_f) + c \log(2N_i) \pm Z \hat{S}_{y.x} \} \quad (A-12)$$

In Eq. A-10,  $\mu$  = mean  $\log(\Delta \epsilon_{e/2})$  or mean  $\log(\Delta \epsilon_{p/2})$ ,  $Z$  = number of standard deviations from the mean and  $\hat{S}_{y.x}$  = standard error of estimate for log strain amplitude sample. For a 95% scatter band,  $Z = 1.96$ . Using Eq. A-11 and  $Z = 1.96$ , the  $\Delta \epsilon_{e/2}$  value corresponding to the 2.5 and 97.5 percentiles can be determined. The same information can be determined for  $\Delta \epsilon_{p/2}$  using Eq. A-12 and  $Z = 1.96$ .

The estimated 95% scatter bands for the elastic and plastic strain amplitude segments are shown in Figs. A-3 and A-4 for dry air and 3.5% NaCl solution, respectively. Coffin-Manson constants are summarized in Table A-3, including the  $(\sigma'_{f/E})$  and  $\epsilon'_f$  values corresponding to the upper and lower bounds of the 95% scatter band.

Total strain amplitude experimental results are plotted in Figs. A-5 and A-6 for dry air and for 3.5% NaCl solution, respectively. Empirical total strain amplitude curves for  $P = 0.50$  are also plotted. These plots are based on the applicable constants shown in Table A-3.

AD-A160 378

DEVELOPMENT OF FATIGUE AND CRACK PROPAGATION DESIGN AND  
ANALYSIS METHODOLOGY (U) GENERAL DYNAMICS FORT WORTH TX  
FORT WORTH DIV S D MANNING ET AL OCT 84

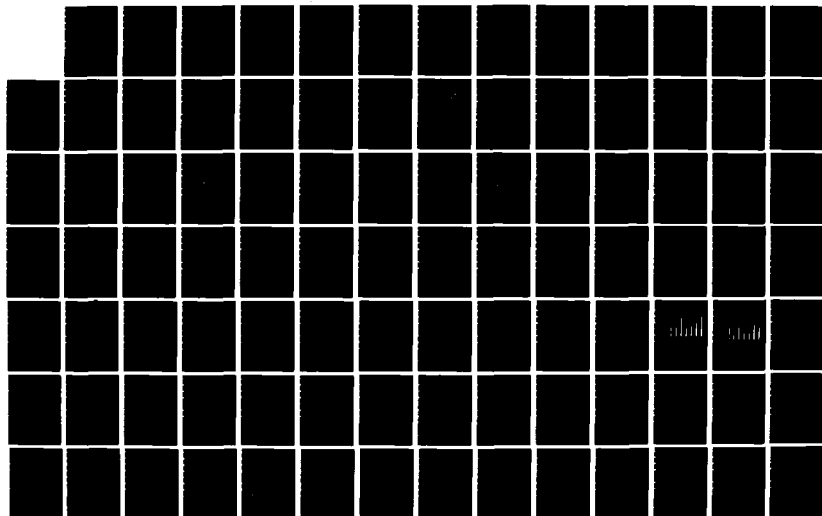
3/4

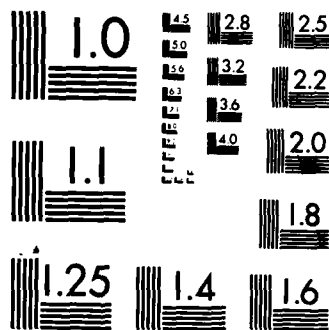
UNCLASSIFIED

NADC-83126-60-VOL-3 N62269-81-C-0268

F/G 11/6

NL





MICROCOPY RESOLUTION TEST CHART  
NATIONAL BUREAU OF STANDARDS 1963-A

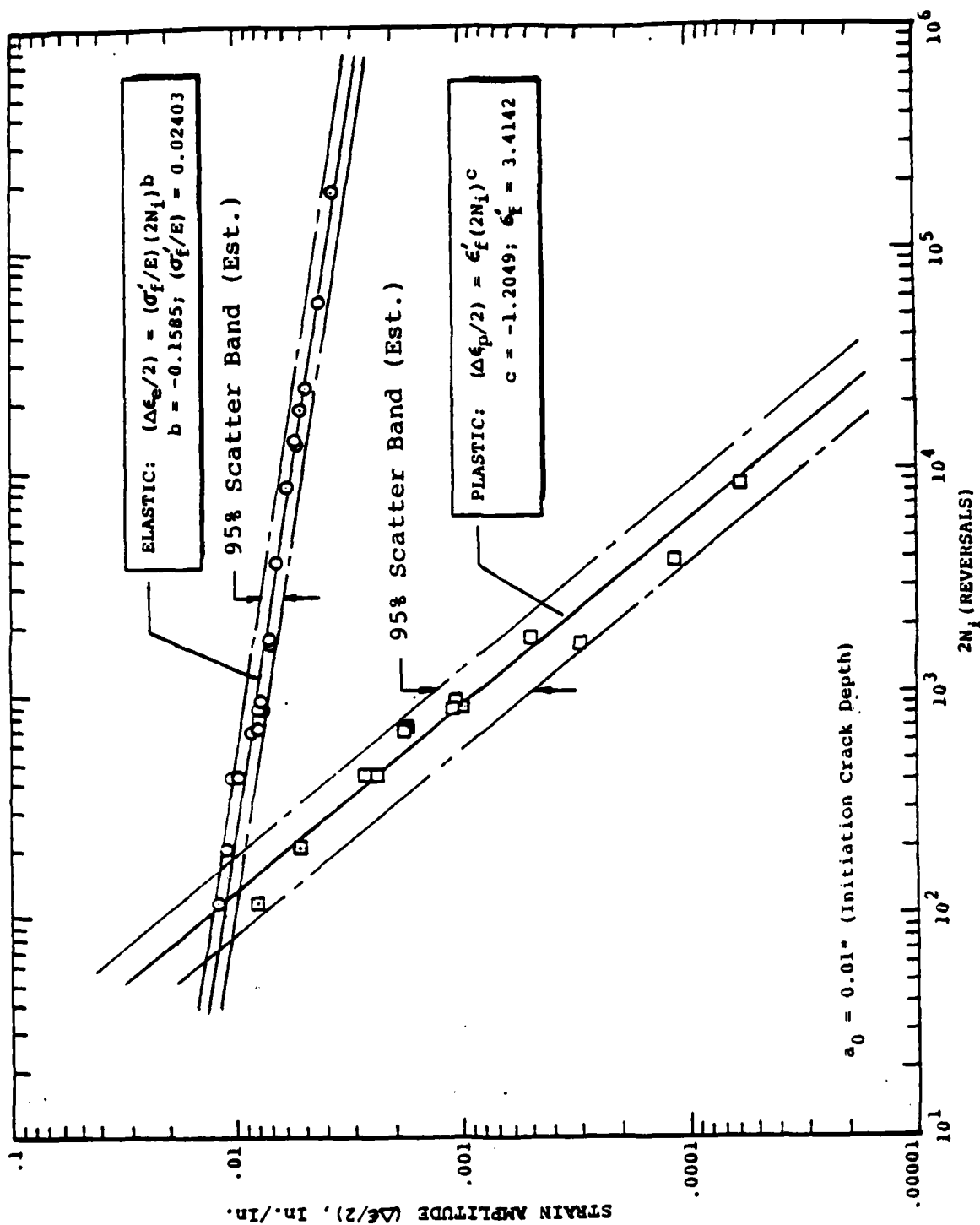


Fig. A-3 Strain Amplitude Versus  $2N_f$  (Reversals) for 7075-T7651 Aluminum in Dry Air

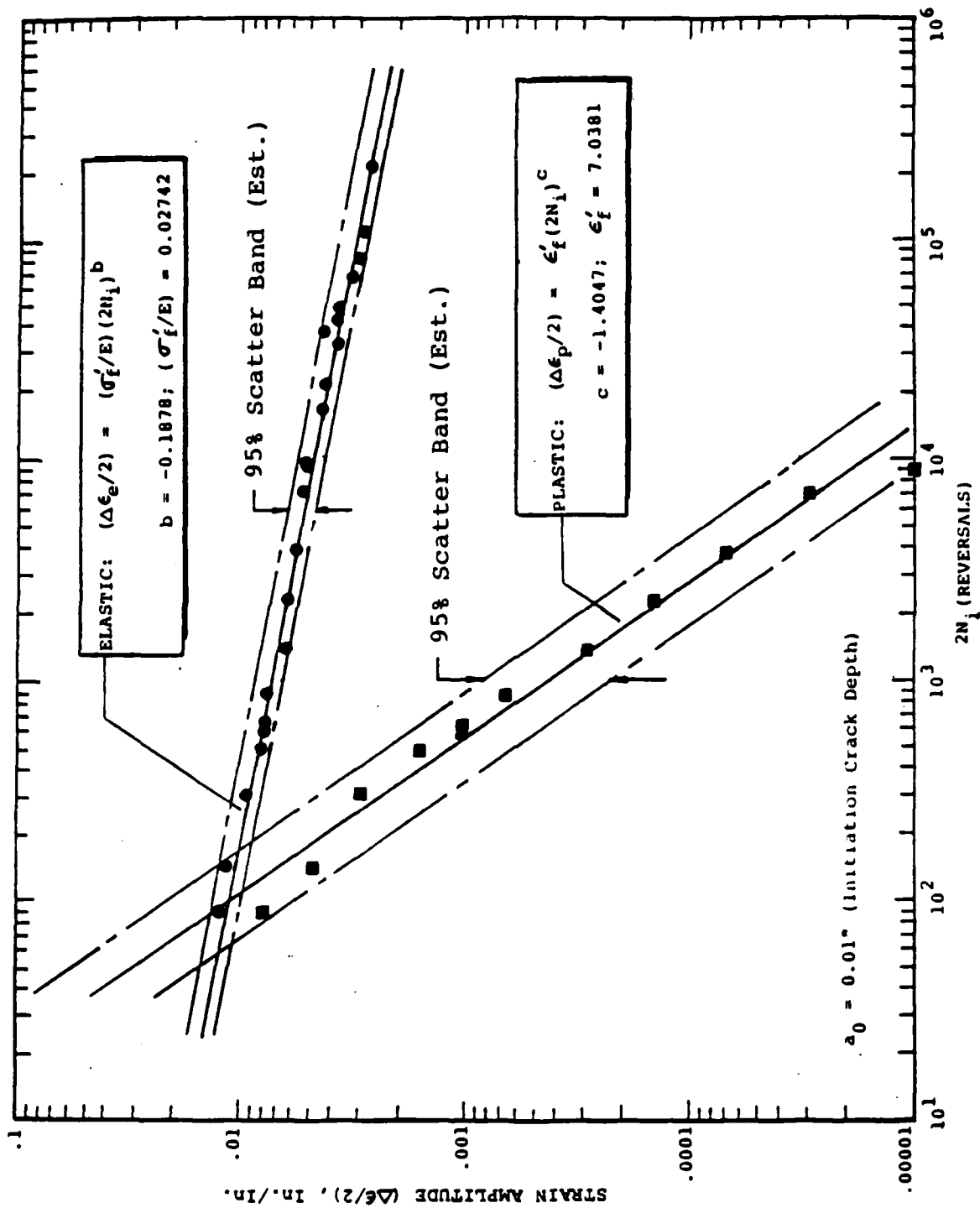


Fig. A-4 Strain Amplitude Versus  $2N_i$  (Reversals) for  
 7075-T7651 Aluminum in 3.5% NaCl Solution at  
 Room Temperature

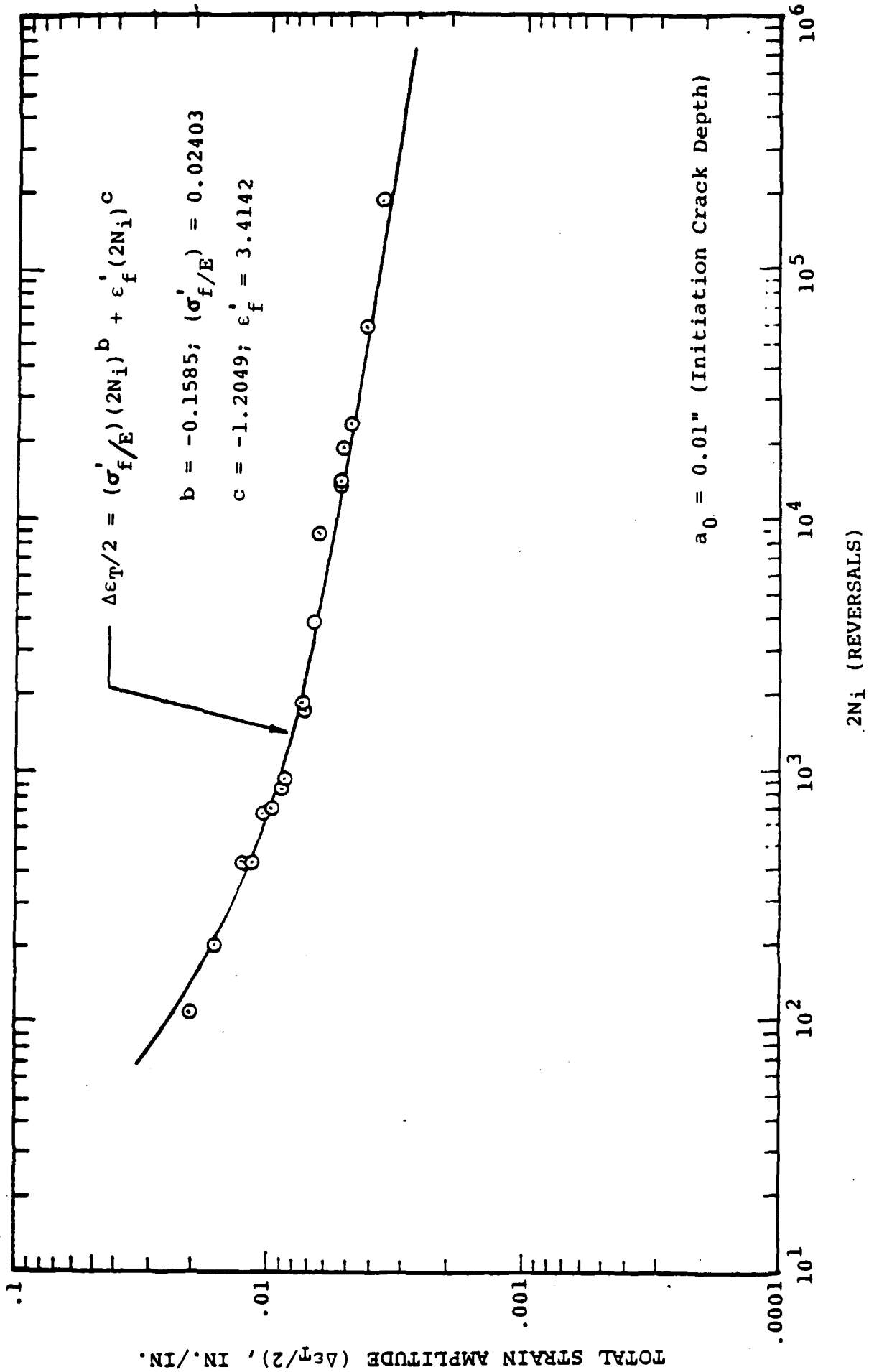


Fig. A-5 Total Strain Amplitude Versus  $2N_i$  (Reversals) for 7075-T7651 Aluminum in Dry Air

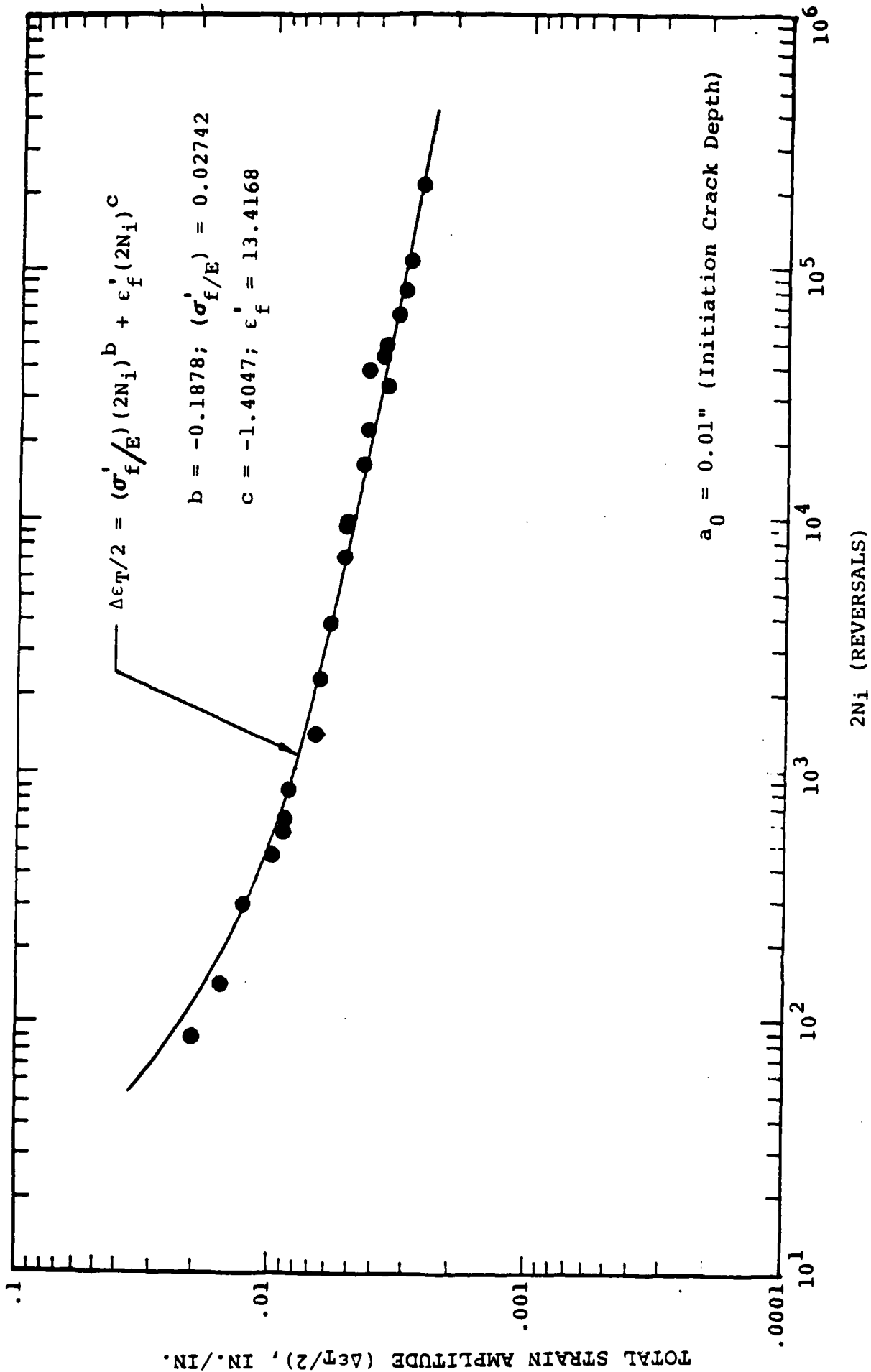
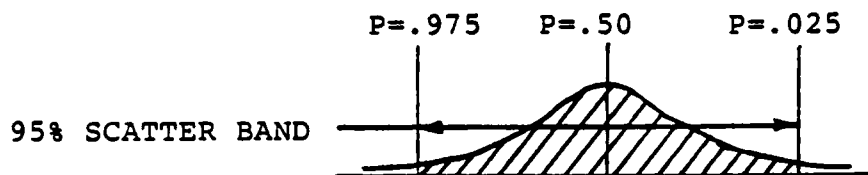


Fig. A-6 Total Strain Amplitude Versus  $2N_i$  (Reversals)  
 for 7075-T7651 Aluminum in 3.5% NaCl Solution  
 at Room Temperature

TABLE A-3 SUMMARY OF STRAIN-LIFE CONSTANTS FOR  
BOTH DRY AIR AND 3.5% NaCl SOLUTION



ENVIRONMENT	CONSTANT	P=.975	P=.50	P=.025
DRY AIR $\updownarrow$ DRY AIR	$(\sigma'_f/E)$	.02191	.02403	.02636
	b	--	-.1585	--
	$\epsilon'_f$	2.0957	3.4142	5.5619
	c	--	-1.2049	--
3.5% NaCl $\updownarrow$ 3.5% NaCl	$(\sigma'_f/E)$	.02471	.02742	.03426
	b	--	-.1878	--
	$\epsilon'_f$	3.6919	7.0381	13.4168
	c	--	-1.4047	--

NADC-83126-60-VOL. III

(This page intentionally left blank)

APPENDIX B

EVALUATION OF DA/DN VERSUS  $\Delta K$  EXPERIMENTAL DATA  
AND CRACK GROWTH MODELS FOR 7075-T7651 ALUMINUM

Contents

<u>Section</u>		<u>Page</u>
B.1	Introduction	B-2
B.2	Evaluation of Paris Crack Growth Model	B-4
B.3	Study Sensitivity of Paris Crack Growth Model Parameters with Respect to Various Factors	B-15
B.4	Evaluation of Superposition Crack Growth Model	B-17
B.5	Evaluation of Forman Crack Growth Model	B-25

## APPENDIX B

EVALUATION OF  $da/dN$  VERSUS  $\Delta K$  EXPERIMENTAL DATA  
AND CRACK GROWTH MODELS FOR 7075-T7651 ALUMINUM

## B.1 INTRODUCTION

The studies herein provide the basis for selecting a "suitable" crack growth model to be used later to make corrosion fatigue crack growth analysis predictions. The purpose of this appendix is to evaluate the  $da/dN$  data from Phase I for application in the crack growth analyses and in particular to:

1. Fit the Paris crack growth model parameters in Eq. B-1 using  $da/dN$  versus  $\Delta K$  data for 7075-T7651 aluminum from Phase I [85,86]. In Eq. B-1,  $da/dN$  = crack growth rate (in./cycle),  $C$  and  $m$  are empirical constants and  $\Delta K$  is the stress intensity range.

$$da/dN = C(\Delta K)^m \quad (B-1)$$

2. Study the influence of various factors (e.g., R ratio, loading frequency and environment) on the Paris crack growth model parameters  $m$  and  $C$  in Eq. B-1.

3. Evaluate the empirical crack growth parameters ( $C_1$ ,  $C_2$  and  $m_1$  in the two-segment superposition model [27] of Eq. B-2 and correlate experimental and predicted results. In Eq. B-2,  $(da/dN)_e$  = rate of fatigue crack growth in an aggressive environment,  $(da/dN)_r$  = rate of fatigue crack growth in an inert environment and  $(da/dN)_{cf}$  = cycle-dependent corrosion fatigue crack growth rate.

$$\begin{aligned} (da/dN)_e &= (da/dN)_r + (da/dN)_{cf} \\ &= \underbrace{C_1 (\Delta K)^{m_1}}_{\text{Dry Air}} + C_2 (\Delta K)^2 \end{aligned} \quad (B-2)$$

4. Evaluate the Forman crack growth model parameters in Eq. B-3 (i.e.,  $n$  and  $C$ ) and study the effects of R-ratio and environment on  $da/dN$ . Also, investigate the use of  $da/dN$  versus  $\Delta K$  data for one R-ratio to make predictions for another R-ratio and goodness-of-fit.

$$da/dN = C(\Delta K)^n / ((1-R)K_c - \Delta K) \quad (B-3)$$

In Eq. B-3,  $da/dN$  = crack growth rate (in./cycle),  $C$  and  $n$  are empirical constants,  $R$  = stress ratio,  $K_c$  = critical stress intensity factor and  $\Delta K$  = stress intensity range.



There are usually many different R-ratios in a loading spectrum and the effects of the R-ratio on the corrosion fatigue crack growth predictions must be accounted for. Various crack growth models have been proposed which account for the effects of the R-ratio on the crack growth rate; e.g., Forman [87], Modified Forman [88], Collipriest [89], Walker -  $\Delta K$  [90] and Badalian [91]. To minimize  $da/dN$  versus  $\Delta K$  data requirements for different R-ratios and environments, the ideal crack growth model would be one that could be calibrated using  $da/dN$  versus  $\Delta K$  data for one or more R-ratios and the model could then be used to predict  $da/dN$  for selected  $\Delta K$ s for a practical range of R-ratios.

Experimental results for  $da/dN$  versus  $\Delta K$  for 7075-T7651 aluminum from the Phase I effort [22] are presented in Tables B-1 through B-4 for dry air ( $R = .05$ ), 3.5% NaCl ( $R = .05$ ), dry air ( $R = .3$ ), and 3.5% NaCl ( $R = .3$ ), respectively. These results are used for the evaluations herein.

## B.2 EVALUATION OF PARIS CRACK GROWTH MODEL



The Paris crack growth model parameters  $m$  and  $C$  in Eq. B-1 were fitted herein using the  $da/dN$  versus  $\Delta K$  data presented in Tables B-1 through B-4.

TABLE B-1       $da/dN$  VERSUS  $\Delta K$  RESULTS FOR 7075-T7651 ALUMINUM  
IN DRY AIR ( $R = 0.05$ ;  $f = 0.1$  HZ, 1 HZ, 6 HZ)

ENVIRONMENT	R	FREQ. (HZ)	$\Delta K$ (ksi- $\sqrt{\text{In}}$ )	$da/dN \times 10^6$ (In./Cycle)
Dry  	0.05	0.1	4.3	0.380
			4.3	0.480
			5.5	1.400
			6.7	2.800
		0.1	10.9	9.600
			4.9	0.540
			10	9.500
			15.1	24.000
		1	20.2	54.000
			26.2	170.000
			7.3	3.100
			9.3	5.600
		6	11.1	10.700
			13.9	15.800
			18.7	46.000
			20.8	100.000
Dry	0.05	6	25.2	170.000

- Notes: 1. Compact tension specimen
2. Ref. Fig. 33 in Volume I report [22].

TABLE B-2       $da/dN$  VERSUS  $\Delta K$  RESULTS FOR 7075-T7651 ALUMINUM  
 IN 3.5% NaCl SOLUTION AT ROOM TEMPERATURE  
 (R = 0.05, f = 1 HZ, 3 HZ, 6 HZ)

ENVIRONMENT	R	FREQ. (HZ)	$\Delta K$ (ksi- $\sqrt{\text{In}}$ )	$da/dN \times 10^6$ (In./Cycle)
3.5% NaCl	0.05	1	7.58	2.4
			9.09	10.0
			10.61	23.0
		1	12.84	40.0
		3	5.87	1.2
			6.82	1.8
			13.18	30.0
			14.77	40.0
			17.80	70.0
			23.86	150.0
		3	28.03	160.0
		6	7.39	3.1
			12.35	16.0
			14.85	39.0
			25.00	120.0
		6	27.65	140.0
3.5% NaCl	0.05			

Notes: 1. Compact tension specimen

2. Ref. Fig. 35 in Volume I report [22].

With  $m_1$  and  $C_1$  defined, the constant  $C_2$  was determined using applicable 3.5% NaCl crack growth data and a least squares fit procedure as follows.

$$(da/dN)_e = C_1 (\Delta K)^{m_1} + C_2 (\Delta K)^2 \quad (B-7)$$

$$E^2 = \sum [(da/dN)_e - C_1 (\Delta K)^{m_1} - C_2 (\Delta K)^2]^2 \quad (B-8)$$

In Eq. B-8,  $E^2$  is the sum squared error. Taking the  $\partial E^2 / \partial C_2$  and setting equal to zero, the following expression for  $C_2$  was obtained,

$$C_2 = \frac{\sum (\Delta K)^2 (da/dN)_e - C_1 \sum (\Delta K)^{m_1 + 2}}{(\Delta K)^4} \quad (B-9)$$

The resulting  $m_1$ ,  $C_1$  and  $C_2$  constants based on the procedures described above are shown in Tables B-7 and B-8 for  $R = 0.05$  and  $0.30$ , respectively. Predicted  $(da/dN)_e$  values based on Eq. B-7 are also shown for the applicable  $\Delta K$  values.

Experimental  $da/dN$  versus  $\Delta K$  results for  $R = .05$  and  $0.30$  are plotted in Figs. B-5 and B-6, respectively. The solid line represents the fit of Eq. B-7 to the applicable test results and the dashed lines represent the data scatter. Since Eq. B-7 correlates fairly well with the experimental results in the  $\Delta K$  range considered, it is reasonable to assume that  $(da/dN)_{cf}$  is a function of  $(\Delta K)^2$ . Further research is required to better understand the effect of the  $R$ -ratio on  $(da/dN)_{cf}$ .

In Eq. B-5, the first two terms are considered to be the most significant contributors to the crack growth rate for the 7075-T7651 aluminum alloy. Wei has suggested that the second term in Eq. B-5,  $(da/dN)_{cf}$ , is a function of  $(\Delta K)^2$ . The purpose of this section is to evaluate the  $da/dN$  crack growth results for 7075-T7651 aluminum from Volume I [22] and to determine if  $(da/dN)_{cf}$  depends on  $(\Delta K)^2$  or not.

The  $da/dN$  versus  $\Delta K$  results from Tables B-1 through B-4 were evaluated as follows. Dry and wet results for the same R-ratio were considered. For example, the results in Table B-1 (dry) and Table B-2 (3.5% NaCl) for  $R = 0.05$  were considered together to evaluate the possible dependence of  $(da/dN)_{cf}$  on  $(\Delta K)^2$ . By the same token, the results in Tables B-3 and B-4 were used for  $R = 0.30$ .

The Paris crack growth model was used to define  $(da/dN)_r$  and dry air  $da/dN$  versus  $\Delta K$  results were used to determine  $m_1$  and  $C_1$  in Eq. B-6.

$$(da/dN)_r = C_1 (\Delta K)^{m_1} \quad (B-6)$$

The constants  $m_1$  and  $C_1$  were determined using dry air crack growth data in a selected  $\Delta K$  range (i.e., 8-24 ksi  $\sqrt{\text{in}}$ ). A  $\Delta K$  range was used which included the applicable dry air and 3.5% NaCl crack growth data for the same R-ratio.  $m_1$  and  $C_1$  were determined using a least squares fit procedure.

TABLE B-6 EFFECT OF ENVIRONMENT AND R-RATIO ON  $da/dN$   
BASED ON PARIS MODEL CONSTANTS

EFFECT	ENVIRONMENT	R-RATIO	DATA SET	m	C x 10 <sup>9</sup>	C-RATIO
ENVIRONMENT	Dry Air	.05	①	3.221	4.413	$\frac{4.413}{5.462} = .81$
	3.5% NaCl	.05	②	3.221	5.462	
	Dry Air	.30	③	2.619	30.96	$\frac{30.96}{55.75} = .56$
	3.5% NaCl	.30	④	2.619	55.75	
R-RATIO	Dry Air	.05	①	3.249	4.130	$\frac{4.130}{7.281} = .57$
	Dry Air	.30	③	3.249	7.281	
	3.5% NaCl	.05	②	3.108	7.328	$\frac{7.328}{20.469} = .36$
	3.5% NaCl	.30	④	3.108	20.469	
ENVIRONMENT AND R-RATIO	Dry Air	.05	①	3.115	5.669	$\frac{5.669}{7.180} = .79$
	3.5% NaCl	.05	②	3.115	7.180	
	Dry Air	.30	③	3.115	9.901	$\frac{9.901}{20.170} = .49$
	3.5% NaCl	.30	④	3.115	20.170	
REF. TABLE B-5						

Notes: Paris Model:  $da/dN = C(\Delta K)^m$

- (a) Environment appears to have a greater effect on  $da/dN$  as the R-ratio increases.
- (b) The R-ratio appears to have a greater effect on  $da/dN$  for 3.5% NaCl than for dry air.
- (c) The environment and R-ratio together appear to have a greater effect on  $da/dN$  as the R-ratio increases.

These results, including the applicable C-ratios, are shown in Table B-6. It should be clear that the C-ratio method provides only an estimate of the effect investigated because the actual variance of "m" for each data set is not considered.

The following conclusions are based on the results shown in Tables B-5 and B-6: (1) the environment appears to have a greater effect on  $da/dN$  as the R-ratio increases, and (2) the R-ratio appears to have a greater effect on  $da/dN$  for 3.5% NaCl than for dry air.

#### B.4 EVALUATION OF SUPERPOSITION CRACK GROWTH MODEL

Wei, et al [27] suggested that the environmentally-assisted fatigue crack growth rate  $(da/dN)_e$ , is the sum of three components.

$$(da/dN)_e = (da/dN)_r + (da/dN)_{cf} + (da/dN)_{scc} \quad (B-5)$$

In Eq. B-5,  $(da/dN)_r$  = rate of fatigue crack growth in an inert environment-representing the contribution of "purely mechanical" fatigue,  $(da/dN)_{cf}$  = the cycle-dependent contribution requiring the synergistic interaction of fatigue and environment, and  $(da/dN)_{scc}$  = contribution of sustained-load crack growth (e.g., stress corrosion cracking) at K levels above the stress corrosion cracking threshold ( $K_{Isc}$  or  $K_{scc}$ ).

TABLE B-5 SUMMARY OF PARIS LAW PARAMETERS (m and C) FOR 7075-T7651 ALUMINUM FOR BOTH DRY AIR AND 3.5% NaCl SOLUTION

DATA SET	ENVIRONMENT	R	FREQ. (HZ)	NO. (N)	AK RANGE (ksi- $\sqrt{In}$ )	(a)		(b)		(c)		(d)		(e)	
						m	(f) $C \times 10^9$	m	(f) $C \times 10^9$	m	(f) $C \times 10^9$	m	(f) $C \times 10^9$	m	(f) $C \times 10^9$
①	Dry Air	.05	0.1	5	4.3 - 10.9	3.224	4.693	3.224	4.380	3.221	4.413	3.115	5.669	3.249	4.130
			1	5	4.9 - 26.2	↑	4.021	↑	↑	↑	↑	↑	↑	↑	↑
	Dry Air		6	7	7.3 - 25.2	3.224	4.440	3.224	4.380		4.413		5.669	3.249	4.130
②	1.5% NaCl		1	4	7.58 - 12.84	3.122	9.670	3.122	7.059		5.462		7.180	3.108	7.328
			3	7	5.87 - 28.03	↑	6.661	↑	↑	↑	↑	↑	↑	↑	↑
		.05	6	5	7.39 - 27.65	3.122	5.933	3.122	7.059	3.221	5.462		7.180	3.108	7.328
③	Dry Air	.30	0.1	11	4.75 - 23.34	3.335	6.843	3.335	5.975	2.619	30.960		9.901	3.249	7.281
			1	8	5.09 - 16.31	↑	5.507	↑	↑	↑	↑	↑	↑	↑	↑
			6	9	4.63 - 23.97	3.335	5.441	3.335	5.975		30.960		9.901	3.249	7.281
④	3.5% NaCl		0.1	4	2.27 - 9.42	3.843	4.006	3.843	4.538		55.746		20.170	3.108	20.469
			0.3	7	4.04 - 12.31	↑	3.771	↑	↑	↑	↑	↑	↑	↑	↑
			1	7	4.42 - 14.62		5.059								
			3	10	4.62 - 17.27	↑	4.987	↑	↑						
	3.5% NaCl		6	7	4.42 - 18.27	3.843	4.613	3.843	4.538	2.619	55.746	3.115	20.170	3.108	20.469
						EFFECT OF FREQUENCY		EFFECT OF ENVIR.		EFFECT OF ENVIR. AND R-RATIO		EFFECT OF R-RATIO			

In Figs. B-1 through B-4, the Paris model fit based on "m" and "C" for a given data set is emphasized. A scatter band, denoted by dashed lines (- - -), is also plotted with straight lines parallel to the line based on unpooled data sets.

The following conclusions are based on Figs. B-1 through B-4: (1) the mean value predictions (solid lines), based on the Paris crack growth model, fit the experimental results well for the four data sets considered, (2) the experimental crack growth results for different loading frequencies are bunched close together - indicating that there are no significant effects of loading frequency on the crack growth rate, (3) as expected, the  $da/dN$  variance was greater for the 3.5% NaCl solution than for dry air.

### B.3 STUDY SENSITIVITY OF PARIS CRACK GROWTH MODEL PARAMETERS WITH RESPECT TO VARIOUS FACTORS

The sensitivity of the Paris crack growth model parameters "m" and "C" was studied using the  $da/dN$  versus  $\Delta K$  data shown in Tables B-1 through B-4. The effects of the following factors on m and C were investigated: (1) loading frequency, (2) environment, and (3) R-ratio.

Results for m and C are summarized in Table B-5 for various cases. Also, the data sets were appropriately grouped to focus attention on the particular effect to be investigated.

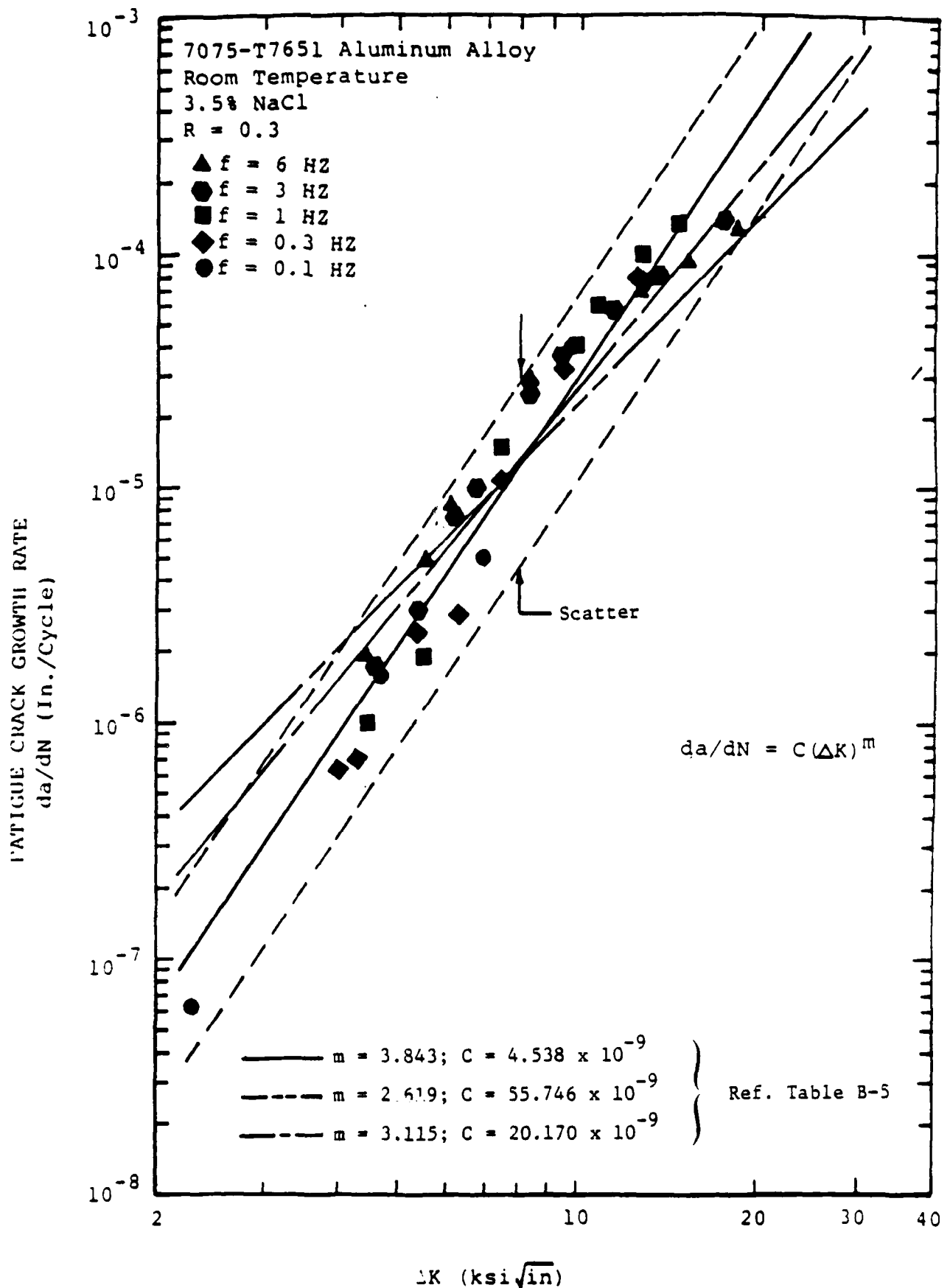


Fig. B-4 da/dN Versus  $\Delta K$  Results for 7075-T7651 Aluminum Alloy Exposed to 3.5% NaCl at Room Temperature (R=0.3; f=0.1 HZ, 0.3 HZ, 1 HZ, 3 HZ and 6 HZ)

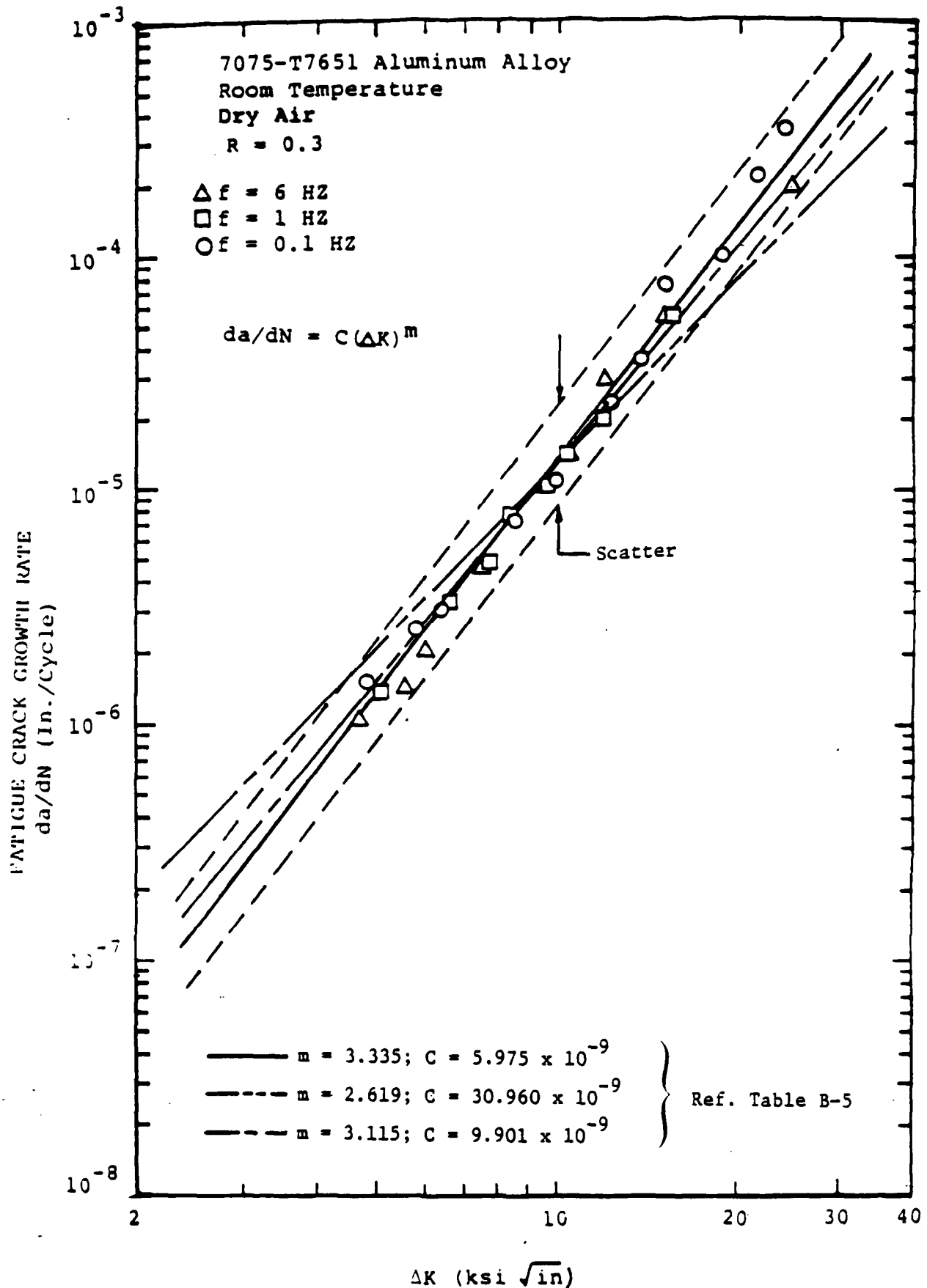


Fig. B-3  $da/dN$  Versus  $\Delta K$  Results for 7075-T7651 Aluminum Alloy Exposed to Dry Air at Room Temperature ( $R=0.3$ ;  $f=0.1\text{HZ}$ ,  $1 \text{ HZ}$  and  $6 \text{ HZ}$ )

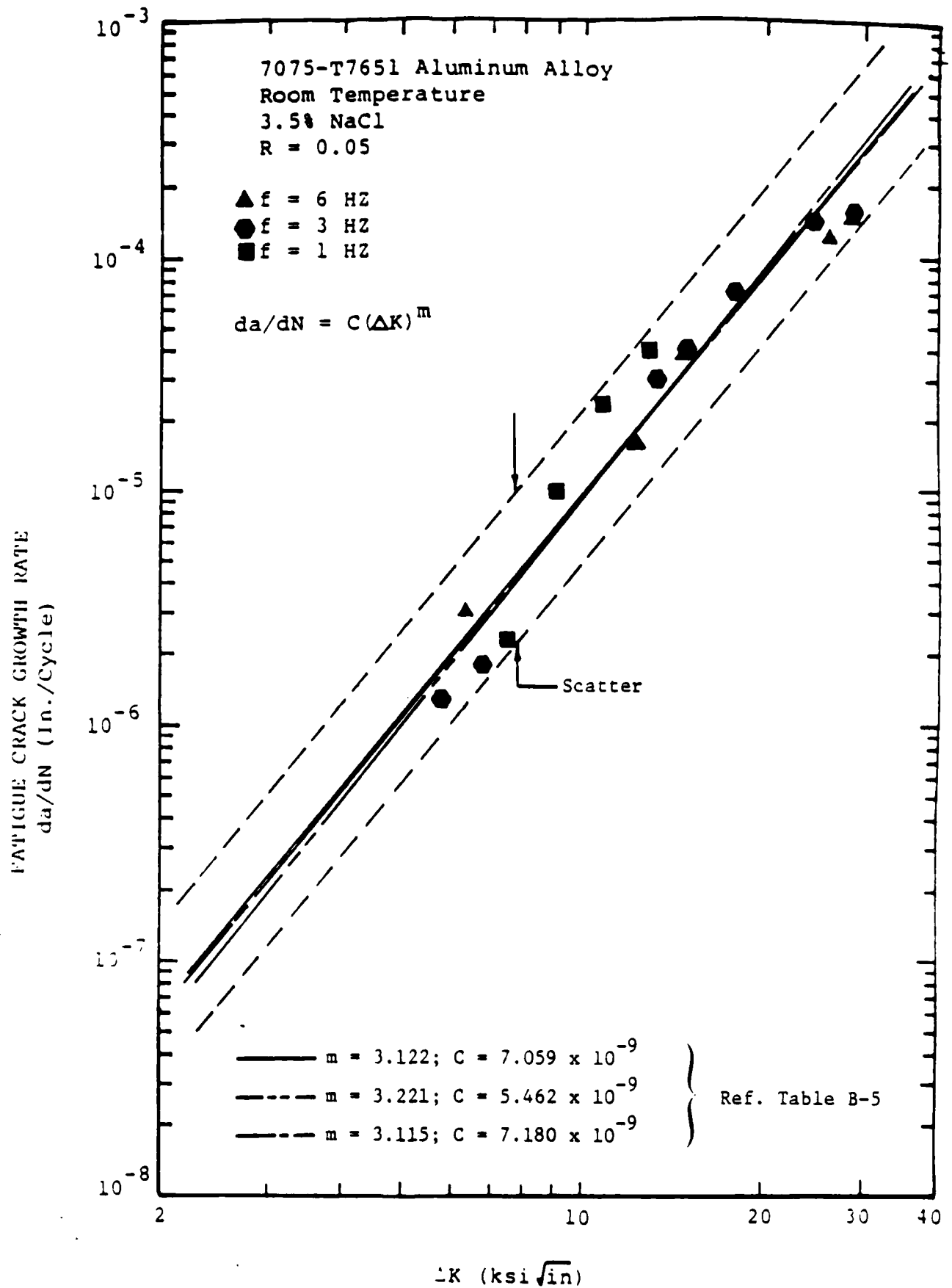


Fig. B-2  $da/dN$  Versus  $\Delta K$  Results for 7075-T7651 Aluminum Alloy Exposed to 3.5% NaCl at Room Temperature ( $R=0.05$ ;  $f=1 \text{ HZ}$ ,  $3 \text{ HZ}$  and  $6 \text{ HZ}$ )

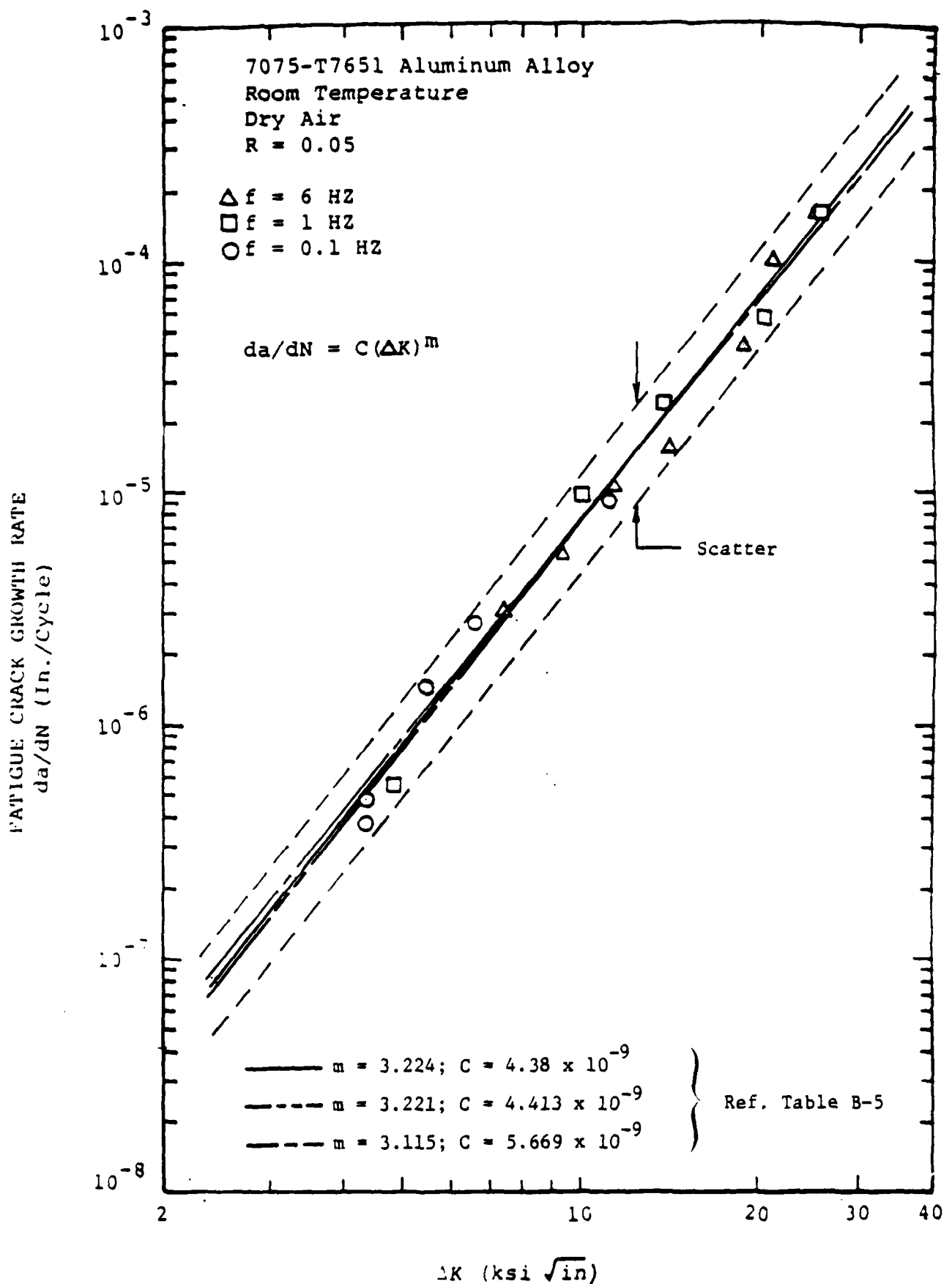


Fig. B-1  $da/dN$  Versus  $\Delta K$  Results for 7075-T7651 Aluminum Alloy Exposed to Dry Air at Room Temperature ( $R=0.05$ ;  $f=0.1\text{Hz}$ ,  $1 \text{ Hz}$  and  $6 \text{ Hz}$ )

5. Data sets with the same environment were pooled to determine "m", the "C" was determined using results for a given data set.

The Paris model constants m and C in Eq. B-1 were determined using a linear least squares fit form of Eq. B-1 as given in Eq. B-4.

$$\underbrace{\log(da/dN)}_Y = \log \underbrace{C}_B + m \underbrace{\log(\Delta K)}_X \quad (B-4)$$

Results for m and C for the various cases studies are summarized in Table B-5.

The da/dN versus  $\Delta K$  results from Tables B-1 through B-4 are plotted in Figs. B-1 through B-4, respectively. To compare the results for different loading frequencies different symbols were used for each frequency. Three different Paris model fits are shown for each figure: (1) "m" and "C" determined for an individual data set and denoted by a solid straight line (—), (2) "m" determined using results for the same R-ratio and "C" determined using results for a given data set (denoted by — — —), and (3) "m" determined using pooled results for different R-ratios and environments and then "C" determined using data for a given data set (denoted by - - - -).

The resulting constants  $m$  and  $C$  for the Paris model were evaluated using dry air and 3.5% NaCl  $da/dN$  versus  $\Delta K$  data and least squares fitting procedures. For purposes of evaluating the effects of R-ratio and environment,  $da/dN$  versus  $\Delta K$  results for selected data sets are pooled to determine a common " $m$ " value in Eq. B-1. By imposing a common " $m$ " value, the variance in a given data set is reflected in a single parameter " $C$ ". Hence, the effects of environment and R-ratio can be estimated by directly comparing the respective " $C$ " values for selected data sets. Data pooling procedures were used to evaluate  $m$  and  $C$  for the following cases:

1. Results for a given data set were pooled to determine " $m$ ", then " $C$ " was determined using results for a selected loading frequency.
2. Same as (1) except " $C$ " was determined using pooled data for all loading frequencies in a given data set.
3. Data sets with the same R-ratio were pooled to determine " $m$ ", then " $C$ " was determined using applicable results for a given data set.
4. Four data sets were pooled to determine " $m$ ", then " $C$ " was determined using results for a given data set.

TABLE B-4  $da/dN$  VERSUS  $\Delta K$  RESULTS FOR 7075-T7651 ALUMINUM  
IN 3.5% NaCl SOLUTION AT ROOM TEMPERATURE  
( $R = 0.3$ ;  $f = 0.1$  HZ, 0.3 HZ, 1 HZ, 3 HZ, 6 HZ)

ENVIRONMENT	R	FREQ. (HZ)	$\Delta K$ (ksi $\sqrt{\text{in}}$ )	$da/dN \times 10^6$ (In./Cyc)
3.5% NaCl ↑	0.3 ↑	0.1	2.27	0.06
		↑	4.65	1.60
		↑	6.88	5.10
		0.1	9.42	40.00
		0.3	4.04	0.62
		↑	4.31	0.70
		↑	5.35	2.30
		↑	6.23	2.90
		↑	7.35	11.00
		↑	9.38	32.00
		0.3	12.31	80.00
		1.0	4.42	1.00
		↑	5.38	1.90
		↑	7.38	16.00
		↑	9.62	40.00
		↑	10.65	60.00
		↑	12.54	100.00
		1.0	14.62	130.00
		3.0	4.62	1.80
		↑	5.35	3.00
		↑	6.15	7.50
		↑	6.81	10.00
		↑	8.31	25.00
		↑	9.42	37.00
		↑	11.42	58.00
		↑	12.69	78.00
		↑	13.50	80.00
		3.0	17.27	130.00
		6.0	4.42	1.90
		↑	5.73	5.00
		↑	6.15	8.50
		↑	8.46	29.00
		↑	12.62	69.00
3.5% NaCl ↓	0.3 ↓	↓	15.04	90.00
		6.0	18.27	120.00

- Notes: 1. Compact tension specimen  
2. Ref. Fig. 36 in Volume I report [22].

TABLE B-3       $da/dN$  VERSUS  $\Delta K$  RESULTS FOR 7075-T7651 ALUMINUM  
IN DRY AIR ( $R = .30$ ,  $f = 0.1$  HZ, 1 HZ, 6 HZ)

ENVIRONMENT	R	FREQ. (HZ)	$\Delta K$ (ksi- $\sqrt{\text{In}}$ )	$da/dN \times 10^6$ (In./Cycle)
Dry Air ↑ ↓ Dry Air	0.3 ↑ ↓ 0.3	0.1 ↑ ↓ 0.1	4.75	1.52
			5.74	2.51
			6.25	3.11
			8.49	7.28
			9.91	11.20
			12.20	23.80
			14.21	37.20
			16.19	76.10
			17.92	100.00
			20.99	217.00
		1 ↑ ↓ 1	23.34	355.00
			5.09	1.43
			6.69	3.20
			7.69	4.90
			8.35	7.79
			9.55	10.50
			10.49	13.80
			12.50	20.00
			16.31	54.40
		6 ↑ ↓ 6	4.63	1.05
			5.46	1.41
			6.00	2.08
			7.41	4.67
			9.39	10.20
			10.34	13.30
			13.29	30.00
			15.85	55.00
			23.97	184.00

- Notes: 1. Compact tension specimen  
2. Ref. Fig. 33 in Volume I report [22].

TABLE B-7 LEAST SQUARES FIT RESULTS FOR TWO-SEGMENT SUPERPOSITION  
 CRACK GROWTH MODEL FOR 7075-T7651 ALUMINUM IN 3.5% NaCl  
 SOLUTION AT ROOM TEMPERATURE ( $R = .05$ )

ENVIRONMENT	R	FREQ. (HZ)	$\Delta K$ (ksi- $\sqrt{\text{in}}$ )	(a)		(a) $C_1 \times 10^9$ (DRY AIR)	EXPERIMENTAL (da/dN) <sub>e</sub> $\times 10^6$ (In./Cycle)	(b) $C_2 \times 10^8$	PREDICTED (c) (da/dN) <sub>e</sub> $\times 10^6$ (In./Cycle)
				$m_1$	$m_1$				
3.5% NaCl	.05	1	9.09	3.037	6.862	<div style="display: flex; align-items: center; justify-content: center;"> <div style="width: 100%; height: 100%; border: 1px solid black; position: relative;"> <div style="position: absolute; top: 0; left: 0; right: 0; bottom: 0; border: 1px solid black;"></div> </div> </div>	10.0	7.921	12.14
		1	10.61				23.0		17.86
		1	12.84				40.0		29.02
		3	13.18				30.0		31.04
		3	14.77				40.0		41.71
		3	17.80				70.0		68.15
3.5% NaCl	.05	3	23.86			<div style="display: flex; align-items: center; justify-content: center;"> <div style="width: 100%; height: 100%; border: 1px solid black; position: relative;"> <div style="position: absolute; top: 0; left: 0; right: 0; bottom: 0; border: 1px solid black;"></div> </div> </div>	150.0	7.921	149.91
		6	12.35				16.0		26.27
		6	14.85	3.037	6.862		39.0		42.29

NOTES: (a)  $(da/dN)_r = (da/dN)_{\text{Dry Air}} = C_1 (\Delta K)^{m_1}$

Used pooled results for dry air in range  
 $8 \leq \Delta K \leq 24$  to compute  $m_1$

(b)  $(da/dN)_{cf} = C_2 (\Delta K)^2$

$$C_2 = \frac{\sum (\Delta K)^2 (da/dN)_e - C_1 \sum (\Delta K)^{m_1+2}}{\sum (\Delta K)^4} \quad (\text{Least Squares Fit})$$

$$\begin{aligned} \text{(c) } da/dN)_e &= (da/dN)_r + (da/dN)_{cf} \\ &= C_1 (\Delta K)^{m_1} + C_2 (\Delta K)^2 \end{aligned}$$

TABLE B-8 LEAST SQUARES FIT RESULTS FOR TWO-SEGMENT SUPERPOSITION CRACK GROWTH MODEL  
FOR 7075-T7651 ALUMINUM IN 3.5% NaCl SOLUTION AT ROOM TEMPERATURE (R=.30)

ENVIRONMENT	R	FREQ. (HZ)	$\Delta K$ (ksi in)	DRY AIR		EXPERIMENTAL (da/dN) <sub>e</sub> × 10 <sup>6</sup> (In./Cycle)	(b) C <sub>2</sub> × 10 <sup>7</sup>	PREDICTED (c) (da/dN) <sub>e</sub> × 10 <sup>6</sup> (In./Cycle)
				(a) m <sub>1</sub>	(a) C <sub>1</sub> × 10 <sup>9</sup>			
3.5% NaCl	.30	.1	9.42	3 528	3.558	40	2.260	29.8
		.3	9.38			32		29.5
		.3	12.31			80		59.2
		1	9.62			40		31.4
		1	10.65			60		40.6
		1	12.54			100		62.2
		1	14.62			130		94.1
		3	8.31			25		21.9
		3	9.42			37		29.8
		3	11.42			58		48.7
		3	12.69			78		64.2
		3	13.50			80		75.8
		3	17.27			130		149.9
		6	8.46			29		22.8
3.5% NaCl	.30	6	12.62			69		63.3
		6	15.04			90		101.8
		6	18.27	3.528	3.558	120	2.260	176.0

NOTES: (a)  $(da/dN)_r = (da/dN)_{\text{DRY AIR}} = C_1 (\Delta K)^{m_1}$

Used pooled results for dry air in range  $8 \leq \Delta K \leq 24$  to compute m<sub>1</sub>.

(b)  $(da/dN)_{cf} = C_2 (\Delta K)^2$

$$C_2 = \frac{\sum (\Delta K)^2 (da/dN)_e - C_1 \sum (\Delta K)^{m_1+2}}{\sum (\Delta K)^4} \quad (\text{Least Squares Fit})$$

(c)  $(da/dN)_e = (da/dN)_r + (da/dN)_{cf} = C_1 (\Delta K)^{m_1} + C_2 (\Delta K)^2$

$$\frac{da}{dN}_e = C_1(\Delta K)^{m_1} + C_2(\Delta K)^2$$

$$\begin{aligned} m_1 &= 3.037; C_1 = 6.862 \times 10^{-9}; \\ C_2 &= 7.921 \times 10^{-8} \end{aligned} \quad \left. \vphantom{\begin{aligned} m_1 &= 3.037; C_1 = 6.862 \times 10^{-9}; \\ C_2 &= 7.921 \times 10^{-8} \end{aligned}} \right\} 8 \leq \Delta K \leq 24 \text{ ksi-}\sqrt{\text{in}}$$

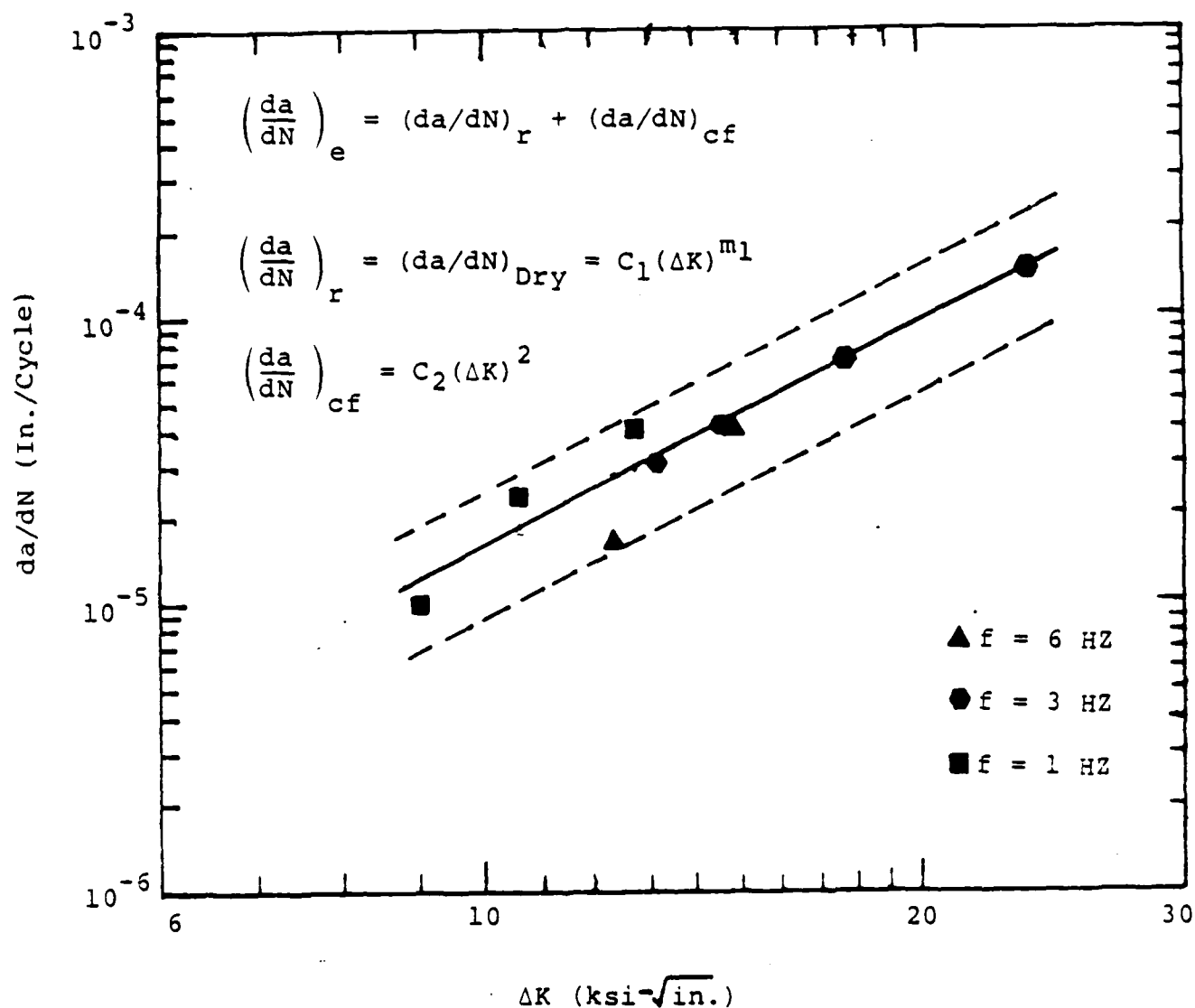


Fig. B-5 Two-Segment Crack Growth Model Fitted to  $da/dN$  Versus  $\Delta K$  Data for 7075-T7651 Aluminum in 3.5% NaCl at Room Temperature ( $R = 0.05$ )

$$\frac{da}{dN}_e = C_1 (\Delta K)^{m_1} + C_2 (\Delta K)^2$$

$$m_1 = 3.528; C_1 = 3.558 \times 10^{-9}$$

$$C_2 = 2.260 \times 10^{-7}$$

$$8 \leq \Delta K \leq 24 \text{ ksi-}\sqrt{\text{in}}$$

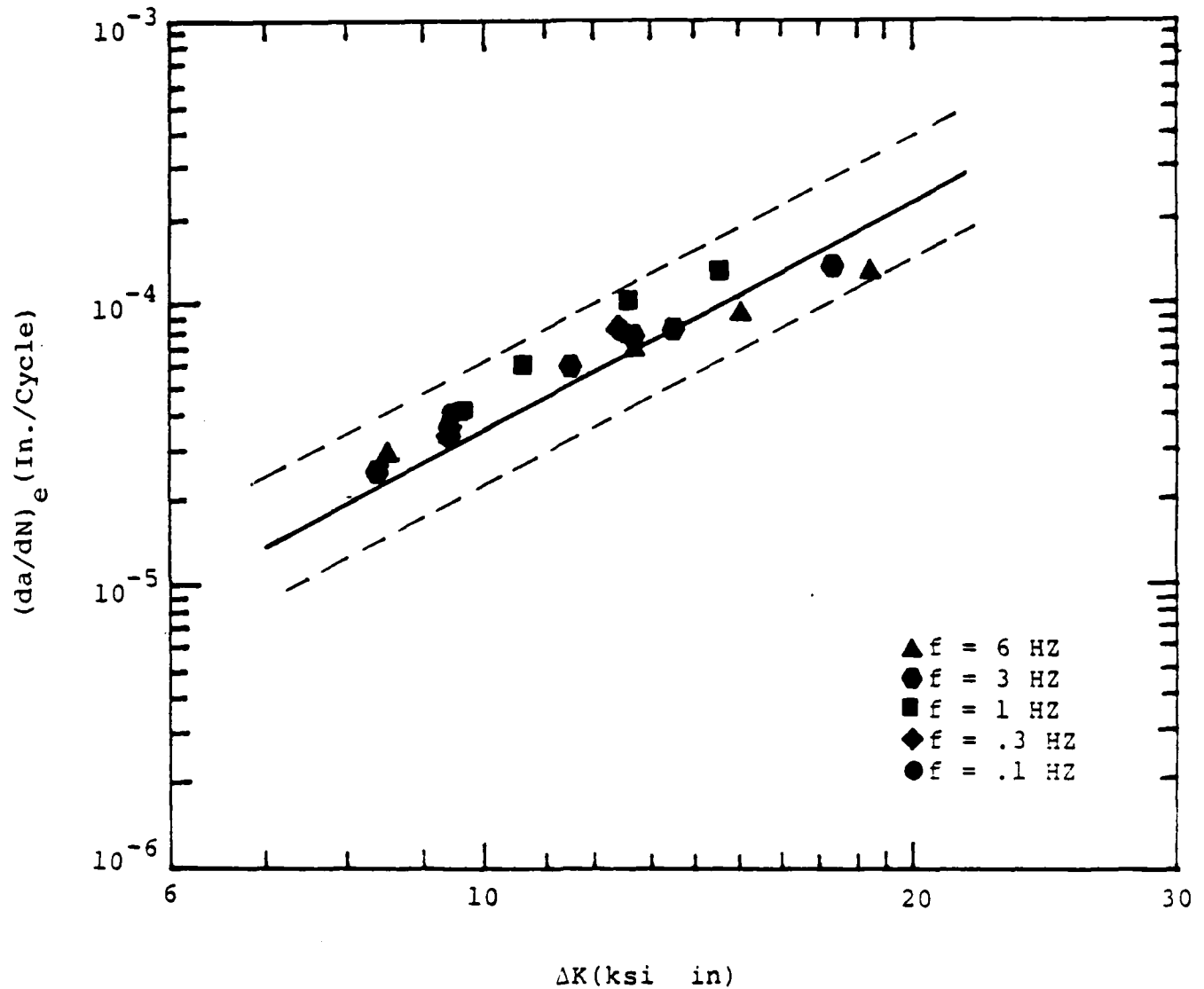


FIG. B-6 TWO-SEGMENT CRACK GROWTH MODEL FITTED TO  $da/dN$  VERSUS  $\Delta K$  DATA FOR 7075-T7651 ALUMINUM IN 3.5% NaCl AT ROOM TEMPERATURE ( $R = 0.30$ )

## B.5 EVALUATION OF FORMAN CRACK GROWTH MODEL

The purpose of this section is to: (1) determine suitable Forman model parameters, ( $C$  and  $n$  in Eq. B-3) to use to make crack growth predictions in Appendix H and (2) evaluate the use of the Forman model to make  $da/dN$  versus  $\Delta K$  predictions for different R-ratios.

Parameters " $C$ " and " $n$ " in Eq. B-3 were determined herein for two different R-ratios (i.e.,  $R = 0.05$  and  $0.3$ ) and for both dry air and 3.5% NaCl environments. A least squares fitting procedure was used. The exponent " $n$ " in Eq. B-3 was determined with and without pooling of  $da/dN$  versus  $\Delta K$  data for different data sets. Data pooling procedures were used for two reasons: (1) to obtain compatible " $n$ " and " $C$ " values for different R-ratios and environments and (2) to provide a rational basis for determining a "scaling factor" or "knock down factor" for accounting for the effects of environment on  $da/dN$ . Furthermore,  $C$  and  $n$  are cross-correlated parameters, i.e., for a given  $n$  there is a corresponding  $C$  and vice versa. By using data pooling procedures a common  $n$  value can be obtained and hence, the scatter in the data can be reflected in the single parameter  $C$ .

Three different cases were considered:

- o Case I - n and C parameters determined using the da/dN versus  $\Delta K$  data for a given data set (i.e., given environment and R-ratio)
- o Case II - n determined using pooled da/dN versus  $\Delta K$  results from Tables B-1 through B-4; C determined using pooled results for same environment and two R-ratios.
- o Case III - n and C based on da/dN versus  $\Delta K$  results for a given environment and R-ratio; results used to predict da/dN versus  $\Delta K$  for different R-ratio.

In all cases a least squares fit procedure was used to compute n and C.

Equation B-3 was transformed into a least squares fit format as shown in Eq. B-10.

$$\underbrace{\ln da/dN + \ln[(1-R)K_c - \Delta K]}_Y = \underbrace{\ln C}_B + n \underbrace{\ln \Delta K}_X \quad (B-10)$$

The parameters  $n$  and  $C$  were determined using the well known least squares fit equations given in Eq. B-11 and B-12, respectively.

$$n = \frac{N\sum xy - (\sum X)(\sum Y)}{N\sum x^2 - (\sum X)^2} \quad (B-11)$$

$$C = \exp \left\{ \frac{\sum Y - n\sum x}{N} \right\} \quad (B-12)$$

In Eqs. B-11 and B-12,  $N$  = number of samples in the fit;  $X$  and  $Y$  are defined in Eq. B-10.

Parameters  $n$  and  $C$  for a given data set were determined using Eq. B-11 and B-12, respectively. A pooled " $n$ " value was determined using Eq. B-11 and the pooled  $da/dN$  versus  $\Delta K$  results for four data sets (Ref. Tables B-1 through B-4). Using the pooled " $n$ " value, the corresponding  $C$  values were determined using Eq. B-11 and the pooled results for the same environment and two different  $R$ -ratios. The resulting  $C$  and  $n$  values for Cases I-III are summarized in Table B-9.

Theoretical predictions for  $da/dN$  versus  $\Delta K$  are compared with experimental results in Figs. B-7 through B-10. Three different curves are plotted in each figure and the resulting  $C$  and  $n$  values used are noted. The basis for each of the three cases (I-III) has been previously described.

Table E-9 Summary of Forman Equation Parameters for 7075-T7651 Aluminum  
for Both Dry Air and 3.5% NaCl Environments

DATA SET	ENVIRONMENT	R-RATIO	ΔK RANGE (ksi- $\sqrt{\text{in}}$ )	SAMPLE SIZE	K <sub>C</sub> (ksi- $\sqrt{\text{in}}$ )	CASE (a)	n (c)	C X 10 <sup>7</sup> (c)	REF TABLE(S) (e)
1	DRY AIR ↓	0.05 ↓	4.3 -26.2 2.27-28.03 4.63-23.97	17 96(b) 28	62.5	I II III	2.967 2.913 2.965	3.722 4.722 4.475	B-1 (d) B-3
2	3.5% NaCl ↓	0.05 ↓	5.87-28.03 2.27-28.03 2.27-18.27	16 96(b) 35		I II III	2.780 2.913 3.609	7.466 8.551 2.554	B-2 (d) B-4
3	DRY AIR ↓	0.3 ↓	4.63-23.97 2.27-28.03 4.3 -26.2	28 96(b) 17		I II III	2.965 2.913 2.967	4.475 4.722 3.722	B-3 (d) B-1
4	3.5% NaCl ↓	0.3 ↓	2.27-18.27 2.27-28.03 5.87-28.03	35 96(b) 16		I II III	3.609 2.913 2.780	2.554 8.551 7.446	B-4 (d) B-2

Notes: (a) Case I - n and C based on da/dN versus ΔK results for given data set

Case II - n based on pooled da/dN versus ΔK results for given data sets 1-4;

C based on results for same environment and two R-ratios

Case III - n and C based on da/dN versus ΔK results for one R-ratio and results  
to be used for different R-ratio

(b) Pooled sample size for determining n

(c) Constants in Forman Equation (Ref. Eq. B-3) determined by least square fit

(d) Tables B-1 through B-4

(e) Data used to determine n and C

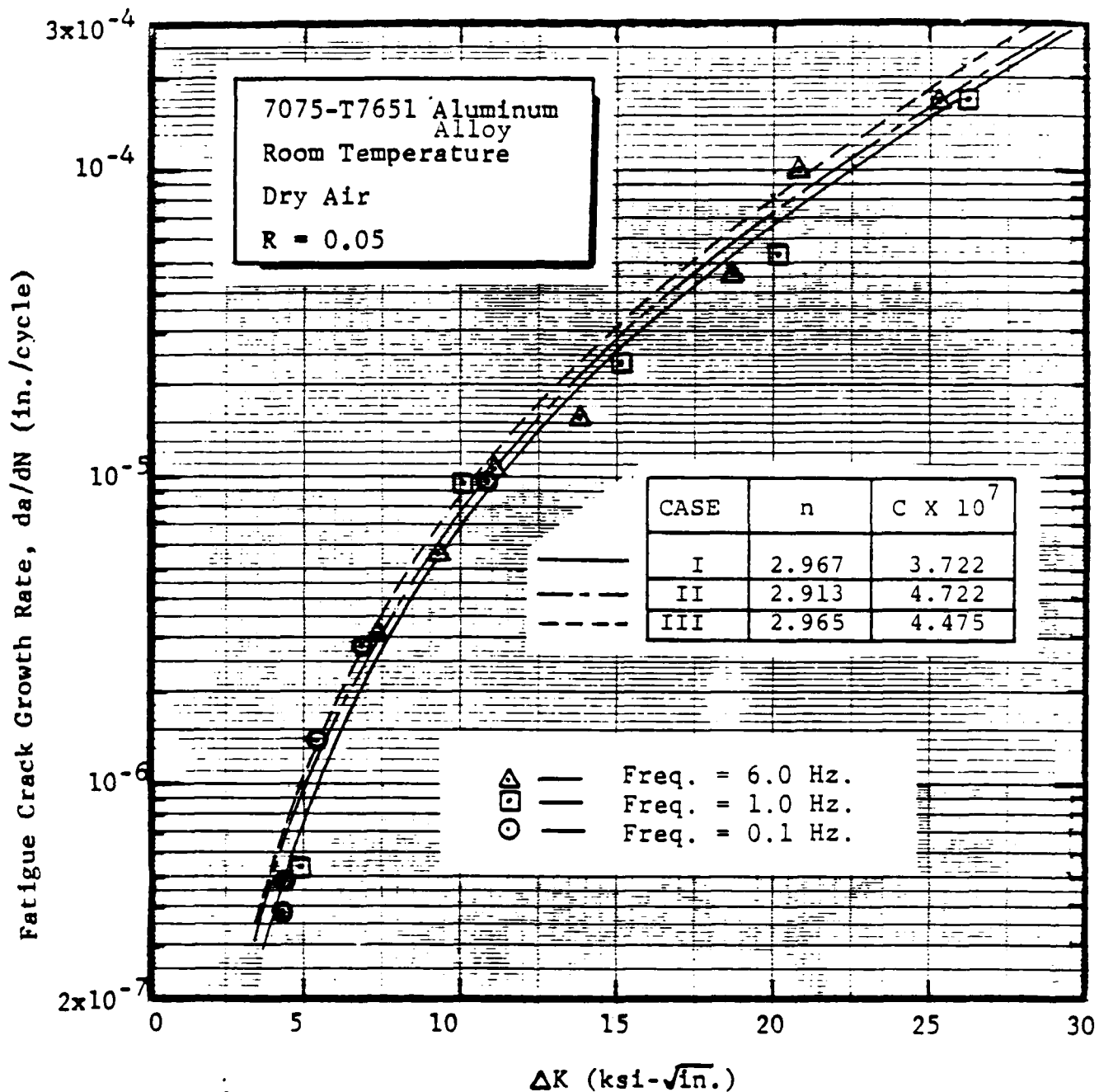


Fig. B-7 Forman Model Goodness-of-Fit Plots for  $da/dN$  Versus  $\Delta K$  (7075-T7651 Aluminum,  $R = 0.05$ , Dry Air Environment)

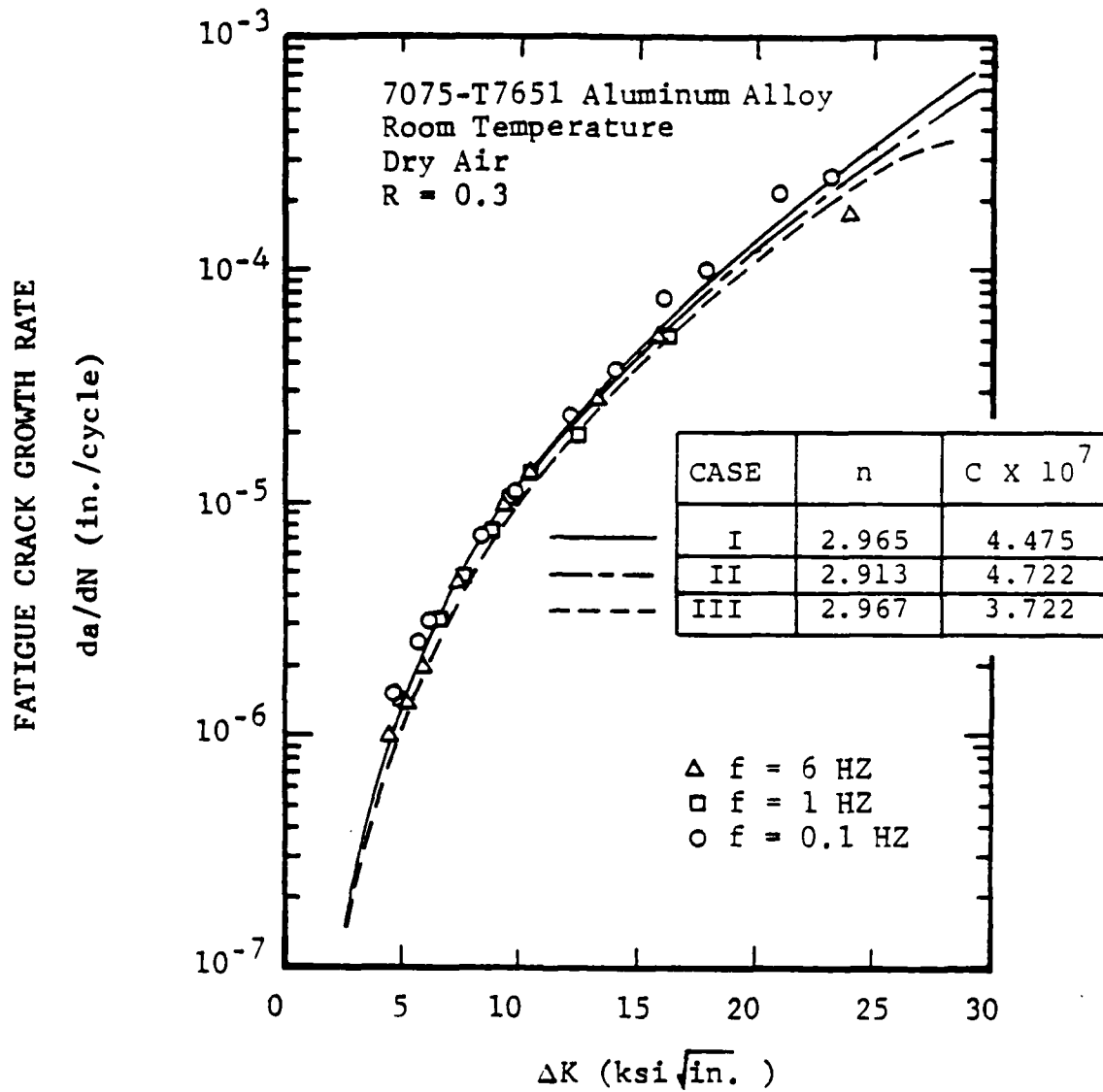


Fig. B-8 Forman Model Goodness-of-Fit Plots for  $da/dN$  Versus  $\Delta K$  (7075-T7651 Aluminum,  $R = 0.3$ , Dry Air Environment)

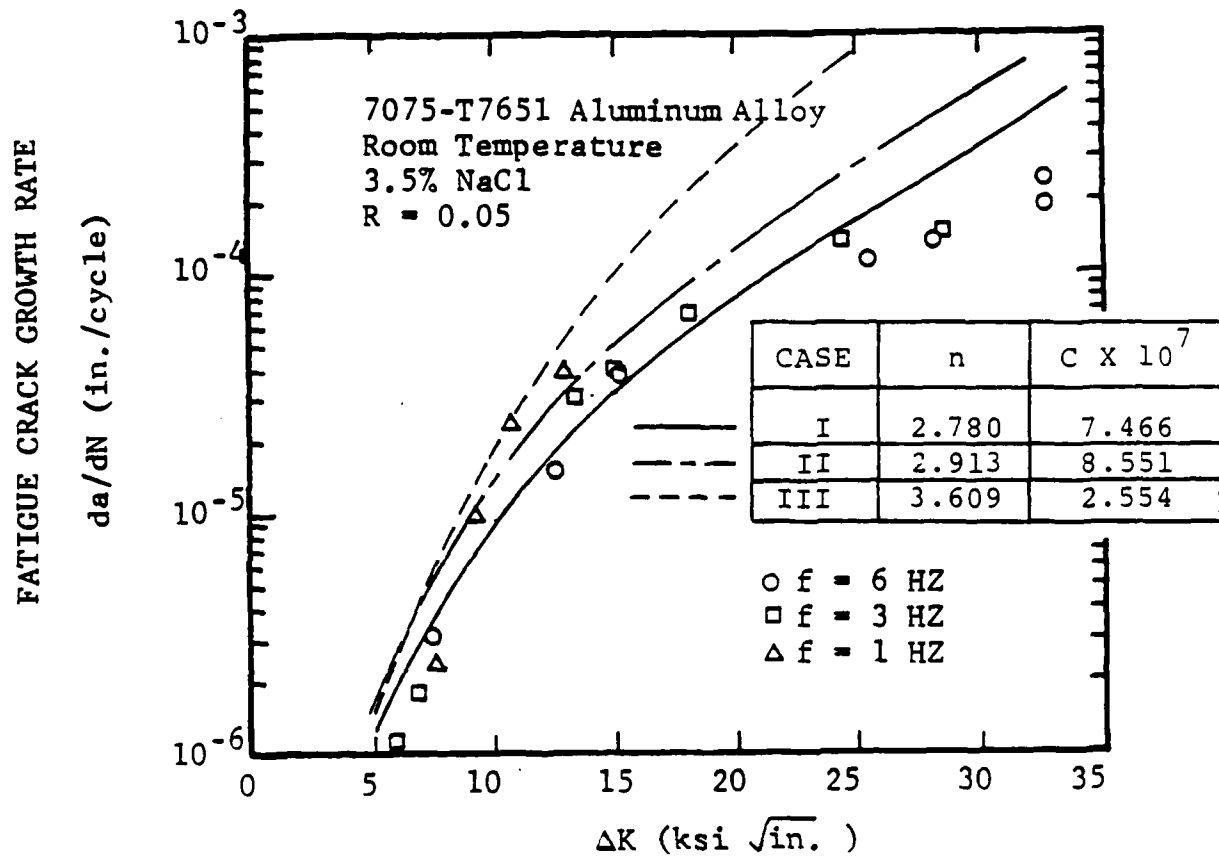


Fig. B-9 Forman Model Goodness-of-Fit Plots for  $da/dN$  Versus  $\Delta K$  (7075-T7651 Aluminum, R = 0.05, 3.5% NaCl Environment)

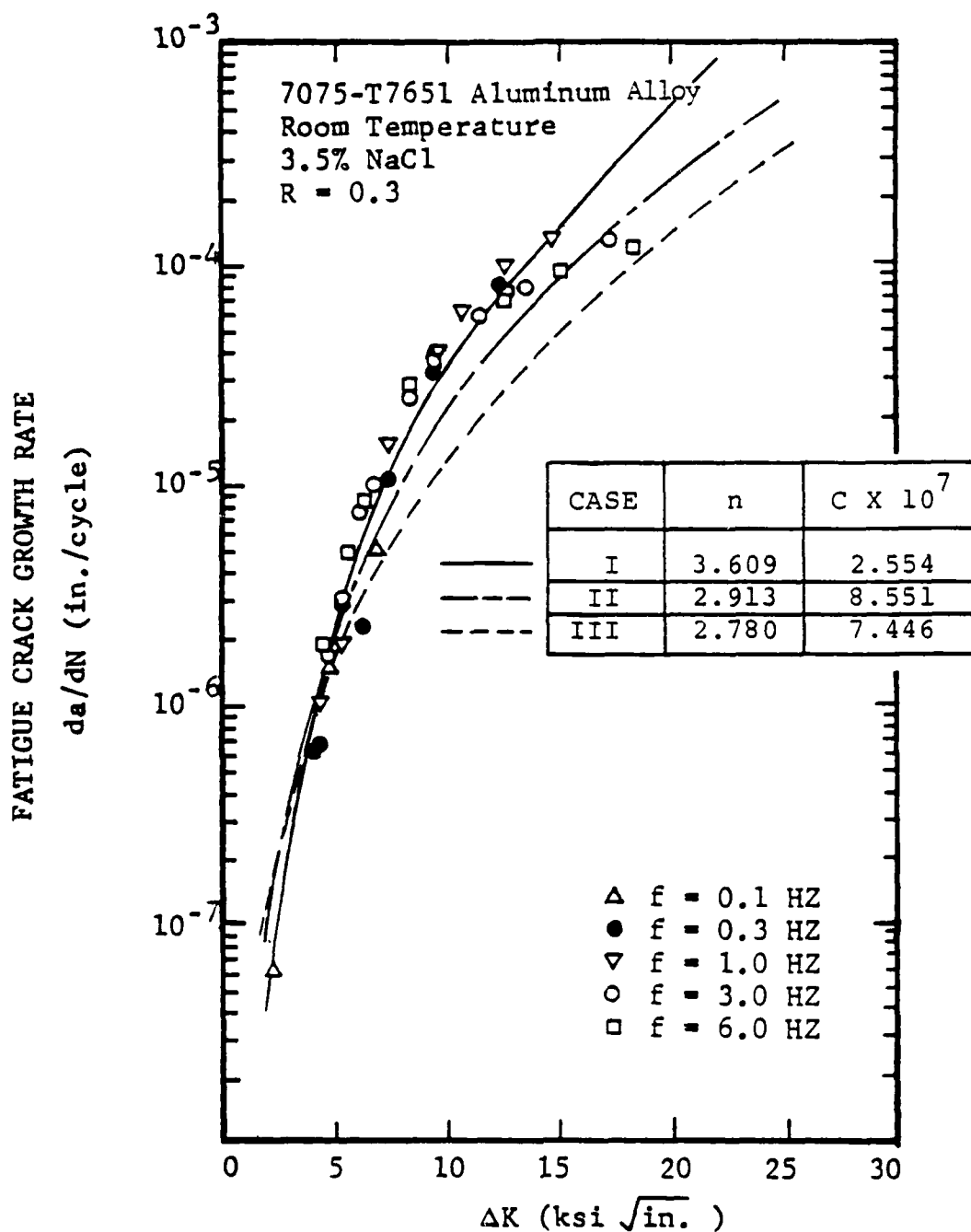


Fig. B-10 Forman Model Goodness-of-Fit Plots for  $da/dN$  Versus  $\Delta K$  (7075-T7651 Aluminum, R = 0.3, 3.5% NaCl Environment)

The following observations and discussions are based on the results shown in Figs. B-7 through B-10:

1. As expected, better overall fits were obtained for a given data set when the C and n values in the Forman model were fitted using the  $da/dN$  versus  $\Delta K$  results for that data set (refer to Case I). However, there's no guarantee that the C and n parameters based on one data set, for a given environment and R-ratio, will be acceptable for predicting the  $da/dN$  versus  $\Delta K$  values for the same environment and other R-ratios (e.g., ref. Case III plot shown in Figs. B-9 and B-10).

2. The C and n values for a given environment and R-ratio were used to make  $da/dN$  versus  $\Delta K$  predictions for a different R-ratio (Case III). C and n values were also determined using a data pooling procedure (Case II). Overall, Case II predictions for  $da/dN$  correlated much better than Case III predictions over the  $\Delta K$  range of the data. Therefore, the data pooling procedure is very promising for determining the C and n parameters in the Forman model for applications to different R-ratios.

3. The data pooling procedure described herein is useful for determining "compatible" C and n values for different da/dN versus  $\Delta K$  data sets. Also, since n is constant for the pooled data sets, the resulting C values can be used to determine an "environmental scaling factor" (ESF) for accounting for the effect of the environment on da/dN. For example, an ESF can be determined using Eq. B-13 and C values in Table B-9.

$$ESF = \frac{C_{wet}}{C_{Dry}} \quad (B-13)$$

Then,  $(da/dN)_{wet}$  is given by Eq. B-14.

$$(da/dN)_{wet} = ESF * (da/dN)_{dry} \quad (B-14)$$

Using  $C_{wet} = 8.551 \times 10^{-7}$  and  $C_{dry} = 4.722 \times 10^{-7}$  (from Table B-9 for case III) and Eq. B-13, and ESF of 1.81 is obtained.

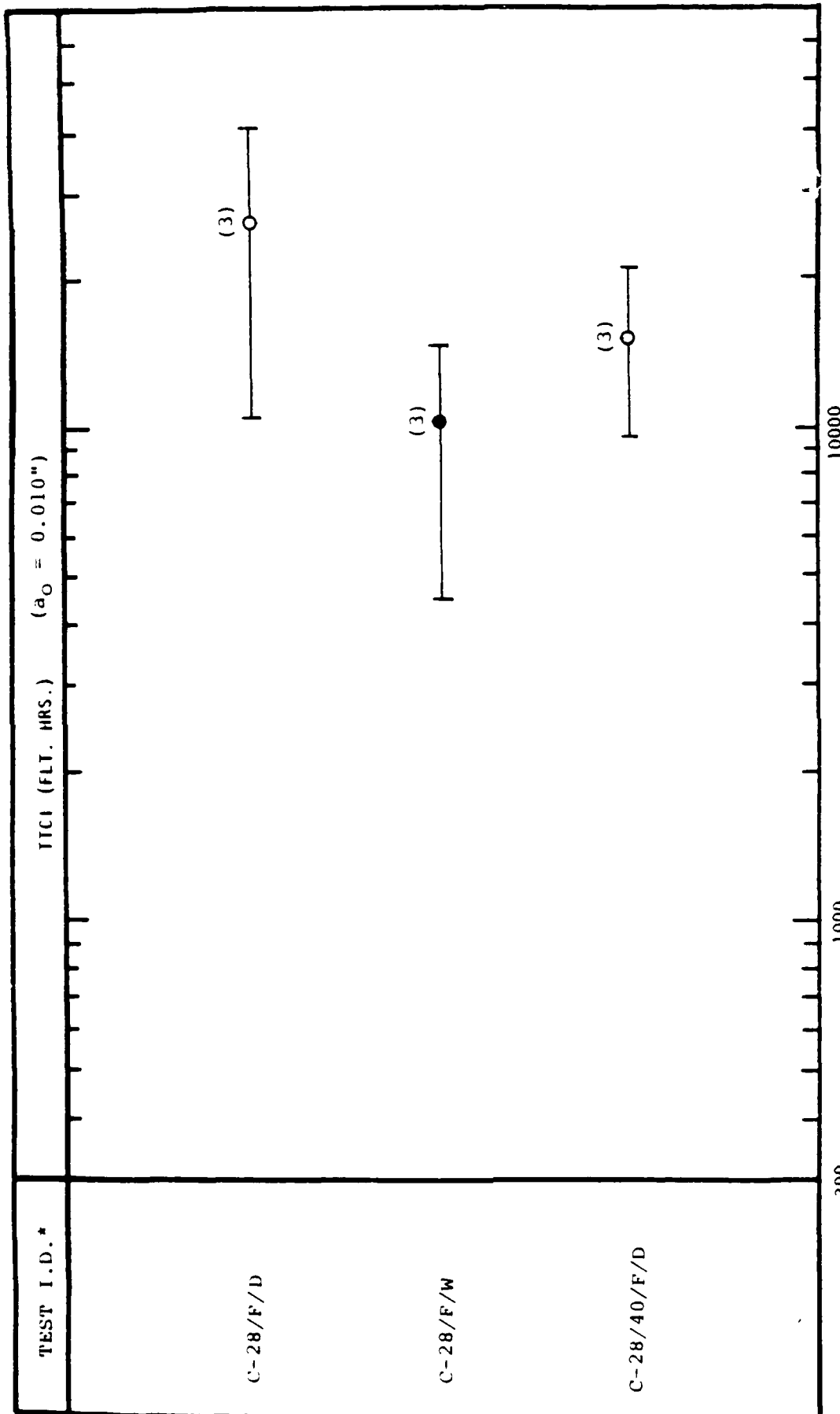


Fig. C-7 Comparison of TICI Test Results for 7075-T7651 Aluminum Dog-Bone Specimens (Open Hole; 40% I.T) Based on F-18 300 Hour (Block) Spectrum ("C") and Dry Air/3.5% NaCl Environments

\*Ref. Table 8

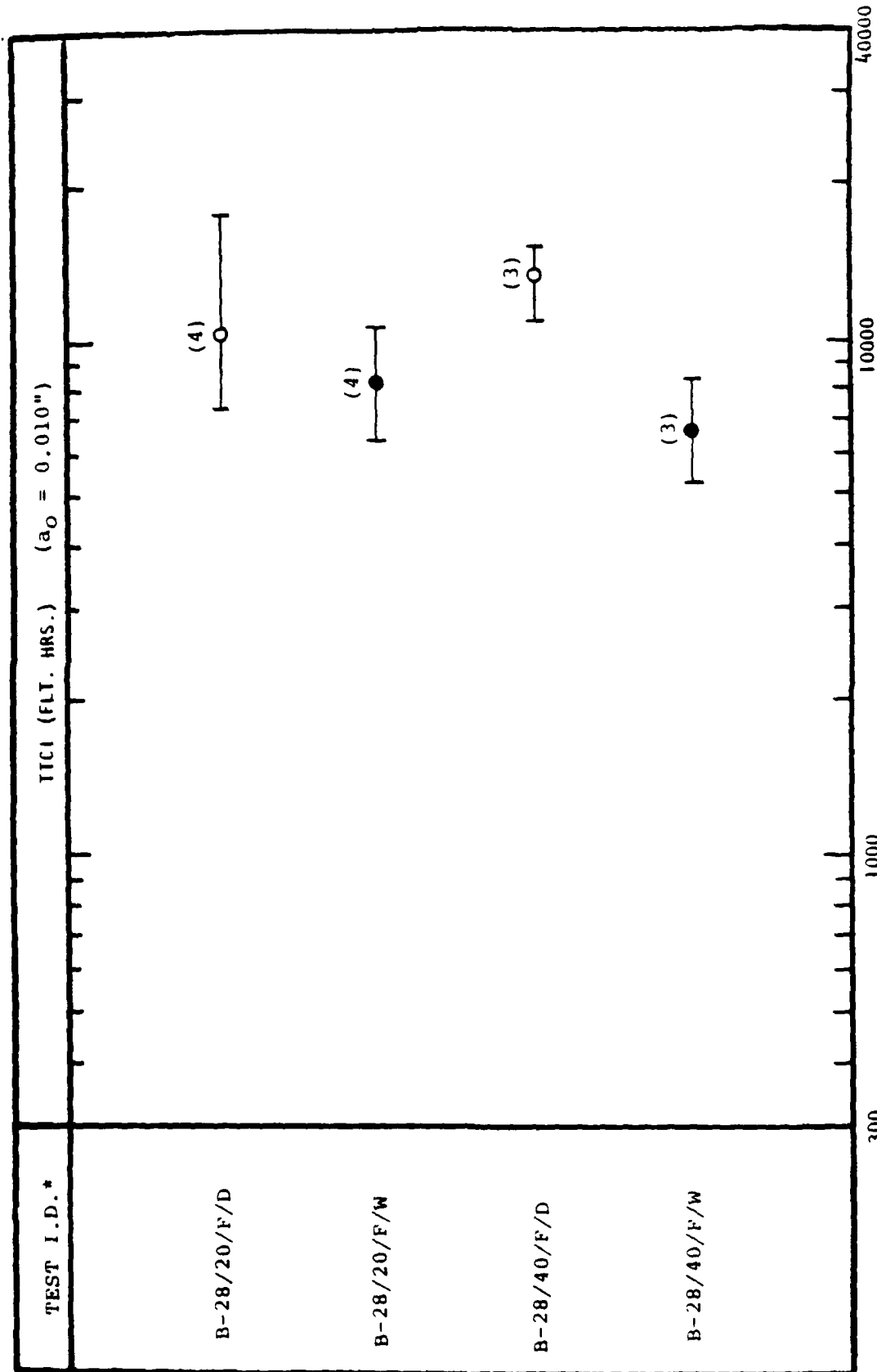


Fig. C-6 Comparison of TlCl Test Results for 7075-T7651 Aluminum Dog-Bone Specimens (20% LT; 40% LT) Based on F-18 300 Hour (Random) Spectrum ("B") and Dry Air/3.5% NaCl Environments

\*Ref. Table 8

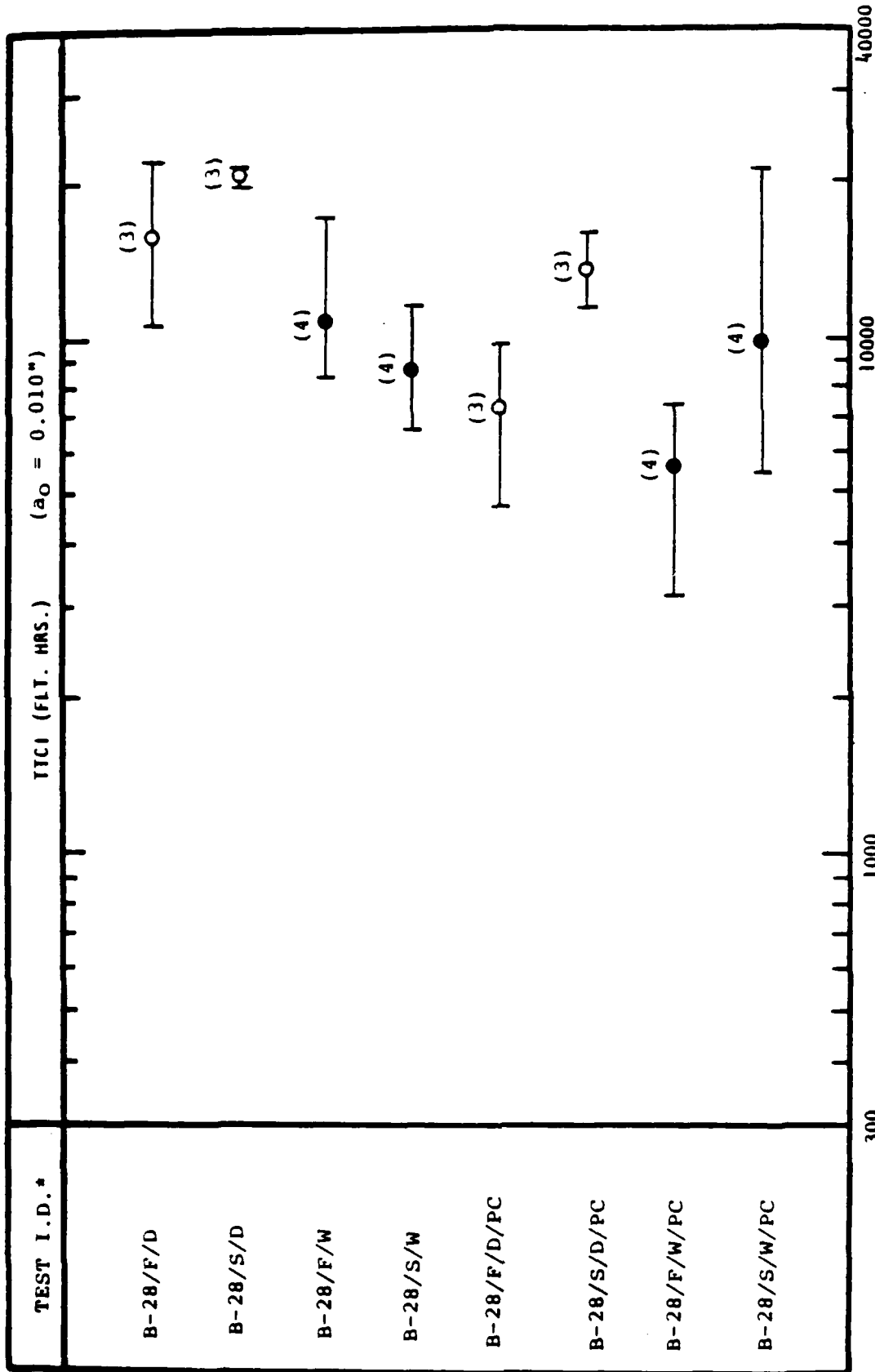


Fig. C-5 Comparison of TICI Test Results for 7075-T7651 Aluminum Dog-Bone Specimens (Open Hole) Based on F-18 300 Hour (Random) Spectrum ("B"), Specimen Preconditioning and Dry Air/3.5% NaCl Environments

\*Ref. Table 8

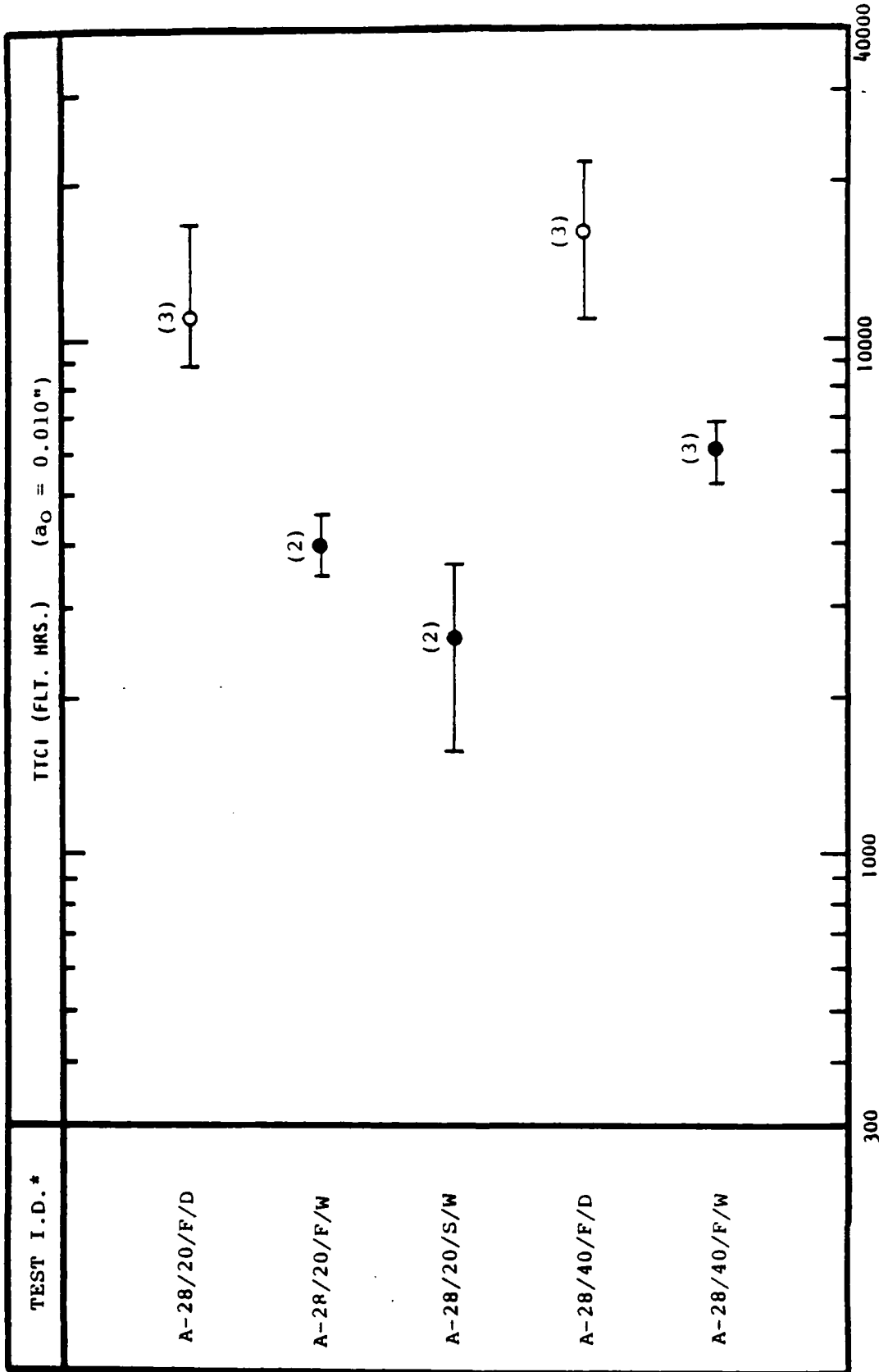


Fig. C-4 Comparison of TICI Test Results for 7075-T7651 Aluminum Dog-Bone Specimens (20% LT; 40% LT) Based on F-16 400 Hour Spectrum ("A") and Dry Air/3.5% NaCl Environments

\*Ref. Table 8

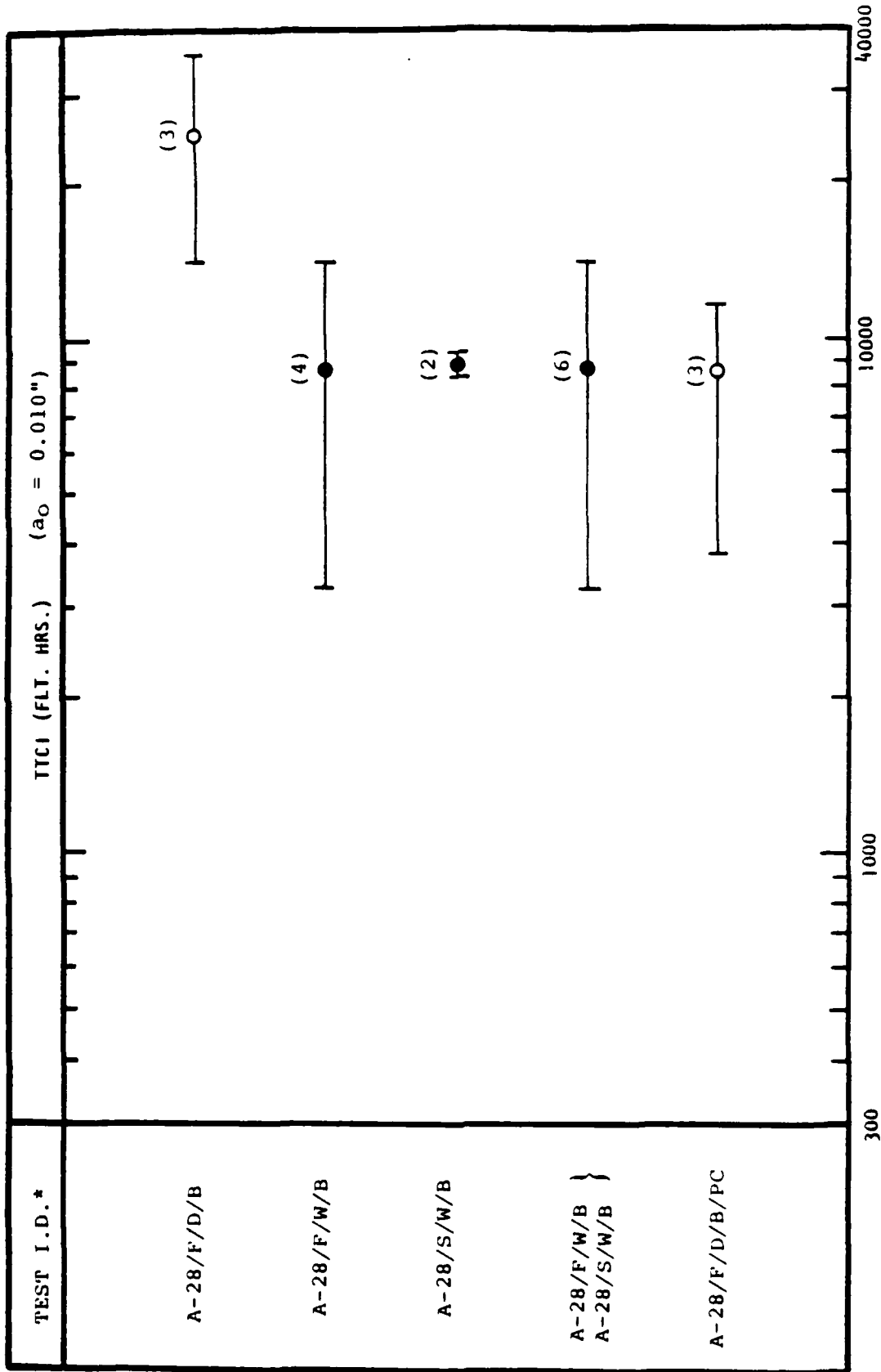


Fig. C-3 Comparison of TCI Test Results for 7075-T7651 Aluminum Dog-Bone Specimens (Bolt-In-Hole) Based on F-16 400 Hour Spectrum ("A"), Specimen Preconditioning Dry Air/3.5% NaCl Environments

\*Ref. Table 8

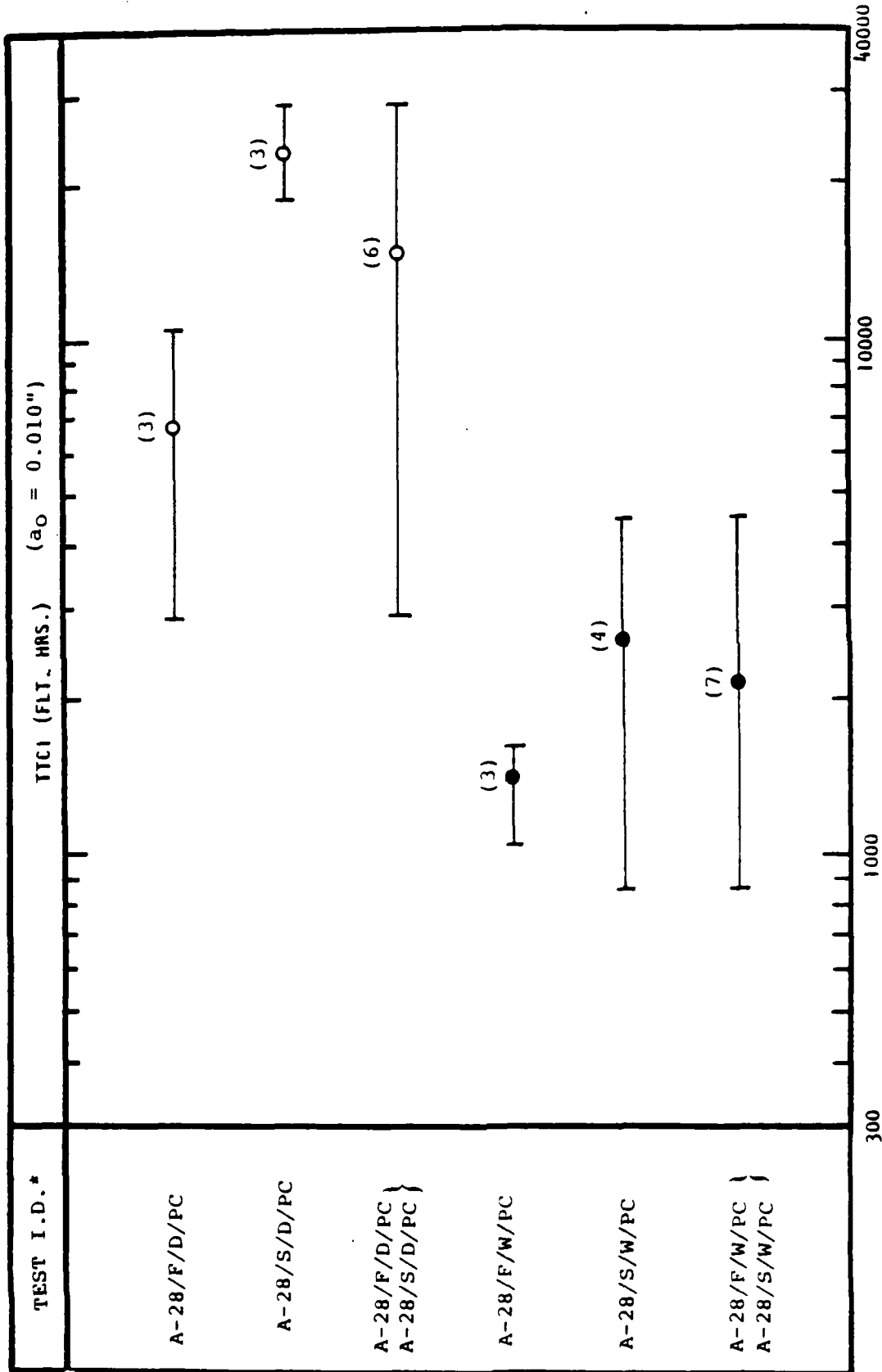


Fig. C-2 Comparison of TICI Test Results for 7075-T7651 Aluminum Dog-Bone Specimens (Open Hole) Based on F-16 400 Hour Spectrum ("A"), Specimen Preconditioning and Dry Air/3.5% NaCl Environments

\*Ref. Table 8

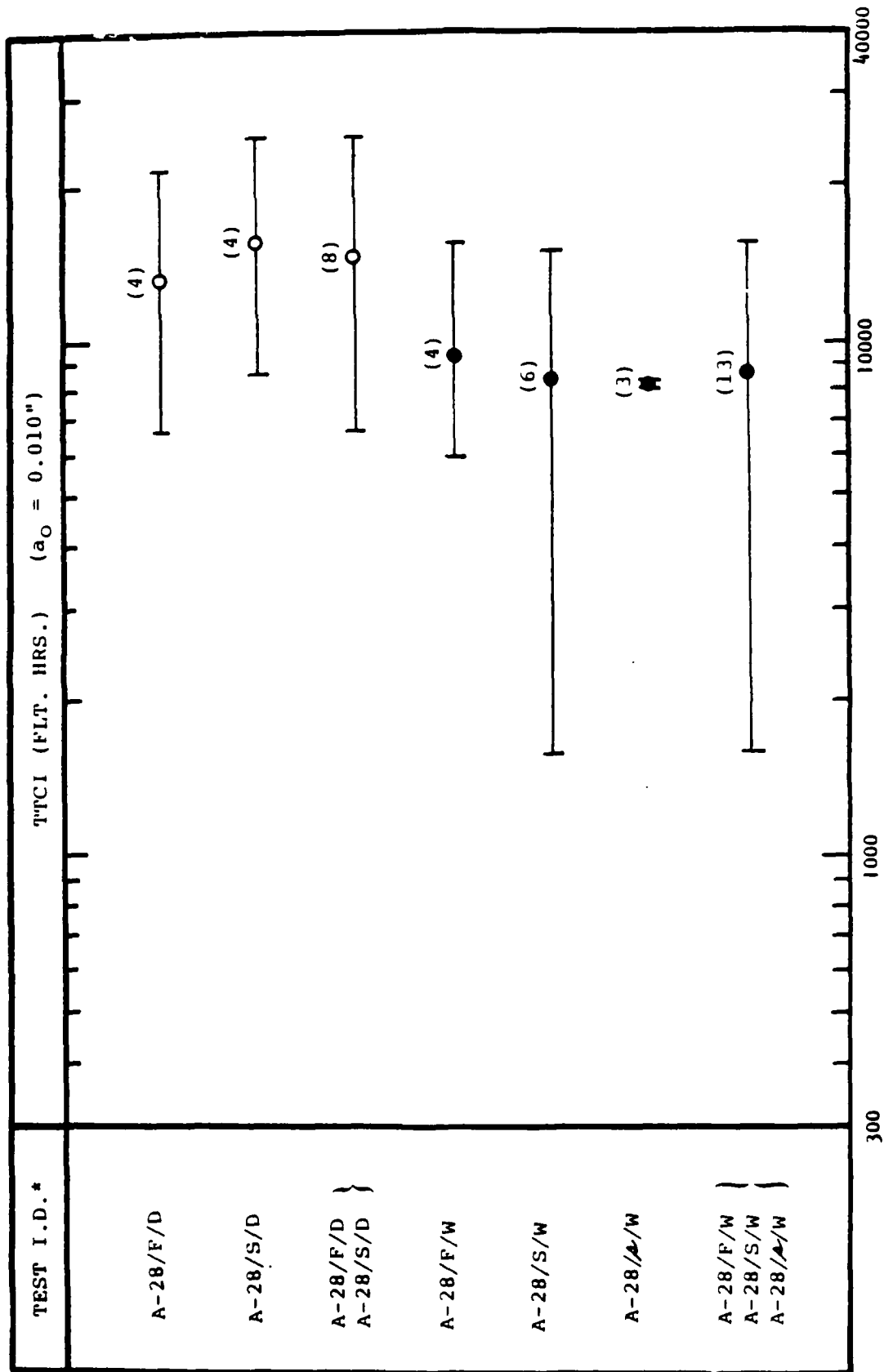


Fig. C-1 Comparison of TTCI Test Results for 7075-T7651 Aluminum Dog-Bone Specimens (Open Hole) Based on F-16 400 Hour Spectrum ("A") and Dry Air/3.5% NaCl Environments

\*Ref. Table 8

- o Test I.D.
- o Data set number
- o Specimen no. for each specimen a given data set
- o Test results for TTCI, TTF, TFCG (i.e., TTF-TTCI) and TTCI/TTF ratio
- o The average TTCI, average TTF and average TFCG are presented for each data set as well as the corresponding coefficient of variation
- o Fatigue crack origin for each specimen in a data set.

The information presented in Tables C-1 and C-2 is evaluated further in the following subsections.

### C.3 BAR GRAPH PLOTS FOR TTCI, TTF AND TFCG

Test results from Tables C-1 and C-2 are plotted in a bar graph format in Figs. C-1 through C-16. The average test result and the high/low values in each data set are plotted in a bar graph format. In Figs. C-1 through C-16, an open or solid circle denotes the average test results and the tic marks at the ends of the horizontal bar denotes the high/low test results considering all specimens in an applicable data set. Data sets are identified by Test I.D. (Refer to Table 8 for description code). The number of specimens in a given data set used to determine the average test result is noted in ( ) above the symbol for the average value.

Table C-2 Summary of 7075-T7651 Aluminum Dog-Bone Specimens for Task 6

TEST I.D. (a)	DATA SET	SPECIMEN NO.	TIME (PLT. HOURS)			TTCI (c)		TTP (d)		TTF-TTCI (e)		TTCI/TTF		FATIGUE CRACK ORIGIN (b)
			(c) TTCI	(d) TTP	(e) TTF-TTCI	AVE (PLT. HRS.)	C.O.V. (%)	AVE (PLT. HRS.)	C.O.V. (%)	AVE (PLT. HRS.)	C.O.V. (%)	AVE	C.O.V. (%)	
A-28/20/F/D	15	74	8800	18000	9200	11934	35.8	22000	24.0	10066	10.2	0.53	11.0	B
		75	10203	20000	9797									B
		80	16800	28000	11200									B
A-28/20/S/D	17	73	16100	24800	10700									B
A-28/20/F/W	16	66	3400	8904	5504	3934	19.8	8252	11.2	4298	39.7	0.49	30.3	B
		68	4508	7600	3092	2664	53.2	6338	16.3	3674	10.4	0.40	40.7	B
		69	1662	5607	3945	16651	31.7	30282	18.5	13631	3.5	0.54	13.9	B
A-28/20/S/W	18	70	3665	7068	3403									B
		506	11736	24835	13099									B
		507	16000	30006	14006									B
A-28/40/F/W	19	508	22218	36006	13788									B
		509	6048	11206	5158	6006	13.9	9747	14.4	3741	33.3	0.62	13.8	B
		510	5149	8400	3251									B
B-28/20/F/D	30	511	6821	9615	2814									B
		308	7228	11161	3935	10302	44.5	14038	33.4	3737	10.4	0.72	10.1	B
		309	8100	12037	3937									B
B-28/20/F/W	29	310	17115	21037	3922									B
		311	8764	11916	3152									B
		332	6343	11358	5015	8041	28.2	11182	19.9	3160	41.4	0.72	15.1	B
B-28/40/F/D	31	500	12900	19650	6750	13030	10.9	20672	8.3	7672	9.9	0.63	5.7	B
		501	14550	22650	8100									B
		502	11700	19216	8016									B
B-28/40/F/W	32	503	6633	8916	2283	6659	23.2	9399	19.7	2740	17.3	0.70	6.8	B
		504	8218	11446	3228									B
		505	5127	7876	2709									B
C-28/F/W	36	524	6900	13500	6600	6750	3.1	13650	1.6	6900	6.1	0.49	4.3	B
		525	6600	13800	7200									B
		526(h)	955(f)	9900	8945									B
C-28/40/F/D	35	521	9591(f)	30600	21009	15689	37.4	34700	14.3	19010	10.3	0.44	26.6	B
		522	16200	33300	17100									B
		523	21278	40200	18922									B

Notes: (a) Ref. Table 8 for description code

(b) Fatigue crack origin: B = bore of hole

(c) Time-to-crack-initiation ( $a_i = 0.01$ " depth) in fastener hole (determined from fractographic results)

(d) Time-to-failure

(e) Time spent in crack growth

(f) Value extrapolated to  $a_i = 0.01$ " crack depth using fractographic results (Vol. IV)

(g) Initial manufacturing scratch in corner of hole in dog-bone test specimen

(h) Results not reflected in statistics because of (g)

Table C-1 Summary of 7075-T7651 Aluminum Dog-Bone Test Results for Task 5 (Continued)

TEST	I.D. (a)	DATA SET	SPECIMEN NO.	(FLT. HOURS)			TTCI		TTCI (c)		TTF (d)		TTF-TTCI (e)		TTCI/TTF		FATIGUE CRACK ORIGIN
				(c) TTCI	(d) TTF	(e) TTF-TTCI	(AVE (FLT. HRS.))	(C.O.V. (Z))	(AVE (FLT. HRS.))	(C.O.V. (Z))	(AVE (FLT. HRS.))	(C.O.V. (Z))	(AVE (FLT. HRS.))	(C.O.V. (Z))	(AVE (FLT. HRS.))	(C.O.V. (Z))	
C-20/P/W	↓	↓	518	15300	20400	5100	10300	52.9	19700	3.2	9400	54.0	0.52	50.9	↓	↓	C
			519	4500	19500	15000	0.75	↓	↓	↓	↓	↓	↓	↓	↓	↓	C
			520	11100	19200	8100	0.23	↓	↓	↓	↓	↓	↓	↓	↓	↓	C
							0.58										B

NOTES: (a) Ref. Table 8 for description code

(b) Fatigue Crack origins: B = bore of hole and C = corner of hole

(c) Time-to-crack-initiation ( $a_1 = 0.01$ " depth) in fastener hole (determined from fractographic results)

(d) Time-to-Failure

(e) Time spent in crack growth

(f) Testing Anomaly

(g) Value extrapolated to  $a_1 = 0.01$ " crack depth using fractographic results (Vol. IV)

(h) Inadequate data to compute

Table C-1 Summary of 7075-T7651 Aluminum Dog-Bone Test Results for Task 5 (Continued)

TEST (a)	I.D.	DATA SET	SPECIMEN NO.	(FLT. HOURS)			TTCI (c)		TTF (d)		TTF-TTCI (e)		TTCI/ITF		FATIGUE CRACK ORIGIN
				(c) TTCI	(d) TTF	(e) TTF-TTCI	AVE (FLT. HRS.)	C.O.V. (z)	AVE (FLT. HRS.)	C.O.V. (z)	AVE (FLT. HRS.)	C.O.V. (z)	AVE.	C.O.V. (z)	
A-28/F/D/B/PC	↓	13	140	3857(g)	17440	13583	8486	50.9	21280	16.6	12794	6.2	0.38	39.1	B
			141	9200	22000	12800	↑	↑	↑	↑	↑	↑	↑	↑	B
			412	12400	24400	12000	↑	↑	↑	↑	↑	↑	↑	↑	B
A-28/F/N/B/PC	↓	14	112	3120	9635	6515	3331	31.9	10157	6.0	6826	10.9	0.32	29.7	B
			114	2323(g)	10000	7677	↑	↑	↑	↑	↑	↑	↑	↑	B
			116	4549	10835	6286	↑	↑	↑	↑	↑	↑	↑	↑	C
A-28/20/F/N/PC	↓	37	101	3775	6007	2232	↑	↑	↑	↑	↑	↑	↑	↑	B
			104(f)	2812	5550	2738	↑	↑	↑	↑	↑	↑	↑	↑	B
			338	2000	3959	1959	↑	↑	↑	↑	↑	↑	↑	↑	B
A-28/20/S/N/PC	↓	21	315	15752(g)	20853	5101	16395	36.1	24167	12.3	7772	72.3	0.68	32.5	B
			316	22608(g)	26595	3987	↑	↑	↑	↑	↑	↑	↑	↑	B
			317	10824(g)	25053	14229	↑	↑	↑	↑	↑	↑	↑	↑	B
B-28/S/D	↓	22	326	20143	22716	2573	20589	5.3	23226	4.8	2637	2.3	0.89	0.6	B
			327	21824	24516	2692	↑	↑	↑	↑	↑	↑	↑	↑	B
			328	19800	22446	2646	↑	↑	↑	↑	↑	↑	↑	↑	B
B-28/F/W	↓	23	300	13002(g)	16646	3644	11917	34.9	15497	29.4	3579	12.7	0.76	7.2	B
			301	9077	12152	3075	↑	↑	↑	↑	↑	↑	↑	↑	B
			302	8267	11717	3470	↑	↑	↑	↑	↑	↑	↑	↑	B
B-28/S/W	↓	24	303	17323(g)	21452	4129	8536	28.9	11819	17.5	3283	21.4	0.72	11.9	B
			318	12038	14676	2638	↑	↑	↑	↑	↑	↑	↑	↑	B
			319	6517	10707	4190	↑	↑	↑	↑	↑	↑	↑	↑	B
B-28/F/D/PC	↓	25	320	8447	11916	3469	7186	34.2	14034	15.9	6848	12.4	0.50	20.3	B
			321	7140	9975	2835	↑	↑	↑	↑	↑	↑	↑	↑	B
			312	9650	15693	6043	↑	↑	↑	↑	↑	↑	↑	↑	B
B-28/S/D/PC	↓	26	313	7176(g)	14916	7740	13541	13.7	16854	9.8	3113	6.3	0.80	3.3	B
			314	4733	11493	6760	↑	↑	↑	↑	↑	↑	↑	↑	B
			329	12797(g)	16116	3319	↑	↑	↑	↑	↑	↑	↑	↑	B
B-28/F/W/PC	↓	27	330	15650	18753	3103	↑	↑	↑	↑	↑	↑	↑	↑	B
			331	12175(g)	15693	3518	↑	↑	↑	↑	↑	↑	↑	↑	B
			304	7310(g)	10716	3406	5540	31.7	8588	24.0	3048	13.4	0.63	11.2	B
B-28/S/W/PC	↓	28	305	5548(g)	8163	2615	↑	↑	↑	↑	↑	↑	↑	↑	B
			306	3141(g)	5916	2775	↑	↑	↑	↑	↑	↑	↑	↑	B
			307	6161(g)	9538	3397	↑	↑	↑	↑	↑	↑	↑	↑	B
B-28/S/W/PC	↓	28	322	6076	8338	2282	9828	81.1	12661	65.0	2832	18.5	0.73	13.7	B
			323B	6097(g)	9453	3356	↑	↑	↑	↑	↑	↑	↑	↑	B
			324	21772	24969	3197	↑	↑	↑	↑	↑	↑	↑	↑	B
C-28/F/D	↓	33	325	5368(g)	7863	2495	26333	56.6	48871	34.2	22538	8.0	0.50	29.1	B
			515	27709	50100	22391	↑	↑	↑	↑	↑	↑	↑	↑	B
			516	10789	31596	20807	↑	↑	↑	↑	↑	↑	↑	↑	B
			517	40500(g)	64916	24416	↑	↑	↑	↑	↑	↑	↑	↑	B

Table C-1 Summary of 7075-T7651 Aluminum Dog-Bone Test Results for Task 5

TEST I.D. (a)	DATA SET	SPECIMEN NO.	(FLT. HOURS)			TTCI (c)		TTF (d)		TTF-TTCI (e)		TTCI/TF		FATIGUE CRACK ORIGIN
			(c) TTCI	(d) TTF	(e) TTF-TTCI	AVE (FLT. HRS.)	C.O.V. (Z)	AVE (FLT. HRS.)	C.O.V. (Z)	AVE (FLT. HRS.)	C.O.V. (Z)	AVE.	C.O.V. (Z)	
A-28/P/D	1	45	14000	22000	8000	11200	48.2	22099	34.3	8899	20.7	0.58	19.7	B
		46	6600	16035	9435	11200	48.2	22099	34.3	8899	20.7	0.58	19.7	B
		79	10600	17558	6958	11200	48.2	22099	34.3	8899	20.7	0.58	19.7	B
		89	21600	32806	11206	11200	48.2	22099	34.3	8899	20.7	0.58	19.7	B
A-28/S/D	2	72	8471	16435	7964	15930	44.3	24807	28.4	8877	16.4	0.62	17.9	B
		83	25200	33677	8477	15930	44.3	24807	28.4	8877	16.4	0.62	17.9	B
		87	16800	24835	8035	15930	44.3	24807	28.4	8877	16.4	0.62	17.9	B
		92	13249(g)	24279	11030	15930	44.3	24807	28.4	8877	16.4	0.62	17.9	B
A-28/P/M	3	62	5872	12035	6163	9243	52.5	15004	31.5	5762	6.7	0.59	18.8	B
		76	8000	13999	5999	9243	52.5	15004	31.5	5762	6.7	0.59	18.8	B
		77	16400	21949	5549	9243	52.5	15004	31.5	5762	6.7	0.59	18.8	B
		82	6700	17035	5335	9243	52.5	15004	31.5	5762	6.7	0.59	18.8	B
A-28/S/M	4	67	7531(a)	14835	7304	8291	63.0	14029	41.8	5738	42.0	0.54	38.9	C
		71	1600	7606	6006	8291	63.0	14029	41.8	5738	42.0	0.54	38.9	C
		81	1434	6749	3315	8291	63.0	14029	41.8	5738	42.0	0.54	38.9	B
		88	12554(g)	15074	2520	8291	63.0	14029	41.8	5738	42.0	0.54	38.9	B
A-28/P/PC	5	90	15226(g)	21635	6409	6750	59.3	19349	42.6	12599	33.9	0.33	21.2	C
		91	9400	18276	8876	6750	59.3	19349	42.6	12599	33.9	0.33	21.2	B
		84	8063(g)	10228	2165	8134	0.8	11021	10.9	2888	40.2	0.74	9.8	B
		85	8160(g)	10430	2270	8134	0.8	11021	10.9	2888	40.2	0.74	9.8	B
A-28/S/D/PC	6	103	10800	27235	16435	23333	20.6	35640	19.4	12307	29.4	0.66	11.6	C
		105	6651	20007	13356	23333	20.6	35640	19.4	12307	29.4	0.66	11.6	B
		106	2800	10806	8006	23333	20.6	35640	19.4	12307	29.4	0.66	11.6	B
		109	28000	43596	15596	23333	20.6	35640	19.4	12307	29.4	0.66	11.6	C
A-28/P/M/PC	8	110	18400	31125	12925	1439	20.6	5278	25.8	3838	30.9	0.28	18.9	C
		117	23600	32000	8400	1439	20.6	5278	25.8	3838	30.9	0.28	18.9	B
		102	1622	4835	3213	1439	20.6	5278	25.8	3838	30.9	0.28	18.9	B
		107	1600	6806	5206	1439	20.6	5278	25.8	3838	30.9	0.28	18.9	B
A-28/S/M/PC	9	108	1092	4192	3095	2656	77.9	4761	44.5	2105	29.7	0.49	49.1	B
		113	875	2806	1931	2656	77.9	4761	44.5	2105	29.7	0.49	49.1	B
		115	4440	7245	2805	2656	77.9	4761	44.5	2105	29.7	0.49	49.1	B
		336	851	3200	2349	2656	77.9	4761	44.5	2105	29.7	0.49	49.1	B
A-28/P/D/B	10	137	4456	5792	1336	2667	42.3	34539	26.4	9873	26.3	0.69	17.5	B
		126	23600	36035	12435	2667	42.3	34539	26.4	9873	26.3	0.69	17.5	B
		127	14800	24748	9948	2667	42.3	34539	26.4	9873	26.3	0.69	17.5	B
		128	33600	42815	7215	2667	42.3	34539	26.4	9873	26.3	0.69	17.5	B
A-28/P/M/B	11	122	3200	16006	12806	8611	57.6	15518	23.5	6907	57.1	0.54	44.7	B
		123	13868	18902	5034	8611	57.6	15518	23.5	6907	57.1	0.54	44.7	B
		124	11600	16806	5206	8611	57.6	15518	23.5	6907	57.1	0.54	44.7	B
		125	5777	10358	4581	8611	57.6	15518	23.5	6907	57.1	0.54	44.7	B
A-28/S/M/B	12	131	8759(g)	14007	5248	8829	7.5	17221	26.4	8392	46.2	0.52	17.7	C
		132	9100(g)	20435	11335	8829	7.5	17221	26.4	8392	46.2	0.52	17.7	C

## APPENDIX C

### EVALUATION OF CORROSION FATIGUE TEST RESULTS FOR 7075-T7651 ALUMINUM DOG-BONE SPECIMENS

#### C.1 INTRODUCTION

The purpose of this appendix is to: (1) summarize 7075-T7651 aluminum dog-bone specimen test results from Volume IV [24], and (2) evaluate test results to determine the effects of selected test variables on TTCI, TTF and TFCG. Test results are evaluated and plotted in various forms to facilitate evaluating the effects of the test variables. Statistical analyses of the test results are performed to gain insight into the significance of selected variables and their sensitivity.

#### C.2 SUMMARY OF DOG-BONE SPECIMEN TEST RESULTS AND STATISTICAL PROPERTIES

Test results for 7075-T7651 aluminum dog-bone specimens and useful statistical properties are summarized in Tables C-1 and C-2 for Tasks 5 and 6, respectively. The following information is presented for each data set tested:

APPENDIX C

EVALUATION OF CORROSION FATIGUE TEST RESULTS FOR  
7075-T7651 ALUMINUM DOG BONE SPECIMENS

Contents

<u>Section</u>		<u>Page</u>
C.1	Introduction	C-2
C.2	Summary of Dog-Bone Specimen Test Results and Statistical Properties	C-2
C.3	Bar Graph Plots for TICI, TTF and TFCG	C-7
C.4	Dry/Wet Ratios	C-25
C.5	Evaluation of TICI/TTF Ratio	C-28
C.6	Conclusions Based on Dog-Bone Specimen Test Results	C-32
	C.6.1 Time-To-Crack Initiation (TICI)	C-32
	C.6.2 Time-For-Crack-Growth (TFCG)	C-35
	C.6.3 Time-To-Failure (TTF)	C-37

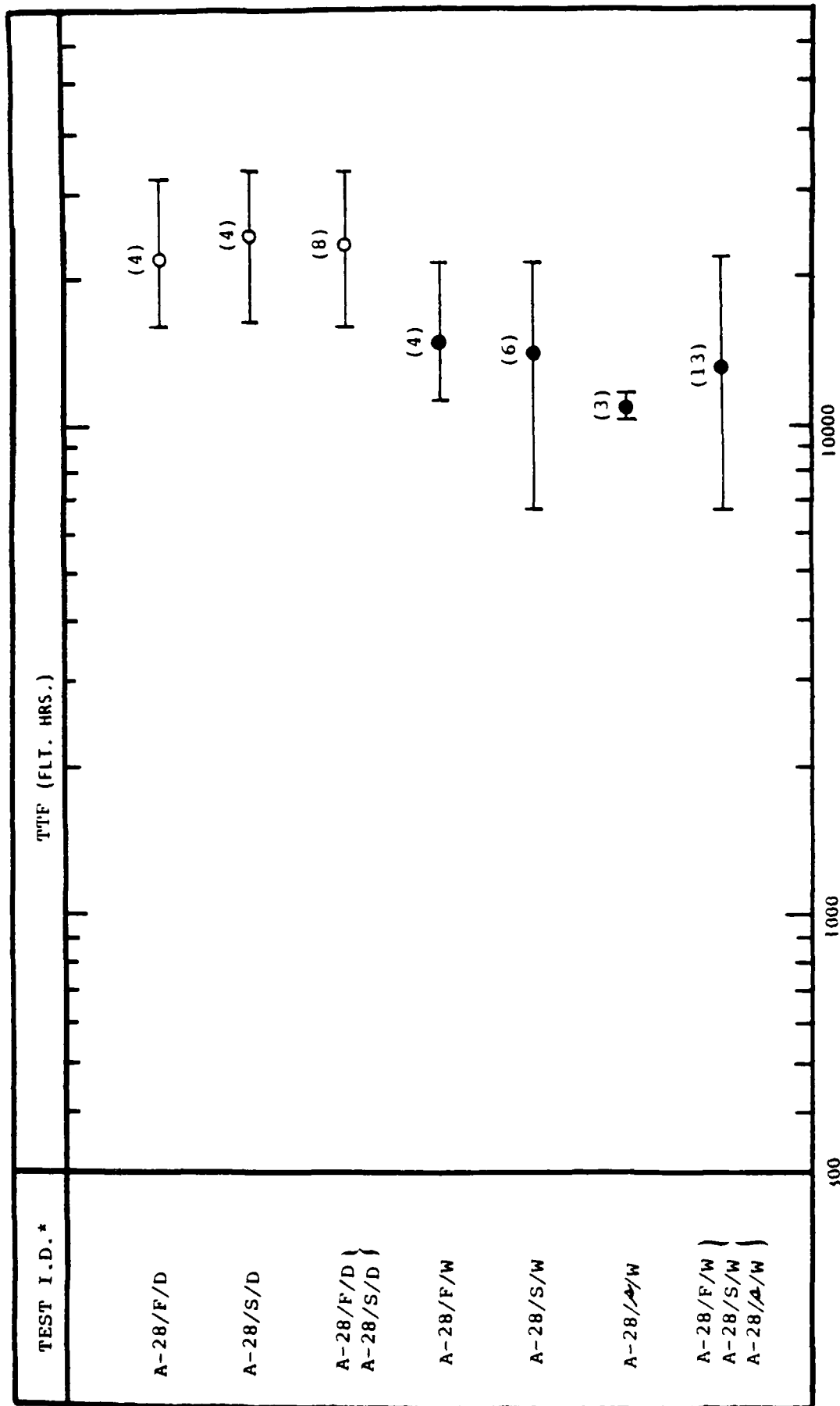


Fig. C-8 Comparison of TTF Test Results for 7075-T7651 Aluminum Dog-Bone Specimens (Open Hole) for F-16 400 Hour Spectrum ("A") and Dry Air/3.5% NaCl Environments

\*Ref. Table 8

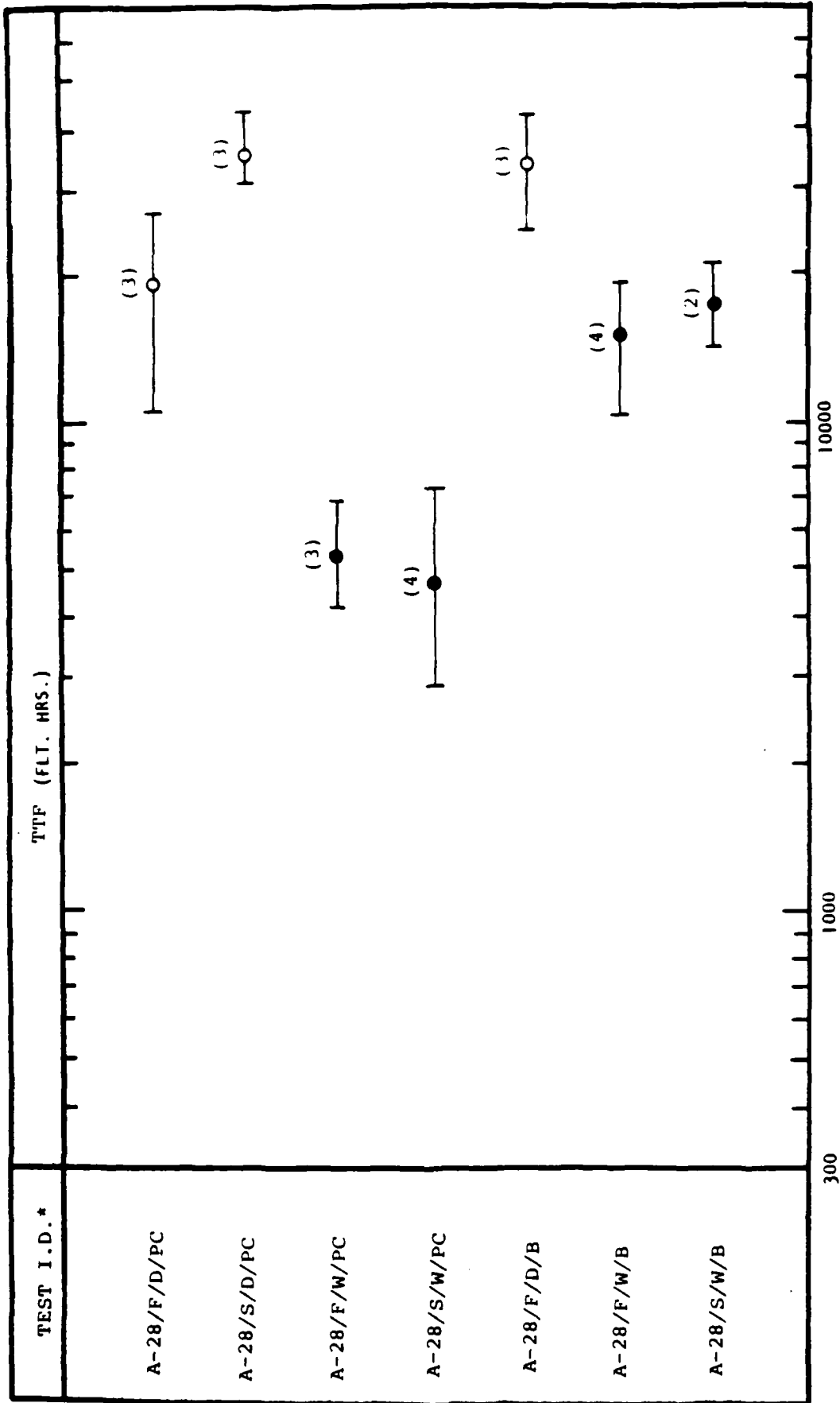


Fig. C-9 Comparison of TTF Test Results for 7075-T7651 Aluminum Dog-Bone Specimens (Open Hole; Bolt-In-Hole) Based on F-16 400 Hour Spectrum ("A"), Dry Air/3.5% NaCl Environments and Specimen Preconditioning

\*Ref. Table 8

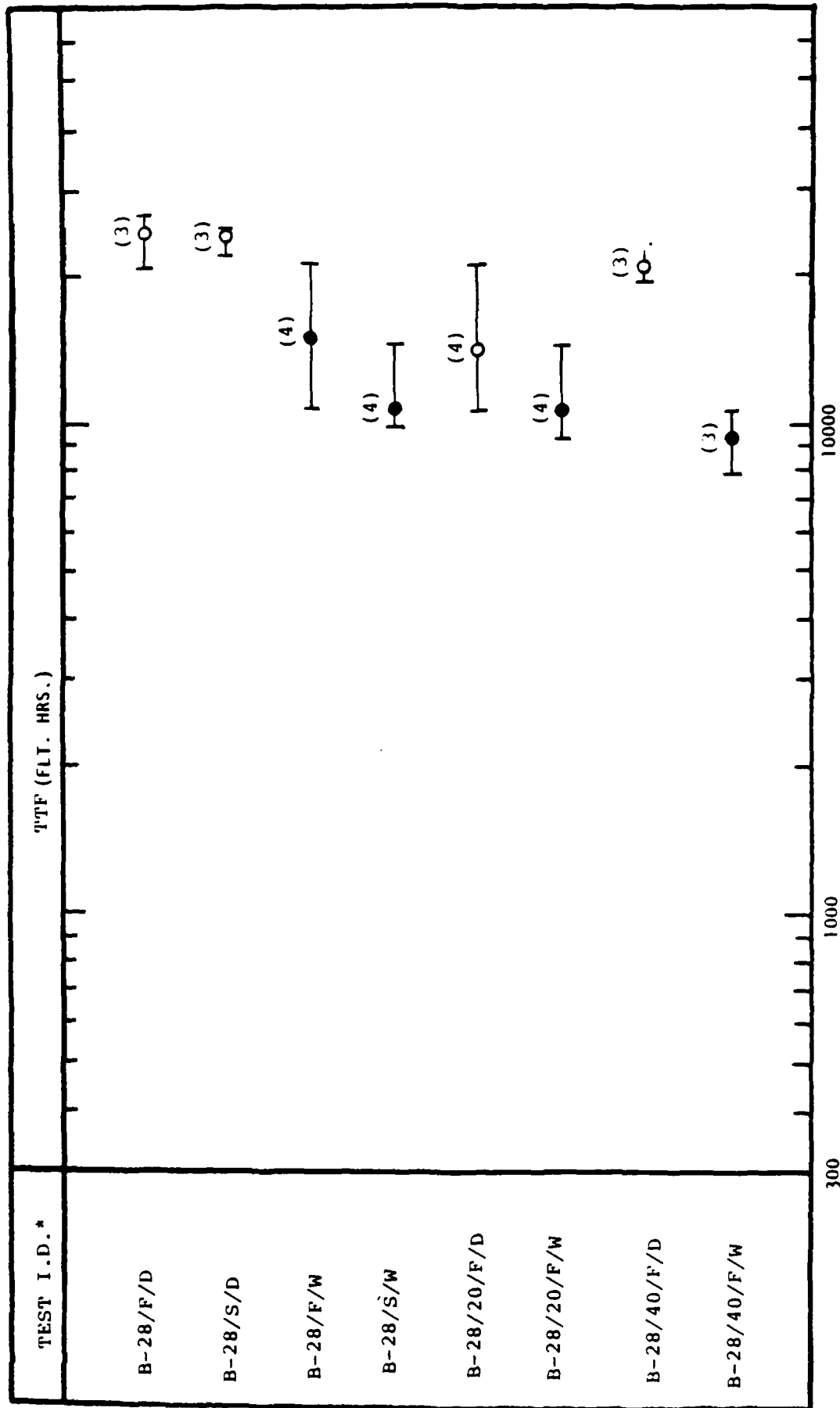


Fig. C-10 Comparison of TTF Test Results for 7075-T7651 Aluminum  
Dog-Bone Specimens (Open Hole; 20% LT; 40% LT)  
Based on F-18 300 Hour (Random) Spectrum ("B") and  
Dry Air/3.5% NaCl Environments

\*Ref. Table 8

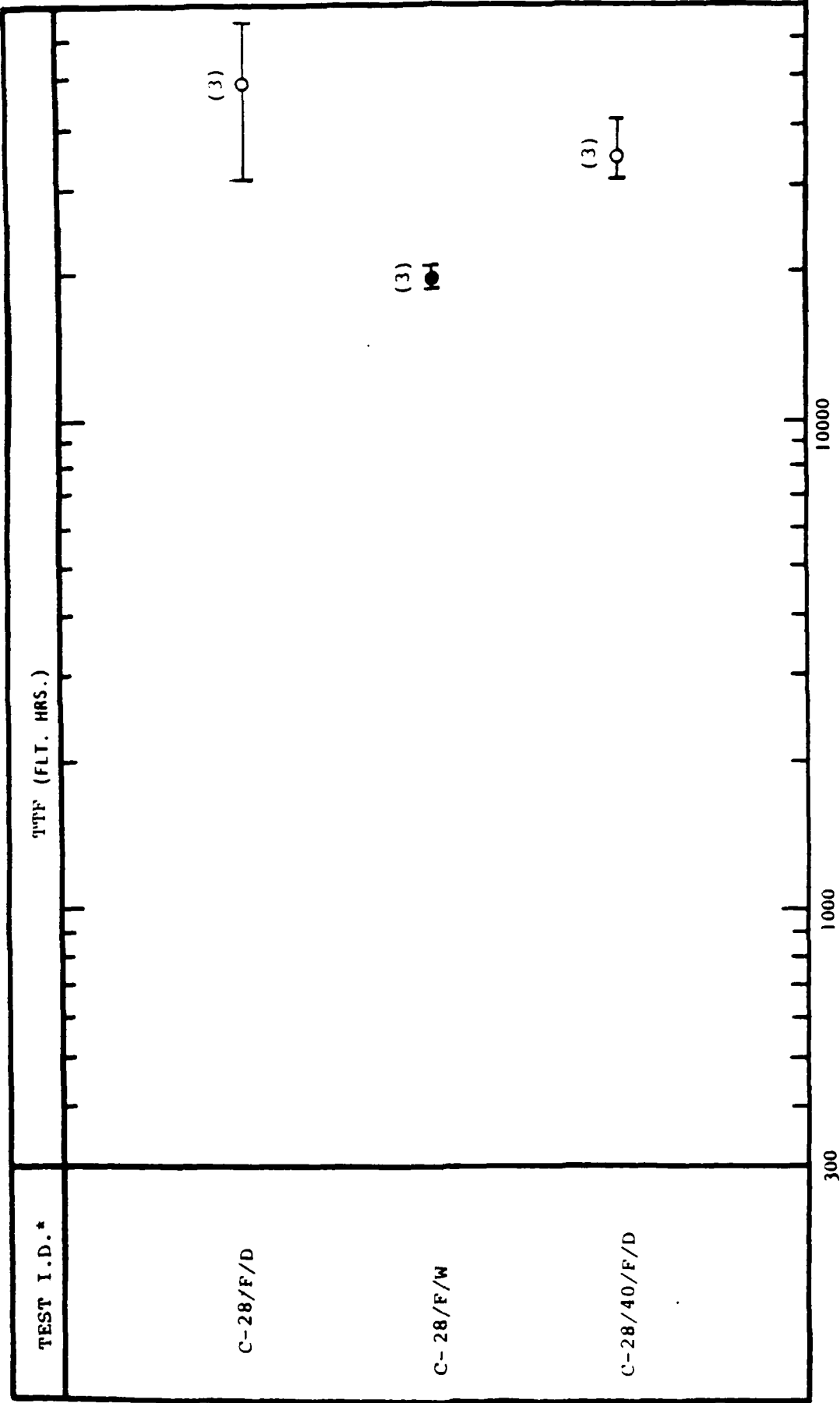


Fig. C-11 Comparison of TTF Test Results for 7075-T7651 Aluminum Dog-Bone Specimens (Open Hole; 40% LT) Based on F-18 300 Hour (Block) Spectrum ("C") and Dry Air/3.5% NaCl Environments

\*Ref. Table 8

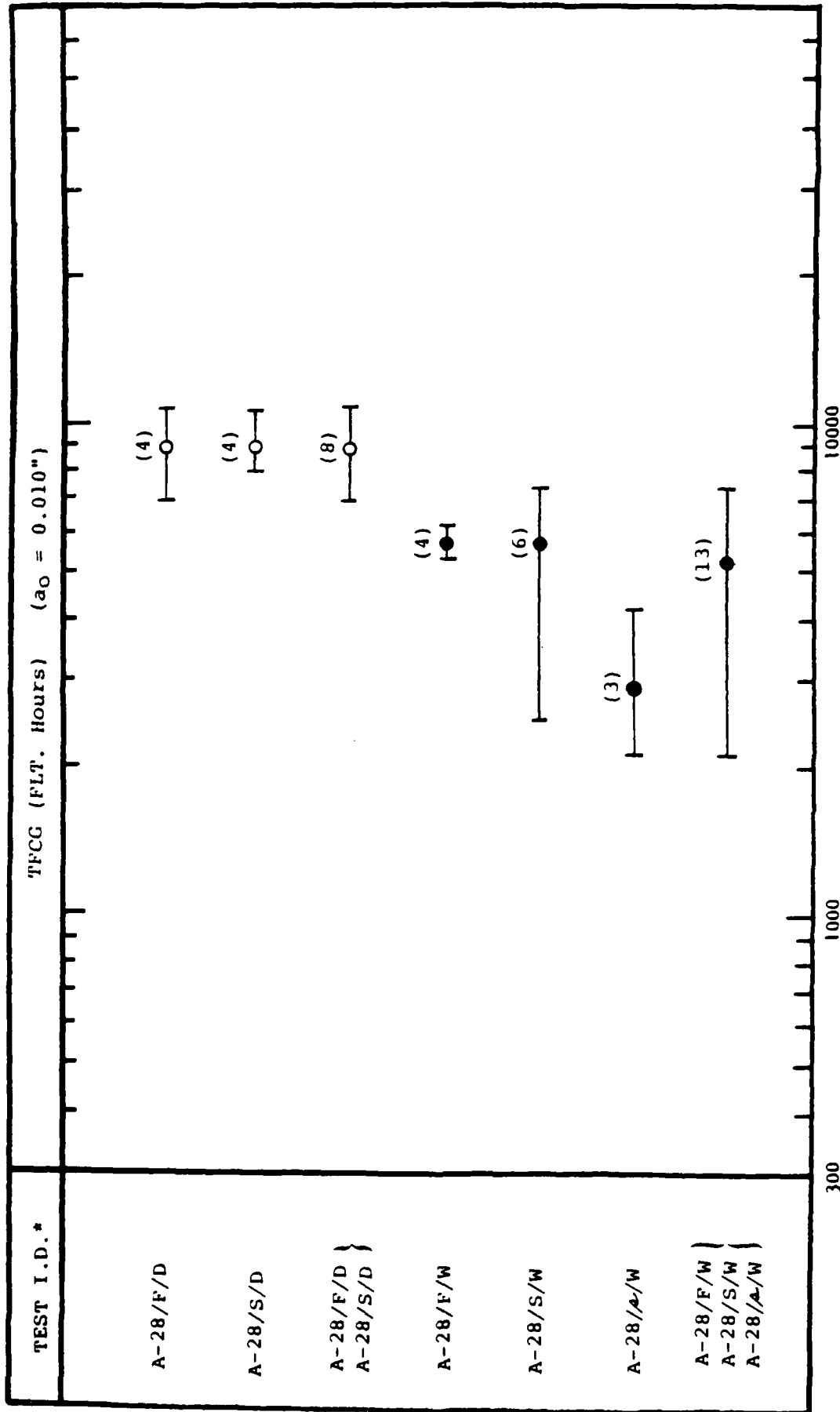


Fig. C-12 Comparison of Crack Growth Test Results for 7075-T7651 Aluminum Dog-Bone Specimens (Open Hole) for F-16 400 Hour Spectrum ("A") and Dry Air/3.5% NaCl Environments

\*Ref. Table 8

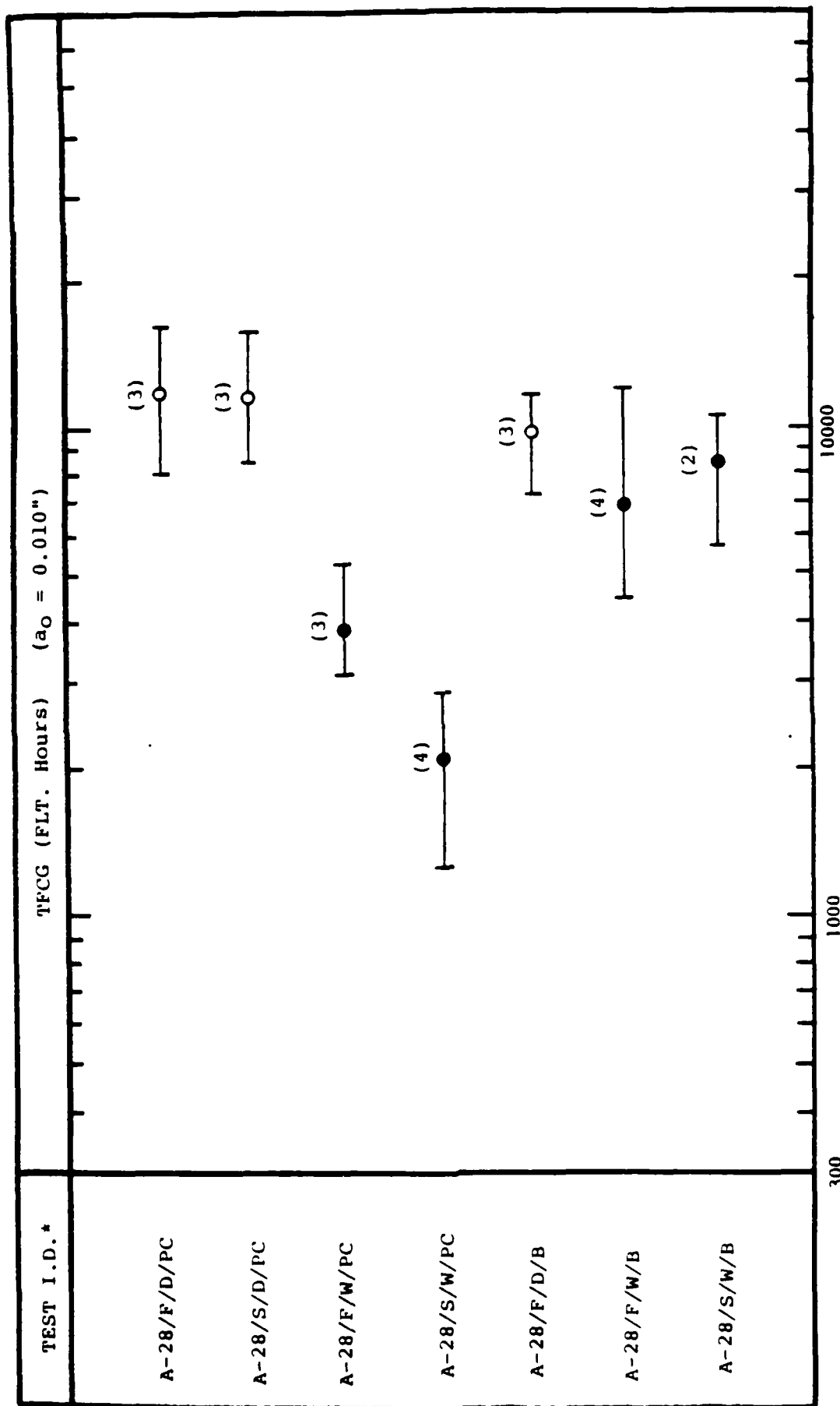


Fig. C-13 Comparison of Crack Growth Test Results for 7075-T7651 Aluminum Dog-Bone Specimens (Open Hole; Bolt-In-Hole) Based on F-16 400 Hour Spectrum ("A"), Dry Air/3.58 NaCl Environments and Specimen Preconditioning

\*Ref. Table 8

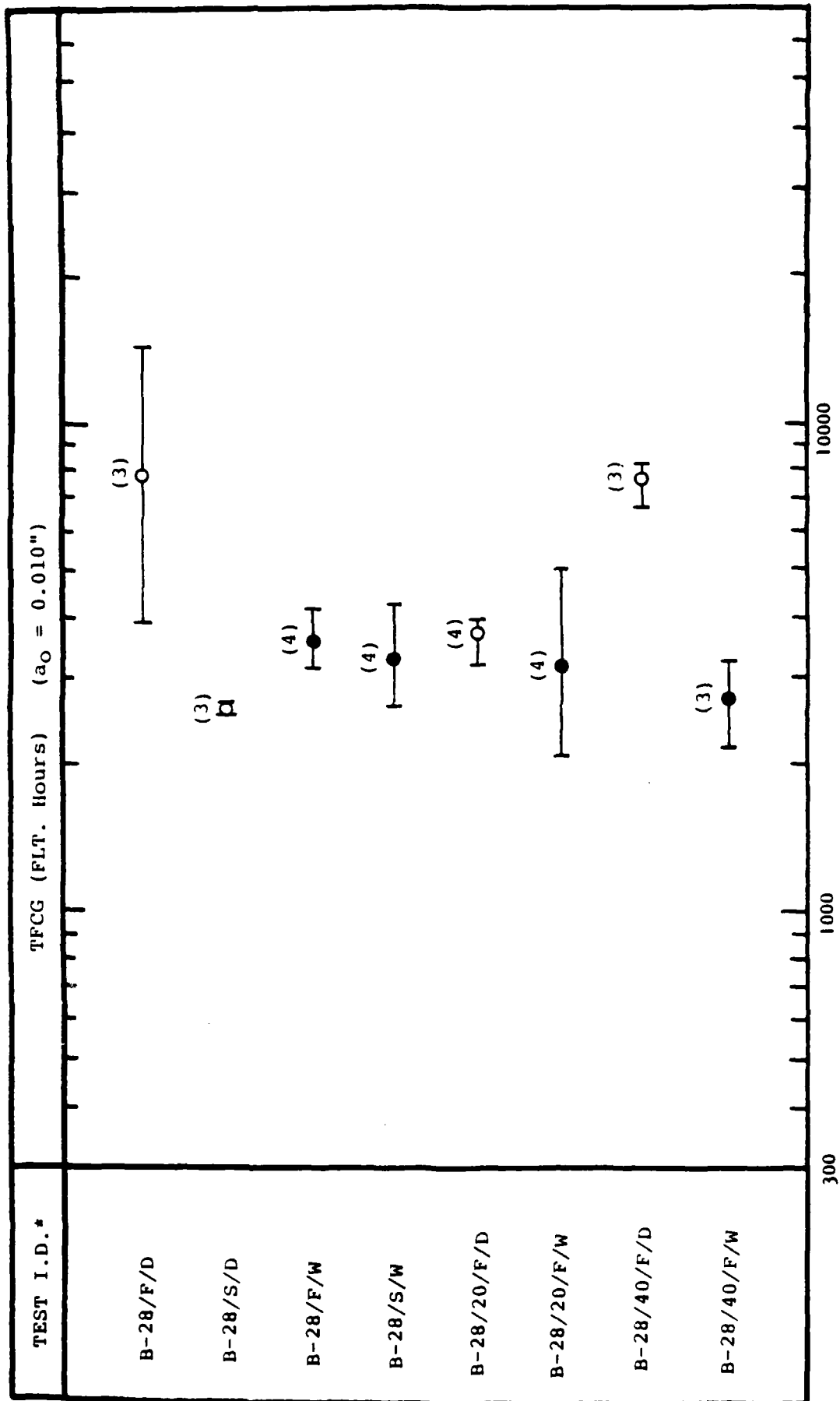


Fig. C-14 Comparison of Crack Growth Test Results for 7075-T7651 Aluminum Dog Bone Specimens (Open Hole; 20% LT; 40% LT) Based on F-18 300 Hour (Random) Spectrum ("B") and Dry Air/3.5% NaCl Environments

\*Ref. Table 8

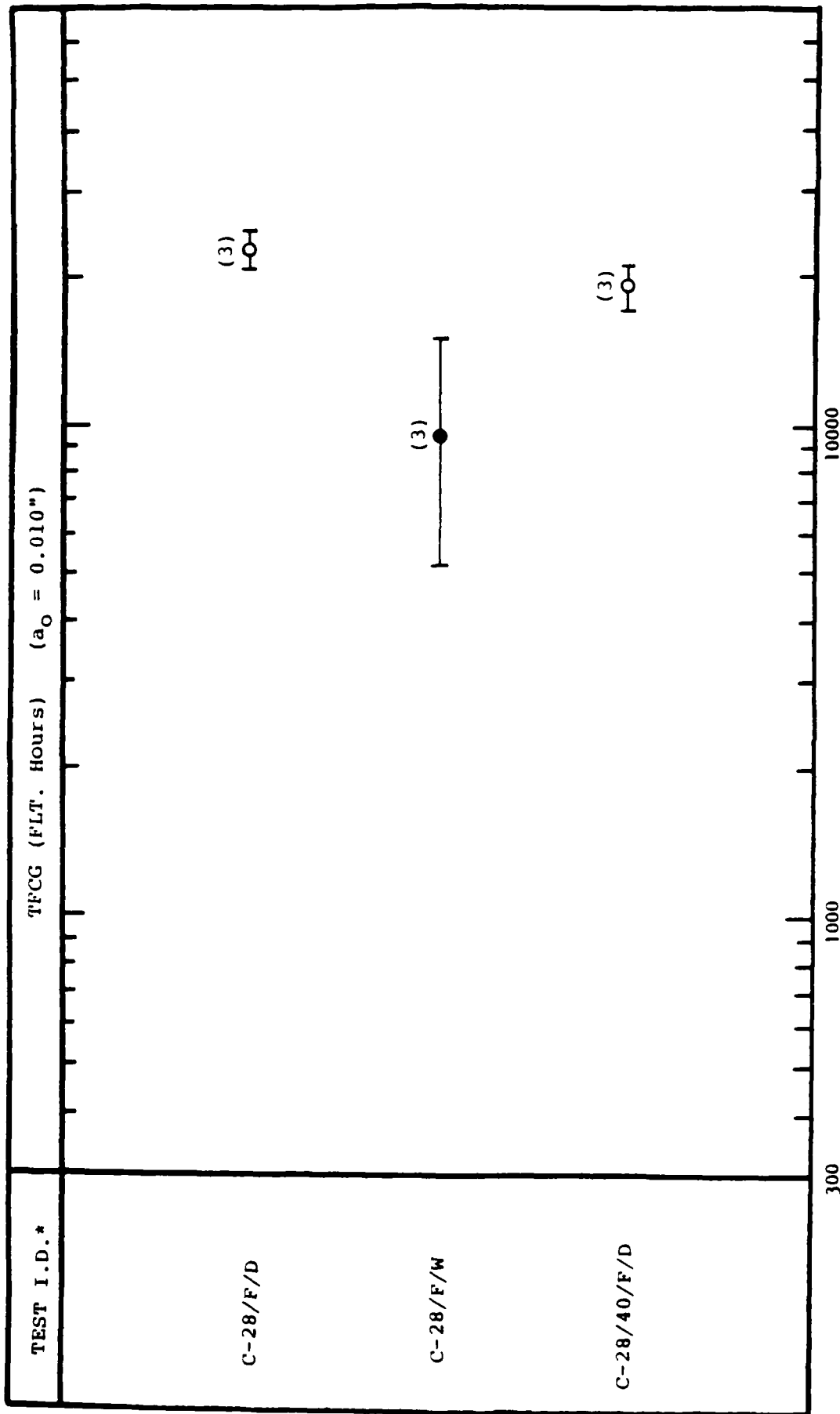


Fig. C-15 Comparison of Crack Growth Test Results for 7075-T7651 Aluminum Dog-Bone Specimens (Open Hole; 40% LT) Based on F-18 300 Hour (Block) Spectrum ("C") and Dry Air/3.5% NaCl Environments

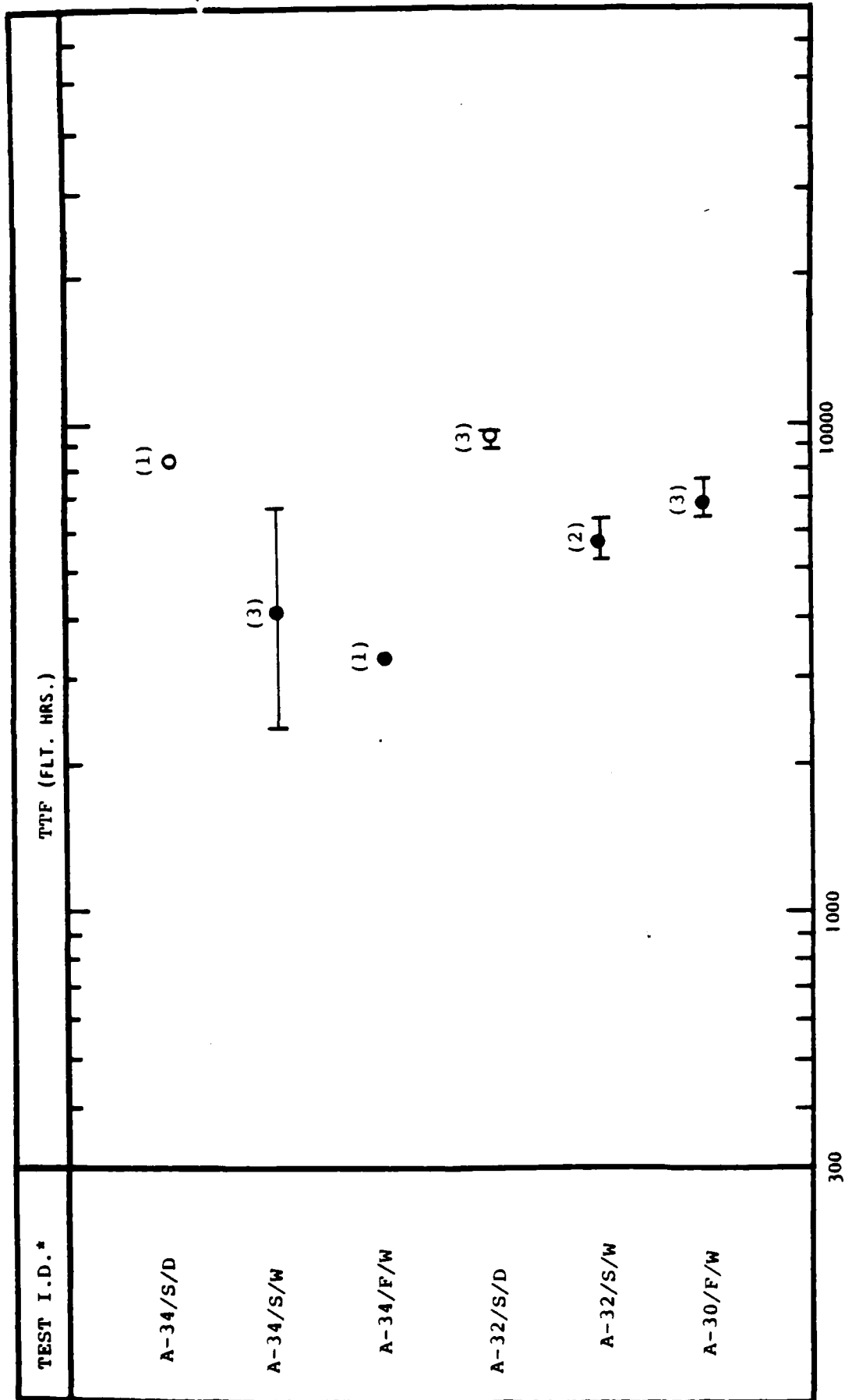


Fig. C-16 Comparison of Crack Growth Test Results for 7075-T7651 Aluminum Dog-Bone Specimens (Open Hole) Based on F-16 400 Hour (Block) Spectrum ("A"), Different stress Levels and Dry Air/3.5% NaCl Environments

\*Ref. Table 8

The plots shown in Figs. C-1 through C-16 are useful for comparing the test results and extremes for a given data set against other data sets. These plots provide a means for qualitatively evaluating the effects of selected test variables on TTCI, TTF or TFCG.

Plots for TTCI ( $a_i = 0.010"$ ) are shown in Figs. C-1 through C-7 and plots for TTF are shown in Figs. C-8 through C-11. The TFCG results are plotted in Figs. C-12 through C-15. TTF results for different stress levels are plotted in Fig. C-16.

In some cases, the results for different data sets were pooled to determine the average result and the corresponding high/low extremes. Data sets were pooled for a given specimen configuration, loading spectrum and environment. Applicable results for different loading frequencies were pooled to compare with results for individual data sets and to qualitatively evaluate the effects of loading frequency on the particular test result (i.e., TTCI, TTF or TFCG). For example, in Fig. C-1 test results for TTCI ( $a_i = 0.010"$ ) for data sets A-28/F/D and the A-28/S/D were pooled for two different loading frequencies (i.e., F = Fast = 8000 flight hours/2 days and S = slow = 8000 flight hours/16 days).

## C.4 DRY/WET RATIOS

Can the effects of the environment on TICI, TTF, and TFCG be "scaled" for 7075-T7651 aluminum? To address this question the applicable experimental results for TICI, TTF and TFCG for both dry air and 3.5% NaCl ("wet") environments from Tables C-1 and C-2 were used to compute "dry/wet" ratios. The results for the F-16 400-hour spectrum ("A") are plotted in a bar graph format in Fig. C-17 and those for the F-18 300-hour spectra (random ("B") and block ("C")) are shown in Fig. C-18. In all cases, the "dry/wet" ratios are based on test results for the same: loading frequency, specimen configuration, stress level and load spectrum.

Fig. C-17 Summary of Dry/Wet Ratios for 7075-T7651 Aluminum Dog-Bone Specimens for F-16 400 Hour Spectrum ("A") and Dry Air/3.5% NaCl Environments

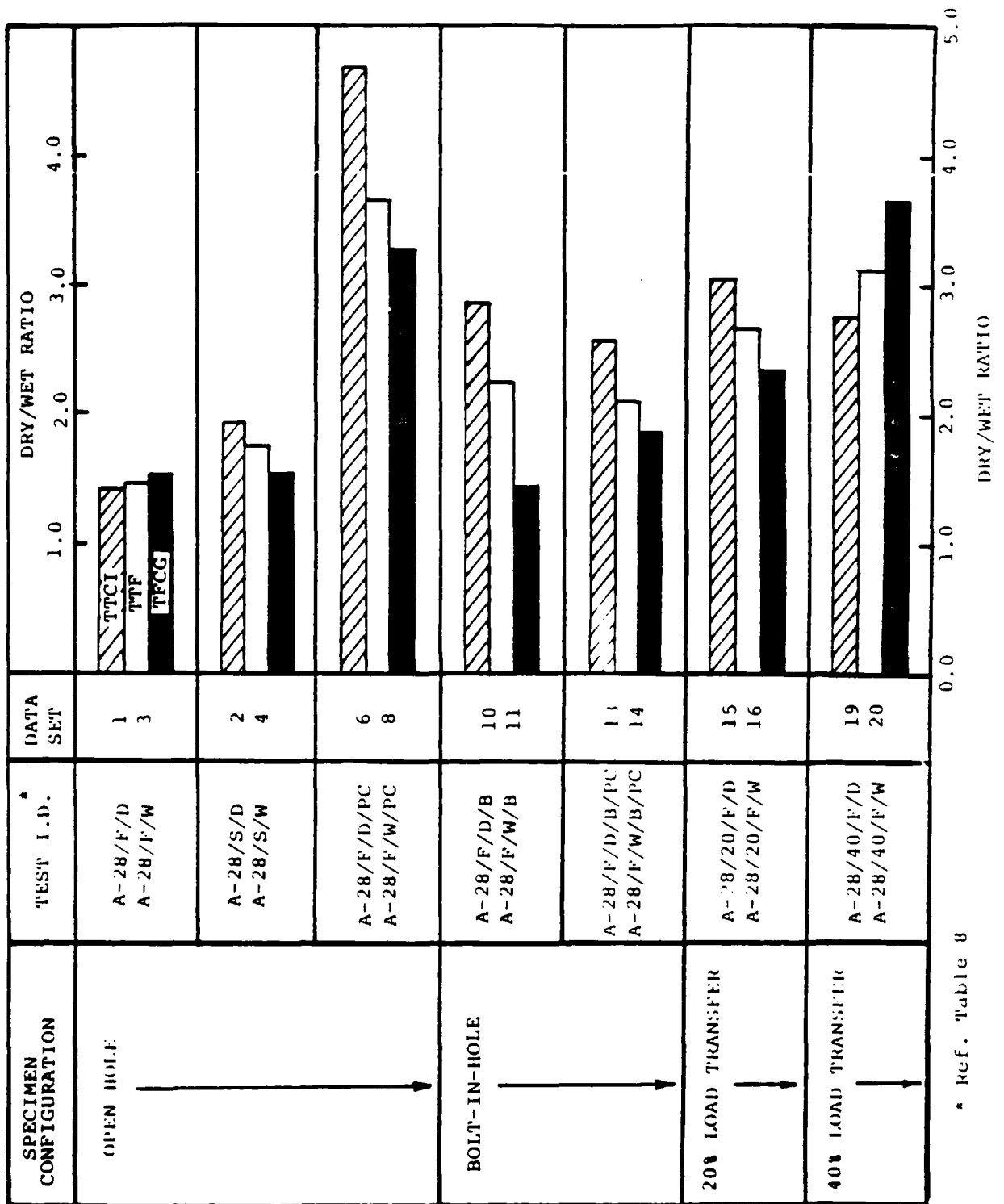
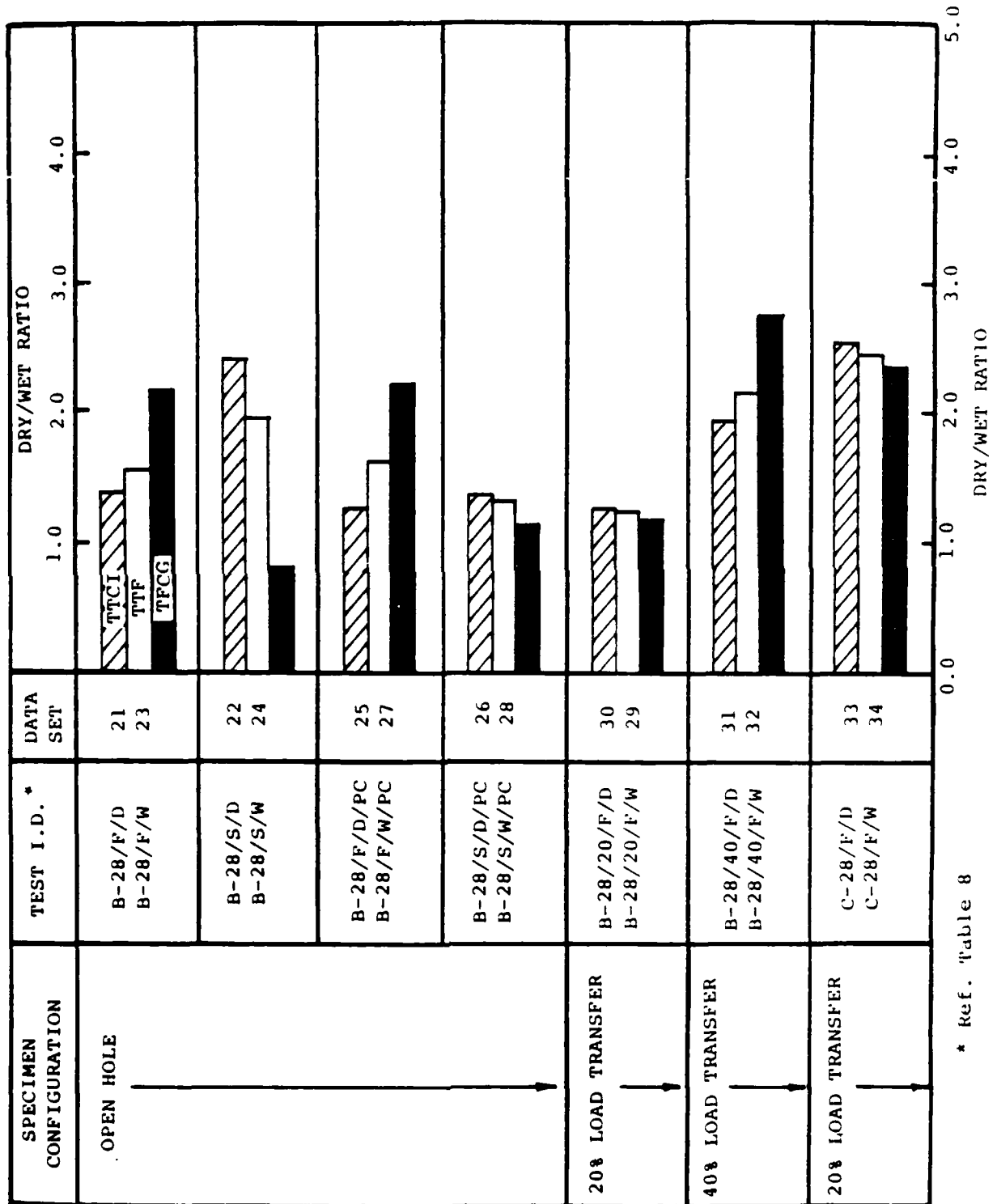


Fig. C-18 Summary of Dry/Wet Ratios for 7075-T7651 Aluminum Dog-Bone Specimens for F-18 300 Hour (Spectra "B" and "C") and Dry Air/3.5% NaCl Environments



\* Ref. Table 8

## C.5 EVALUATION OF TTCI/TTF RATIO

Test results from Tables C-1 and C-2 were used to study the ratio of TTCI to TTF for selected data sets. The purpose of this investigation was to study the statistics and sensitivity of the TTCI/TTF ratio for different environments, loading frequency, % bolt load transfer and load spectra.

Computed TTCI/TTF ratios and the corresponding statistical information (i.e., mean, standard deviation and coefficient of variation) are presented in Tables C-3 through C-5. Results are presented separately for dry air and 3.5% NaCl environments for load spectra "A", "B" and "C" in Tables C-3, C-4 and C-5, respectively.

The following observations are based on the results presented in Tables C-3 through C-5.

1. The environment, loading frequency and % bolt load transfer don't have a significant effect on the average TTCI/TTF ratio for 7075-T7651 aluminum.

2. It appears that the load spectra and maybe stress level have the greatest influence on the TTCI/TTF ratio.

F = Fast Frequency = 8000 Flt. Hrs/2 days  
S = Slow Frequency = 8000 Flt. Hrs/16 days

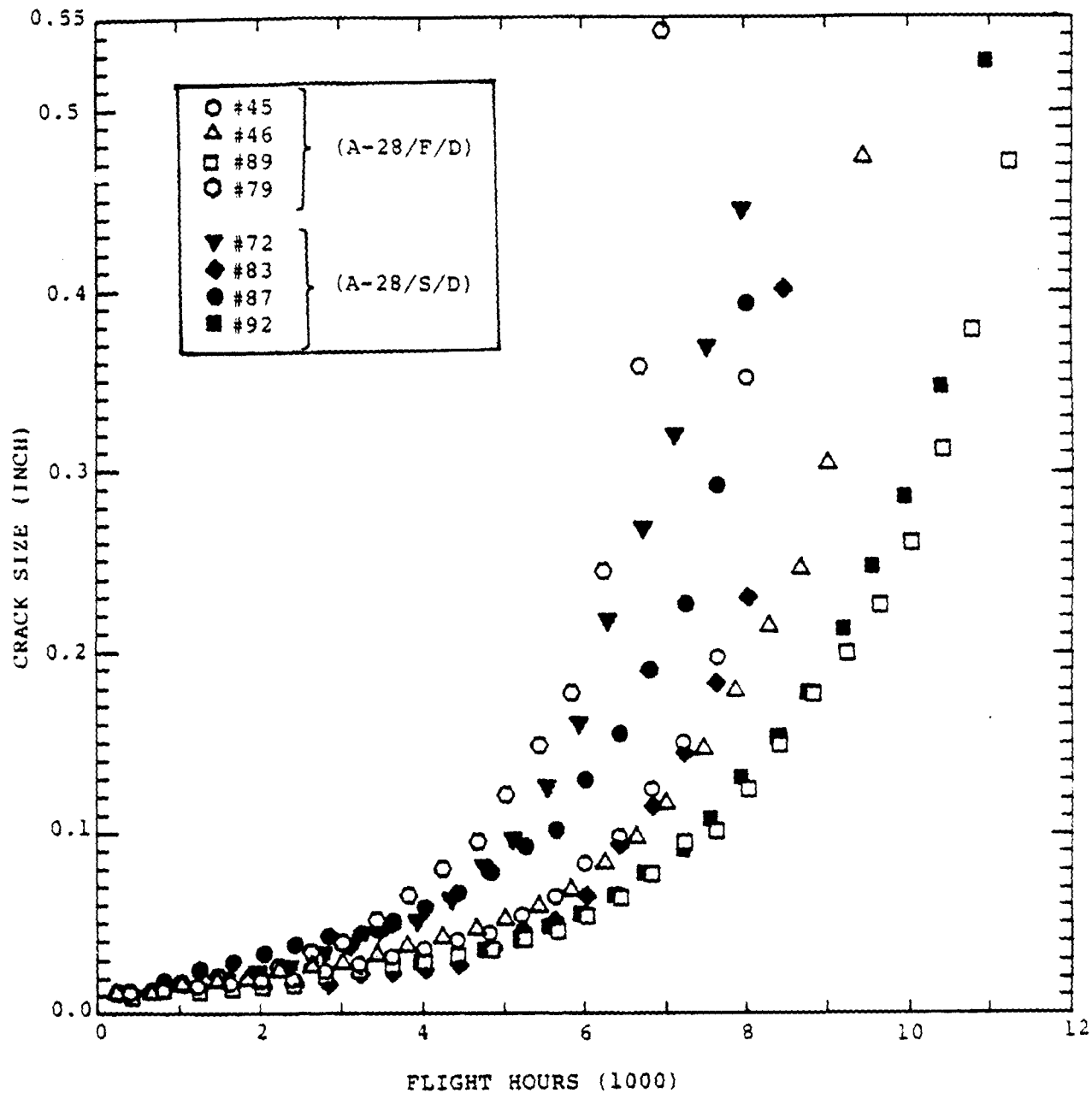


Fig. D-1 Normalized Crack Growth Results ( $a_i = 0.01"$ ) for 7075-T7651 Aluminum Dog-Bone Specimens (Open Hole)  
Tested Using: F-16 400 Hour Block Spectrum ( $\sigma_{GROSS} = 28$  ksi Max.), Dry Air Environment and Two Loading Frequencies (FAST, SLOW)

APPENDIX D

NORMALIZED CRACK GROWTH RESULTS FOR 7075-T7651  
ALUMINUM DOG-BONE SPECIMENS TESTED UNDER  
SPECTRUM LOADING

Experimental crack growth results for dog-bone specimens are plotted herein. Most results are normalized to a crack size of 0.010". In some cases reliable fractographic readings could not be made at a crack size of 0.010". Back-extrapolation to a crack size of 0.010" were possible in most cases. However, in some cases reliable extrapolations to a crack size of 0.010" were not possible. For this reason, and to minimize the effects of scatter in the crack growth results, a larger reference crack size was used in some cases (e.g.,  $a_i=0.035$ ").

(This page intentionally left blank.)

Further tests and evaluations are needed to better understand the effects of bolt load transfer on the TTF in mechanically-fastened joints.

7. The trends in the average TTF lives shown in Fig. C-11 are consistent with those observed in Fig. C-10 for the F-18 300 hour (random) spectrum. For example, the average TTF life for the open hole specimens tested in dry air environment is larger than that for the 40% load transfer specimens. Also, as expected, the open hole specimens tested in a 3.5% NaCl environment had a shorter average TTF life than comparable specimens tested in a dry air environment.

significant effect on the average TTF lives for open hole specimens tested under a dry environment and spectrum "A" (Ref. Fig. C-8). However, preconditioned specimens tested in the 3.5% NaCl environment showed considerably shorter average TTF lives than those tested in the dry air environment.

4. Specimens tested with a clearance-fit bolt in the hole for the dry air environment had a longer average TTF life than open hole specimens for spectrum "A" (Ref. Figs. C-8 and C-9). No significant difference was found between the average TTF life for open hole specimens and for specimens with a clearance-fit bolt in hole based on tests in a 3.5% NaCl environment.

5. No significant differences were observed in the average TTF lives for open hole tested under fast and slow loading frequencies and spectrum "B" (Ref. Fig. C-10).

6. The average TTF life for the open hole specimens tested using spectrum "B" was longer than either the 20% or 40% load transfer specimens tested in dry air (Ref. Fig. C-10). However, the effects of the load transfer on the average TTF life are not clear because the average TTF life for the 20% load transfer specimens was actually shorter than for the 40% load transfer specimens. Based on our test results, we cannot say with certainty that the average TTF life decreases as the % bolt load transfer increases.

average crack growth lives were observed for open hole, 20% load transfer of 40% load transfer specimens. Test results were not available for the case with no load transfer and a bolt in the hole for direct comparisons with the 20% and 40% load transfer results.

7. The average crack growth life for the 40% load transfer specimens tested using spectrum "C" was not significantly different than that for the open hole specimens tested in dry air (Ref. Fig. C-15).

8. The 3.5% NaCl environment significantly reduced the crack growth life for open hole specimens tested using spectrum "C" (Ref. Fig. C-15).

#### C.6.3 Time-to-Failure (TTF)

The following observations are based on the results plotted in Figs. C-8 thru C-11.

1. No significant effect of loading frequency on the average TTF life for either dry air or 3.5% NaCl environments based on the open hole specimens and spectrum "A" (Ref. Fig. C-8).

2. Testing in a 3.5% NaCl environment results in a shorter average TTF life than when tested in a dry air environment and spectrum "A" (Ref. Fig. C-8).

3. Specimen preconditioning did not seem to have a

without preconditioning but tested in the same environment.

Preconditioning is intimately associated with the effect of stress enhanced corrosion and depends strongly on the environment, surface condition and geometry.

4. Specimens with a clearance-fit bolt had slightly longer average crack growth lives than open hole specimens for both the dry air and 3.5% NaCl environments. The bolt increases the crack growth resistance to some degree (Ref. Figs. C-12 and C-13).

5. The average crack growth life for the open hole specimens was considerably longer for the fast loading frequency than for the slow loading frequency for the dry air environment (Ref. Fig. C-14). For example, the average crack growth life for B-28/F/D and B-28/S/D was 7772 flight hours and 2637 flight hours, respectively (Ref. Table C-1). A much smaller difference in the average crack growth results was observed for the open hole specimens tested in a 3.5% NaCl environment than for the dry air environment. For example, B-28/F/W and B-28/S/W had an average crack growth life of 3579 flight hours and 3283 flight hours, respectively.

6. The effect of the % bolt load transfer on crack growth life for spectrum "B" was not clear from the test results (Ref. Fig. C-14). For example, the average crack growth life for open hole specimens tested under a dry air environment was longer than that for the 20% load transfer specimens but about the same for the 40% load transfer specimens. In the 3.5% NaCl environment, no significant differences in the

## C.6.2 Time-for-Crack Growth (TFCG)

The following observations are based on the test results plotted in Figs. C-12 thru C-15.

1. No significant effect of loading frequency on the crack growth lives for open hole specimens tested in a dry air or 3.5% NaCl; environment and spectrum "A" (Ref. Fig. C-12). Two frequencies were considered: F = fast and S = slow.

2. Open hole specimens tested using the extra slow loading frequency ( $s = 8000$  flt hrs/90 days) had approximately one-half the average crack growth life as specimens tested using the fast (F) or slow(S) loading frequencies for spectrum "A" (Ref. Fig. C-12). The separate effects of long term environmental exposure and slow loading frequency on the average TTF life need to be studied further to clarify the effects of environment and loading frequency on TTF of mechanically-fastened joints.

3. Specimen preconditioning did not have a significant effect on the average TFCG life for open hole specimens tested under dry air environment and spectrum "A" (Ref. Figs. C-12 and C-13). Preconditioned specimens tested in a 3.5% NaCl environment had shorter average TFCG lives than specimens

8. No significant differences in the average TTCI lives were observed for the open hole specimens for Spectrum "B" for either the dry air or the 3.5% NaCl environments. Two frequencies were considered: Fast and Slow (Ref. Fig. C-5).

9. Loading frequency did not appear to have a significant effect on the average TTCI lives for preconditioned specimens for either the dry air or 3.5% NaCl environments for load spectrum "B" (Ref. Fig. C-5).

10. The average TTCI lives for the 20% and 40% load specimens were shorter than for the open hole specimens subjected to spectrum "B". Increasing the % bolt load transfer from 20% to 40% did not significantly change the average TTCI life for either the dry air or 3.5% NaCl environments (Ref. Figs. C-5 and C-6).

11. The average TTCI life for the 40% load transfer specimens in a dry air environment was shorter than that for the open hole specimen for spectrum "C" (Ref. Fig. C-7).

12. The environment has a significant effect on average TTCI lives for the open hole specimens for spectrum "C" (Ref. Fig. C-7).

3. The average TTCI life for the open hole specimens under dry air and fast frequency was shorter than the life for specimens with a clearance-fit bolt in the hole. In this case, the bolt apparently increases the resistance to crack initiation (Ref. Figs. C-1 and C-3).

4. There was no significant difference in the average TTCI life for the open hole specimen and the specimens with a clearance-fit bolt (with 0% load transfer) for the 3.5% NaCl environment (Ref. Figs. C-1 and C-3).

5. No significant effects of the loading frequency on the TTCI life was observed for the specimens with a clearance-fit bolt in hole for the 3.5% NaCl environment for the fast (F) or slow (S) loading frequencies (Ref. Fig. C-3).

6. There was no significant difference between the average TTCI lives for an open hole specimen and 20% or 40% load transfer specimens tested in a dry air environment. In this case, specimens with bolt load transfer did not have a significantly different average TTCI life than the open hole specimens (Ref. Figs. C-1 and C-4). The average TTCI life for the open hole specimens was approximately 54% of that for the zero load transfer specimens with a bolt in the hole. As expected, the presence of a clearance-fit bolt in the hole increased the crack initiation life.

7. The test results suggest that the environment had a greater effect on the average TTCI life than the three % load transfer considered (i.e., 0%, 20% and 40%)(Ref. Figs. C-1 and C-4).

## C.6 CONCLUSIONS BASED ON DOG-BONE SPECIMEN TEST RESULTS

## C.6.1 Time-to-Crack Initiation (TTCI)

The following observations are based on the TTCI test results for 7075-T7651 aluminum dog-bone specimens, three load spectra (i.e., "A", "B" and "C") and the results plotted in Figs. C-1 thru C-7.

1. Loading frequency did not have a significant effect on the average TTCI for the open hole specimen for either the dry air or 3.5% NaCl environments (Fig. C-1). Three loading frequencies were considered: F = fast = 8000 flight hours/2 days; S = slow = 8000 flight hours/16 days; s = extra slow = 8000 flight hours/90 days. As expected, the average TTCI life was shorter for the 3.5% NaCl environment than for the dry air environment.

2. The effect of specimen preconditioning on the average TTCI life for open hole specimens is more significant for the 3.5% NaCl environment than for the dry air environment. For example, the average TTCI lives for the preconditioned specimens tested under a 3.5% NaCl environment were over three times shorter than for the specimens without preconditioning (Ref. Figs. C-1 and C-2).

Table C-5 Summary of Statistics for TTCl/TTF Ratio for 7075-T7651 Aluminum Dog-Bone Specimens,  
F-18 300 Hour (Block Spectrum and Dry Air/3.5% NaCl Environments

DRY AIR ENVIRONMENT				3.5% NaCl ENVIRONMENT			
TEST I.D.*	DATA SET	SPEC NO.	TTCl/TTF (a)	TEST I.D.*	DATA SET	SPEC NO.	TTCl/TTF (a)
C-28/F/D	33	515 516 517	.55 .34 .62	C-28/F/W	34	518 519 520	.75 .23 .58
C-28/40/F/D	35	521 522 523	.31 .49 .53	N = 3 X = Ave. (TTCl/TTF) = 0.520 (X) = Std Dev = 0.2651 C.O.V. = 50.9%			
N = 6 $\bar{X}$ = 0.473 $\sigma(\bar{X})$ = 0.1227 C.O.V. = 25.9%							

\*Ref. Table 8

NOTES: (a)  $a_1 = 0.010"$

Table C- 4 Summary of Statistics for TTCl/TTF Ratio for 7075-T7651 Aluminum Dog-Bone Specimens,  
F-18 300 Hour (Random) Spectrum and Dry Air/3.5% Nacl Environments

DRY AIR ENVIRONMENT				3.5% NACL ENVIRONMENT			
TEST I.D.*	DATA SET	SPEC NO.	TTCl/TTF (a)	TEST I.D.*	DATA SET	SPEC NO.	TTCl/TTF (a)
B-28/F/D	21	315 316 317	.76 .85 .43	B-28/F/W	23	300 301 302 303	.78 .75 .70 .81
B-28/S/D	22	326 327 328	.89 .89 .88	B-28/S/W	24	318 319 320 321	.82 .61 .71 .72
B-28/20/F/D	30	308 309 310 311	.65 .67 .81 .74	B-28/20/F/W	29	332 333 334 335	.56 .79 .72 .79
B-28/40/F/D	31	500 501 502	.66 .64 .59	B-28/40/F/W	32	503 504 505	.74 .72 .65
N = 13 $\bar{X}$ = Ave. (TTCl/TTF) = 0.728 $\sigma(\bar{X})$ = Std. Dev. = 0.1378 C.O.V. = 18.9%				N = 15 $\bar{X}$ = 0.725 $\sigma(\bar{X})$ = 0.0735 C.O.V. = 10.1%			

\*Ref. Table 8

NOTES: (a)  $a_i = 0.010''$

Table C-3 Summary of Statistics for TTCl/TTf Ratio for 7075-T7651 Aluminum Dog-Bone Specimens, F-16 400 Hour (Block) Spectrum and Dry Air/3.5% NaCl Environments

DRY AIR ENVIRONMENT				3.5% NaCl ENVIRONMENT			
TEST I.D.*	DATA SET	SPEC NO.	TTCl/TTf (a)	TEST I.D.*	DATA SET	SPEC NO.	TTCl/TTf (a)
A-28/F/D	1 ↓	45	.64	A-28/F/W	3 ↓	62	.49
		46	.41			76	.57
		79	.60			77	.75
		89	.66			82	.56
A-28/S/D	2 ↓	72	.52	A-28/S/W	4 ↓	67	.51
		83	.75			71	.21
		87	.68			81	.51
		92	.54			88	.83
A-28/F/D/B	10 ↓	126	.65	A-28/R/W	5 ↓	90	.70
		127	.60			91	.51
		128	.83			84	.79
A-28/20/F/D	15 ↓	74	.49	A-28/F/W/B	11 ↓	85	.78
		75	.51			86	.66
		80	.60			122	.20
A-28/20/S/D	17 ↓	73	.57	A-28/S/W/B	12 ↓	123	.73
		506	.47			124	.69
		507	.53			125	.56
A-28/40/F/D	19 ↓	508	.62	A-28/20/F/W	16 ↓	131	.59
						132	.46
						66	.38
A-28/40/F/W	20 ↓			A-28/20/S/W	18 ↓	68	.59
						69	.29
						70	.52
A-28/40/F/W	20 ↓			A-28/40/F/W	20 ↓	509	.54
						510	.61
						511	.71
N = 18 X̄ = Ave.(TTCl/TTf) = 0.593 σ(X̄) = Std. Dev. = 0.1023 C.O.V. = 17.2%				N = 26 X = 0.567 σ(X) = 0.1665 C.O.V. = 29.42%			

\*Ref Table 8 NOTES: (a)  $a_1 = 0.010^{10}$

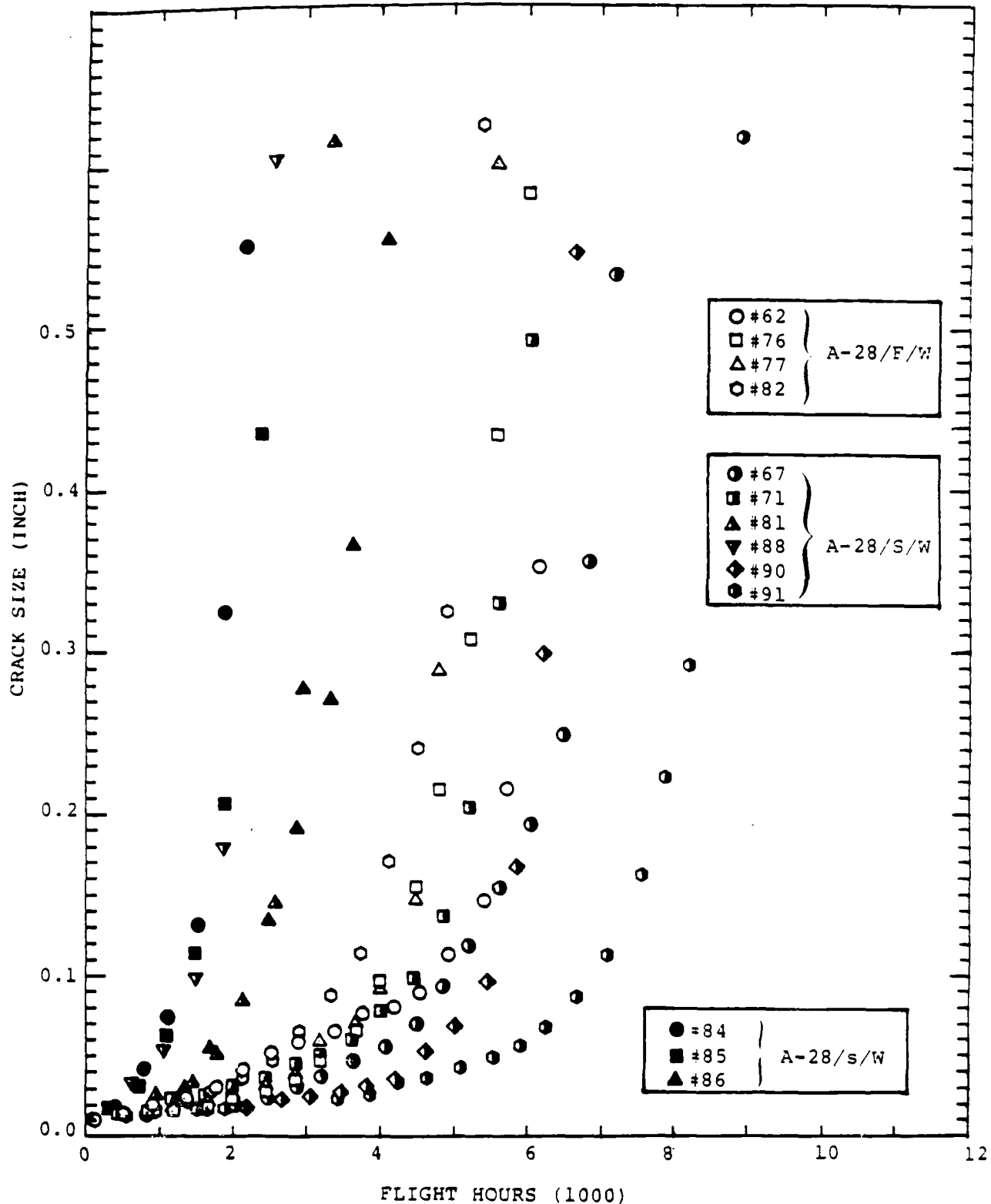


Fig. D-2 Normalized Crack Growth Results ( $a_i = 0.01"$ ) for 7075-T7651 Aluminum Dog-Bone Specimens (Open Hole)  
 Tested Using: F-16 400 Hour Block Spectrum  
 $\sigma_{GROSS} = 28$  ksi Max.), 3.5% NaCl Environment  
 and Three Loading Frequencies (Fast, Slow, Extra Slow)

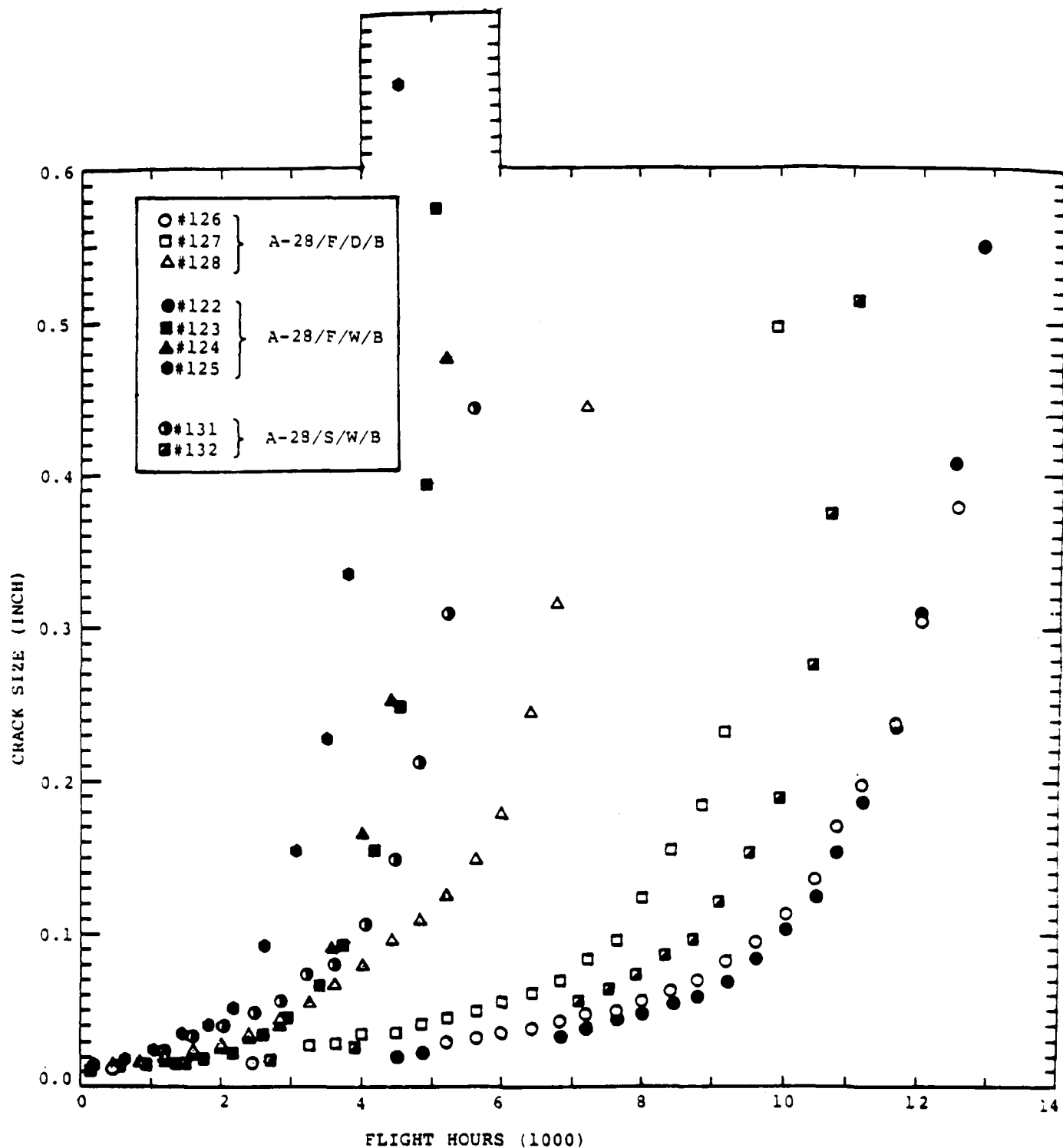


Fig. D-3 Comparison of Normalized Crack Growth Results ( $a_i = 0.01"$ , Dry Air Versus 3.5% NaCl) for 7075-T7651 Aluminum Dog-Bone Specimens (Bolt-In-Hole) Tested Using F-16 400 Hour Block Spectrum ( $\sigma_{GROSS} = 28$  ksi Max.) and Two Loading Frequencies (Fast, Slow)

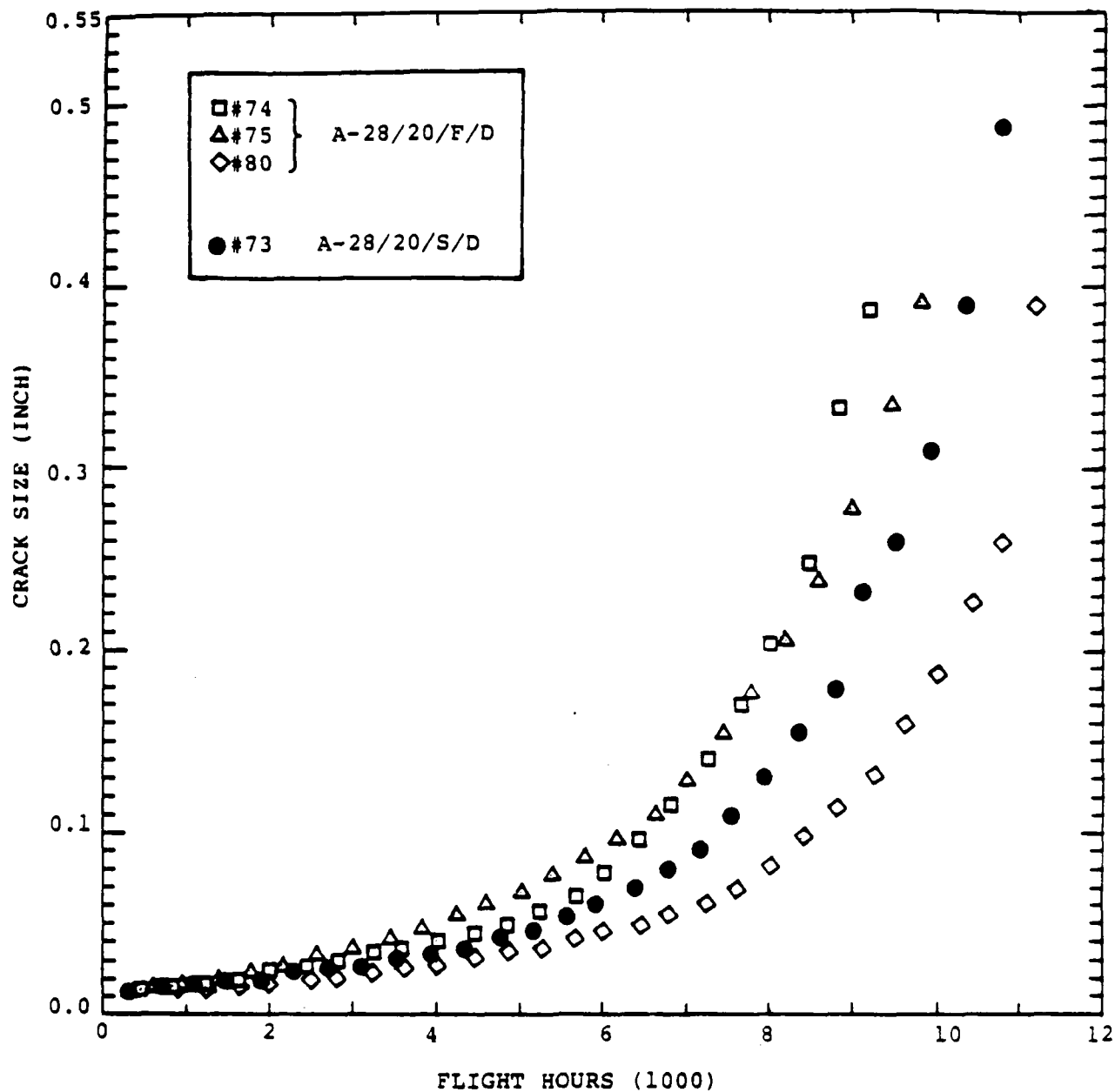


Fig. D-4 Normalized Crack Growth Results ( $a_i = 0.01"$ ) for 7075-T7651 Aluminum Dog-Bone Specimens (20% Load Transfer) Tested Using: F-16 400 Hour Block Spectrum ( $\sigma_{GROSS} = 28$  ksi Max.), Dry Air Environment and Two Loading Frequencies (Fast, Slow)

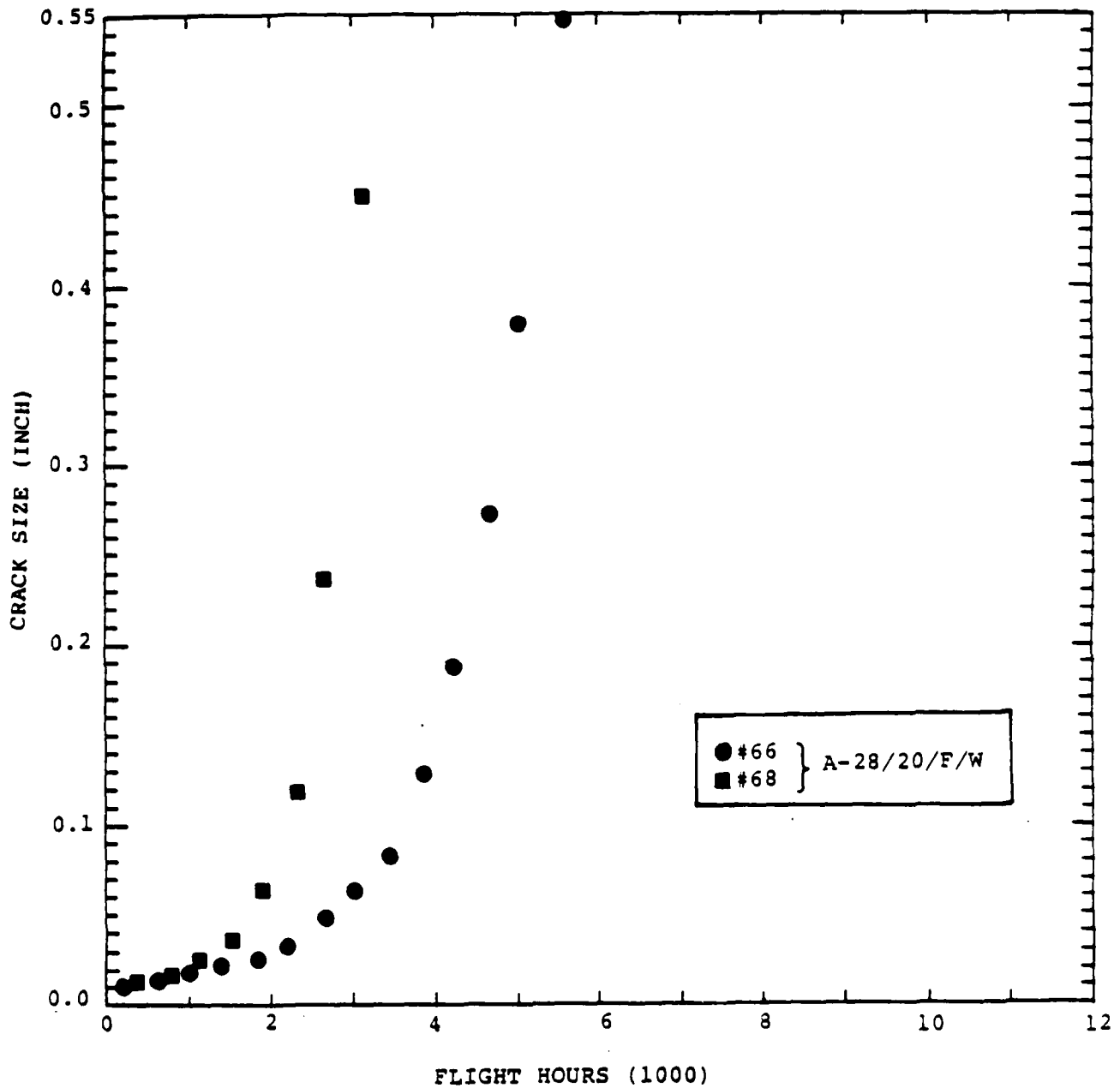


Fig. D-5 Normalized Crack Growth Results ( $a_i = 0.01"$ ) for 7075-T7651 Aluminum Dog-Bone Specimens (20% Load Transfer) Tested Using: F-16 400 Hour Block Spectrum ( $\sigma_{GROSS} = 28$  ksi Max.), 3.5% NaCl Environments and Fast Frequency

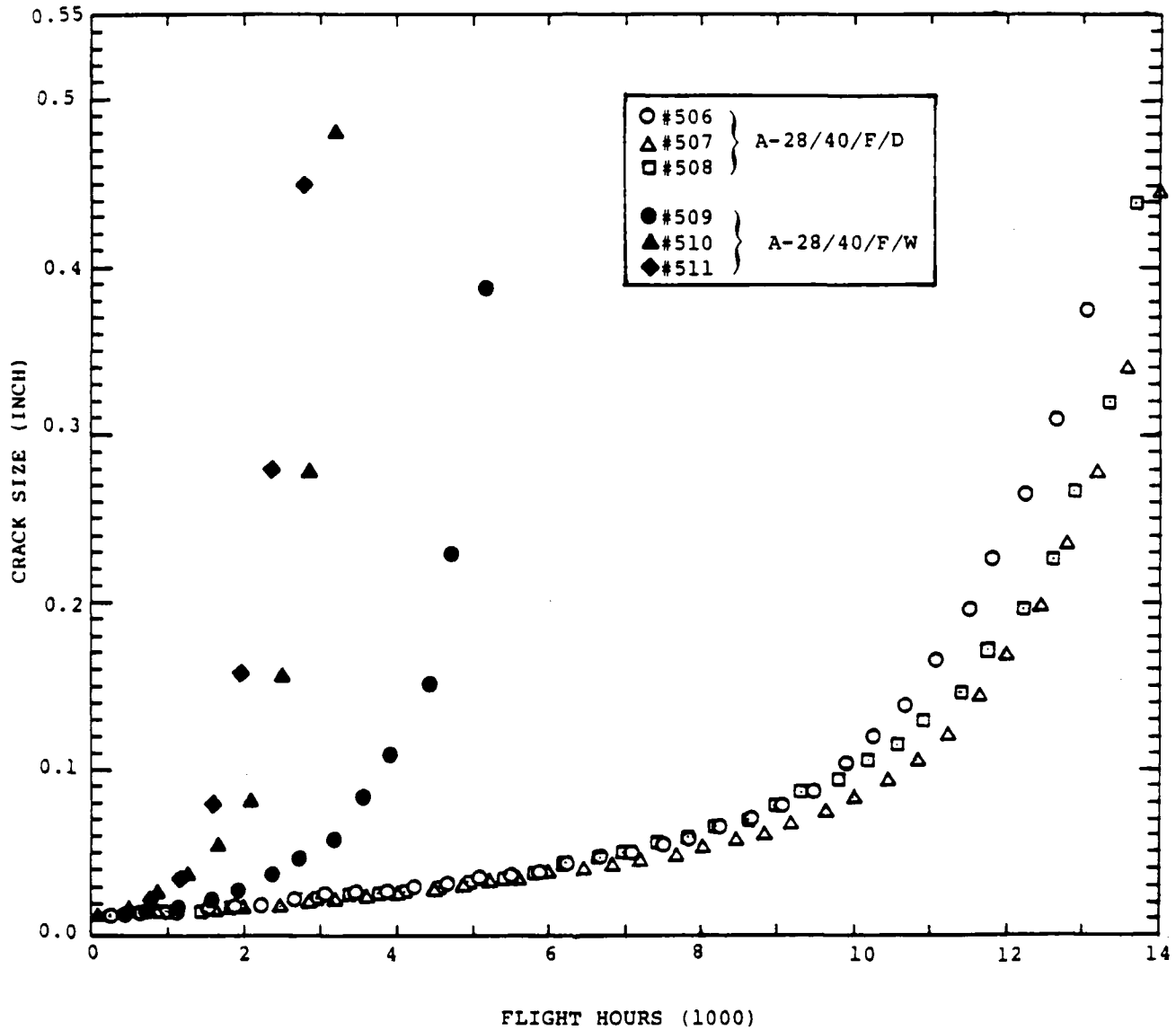


Fig. D-6 Comparison of Normalized Crack Growth Results ( $a_i = 0.01"$ , Dry Air Versus 3.5% NaCl) for 7075-T7651 Aluminum Dog-Bone Specimens (40% Load Transfer) Tested Using: F-16 400 Hour Block Spectrum ( $\sigma_{GROSS} = 28$  ksi Max.) and Fast Loading Frequency

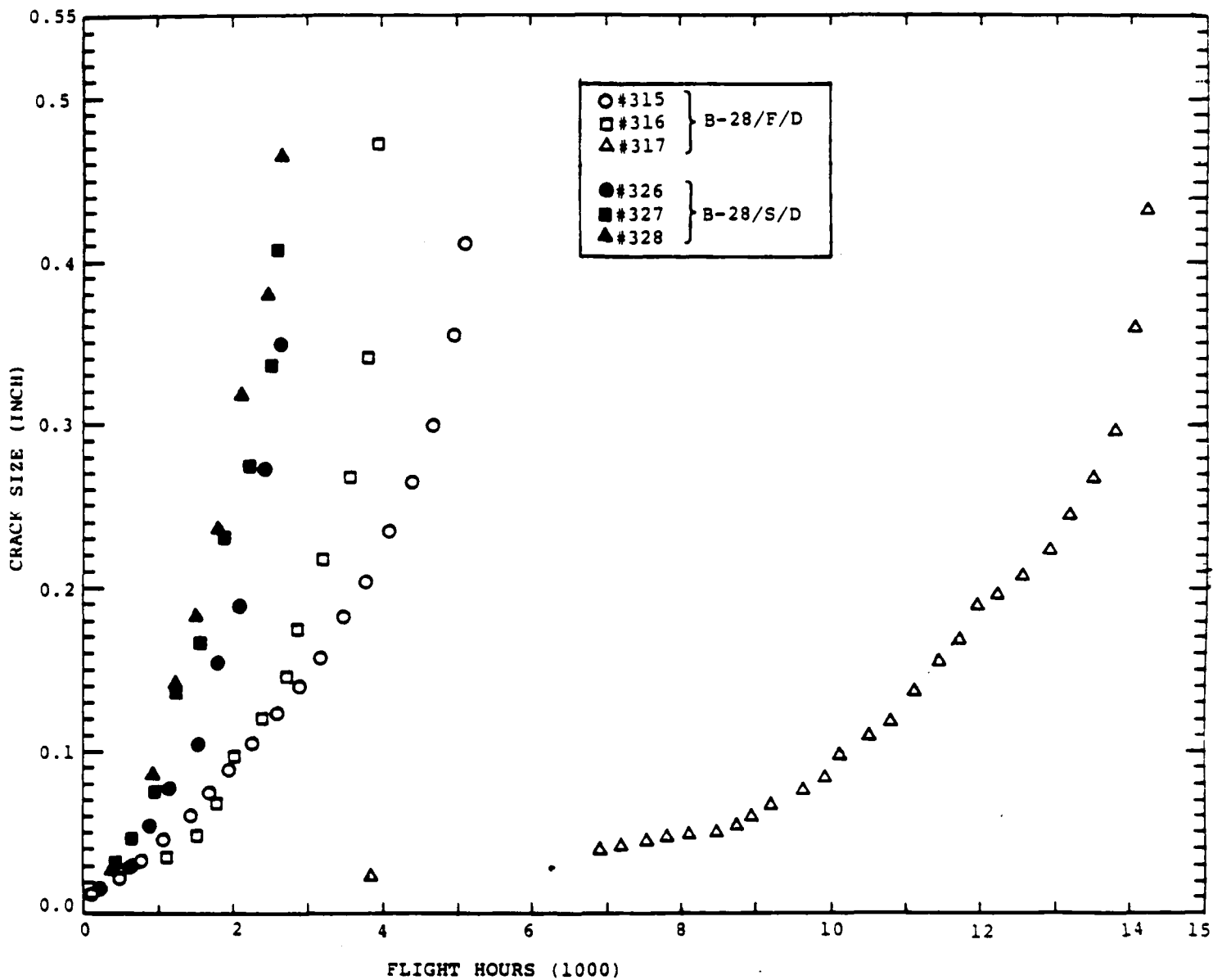


Fig. D-7 Comparison of Normalized Crack Growth Results ( $a_i = 0.01"$ ; Fast Versus Slow Loading Frequency) for 7075-T7651 Aluminum Dog-Bone Specimens (Open Hole) Tested Using: F-18 300 Hour (Random) Spectrum ( $\sigma_{Gross} = 28$  ksi Max.) and Dry Air Environment.

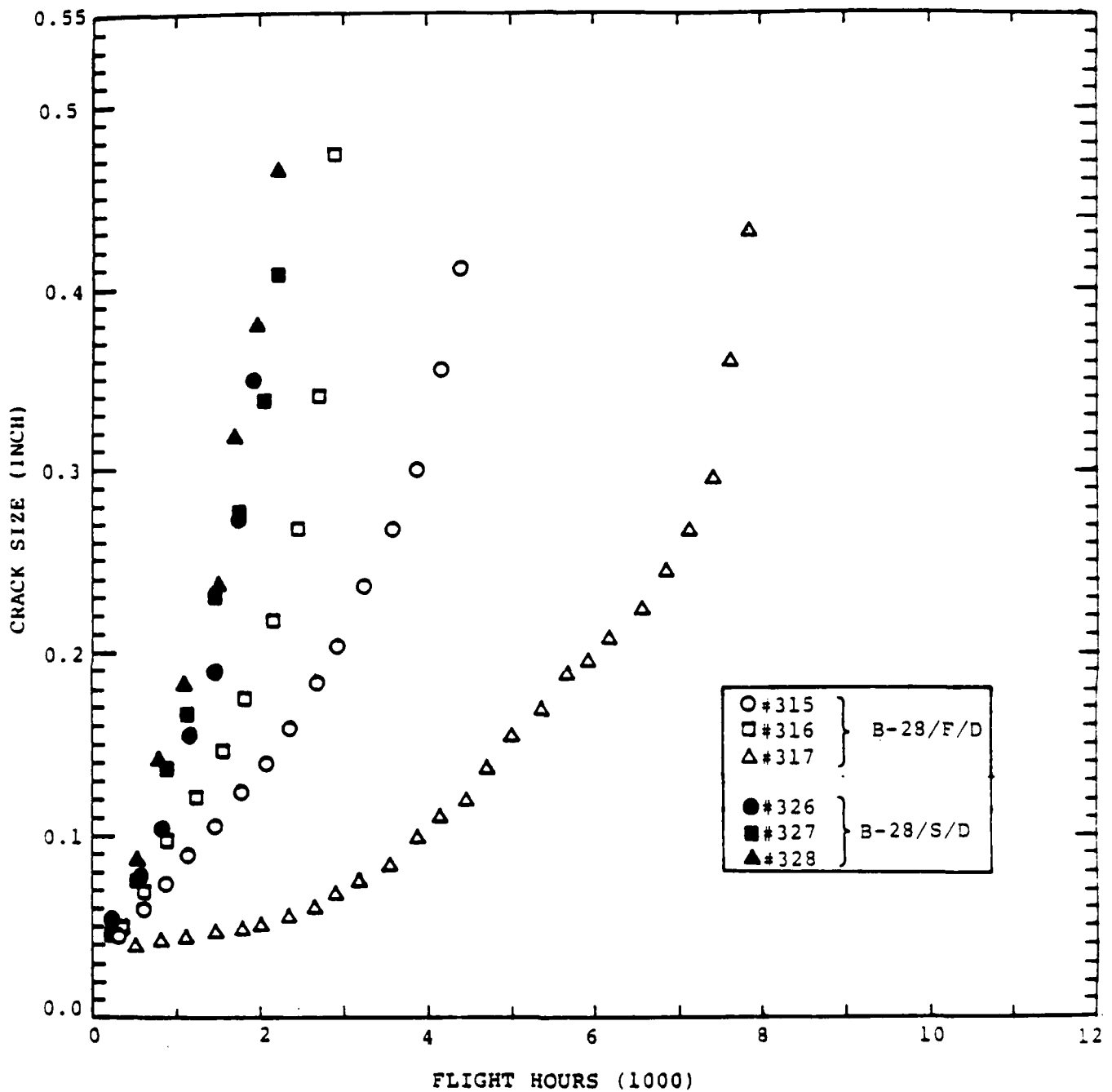


Fig. D-8 Comparison of Normalized Crack Growth Results  
 ( $a_i = 0.035"$ ; Fast Versus Slow Loading Frequency)  
 for 7075-T7651 Aluminum Dog-Bone Specimens (Open Hole)  
 Tested Using: F-18 300 Hour (Random) Spectrum  
 ( $\sigma_{Gross} = 28$  ksi Max.) and Dry Air Environment

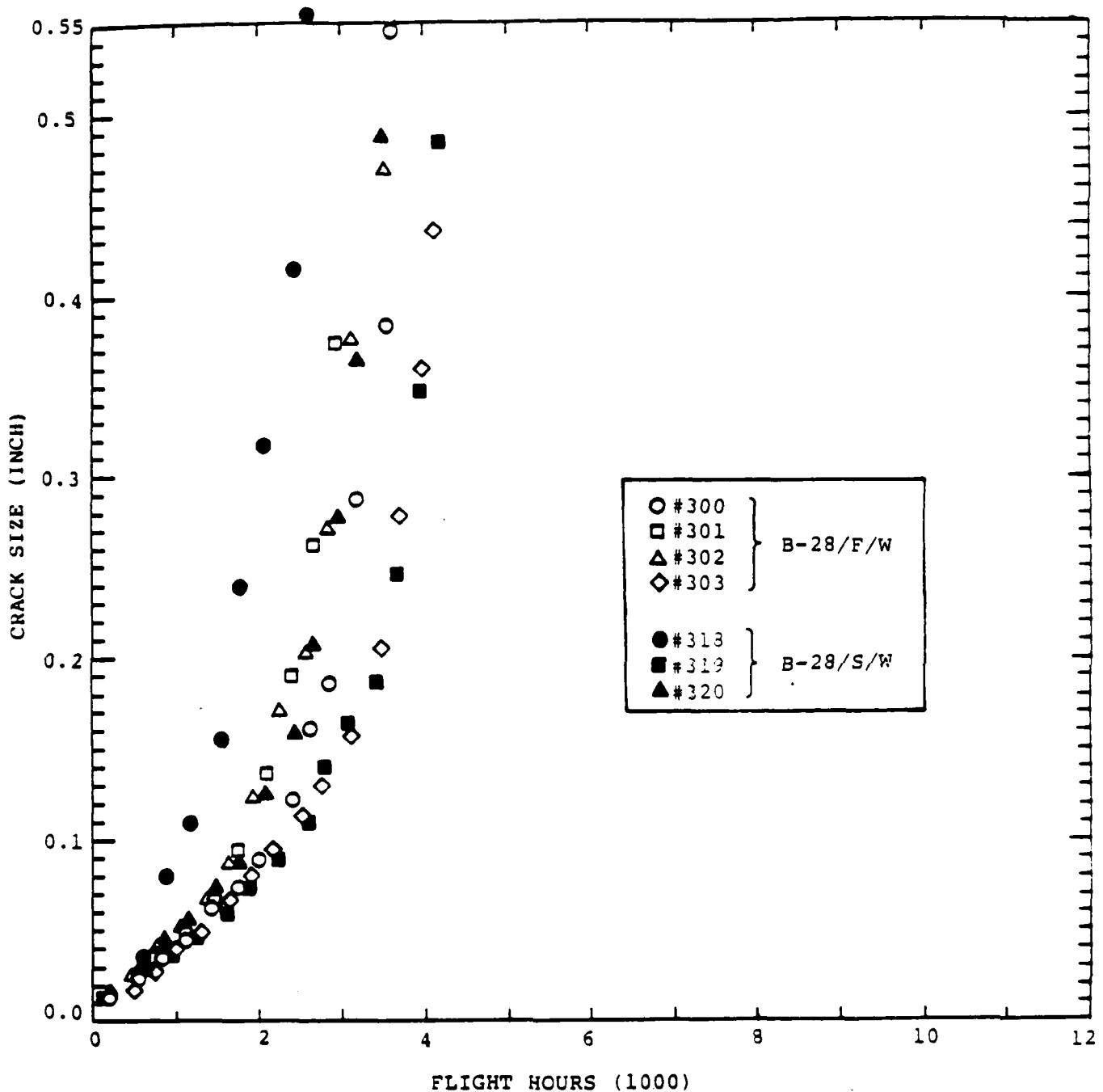


Fig. D-9 Comparison of Normalized Crack Growth Results  
 $(a_i = 0.01"$ ; Fast Versus Slow Loading Frequency)  
 for 7075-T7651 Aluminum Dog-Bone Specimens  
 (Open Hole) Tested Using: F-18 300 Hour (Random)  
 Spectrum ( $\sigma_{Gross} = 28$  ksi Max.) and 3.5% NaCl  
 Environment

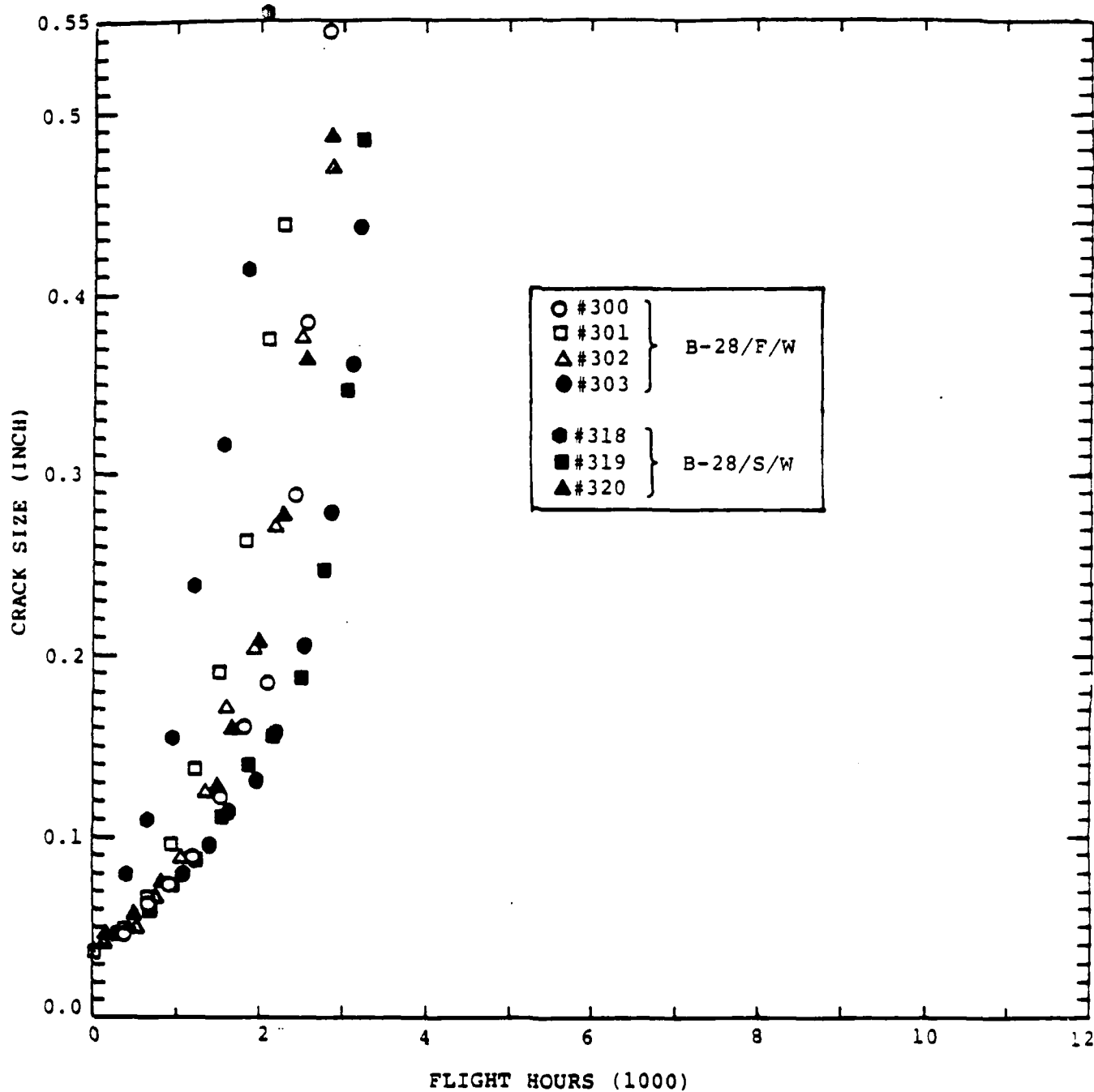


Fig. D-10 Comparison of Normalized Crack Growth Results  
 ( $a_i = 0.035"$ ; Fast Versus Slow Loading Frequency)  
 for 7075-T7651 Aluminum Dog-Bone Specimens  
 (Open Hole) Tested Using: F-18 300 Hour (Random)  
 Spectrum ( $\sigma_{Gross} = 28$  ksi Max.) and 3.5% NaCl  
 Environment

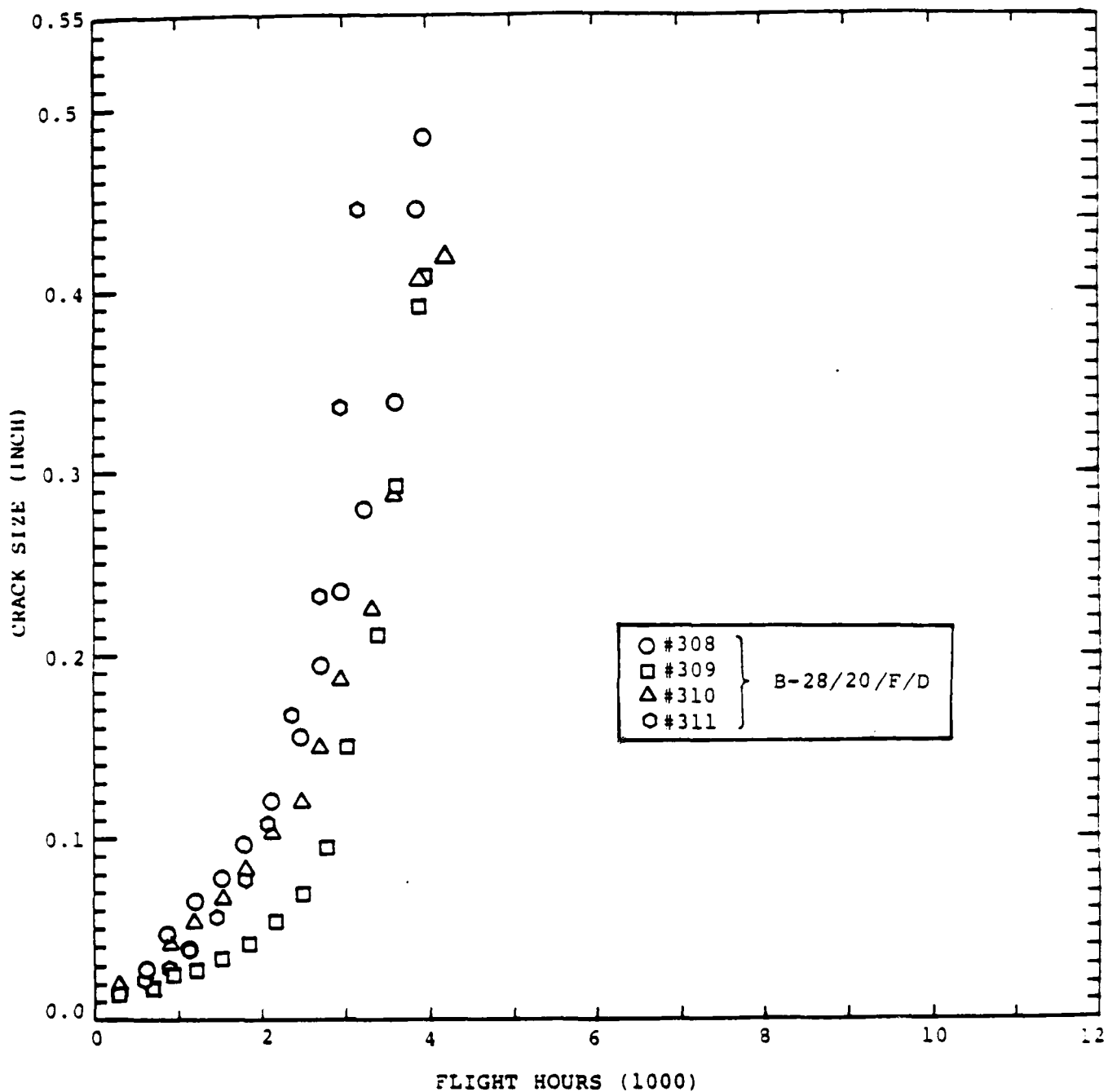


Fig. D-11 Normalized Crack Growth Results ( $a_0 = 0.01"$ ) for 7075-T7651 Aluminum Dog-Bone Specimens (20% Load Transfer) Tested Using: F-18 300 Hour (Random) Spectrum ( $\sigma_{Gross} = 28$  ksi Max.), Dry Air Environment and Fast Loading Frequency.

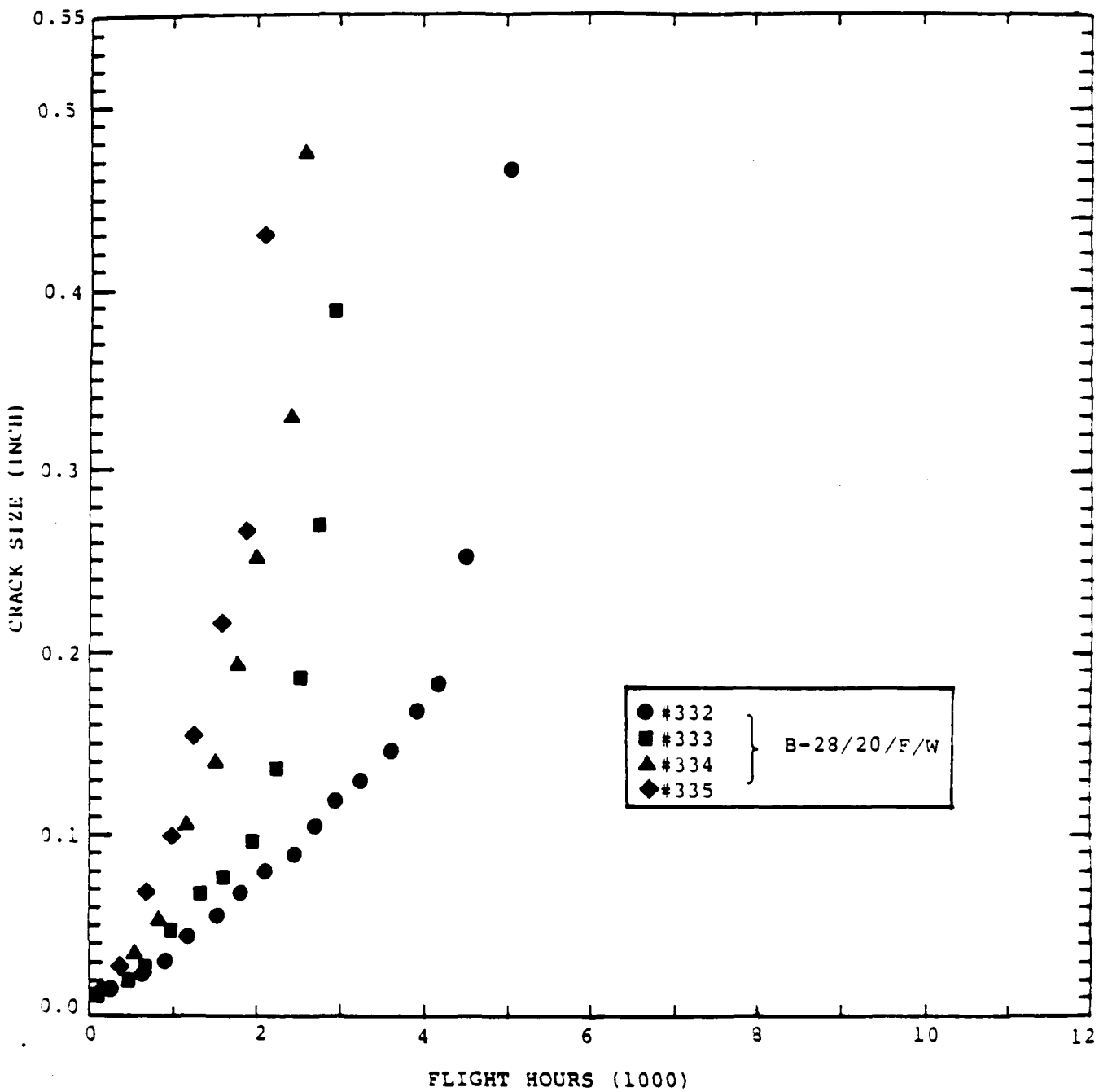


Fig. D-12 Normalized Crack Growth Results ( $a_i = 0.01"$ )  
for 7075-T7651 Aluminum Dog-Bone Specimens  
(20% Load Transfer) Tested Using: F-18 300 Hour  
(Random) Spectrum ( $\sigma_{\text{Gross}} = 28$  ksi Max.), 3.5%  
NaCl Environment and Fast Loading Frequency.

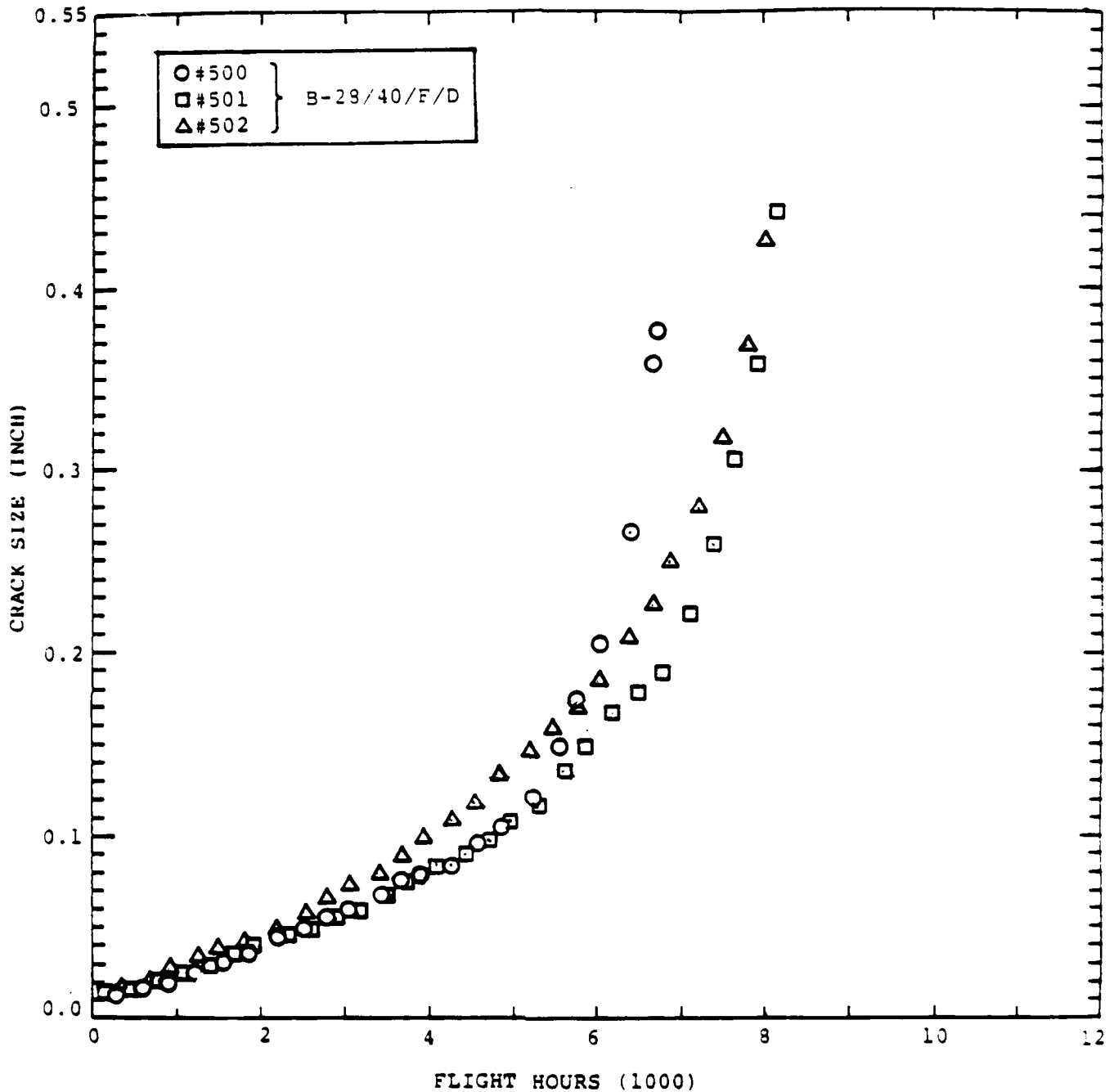


Fig. D-13 Normalized Crack Growth Results ( $a_i = 0.01"$ ) for 7075-T7651 Aluminum Dog-Bone Specimens (40% Load Transfer) Tested Using: F-18 300 Hour (Random) Spectrum, Dry Air Environment and Fast Loading Frequency.

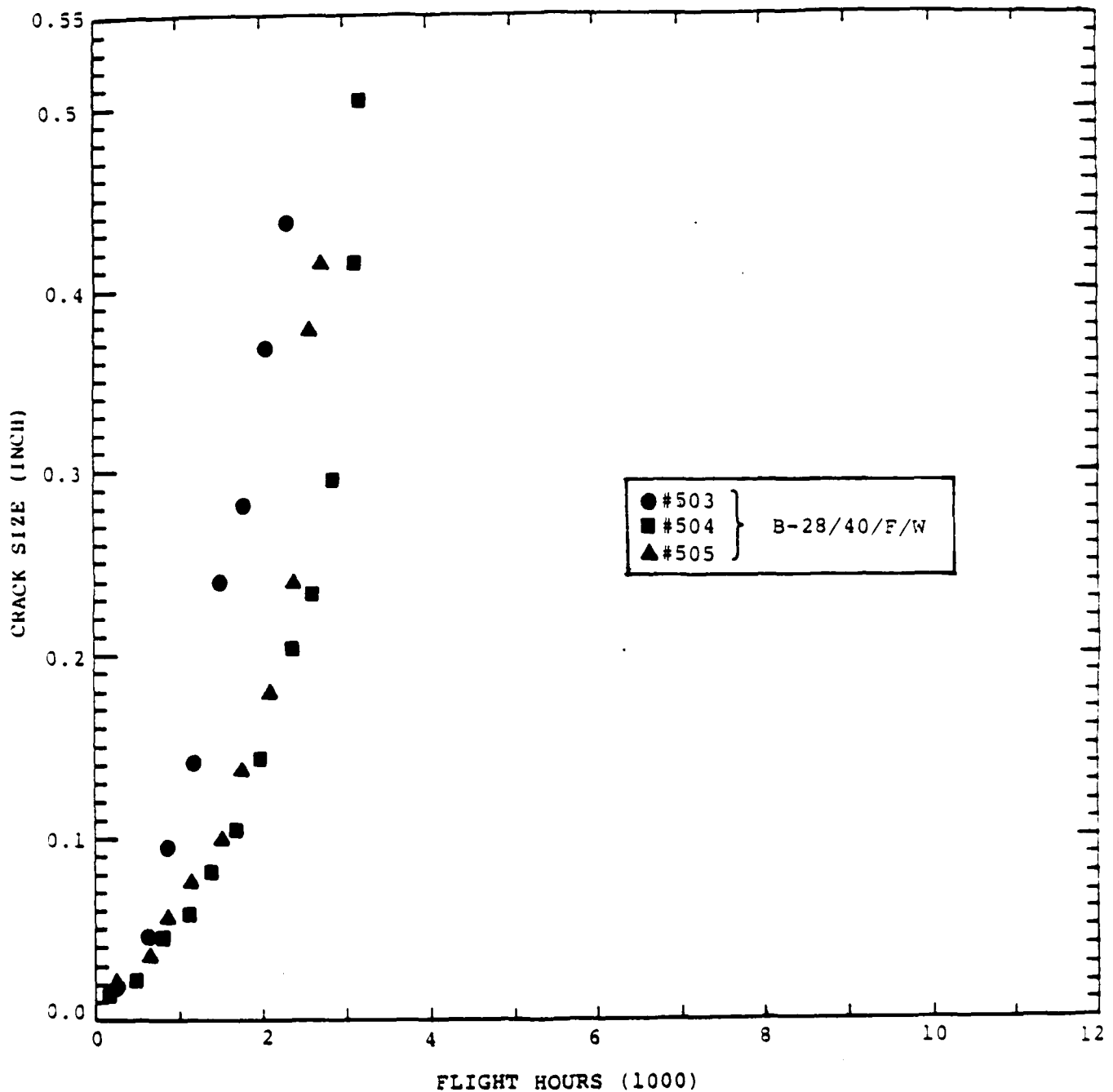


Fig. D-14 Normalized Crack Growth Results ( $a_i = 0.01"$ ) for 7075-T7651 Aluminum Dog-Bone Specimens (40% Load Transfer) Tested Using: F-18 300 Hour (Random) Spectrum, 3.5% NaCl Environment and Fast Loading Frequency.

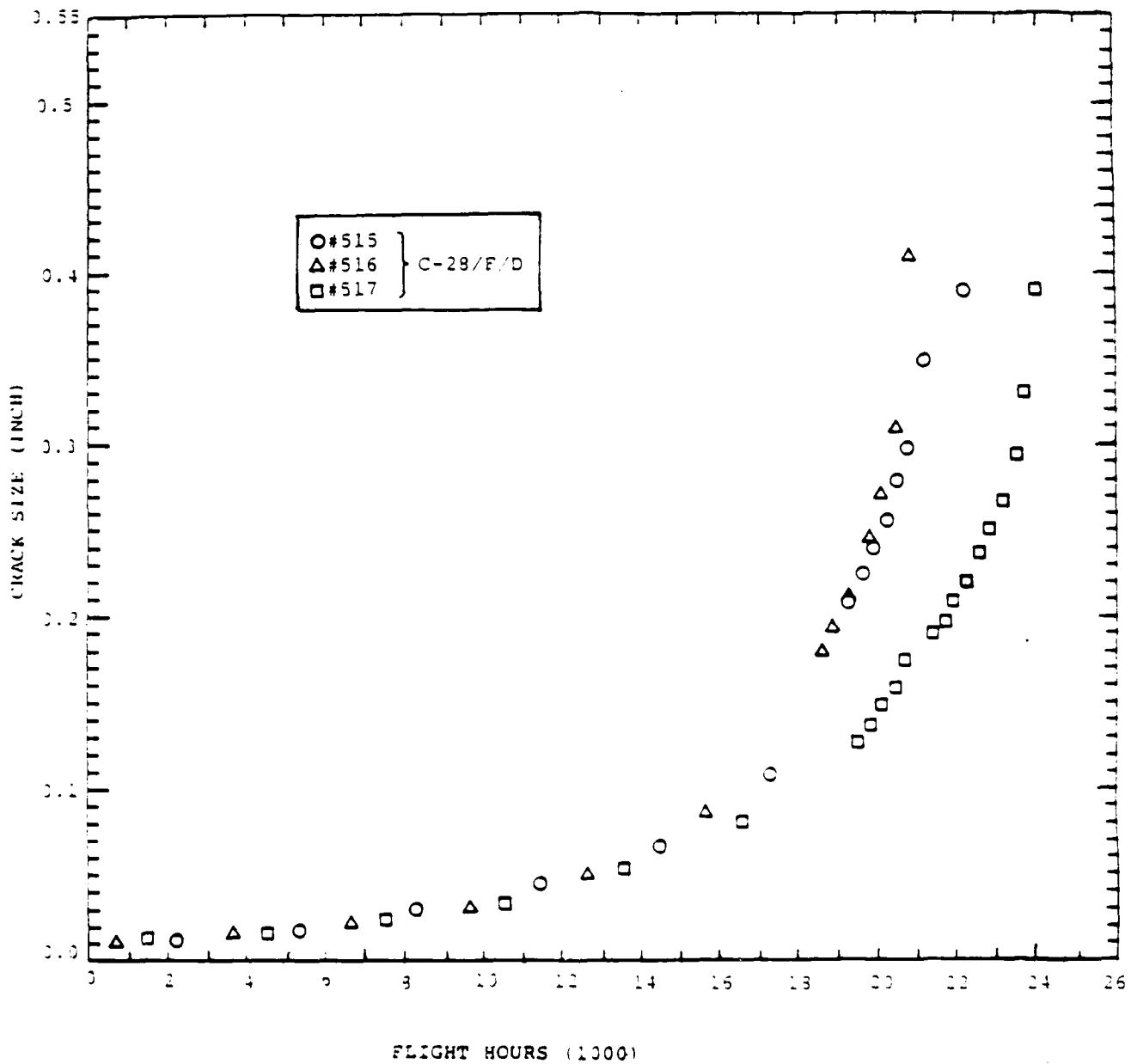


Fig. D-15 Normalized Crack Growth Results ( $a_1 = 0.01"$ )  
for 7075-T7651 Aluminum Dog-Bone Specimens  
(Open Hole; Dia. = 0.4375") Tested Using: F-18  
300 Hour (Block) Spectrum (Gross = 28 ksi Max.,  
Dry Air Environment, and Fast Loading Frequency)

AD-A160 378 DEVELOPMENT OF FATIGUE AND CRACK PROPAGATION DESIGN AND ANALYSIS METHODOL. (U) GENERAL DYNAMICS FORT WORTH TX 4/4

AD-A160 378 DEVELOPMENT OF FATIGUE AND CRACK PROPAGATION DESIGN AND ANALYSIS METHODOL. (U) GENERAL DYNAMICS FORT WORTH TX 4/4

AD-A160 378 DEVELOPMENT OF FATIGUE AND CRACK PROPAGATION DESIGN AND ANALYSIS METHODOL. (U) GENERAL DYNAMICS FORT WORTH TX 4/4

UNCLASSIFIED NADC-83126-60-VOL-3 N62269-81-C-0268

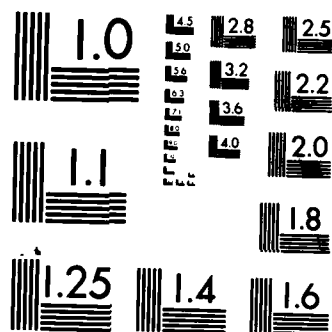
UNCLASSIFIED NADC-83126-60-VOL-3 N62269-81-C-0268

UNCLASSIFIED NADC-83126-60-VOL-3 N62269-81-C-0268 F/G 11/6 NL

UNCLASSIFIED NADC-83126-60-VOL-3 N62269-81-C-0268 F/G 11/6 NL

FALM 7

DTM



MICROCOPY RESOLUTION TEST CHART  
NATIONAL BUREAU OF STANDARDS-1963-A

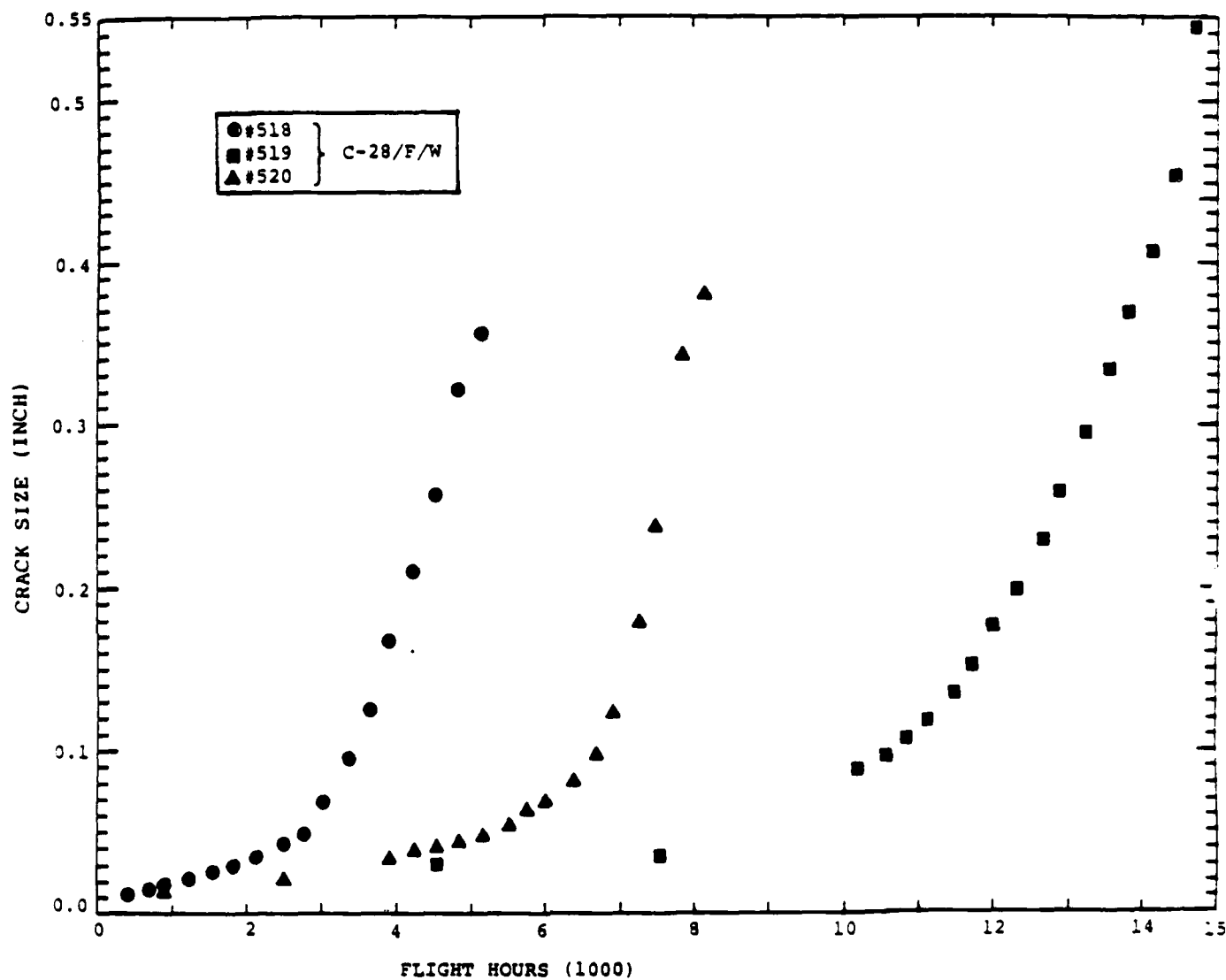


Fig. D-16 Normalized Crack Growth Results ( $a_i = 0.01"$ )  
for 7075-T7651 Aluminum Dog-Bone Specimens  
(Open Hole: Dia = 0.4375") Tested Using: F-18  
300 Hour (Block) Spectrum ( $\sigma_{Gross} = 28$  ksi Max.),  
3.5% NaCl Environment and Fast Loading Frequency.

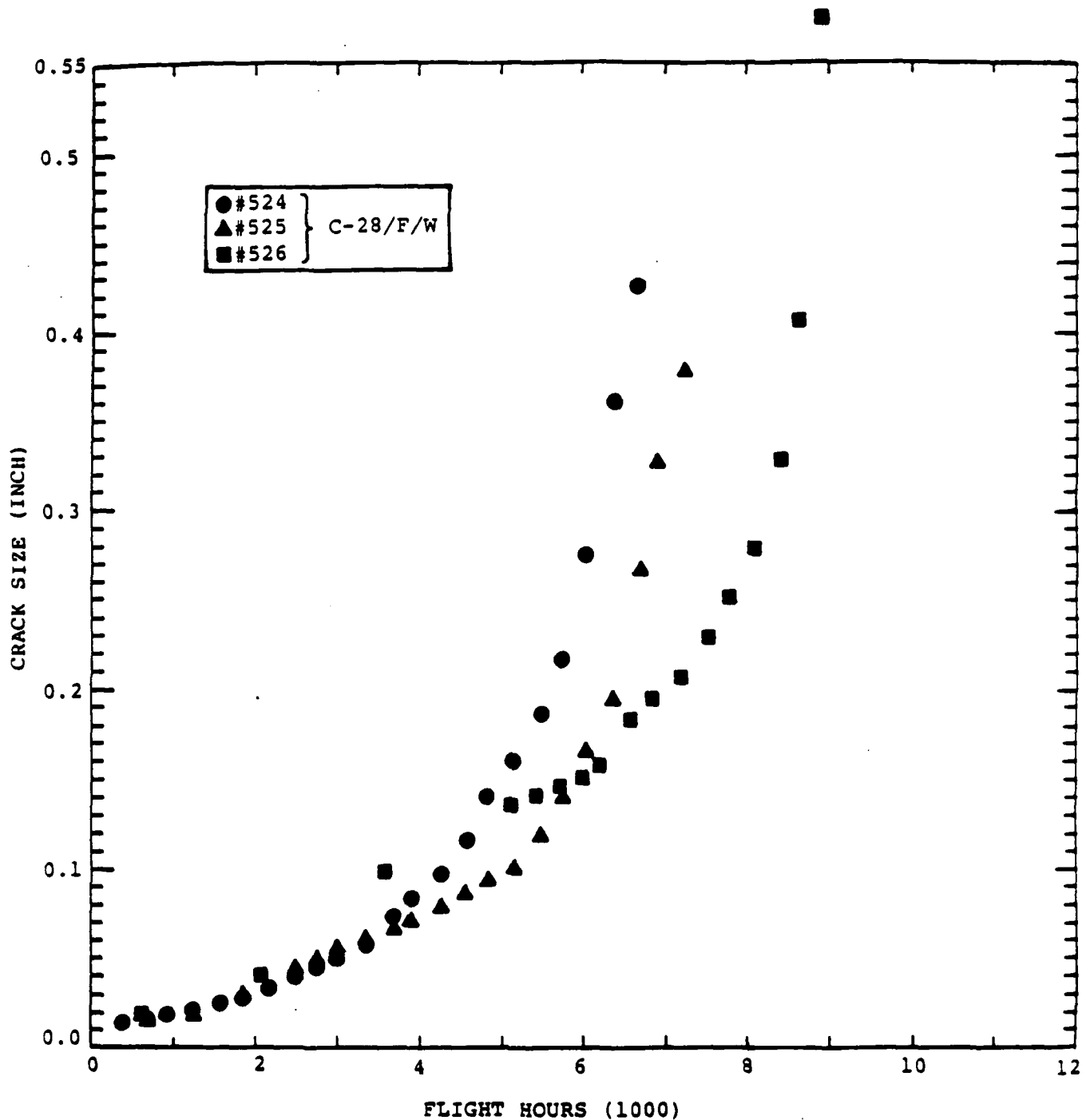


Fig. D-17 Normalized Crack Growth Results ( $a_i = 0.01"$ )  
for 7075-T7651 Aluminum Dog-Bone Specimens  
(Open Hole; Dia = 0.500") Tested Using: F-18  
300 Hour (Block) Spectrum ( $\sigma_{Gross} = 28$  ksi Max.),  
3.5% NaCl Environment and Fast Loading Frequency.

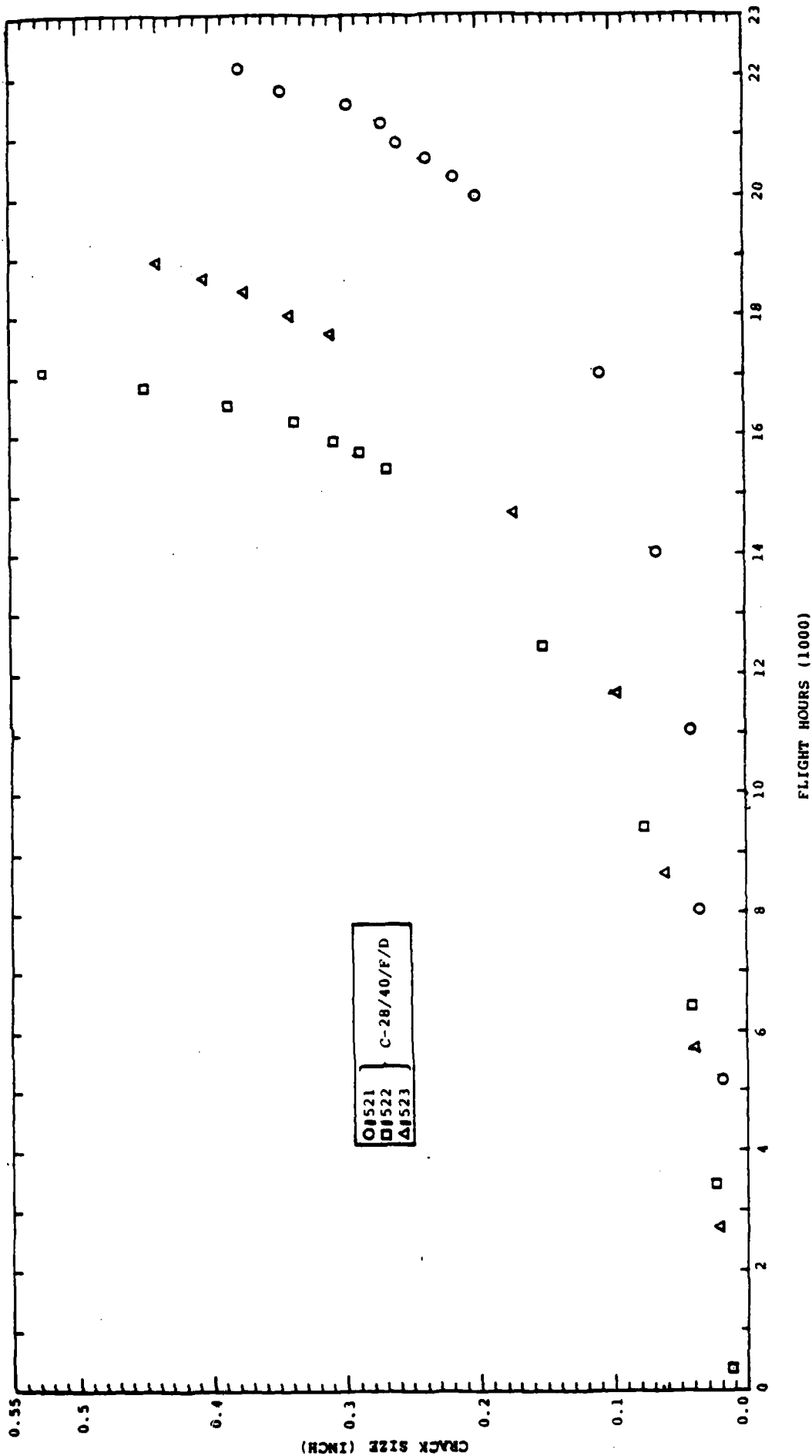


Fig. D-18 Normalized Crack Growth Results ( $a_i = 0.01"$ )  
for 7075-T7651 Aluminum Dog-Bone Specimens  
(40% Load Transfer) Tested Using: F-18 300 Hour  
(Block) Spectrum ( $\sigma_{Gross} = 28$  ksi Max.), Dry Air  
Environment and Fast Loading Frequency

(This page intentionally left blank)

APPENDIX E

DESCRIPTION OF LOCAL-STRAIN COMPUTER PROGRAM (BROSE)

E.1 INTRODUCTION

The local strain analysis computer program described herein was used to predict the time-to-crack-initiation (TTCI) for various dog-bone specimen configurations. Essential features and capabilities of the computer program are briefly described herein and details are described in Ref. 45. Example input/output is presented to show the features of the program. A complete listing of the computer program can be obtained from Dr. Y. T. Wu of the University of Arizona.

A general purpose local strain analysis computer program was developed by Dr. W. R. Brose as a M.S. thesis in the Department of Theoretical and Applied Mechanics at the University of Illinois. This program was later modified by Scott Martindale and Yih-Tsuen Wu while graduate students at the University of Arizona under Dr. Paul H. Wirsching. The updated version of the local strain analysis program was rehosted at General Dynamics/Fort Worth Division for use on the VAX 11/780.

## E.2 PROGRAM CAPABILITIES

The local strain analysis program can be used to predict the time-to-failure (TTF) or the TFCI in notches or fastener holes where cyclic plasticity is a possibility. Also, the program applies to either constant amplitude or random loading. It also features two options for estimating the local notch stress-strain behavior:

- (1) Neuber's rule [48] and (2) generalized Neuber's rule proposed by T. Seeger and P. Heuler [50]. The effects of cyclic mean stresses on the TTF or TFCI can also be accounted for. The rain-flow cycle counting scheme is used for spectrum load history [e.g., 28].

A typical problem for predicting the TFCI in a fastener hole using the local strain analysis approach is illustrated in Fig. E.1. Typical input output for the computer program is presented in Table E-1.

## E.3 SUMMARY OF ESSENTIAL EQUATION USED IN LOCAL STRAIN ANALYSIS COMPUTER PROGRAM

For reference purposes, the main equations reflected in computer program BROSE are summarized below:

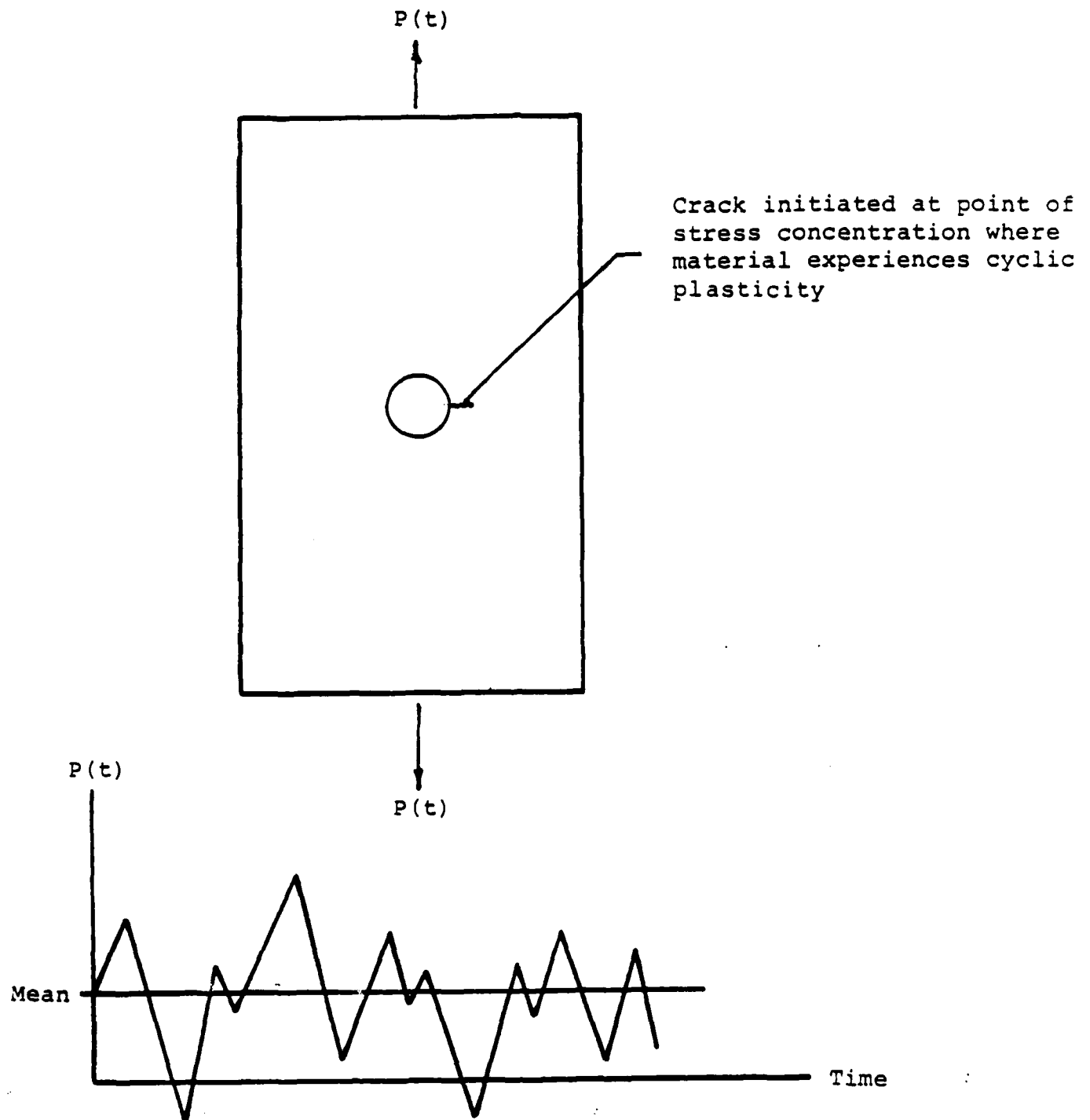


Fig. E-1 Typical Problem for Predicting the TTCI in Fastener Hole Using the Local Strain Analysis Approach

Table E-1 Typical Input/Output For Local Strain  
Analysis Computer Program (BROSE)

Summary of Input Data

Version 2: The load-strain relation is generated using Neuber's rule.

A correction for the effect of mean stress is employed  
Number of terms in stress-strain range 100

Material 7075-t7651 Aluminum Average Values (DRY)

Elastic Modulus (ksi) = 10300.  
Fatigue Strength Coefficient (ksi) = 247.5  
Fatigue Strength Exponent = -0.1585  
Fatigue Ductility Coefficient = 3.414  
Fatigue Ductility Exponent = -1.2049  
Cyclic Strength Coefficient = 104.9  
Cyclic Strain Hardening Exponent = 0.103  
Data for Neuber's rule:  $K_t = 3.430$   $F(IN^{*-2}) = 1.000$   
Mean Stress Factor  $K_m = 1.000$

Summary of Fatigue Life Predictions

Version 2: The load-strain relation is generated using Neuber's rule.

A correction for the effect of mean stress is employed

Material 7075-t7651 Aluminum Average Values (DRY)

Data for Neuber's rule:  $K_t = 3.430$   $F(IN^{*-2}) = 1.000$

History F-18 Fighter Spectrum

Load Scale Factor = 358.0000

Damage = 0.0386

Predicted Life in blocks = 25 89

Predicted Life in cycles = 0.3892E+05

Table E-1 Typical Input/Output For Local Strain  
Analysis Computer Program (BROSE)  
(Continued)

Strain - Life Fatigue Analysis F18BLC						
Material 7475-t/651 Aluminum Average Values (DRY)						
History F-18 Fighter Spectrum						
Level	Stress Range psi	Strain Range	No of Cycles	Percent of Total Cycles	Percent of Total Cycles Above Level	Damage
1	1248.	0.000416	0	0.000	100.000	0.0000E+00
2	2496.	0.000832	0	0.000	100.000	0.0000E+00
3	3746.	0.001248	0	0.000	100.000	0.0000E+00
4	4994.	0.001664	0	0.000	100.000	0.0000E+00
5	6244.	0.002080	0	0.000	100.000	0.0000E+00
6	7492.	0.002496	0	0.000	100.000	0.0000E+00
7	8742.	0.002911	0	0.000	100.000	0.0000E+00
8	9990.	0.003327	0	0.000	100.000	0.0000E+00
9	11240.	0.003743	1	0.067	99.933	0.0000E+00
10	12480.	0.004159	231	15.369	84.564	0.5408E-06
11	13736.	0.004575	0	0.000	84.564	0.1226E-03
12	14984.	0.004991	100	7.186	77.379	0.0000E+00
13	16228.	0.005407	348	23.154	54.225	0.2527E-03
14	17470.	0.005823	0	0.000	54.225	0.9609E-03
15	18704.	0.006239	300	25.283	28.942	0.0000E+00
16	19928.	0.006655	37	2.461	26.480	0.2866E-02
17	21136.	0.007071	0	0.000	26.480	0.2740E-03
18	22322.	0.007487	236	15.702	10.778	0.5216E-02
19	23480.	0.007903	2	0.133	10.645	0.3913E-04
20	24602.	0.008319	0	0.000	10.645	0.0000E+00
21	25684.	0.008734	95	6.321	4.325	0.0000E+00
22	26726.	0.009150	6	0.399	3.925	0.5577E-02
23	27726.	0.009566	0	0.000	3.925	0.3310E-03
24	28688.	0.009982	0	0.532	3.393	0.0000E+00
25	29612.	0.010398	29	1.929	1.464	0.1340E-02
26	30504.	0.010814	0	0.000	1.464	0.4692E-02
27	31366.	0.011230	0	0.000	1.464	0.0000E+00
28	32202.	0.011646	0	0.000	1.464	0.0000E+00
29	33012.	0.012062	15	0.998	0.466	0.6008E-02
30	33802.	0.012478	0	0.000	0.466	0.0000E+00
31	34570.	0.012894	0	0.000	0.466	0.0000E+00
32	35320.	0.013310	0	0.000	0.466	0.0000E+00
33	36054.	0.013726	4	0.266	0.200	0.3478E-02
34	36772.	0.014142	0	0.000	0.200	0.0000E+00
35	37476.	0.014557	0	0.000	0.200	0.0000E+00
36	38166.	0.014973	0	0.000	0.200	0.0000E+00
37	38846.	0.015389	0	0.000	0.200	0.0000E+00
38	39512.	0.015805	0	0.000	0.200	0.0000E+00
39	40168.	0.016221	2	0.133	0.067	0.3185E-02
40	40814.	0.016637	0	0.000	0.067	0.0000E+00
41	41450.	0.017053	0	0.000	0.067	0.0000E+00
42	42078.	0.017469	0	0.000	0.067	0.0000E+00
43	42698.	0.017885	0	0.000	0.067	0.0000E+00
44	43308.	0.018301	0	0.000	0.067	0.0000E+00
45	43910.	0.018717	0	0.000	0.067	0.0000E+00
46	44506.	0.019133	0	0.000	0.067	0.0000E+00
47	45094.	0.019549	0	0.000	0.067	0.0000E+00
48	45674.	0.019965	0	0.000	0.067	0.0000E+00
49	46250.	0.020380	0	0.000	0.067	0.0000E+00
50	46818.	0.020796	1	0.067	0.000	0.4280E-02

General Strain Life Curve

$$\epsilon_a = \frac{\sigma'_f}{E} (2N_f)^b + \epsilon'_f (2N_f)^c \quad (E-1)$$

where  $\epsilon_a$  = strain amplitude

$E$  = Modulus of Elasticity

$\sigma'_f$  = Fatigue strength coefficient

$b$  = Fatigue strength exponent

$\epsilon'_f$  = Fatigue ductility coefficient

$c$  = Fatigue ductility exponent

$N_f$  = Number of cycles to failure or initiation

When the mean stress,  $\sigma_o$ , must be accounted for use Manson's formulation (83) given by Eq. E-2.

$$\epsilon_a = \left[ \frac{\sigma_f - K_m \sigma_o}{E} \right] (2N_f)^b + \left[ \frac{\sigma_f - K_m \sigma_o}{\sigma'_f} \right]^{c/b} \epsilon'_f (2N_f)^c \quad (E-2)$$

In Eq. E-2,  $K_m$  is the mean stress factor, equal to unity in Morrow's model (84).

Neuber's Rule [49]

The rule correlates nominal stress  $S$  and nominal strain  $e$  and local stress-strain behavior.

$$\sigma_e = K_t^2 S e \quad (E-3)$$

where  $K_t$  = stress concentration factor

$\sigma$  = Local stress amplitude

If the gross deformation at the notch is elastic, Eq. E-3 becomes

$$\sigma_e = \left( \frac{K_t S}{E} \right)^2 \quad (E-4)$$

Generalized Neuber Rule by Seeger and Heuler [50]

Use Eq. E-5 when nonlinear net section behavior has to be considered:

$$\sigma_e = (S^2 K_t^2 / E) (e^* E / S^*) \quad (E-5)$$

In Eq. E-5,  $e^*$  = modified nominal strain and  $S^*$  = modified nominal stress

Cyclic Stress-Strain Curve

$$\epsilon = \sigma/E + (\sigma/K')^{1/n'} \quad (E-6)$$

where  $n'$  = cyclic strain hardening exponent and  $K'$  = cyclic strength coefficient.

TABLE F-6 SUMMARY OF CONSTANTS IN  $K_t = (A(TTCI))^B$  FOR TTCI  
 ( $\sigma_c = 0.01$ ) PREDICTIONS FOR 7075-T7651 ALUMINUM  
 BASED ON: LOCAL STRAIN ANALYSIS, F-18 300 HOUR  
 (BLOCK) SPECTRUM ("C") AND  $\sigma_{GROSS} = 28$  KSI

ENVIRONMENT	$K_t$	LWR BOUND		AVERAGE		UPR. BOUND	
		TTCI 1000 (FLT.HRS.)	A	TTCI 1000 (FLT.HRS.)	A	TTCI 1000 (FLT.HRS.)	A
DRY AIR	3.02	9.9	4.285	18.1	4.672	33.0	5.043
	3.18	7.3		13.3		24.1	
	3.25	6.2		11.2		20.2	
	3.43	4.3		7.8		13.9	
3.5% NaCl	3.02	4.1	3.817	10.1	4.523	24.1	5.199
	3.18	3.2		7.9		18.6	
	3.25	2.7		6.7		15.8	
	3.43	1.9		4.9		11.5	

NOTE: (a)  $K_t = A(TTCI)^B$

(b)  $\sigma_{Net} = 35.8$  ksi (peak stress) used in local strain analysis

(c) Local strain analysis based on Neuber's rule

TABLE F-5 SUMMARY OF CONSTANTS IN  $K_t = A(TTCI)^B$  FOR TTCI  
 ( $a_1 = 0.01$ ) PREDICTIONS FOR 7075-T7651 ALUMINUM  
 BASED ON: LOCAL STRAIN ANALYSIS, F-18 300 HOUR  
 (RANDOM) SPECTRUM ("B") AND  $\sigma_{GROSS} = 28$  ksi

ENVIRONMENT	K <sub>L</sub>	LMR BOUND		AVERAGE			UPR BOUND				
		(1000 FLT HRS)		A	B	TTCI 1000 (FLT.HRS)	A	B	TTCI 1000 (FLT.HRS)	A	B
DRY AIR	3.02	9.8		4.142	-0.139	17.6	4.459	-0.136	31.5	4.798	-0.134
	3.18	6.6				11.8			20.9		
	3.25	5.8				10.2			18.1		
	3.43	3.9				6.9			12.2		
3.5% NaCl	3.02	4.7		3.850	-0.158	11.2	4.421	-0.158	26.1	4.939	-0.151
	3.18	3.3				7.9			18.3		
	3.25	2.9				7.0			16.1		
	3.43	2.1				5.0			11.2		

NOTE: (a)  $K_t = A(TTCI)^B$

(b)  $\sigma_{NET} = 35.8$  ksi (peak stress) used in local strain analysis (equivalent to  $\sigma_{GROSS} = 28$  ksi)

(c) Local strain analysis based on Neuber's rule.

TABLE F-4 SUMMARY OF CONSTANTS IN  $K_L = A(TTCI)^B$  FOR TTCI ( $a_i = 0.01$ ) PREDICTIONS FOR 7075-T7651 ALUMINUM BASED ON: LOCAL STRAIN ANALYSIS, F-16 400 HOUR (BLOCK) SPECTRUM AND  $\sigma_{GROSS} = 28$  KSI

ENVIRONMENT	K <sub>t</sub>	LMR BOUND			AVE			UPR. BOUND		
		TTCI 1000 (FLT. HRS.)	A	B	TTCI 1000 (FLT. HRS.)	A	B	TTCI 1000 (FLT. HRS.)	A	B
DRY AIR	2.5	39.88	4.423	-0.162	73.48	4.842	-0.159	135.16	5.296	-0.158
	3.0	11.88			21.71			39.59		
	3.5	4.18			7.56			13.64		
	4.0	1.66			2.96			5.30		
	4.5	0.78			1.38			2.43		
	5.0	0.39			0.68			1.18		
	10.0	0.008			0.013			0.022		
3.5% NaCl	2.5	11.09	3.033	-0.184	27.94	4.486	-0.178	67.48	5.141	-0.172
	3.0	4.00			10.03			23.97		
	3.5	1.67			4.13			9.70		
	4.0	0.74			1.82			4.19		
	4.5	0.39			0.94			2.09		
	5.0	0.21			0.49			1.08		
	10.0	0.006			0.012			0.022		

NOTE: (a)  $K_f = A(TfCl)^B$

(b)  $\sigma_{NET} = 35.8$  ksi used in local strain analysis (equivalent to  $\sigma_{GROSS} = 20$  ksi)

(c) Local strain analysis based on Neuber's rule.

Table F-3 Example Output from Strain-Life Computer Program  
(Generalized Neuber Rule Option) (Cont'd)  
Strain-Life Fatigue Analysis  
F16/D

891.881.49

12-SEP-84

## Summary of Fatigue Life Predictions

## Version 4: Neuber's Rule, Seeger's Version

A correction for the effect of mean stress is employed

Material 7075-T7651 Aluminum Average Values (DR7)

Date for Neuber's rule  
 $K_t = 3.500$   $K_p = 3.500$   $S_{t(N+2)} = 1.000$

History F-16 fighter 400 Hour Block Spectrum

Load Scale factor = 350.0000

Damage = 0.0532

Predicted Life in blocks = 18.78

Predicted Life in cycles = 6.3552E+06

Table F-3 Example Output from Strain-Life Computer Program  
(Generalized Neuber Rule Option) (Cont'd)Strain - Life Fatigue Analysis  
F16/D

## Summary of Fatigue Life Predictions

Version 4: Neuber's Rule, Seeger's Version

A correction for the effect of mean stress is employed

Material 7075-T7651 Aluminum Average Values (DRY)

Data for Neuber's rule  
 $K_t = 3.500$   $K_p = 3.500$   $f(1N^{m-2}) = 1.000$ 

History F-16 fighter 400 Hour Block Spectrum

Load Scale factor = 350.0000

Damage = 0.0532

Predicted Life in blocks = 10.70

Predicted Life in cycles = 0.3652E+06

Table F-3 Example Output from Strain-Life Computer Program  
(Generalized Neuber Rule Option) (Cont'd)

Strain - Life Fatigue Analysis  
F16/D

Material 7075-T7651 Aluminum Average Values (DRY) History F-16 Fighter 400 Hour Block Spectrum							
Level	Stress Range Psi	Strain Range	No of Cycles	Percent of Total Cycles	Percent of Total Cycles Above Level	Percent of Total Damage	Damage
1	1320.	0.000449	19	0.100	99.900	0.00	0.4267E-11
2	2642.	0.00090	9	0.040	99.852	0.00	0.1013E-09
3	3964.	0.001340	14	0.074	99.778	0.00	0.3200E-08
4	5286.	0.001797	21	0.111	99.667	0.00	0.3205E-07
5	6600.	0.002246	1917	10.136	89.530	0.02	0.1000E-04
6	7930.	0.002695	5024	30.795	58.735	0.25	0.1325E-03
7	9252.	0.003145	2350	12.460	46.267	0.33	0.1761E-03
8	10574.	0.003594	2231	11.797	34.470	0.70	0.4154E-03
9	11896.	0.004043	2126	11.242	23.229	1.60	0.0940E-03
10	13210.	0.004492	232	1.227	22.002	0.29	0.1527E-03
11	14530.	0.004941	1260	6.662	15.339	2.56	0.1364E-02
12	15856.	0.005391	894	4.727	10.612	4.45	0.2360E-02
13	17170.	0.005840	1155	6.107	4.505	10.61	0.5650E-02
14	18476.	0.006289	82	0.434	4.071	1.15	0.6113E-03
15	19760.	0.006738	156	0.825	3.247	4.26	0.2265E-02
16	21042.	0.007187	300	2.052	1.195	13.75	0.7322E-02
17	22200.	0.007637	33	0.174	1.021	1.30	0.6933E-03
18	23500.	0.008086	121	0.640	0.381	0.54	0.4549E-02
19	24666.	0.008535	6	0.032	0.349	0.52	0.2790E-03
20	25780.	0.008984	10	0.053	0.296	1.17	0.6244E-03
21	26862.	0.009434	1	0.005	0.291	0.12	0.6460E-04
22	27892.	0.009883	4	0.021	0.270	0.75	0.3971E-03
23	28070.	0.010332	0	0.000	0.270	0.00	0.0000E+00
24	29026.	0.010781	4	0.021	0.249	1.54	0.0193E-03
25	30740.	0.011230	32	0.169	0.079	16.00	0.0559E-02
26	31622.	0.011600	0	0.000	0.079	0.00	0.0000E+00
27	32470.	0.012129	1	0.005	0.074	0.70	0.3740E-03
28	33300.	0.012578	1	0.005	0.069	0.76	0.4020E-03
29	34116.	0.013027	1	0.005	0.063	1.00	0.5746E-03
30	34904.	0.013477	9	0.048	0.016	13.00	0.6919E-02
31	35672.	0.013926	0	0.000	0.016	0.00	0.0000E+00
32	36424.	0.014375	0	0.000	0.016	0.00	0.0000E+00
33	37162.	0.014824	1	0.005	0.011	1.97	0.1047E-02
34	37804.	0.015273	1	0.005	0.005	2.27	0.1208E-02
35	38592.	0.015723	0	0.000	0.005	0.00	0.0000E+00
36	39200.	0.016172	0	0.000	0.005	0.00	0.0000E+00
37	39972.	0.016621	0	0.000	0.005	0.00	0.0000E+00
38	40646.	0.017070	0	0.000	0.005	0.00	0.0000E+00
39	41310.	0.017520	0	0.000	0.005	0.00	0.0000E+00
40	41962.	0.017969	0	0.000	0.005	0.00	0.0000E+00
41	42606.	0.018410	0	0.000	0.005	0.00	0.0000E+00
42	43242.	0.018867	0	0.000	0.005	0.00	0.0000E+00
43	43860.	0.019316	0	0.000	0.005	0.00	0.0000E+00
44	44406.	0.019766	0	0.000	0.005	0.00	0.0000E+00
45	45090.	0.020215	0	0.000	0.005	0.00	0.0000E+00
46	45702.	0.020664	0	0.000	0.005	0.00	0.0000E+00
47	46290.	0.021113	0	0.000	0.005	0.00	0.0000E+00
48	46800.	0.021562	0	0.000	0.005	0.00	0.0000E+00
49	47472.	0.022012	0	0.000	0.005	0.00	0.0000E+00
50	48040.	0.022461	1	0.005	0.000	10.10	0.5375E-02

16.12.68

Table F-2 Example Output from Strain-Life Computer  
Program (Neuber's Rule Option) (Cont'd)  
Strain - Life Fatigue Analysis  
F16/D

1-SEP-84

## Summary of Fatigue Life Predictions

Version 2: The load-strain relation is generated using Neuber's rule.

A correction for the effect of mean stress is employed

Material 7075-T7651 Aluminum Average Values (ORV)

Data for Neuber's rule:  $K_t = 3.500$   $f(LN-2) = 1.000$

History F-16 fighter 400 Hour Block Spectrum

Load Scale Factor = 350.0000

Damage = 0.0529

Predicted Life in blocks = 10.90

Predicted Life in cycles = 0.3575E+06

Table F-2 Example Output from Strain-Life Computer Program (Neuber's Rule Option) (cont'd)

Strain - Life Fatigue Analysis  
F16/D

Summary of Fatigue Life Predictions

Version 2: The load-strain relation is generated using Neuber's rule.

A correction for the effect of mean stress is employed

Material 7075-T7651 Aluminum Average Values (DRV)

Data for Neuber's rule:  $K_t = 3.500$   $F(LN^{*-2}) = 1.000$

History F-16 Fighter 400 Hour Block Spectrum

Load Scale Factor = 350.0000

Damage = 0.0529

Predicted Life in blocks = 10.90

Predicted Life in cycles = 0.3576E+06

Table F-2 Example Output from Strain-Life Computer  
Program (Neuber's Rule Option)  
Strain - Life Fatigue Analysis  
F16/D

Material 7075-T7651 Aluminum Average Values (DRV) History F-16 Fighter 400 Hour Block Spectrum						
Level	Stress Range Psi	Strain Range	No of Cycles	Percent of Total Cycles	Percent of Total Cycles Above Level	Damage
1	1260.	0.000431	20	0.106	99.894	0.3496E-11
2	2530.	0.000653	11	0.058	99.836	0.1605E-09
3	3080.	0.001294	11	0.058	99.778	0.1976E-08
4	5070.	0.001726	22	0.116	99.662	0.2600E-07
5	6340.	0.002157	567	2.990	96.663	0.2007E-06
6	7616.	0.002509	7142	37.764	58.899	0.1199E-03
7	8086.	0.003020	2209	11.600	47.219	0.1267E-03
8	10156.	0.003452	1193	6.300	40.911	0.1412E-03
9	11426.	0.003803	2500	13.219	27.691	0.0076E-03
10	12694.	0.004314	1057	5.509	22.182	0.6220E-03
11	13964.	0.004746	950	5.066	17.037	0.0069E-03
12	15230.	0.005177	1037	5.403	11.554	0.1007E-02
13	16494.	0.005609	019	4.331	7.223	0.3467E-02
14	17752.	0.006040	527	2.707	4.436	0.2602E-02
16	19002.	0.006472	71	0.376	4.061	0.6663E-03
16	20230.	0.006903	101	0.567	3.104	0.2944E-02
17	21454.	0.007335	362	1.914	1.190	0.7329E-02
18	22642.	0.007766	112	0.592	0.690	0.3134E-02
19	23794.	0.008197	43	0.227	0.370	0.1640E-02
20	24984.	0.008629	4	0.021	0.349	0.2090E-03
21	26974.	0.009060	10	0.053	0.296	0.6720E-03
22	26990.	0.009492	2	0.011	0.206	0.1665E-03
23	27902.	0.009923	3	0.016	0.270	0.2063E-03
24	29020.	0.010355	3	0.016	0.264	0.5026E-03
26	29036.	0.010706	2	0.011	0.243	0.4179E-03
26	30714.	0.011210	1	0.005	0.230	0.2299E-03
27	31564.	0.011649	30	0.159	0.079	0.9724E-02
28	32380.	0.012000	1	0.005	0.074	0.3696E-03
29	33100.	0.012512	1	0.005	0.069	0.3937E-03
30	33966.	0.012943	9	0.048	0.021	0.6649E-02
31	34720.	0.013375	1	0.005	0.016	0.6541E-03
32	36470.	0.013806	0	0.000	0.016	0.0000E+00
33	36190.	0.014230	0	0.000	0.016	0.0000E+00
34	36910.	0.014669	1	0.005	0.011	0.9709E-03
36	37600.	0.015101	0	0.000	0.011	0.0000E+00
36	38294.	0.015632	1	0.005	0.006	0.1290E-02
37	38960.	0.015964	0	0.000	0.006	0.0000E+00
38	39630.	0.016395	0	0.000	0.006	0.0000E+00
39	40202.	0.016826	0	0.000	0.005	0.0000E+00
40	40926.	0.017250	0	0.000	0.005	0.0000E+00
41	41550.	0.017609	0	0.000	0.005	0.0000E+00
42	42104.	0.018121	0	0.000	0.005	0.0000E+00
43	42000.	0.018552	0	0.000	0.005	0.0000E+00
44	43406.	0.018984	0	0.000	0.005	0.0000E+00
45	44000.	0.019415	0	0.000	0.005	0.0000E+00
45	44600.	0.019847	0	0.000	0.005	0.0000E+00
47	45106.	0.020270	0	0.000	0.005	0.0000E+00
48	45766.	0.020709	0	0.000	0.005	0.0000E+00
49	46340.	0.021141	0	0.000	0.005	0.0000E+00
50	46906.	0.021572	0	0.000	0.005	0.0000E+00
51	47466.	0.022004	0	0.000	0.005	0.0000E+00
52	48022.	0.022435	1	0.006	0.000	0.5306E-02

TABLE F-1 SUMMARY OF LOCAL STRAIN ANALYSIS RESULTS FOR 7075-T7651 ALUMINUM: TTCI ( $a_i = 0.01"$ ) PREDICTIONS FOR SELECTED EFFECTIVE  $K_t$  VALUE,  $\sigma_{GROSS} = 28$  ksi AND F-16 400 HOUR (BLOCK) SPECTRUM

ENVIRONMENT	$K_t$	TTCI (1000 FLT. HRS.)					
		NEUBER'S RULE			SEEGER/HEULER(e)		
		LWR.	AVE.	UPR.	LWR.	AVE.	UPR.
DRY AIR ↓	2.5	39.88	73.48	135.16	39.59	73.08	134.68
	3.0	11.88	21.71	39.59	11.22	20.53	37.49
	3.5	4.18	7.56	13.64	4.15	7.51	13.57
	4.0	1.66	2.96	5.30	1.65	2.96	5.28
	4.5	0.78	1.38	2.43	0.76	1.34	2.37
	5.0	0.39	0.68	1.18	0.38	0.67	1.18
	10.0	0.008	0.013	0.022	0.008	0.013	0.021
3.5% NaCl ↓	2.5	11.09	27.94	67.48	11.04	27.90	67.52
	3.0	4.00	10.03	23.97	3.85	9.65	23.09
	3.5	1.67	4.13	9.70	1.66	4.11	9.66
	4.0	0.74	1.82	4.19	0.75	1.84	4.23
	4.5	0.39	0.94	2.09	0.38	0.91	2.04
	5.0	0.21	0.49	1.08	0.20	0.49	1.07
	10.0	0.006	0.012	0.022	0.006	0.013	0.022

- NOTES: (a) Lower, average and upper bound TTCI predictions based on applicable strain-life constants shown in Table A-3 and the local strain analysis computer program described in Appendices E.  
 (b)  $a_i = 0.01"$  crack depth  
 (c) Ref. Table F-3 for typical output of strain-life analysis.  
 (d)  $\sigma_{NET} = 35.8$  ksi used for local strain analysis (equivalent to  $\sigma_{GROSS} = 28$  ksi)  
 (e) Generalized Neuber's Rule (48).

the corrosion fatigue tests performed in Phase II. TTCI predictions were made for both Neuber's rule [48] and the generalized Neuber rule proposed by Seeger and Heuler[50] for spectrum "A" (F-16 400 hour block).

Local strain analysis results for different assumed effective  $K_t$  values are summarized in Table F-1 for the F-16 400 hour block spectrum ("A") for both the dry air and 3.5% NaCl environments. TTCI predictions ( $a_0 = 0.01"$ ) are shown for the average as well as the 95% scatter band (referred to as upper and lower bound TTCI predictions). Example computer output for the strain life analysis are shown in Table F-2 and F-3 based on Neuber's rule and the generalized Neuber rule, respectively. As shown in Table F-2, there were no significant differences in the TTCI results for the two versions of Neuber's rule.

Strain analysis results for TTCI based on selected effective stress concentration factors are summarized in Table F-4 through F-6 for load spectra "A", "B" and "C", respectively. TTCI predictions are shown for both the dry air and 3.5% NaCl environments for three different strain life allowable curves, i.e., average and the 95% confidence interval (Ref. Appendix A).

Normally, the same effective  $K_t$  values (assumed) should be used for different load spectra in the strain life analysis. However, in the case of load spectra "B" and "C"

## F.2 STRAIN LIFE ANALYSIS RESULTS

Strain life analyses were performed using computer program "BROSE", described in Appendix E and Ref. 45. Predictions were made for TCI ( $a_0 = 0.01"$ ) for 7075-T7651 aluminum different effective  $K_t$  values, three load spectra ("A", "B" and "C"), and both dry air and 3.5% NaCl environments.

Strain life allowables from Appendix A were used. These allowables reflected the mean as well as the 95% scatter bond extremes. Applicable strain life allowables and selected effective  $K_t$  values were used to predict the TCI mean and to estimate the extreme values (referred to as upper and lower bounds). The TCI predictions were used to determine effective  $K_t$  versus TCI relationships (in Section F.3) for the three load spectra considered.

Strain-life analyses were performed using  $\sigma_{Net} = 35.8$  ksi (or  $\sigma_{Gross} = 28$  ksi)\* for each of the three load spectra considered.  $\sigma_{Gross} = 28$  ksi is the baseline stress used for

---

\*Maximum gross stress in the spectrum. The more usual practice specified  $\sigma_{gross}$  as the "design stress" and the maximum value is scaled by an "overload factor" in the spectrum.

## APPENDIX F

## CORROSION FATIGUE CRACK INITIATION ANALYSIS DETAILS

## F.1 INTRODUCTION

The corrosion fatigue (CF) crack initiation methodology recommended for application to the 7000-series aluminum alloy in the over-aged condition is described in Section 5.3 and essential details are given in Fig. 15. In this Appendix, further details and insight are given about implementing the CF crack initiation methodology. Specifically, the following details are presented in this Appendix: (1) strain life analysis predictions are presented, including typical output from computer program "BROSE", (2) how to determine an effective  $K_t$  versus time-to-crack-initiation (TTCI) relationship, using a simple power law, based on the average and extreme strain life allowables, (3) describe and illustrate how to determine  $\bar{K}_t(0)$  and  $\bar{K}_t(LT)$ , and (4) illustrate how to determine the environmental scaling factor for crack initiation based on constant amplitude fatigue test results.

APPENDIX F

CONTENTS

<u>Section</u>		<u>Page</u>
F.1	Introduction	F-2
F.2	Strain Life Analysis Results	F-3
F.3	Effective $K_t$ Relationships	F-15
F.4	Strain Life Analysis Scaling	F-19
F.5	Effective $\bar{K}_t$ (LT) for Bolt Load Transfer	F-25
F.6	Evaluation of Environmental Scaling Factors for Crack Initiation	F-29

preliminary strain life analysis results were available for specific effective  $K_t$  values (i.e., 3.02, 3.18, 3.25 and 3.43). Therefore, these effective  $K_t$  values and applicable strain life analysis results were used herein to establish effective  $K_t$  relationships for load spectra "B" and "C" based on Eq. F-1.

### F.3 EFFECTIVE $K_t$ RELATIONSHIPS

The relationship between effective  $K_t$  and TTCI is needed to: (1) scale or tune the initial strain life predictions for TTCI (based on smooth, un-notch strain controlled data) using dog-bone test results, and (2) make TTCI predictions for different dog-bone specimen configurations.

Two suggested ways to determine the effective  $K_t$  and TTCI relationship are: (1) simply plot the results of the strain life analysis (i.e., effective  $K_t$  versus TTCI) and determine the desired relationship graphically and (2) use a suitable empirical relationship and determine the constants using the strain life analysis results (e.g., Table F-1).

The simple power law relationship for effective  $K_t$ , given in Eq. F-1, worked very well for the three load spectra considered under this program. In Eq. F-1, A and B are empirical constants.

$$\text{Effective } K_t = A(TTCI)^B \quad (F-1)$$

Strain life predictions for assumed effective stress concentrations (e.g., Table F-1) can be used to evaluate the constants A and B in Eq. F-1.

Equation F-1 was transformed into a linear least square fit form by taking the log of both sides of the equation. The constants A and B in Eq. F-1 were determined for both dry air and 3.5% NaCl environments and for three load spectra using a least squares fit procedure. A and B values were determined using the strain life analysis results based on the average and extreme (i.e., upper and lower bounds) strain life allowables (Ref. Appendix A). The resulting A and B constants in Eq. F-1 are summarized in Table F-4 through F-6 for load spectra "A", "B" and "C", respectively. Effective  $K_t$  versus TTCI ( $a_0 = 0.01"$ ) predictions from Table F-1 are plotted in a ln-ln format in Fig. F-1 and F-2 for dry air and 3.5% NaCl environments, respectively. Similar plots were

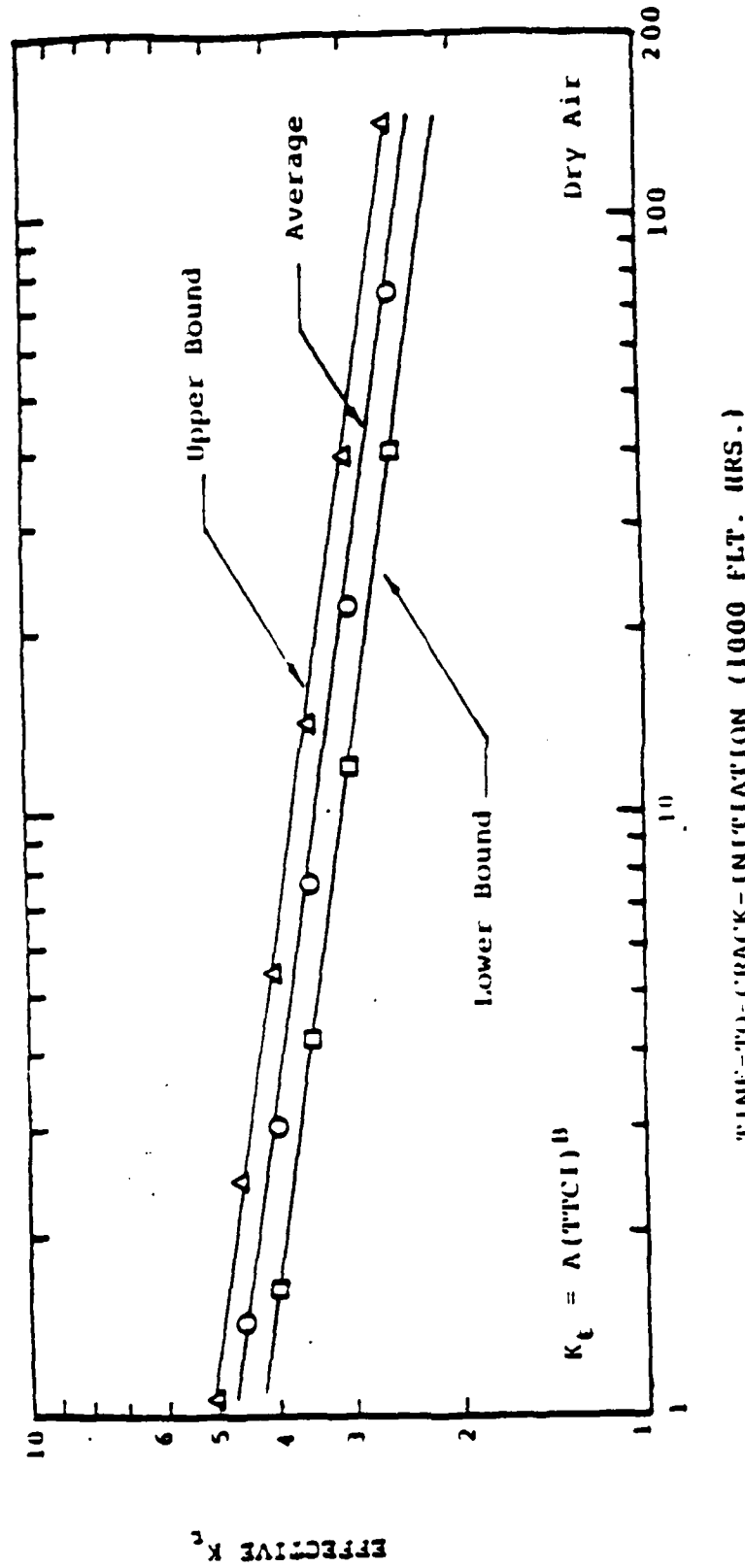


Fig. F-1 Effective  $K_t$  Versus TTCT ( $a_1=0.01"$ ) for 7075-T7651 Aluminum Based on: Strain-Life Analysis, F-16 400 Hour Spectrum,  $\sigma_{Gross} = 28$  ksi (Max.), and Dry Air Environment

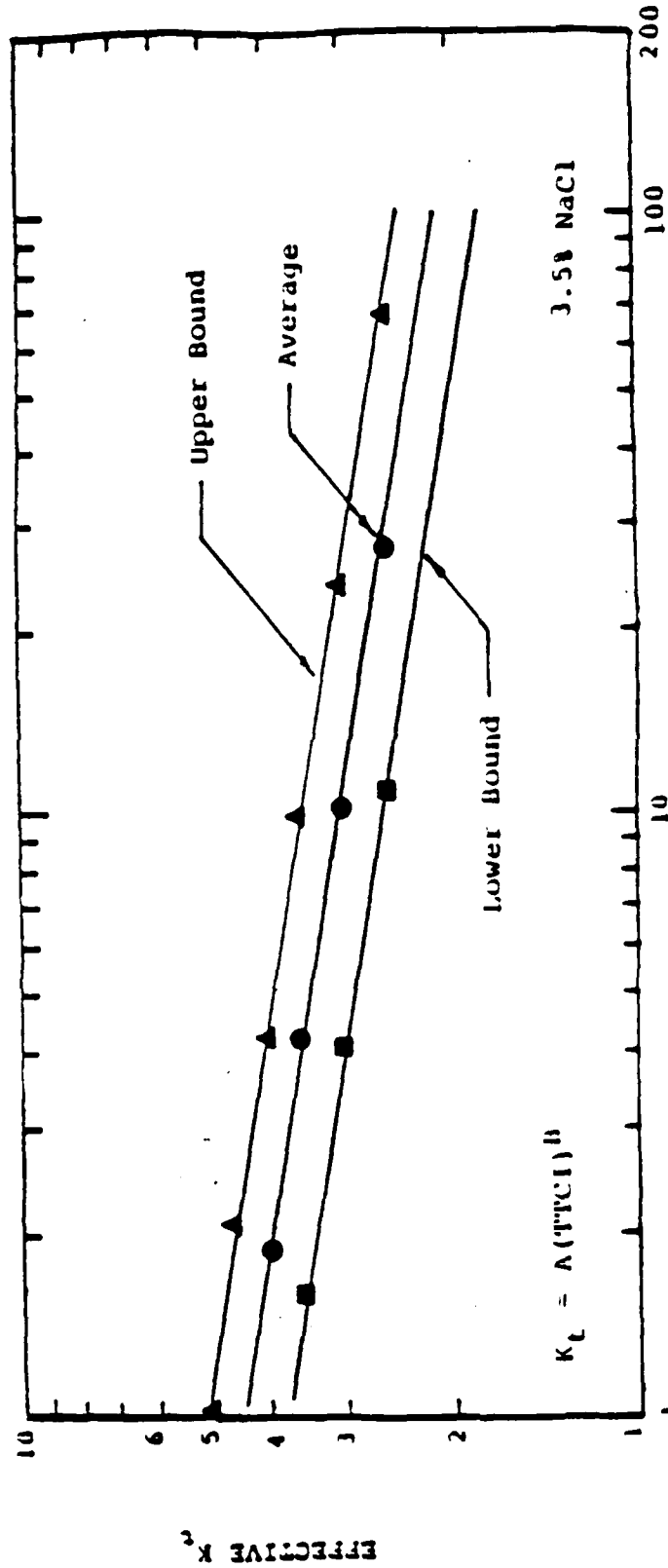


Fig. F-2 Effective  $K_t$  Versus TTCl ( $a_i=0.01"$ ) for 7075-T7651 Aluminum Based on: Strain-Life Analysis, F-16 400 Hour Spectrum,  $\sigma_{G,ross} = 28$  ksi (Max.), and 3.58 NaCl Environment

made for load spectra "B" and "C". In all cases, an excellent fit was obtained using Eq. F-1. The results shown in Tables F-4 through F-6 were used to "tune" or scale the strain life analysis using actual dog-bone specimen spectrum fatigue test results from Volume IV [24].

#### F.4 STRAIN LIFE ANALYSIS SCALING

The strain life analysis needs to be scaled or tuned to dog-bone specimen test results (for a baseline joint configuration, e.g., open hole case) for a baseline load spectrum ("A") and environment (e.g., dry air). This step is essential before TTCI predictions can be made for a different set of conditions (e.g., stress level, load spectra, & bolt load transfer). The baseline scaling factor for the open hole case is denoted as  $\bar{K}_t(0)$ .

A method is illustrated in this section for scaling the strain life analysis results for a given load spectra. Also, it will be shown that the scaling factor  $\bar{K}_t(0)$ , is independent of the load spectra and environment.

Scaling factors can be determined using the applicable effective  $K_t$  versus TTCI relationship (Tables F-4 through F-6) and the TTCI test results (i.e., average, low and high) for selected dog-bone specimen data sets (Tables F-7 through F-9). For comparison purposes, test results for the same loading frequently will be used.

The low, average and high TTCI ( $a_0 = 0.01"$ ) test results for selected data sets are summarized in Table F-10 for three load spectra. These values were obtained from Tables F-7 through F-9. The baseline scaling factor,  $\bar{K}_t(0)$ , for each data set is obtained by substituting the applicable TTCI test results (i.e., low, average or high) in Eq. F-1 and using the applicable A and B constants from Tables F-4 through F-6. For example, the scaling factor for the A-28/F/D (open hole, spectrum "A", fast freq., dry) data set, based on the average TTCI result of 13,200 flight hours, is  $SF = 4.842(13.2)^{-0.159} = 3.21$ . The constants  $A = 4.842$  and  $B = -0.159$  were obtained from Table F-4. The resulting scaling factors for various experimental data sets are summarized in Table F-10 for the dry air and 3.5% NaCl environments for three load spectra.

The following observations are based on the results summarized in Table F-10:

1. Environment does not have a significant effect on

Table 7 Summary of TTCI Results ( $a_i=0.01''$ ) for 7075-T7651 Aluminum Dog-Bone Specimens Tested Using the F-16 400 Hour Spectrum

SPECIMEN CONFIGURATION	TEST I.D.	DATA SET NO.	SPECIMEN NO.	(a) TTCI (FLT. HRS.)	AVE. TTCI (FLT. HRS.)	
					PER DATA SET	PER DATA SET (S)
OPEN HOLE	A-28/F/D	1	45	14000	13200	14565
			46	6600		
			79	10600		
			89	21600		
	A-28/S/D	2	72	3471	15930	
			83	25200		
			87	16800		
			92	13249		
	A-28/F/W	3	62	5872	3243	3548
			76	3000		
			77	16400		
			82	6700		
	A-28/S/W	4	67	7351 (b)	3291	
			71	1600		
			81	3434		
			88	12554 (b)		
			90	15226 (b)		
	A-28/s/W	5	91	9400	8134	
			84	3063 (b)		
			85	8160 (b)		
			86	9178 (b)		
BOLT-IN-HOLE	A-28/F/D/B	10	126	23600	24667	24667
			127	14800		
			128	15600		
	A-28/F/W/B	11	122	3200	3611	3684
			123	13868		
			124	11600		
	A-28/S/W/B	12	125	5777	3329	
			131	3359 (a)		
20% CT	A-28/20/F/D	15	132	3300 (b)	12476	12476
			74	3800		
			75	10203		
	A-28/20/S/D	17	80	16800	3954	3309
			73	4100		
	A-28/20/F/W	16	66	3400	2664	
			68	4508		
40% CT	A-28/40/F/D	18	69	1662	16651	16651
			70	1665		
			506	11736		
	A-28/40/F/W	20	507	16000	5006	5006
			508	22218		
			509	6048		
			510	5149		
			511	6821		

NOTES: (a) Ref. NADC-83126-60-Vol. IV;  $a_i = 0.01''$ (b) Extrapolated results to  $a_i = 0.01''$

Table 8 SUMMARY OF TTCI RESULTS ( $a_1=0.01''$ ) FOR 7075-T7651 ALUMINUM  
DOC-BONE SPECIMENS TESTED USING THE F-18 300 HOUR (RANDOM)  
SPECTRUM ("B")

SPECIMEN CONFIGURATION	TEST I.D.	DATA SET NO.	SPECIMEN NO.	(a) TTCI (FLT. HRS.)	AVE TTCI (FLT. HRS.)	
					PER DATA SET	PER DATA SET(S)
OPEN HOLE	B-28/F/D	21	315	15752(b)	16395	18492
			316	22608(b)		
			317	10824(b)		
	B-28/S/D	22	326	20143	20589	
			327	21824		
			328	19800		
	B-28/F/W	23	300	13002(b)	11917	10226
			301	9077		
			302	8267		
	B-28/S/W	24	303	17323(b)	8536	
			318	12038		
			319	6517		
20X LT	B-28/20/F/D	30	320	8447	10302	10302
			321	7140		
			308	7228		
	B-28/20/F/W	29	309	8100	8041	8041
			310	17115		
			311	8/66		
	B-28/40/F/D	31	312	6343	13050	13050
			313	11311(b)		
			314	6712		
	B-28/40/F/W	32	315	7799(b)	6659	6659
			500	12900		
			501	14550		
40X LT	B-28/40/F/W	32	502	11700		
			503	6633		
			504	8218		
			505	5127		

NOTES: (a) Ref. NADC-38126-60-Vol. IV;  $a_1 = 0.01''$

(b) Extrapolated results to  $a_1 = 0.01''$

Table 9 SUMMARY OF TTCI RESULTS ( $a_1 = 0.01''$ ) FOR 7075-T7651 ALUMINUM  
DOG-BONE SPECIMENS TESTED USING THE F-18 300 HOUR (BLOCK)  
SPECTRUM ("C")

SPECIMEN CONFIGURATION	TEST I. D.	DATA SET NO.	SPECIMEN NO.	TTCI (FLT. HRS.)	AVE. TTCI (FLT. HRS.) PER DATA SET
OPEN HOLE	C-28/F/D	33	515	27709	26333
			516	10789	
			517	40500(b)	
	C-28/F/W	34	518	15300	10300
			519	4500	
	C-28/F/W(c)	36	520	11100	
524			6900	6750	
525			6600		
40X I.T	C-28/40/F/D	35	526(d)	--(d) --	
			521	9591(b)	15689
			522	16200	
			523	21278	

## NOTES:

- (a) Ref. NADC-83126-60-Vol. IV;  $a_1 = 0.01''$   
 (b) Extrapolated results to  $a_1 = 0.01''$   
 (c) Hole diameter = 0.500" (Nominal)  
 (d) Manufacturing anomaly in fastener hole (i.e., 0.014" deep corner scratch).

Table 10 Summary of Scaling Factors for Scaling  
Strain Life Predictions to Dog-Bone  
Specimen Test Results for 7075-T7651 Aluminum

SPECIMEN CONFIGURATION	SPECTRUM	TEST I.D.	(1000 FLT HRS) TTCI ( $a_0 = 0.01"$ )			$\bar{K}_t(0)$ SCALING FACTOR		
			LOW	AVE	HIGH	LOW	AVE	HIGH
OPEN HOLE	"A" ↓	A-28/F/D	6.6	13.2	21.6	3.26	3.21	3.26
		A-28/F/W	5.872	9.243	16.4	2.77	3.02	3.18
BOLT-IN-HOLE		A-28/F/D/B	14.8	24.667	35.6	2.86	2.91	3.01
		A-28/F/W/B	3.2	8.611	13.868	3.09	3.06	3.27
20% LT		A-28/20/F/D	8.8	12.476	16.8	3.11	3.24	3.39
	"A" ↓	A-28/20/F/W	3.4	3.954	4.508	3.06	3.51	3.97
40% LT		A-28/40/F/D	11.736	16.651	22.218	2.97	3.09	3.24
		A-28/40/F/W	5.149	6.006	6.821	2.84	3.26	3.69
OPEN HOLE		B-28/F/D	10.824	16.395	22.608	2.97	3.05	3.16
		B-28/F/W	8.267	11.917	17.323	2.76	2.99	3.21
20% LT	"B" ↓	B-28/20/F/D	7.228	10.302	17.115	3.15	3.25	3.28
		B-28/20/F/W	6.343	8.041	11.311	2.88	3.18	3.42
40% LT		B-28/40/F/D	11.700	13.050	14.550	2.94	3.14	3.35
		B-28/40/F/W	5.127	6.659	8.218	2.97	3.28	3.59
OPEN HOLE		C-28/F/D	10.789	26.333	40.500	2.98	2.86	2.94
	"C" ↓	C-28/F/W	4.5	10.300	15.3	2.99	3.02	3.28
40% LT		C-28/40/F/D	9.591	15.689	21.278	3.04	3.09	3.23

the scaling factor,  $\bar{K}_t(0)$  for the aluminum alloy considered (7075-T7651). For example, compare the scaling factors based on the average TTCI results for the dry air (D) and 3.5% NaCl (W) environments. There is no significant difference in the  $\bar{K}_t(0)$  values for the three load spectra considered.

2. Since the scaling factor is independent of the environment (dry air and 3.5% NaCl), this supports the conclusion that there is no significant synergistic effect of the environment on crack initiation for this alloy (i.e., 7075-T7651 aluminum).

#### F.5 EFFECTIVE $\bar{K}_t$ (LT) FOR BOLT LOAD TRANSFER

To account for the effects of bolt load transfer in the strain life analysis predictions for TTCI, the baseline effective stress concentration factor  $\bar{K}_t(0)$ , is scaled up. This scaled up  $\bar{K}_t(0)$  value denoted by  $\bar{K}_t(LT)$ , can be estimated using Eq. 11 in subsection 5.3.5. Procedures are illustrated in this section for determining: (1)  $K_\sigma(0)$  and  $K_\sigma(LT)$  in Eq. 11 and (2)  $\bar{K}_t(LT)$  for 20% and 40% load transfer cases.

$K_{\sigma}(0)$  and  $K_{\sigma}(LT)$  values were "estimated" for four specimen configurations (i.e., open hole, 20% LT, 40% LT and 100% LT). Detailed procedures are given in subsection 5.3.5. The results are based on  $W = 2.00"$ ,  $d = 0.4375"$ ,  $\sigma_I = 28$  ksi (same baseline stress used in Phase II test program), 7075-T7651 aluminum and  $LT = 0, 0.2, 0.4$  and  $1.0$ . The following values for  $n'$  and  $K$  were used in Eq. F-13:  $n' = 0.103$  and  $K = 104.9$  (Ref. Appendix A).  $K_{\sigma}(LT)$  values obtained and the resulting  $K_{\sigma}(LT)/K_{\sigma}(0)$  ratios are summarized in Table F-11. The  $K_{\sigma}(LT)/K_{\sigma}(0)$  ratios were used in Table 12 to compute the  $K_t(LT)$  values needed to make TTCI predictions for various dog-bone specimen configurations.

Scaling factors,  $\bar{K}_t(LT)$ , are presented in this section for calibrating the strain life analysis for particular dog-bone specimen configurations (i.e., open hole,  $LT = 0.2, 0.4$  and  $1.0$ ). The results herein were used to make TTCI predictions for selected dog-bone specimen geometries and 3 bolt load transfers (see subsection 5.7.2). The scaling factors account for the effects of bolt load transfer in the strain life analysis. The objective is to determine the scaling factor for a given baseline spectrum for the open hole case - then modify the scaling factor to account for the effects of bolt load transfer.

Scaling factors for  $\bar{K}_t(LT)$  are summarized in Table F-12

Table F-11 Summary of  $K\sigma$  (LT) Values for 7075-T7651 Aluminum  
( $W = 2.00"$ ,  $d = 0.4375"$ )

SPECIMEN CONFIGURATION	$\sigma_I$ (KSI)	$\sigma_{NeL}$ (KSI)	LT	$K_T$ (1)	$\sigma_{MAX}$ (KSI) (2)	$K\sigma$ (LT) (3)	$\frac{K\sigma (LT)}{K\sigma (0)}$
OPEN HOLE	28	35.8	0	2.46	88.1	1.614	1.000
20% LT	→	→	0.2	2.93	104.9	1.676	1.038
40% LT			0.4	3.39	121.4	1.721	1.066
100% LT			1.0	4.79	171.5	1.829	1.133

NOTES: (1) Ref. Eq. F-9

(2) Ref. Eq. F-10

(3) Ref. procedure described in subsection 5.3.5.2 for  $\sigma_{max}$   
yield stress of material

Table F-12 Summary of  $\bar{K}_t$  (LT) Scaling Factors for Strain Life Analysis Predictions for TTCI

SPECIMEN CONFIGURATION	BASILINE SPECTRUM	$\frac{K_{\sigma} (LT)}{K_{\sigma} (0)}$	$\bar{K}_t (LT) = \bar{K}_t (0) * \frac{K_{\sigma} (LT)}{K_{\sigma} (0)}$
OPEN HOLE	"A"	1.000	3.12
20% LT	↓	1.038	3.24
40% LT	↓	1.066	3.32
100% LT	↓	1.133	3.53
OPEN HOLE	"B"	1.000	3.02
20% LT	↓	1.038	3.13
40% LT	↓	1.066	3.22
100% LT	↓	1.133	3.42
OPEN HOLE	"C"	1.000	2.94
20% LT	↓	1.038	3.05
40% LT	↓	1.066	3.13
100% LT	↓	1.133	3.33

Note:  $\bar{K}_t$  (LT) values are shown for load spectra "A," "B" and "C." In most cases results for determining  $\bar{K}_t (0)$  will be available for only the baseline environment (e.g., dry air), geometry and load spectrum.  $\bar{K}_t$  (LT) values are shown here for all three spectra because we want to show that reasonable TTCI predictions for one load spectrum can be made using the baseline  $\bar{K}_t (0)$  value based on another load spectrum.

Table H-1 Load Summary for the F-16  
400 Hour Spectrum "A"

<u>MAX LOAD %</u>	<u>MIN LOAD %</u>	<u>No. of Load Points/8000 Flight Hours</u>
-35.00	-30.10	60
-30.00	-25.10	0
-25.00	-20.10	60
-20.00	-15.10	80
-15.00	-10.10	200
-10.00	-5.10	440
-5.00	-0.10	3684
0.00	0.00	10187
5.00	0.10	2880
10.00	5.10	59360
15.00	10.10	312566
20.00	15.10	920
25.00	20.10	3780
30.00	25.10	81300
35.00	30.10	100222
40.00	35.10	39024
45.00	40.10	66050
50.00	45.10	16526
55.00	50.10	35585
60.00	55.10	18770
65.00	60.10	1700
70.00	65.10	8980
75.00	70.10	1950
80.00	75.10	551
85.00	80.10	640
90.00	85.10	0
95.00	90.10	208
100.00	95.10	24

## APPENDIX H

## LOAD SPECTRA DESCRIPTIONS AND COMPARISONS

Three load spectra were used to test 7075-T7651 aluminum dog-bone specimens in Phase II: (1) F-16 400 hour (hi-lo block), (2) F-18 300 hour (random), and (3) F-18 300 hour (hi-lo block). These load spectra, referred to as spectrum "A", "B" and "C", respectively, were also used to perform corrosion fatigue analysis predictions for TCI ( $a_i = 0.01$ ") and TFCG. The purpose of this section is to describe the three load spectra used for this program.

The F-16 400 hour (hi-lo block) spectrum "A", a wing-root bending spectrum, has been used extensively at the General Dynamics, Fort Worth Division, for F-16 preliminary development tests and other structural research programs [25,26]. Maximum and minimum percent loads versus number of load points per 3000 flight hours are summarized in Table H-1 for this spectrum.

An F-18 300 hour spectrum, a modified wing spectrum, was provided by the Naval Air Development Center (Warminster, PA) for this program. Maximum and minimum percent loads versus number of load cycles per 300 flight hours are shown in Table H-2 for this spectrum (referred to as "NADC"). The maximum compressive load in this spectrum was limited to the same percentage of the maximum tension load as that for spectrum

(This page intentionally left blank.)

Table G-3 "Typical Output for "RXN" Computer Run  
(Continued)

***** ** FORMATTING - 1) DADN EQ VARIABLES *** *****											
DM	MAX	C	PARA.	N	PARA.	KC	MOD.	PARA.	Q	PARA.	
100.00000	.4722E-04	2.91300	62.50000	.60000	.00000						
A	C	DELTA	TOTAL	BLK	SPEC	DELTA	DELTA	RETARD	SIGMAX	BETA	TOTAL
(INCH)	(INCH)	(INCH)	PASS	HOURS	MAX	K	A	FACTOR	RATIO	A	C
.01116	.01116	.500	1	300	1	20.00000	.4316E-04	1.00	.20	28.00	.000
.01225	.01225	.500	2	600	1	20.00000	.4913E-04	1.00	.20	28.00	.000
.01350	.01350	.500	3	900	1	20.00000	.5644E-04	1.00	.20	28.00	.000
.01493	.01493	.500	4	1200	1	20.00000	.6533E-04	1.00	.20	28.00	.000
.01598	.01598	.500	5	1500	1	20.00000	.7572E-04	1.00	.20	28.00	.000
.01658	.01658	.500	6	1800	1	20.00000	.8822E-04	1.00	.20	28.00	.000
.01851	.01851	.500	7	2100	1	20.00000	.1033E-03	1.00	.20	28.00	.000
.02077	.02077	.500	8	2400	1	20.00000	.1215E-03	1.00	.20	28.00	.000
.02342	.02342	.500	9	2700	1	20.00000	.1436E-03	1.00	.20	28.00	.000
.02658	.02658	.500	10	3000	1	20.00000	.1703E-03	1.00	.20	28.00	.000
.03034	.03034	.500	11	3300	1	20.00000	.2024E-03	1.00	.20	28.00	.000
.03485	.03485	.500	12	3600	1	20.00000	.2403E-03	1.00	.20	28.00	.000
.04027	.04027	.500	13	3900	1	20.00000	.2840E-03	1.00	.20	28.00	.000
.04679	.04679	.500	14	4200	1	20.00000	.3384E-03	1.00	.20	28.00	.000
.05459	.05459	.500	15	4500	1	20.00000	.4007E-03	1.00	.20	28.00	.000
.06425	.06425	.500	16	4800	1	20.00000	.4800E-03	1.00	.20	28.00	.000
.07613	.07613	.500	17	5100	1	20.00000	.5732E-03	1.00	.20	28.00	.000
.09055	.09055	.500	18	5400	1	20.00000	.6832E-03	1.00	.20	28.00	.000
.10740	.10740	.500	19	5700	1	20.00000	.8111E-03	1.00	.20	28.00	.000
.12737	.12737	.500	20	6000	1	20.00000	.9621E-03	1.00	.20	28.00	.000
.15010	.15010	.500	21	6300	1	20.00000	.1193E-02	1.00	.20	28.00	.000
.17617	.17617	.500	22	6600	1	20.00000	.1469E-02	1.00	.20	28.00	.000
.20665	.20665	.500	23	6900	1	20.00000	.1809E-02	1.00	.20	28.00	.000
.24609	.24609	.500	24	7200	1	20.00000	.2246E-02	1.00	.20	28.00	.000
.29136	.29136	.500	24	7200	1	20.00000	.2746E-02	1.00	.20	28.00	.000
.30180	.30180	.500	24	7200	1	20.00000	.3301E-02	1.00	.20	28.00	.000

\*\*\*\*\* CRACK DEPTH EXCEEDED PLATE THICKNESS TRANSITION ALLOWED RECYCLING FOR THRU CRACK \*\*\*\*\*

Table G-3 Typical Output for "RXN" Computer Run

```

*** CRACK GROWTH PROGRAM ***
*** VERSION 2.0 RELEASED 5/84 ***
*** *****

PROBLEM TITLE : F-18 300 HW FIGHTER SPECTRUM, GROSS STRESS -20.0 KSI
MATERIAL TITLE : 7075-T7651 ALUMINUM 1/2 INCH PLATE STOCK
SPECTRUM TITLE : NO LOAD TRANSFER, DRY AIR, KTM-1.5, OVERLOAD-2.65

*****
** MATERIAL PARAMETER **
*****
MATERIAL YIELD STRENGTH : 67.00000 THICKNESS : .30000
MAXIMUM DADN : .10000 PLATE HALF WIDTH : 1.00000
PLASTIC ZONE CONDITION : PLANE STRESS HOLE RADIUS : .21000
STRESS INTENSITY THRESHOLD (KTM) : 1.50000 BEARING-TO-TENSION RATIO : .00000
STRESS INTENSITY CRITICAL (KTSURC) : 35.00000 ANALYSIS BETA ANGLE SURFACE : 90.00000
NUMBER OF DADN EQUATIONS : 1 ANALYSIS BETA ANGLE DEPTH : 25.00000
COMPRESSIVE CYCLE RATIO CUTOFF : .00000

*****
** CRACK GEOMETRY **
*****
INITIAL CRACK LENGTH (DEPTH) : .01000 SURFACE CORRECTION FACTOR : 1.00000
INITIAL CRACK LENGTH (SURFACE) : .01000 DEPTH CORRECTION FACTOR : 1.00000
MAXIMUM CRACK LENGTH : .50000 COMPRESSIVE LOADS WERE : DELETED
CONSTANT FRONT FACE CORR. (INF-DEPTH) : 1.03000 SPECTRUM INPUT ON : CARDS
CRACK TRANSITION ALLOWED : YES LOAD INPUT SPECTRUM PRINTED : YES
CRACK ASPECT RATIO (A/2C) IS : CONSTANT STRESS INTENSITY TABLES PRINTED : YES
NUMBER OF CRACKS IN SPECIMEN : 1 DESIGN LIMIT STRESS : 20.00000
MAXIMUM VALUE OF A/2C : 10.00000 CODE FOR INPUT SIF FILES : 0

*****
** ANALYSIS FACTORS **
*****

*****
** SPECTRUM MULTIPLIERS **
*****
STRESS MULTIPLIER : 280.00000 PRINT OUT INTERVAL (NO. OF FLIGHTS) : 1
CYCLE MULTIPLIER : 1.00000 PRINTOUT END OF BLOCK : YES
CRACK GROWTH LAW : FORMAN(+-) FLIGHT/PASS NUMBER TERMINATOR : 60
RETARDATION MODEL : MODIF. WILLEN. SLOW CRACK GROWTH CHK PASS NUMBER : 60
WHEELER EXPONENT : .00000 SLOW CRACK GROWTH CHK DELTA A : .00100
MODIF. WILLENBORG OVERLOAD RATIO : 2.65000 FLIGHT HOURS/FLIGHTS (FOR PLOT) : 300.00000

```

TABLE G-2 DESCRIPTION OF STANDARD STRESS INTENSITY FACTORS

SUBBT Number	Description
1	Constant Front Face Correction (Input Value)
2	Front Face Correction - Kobayashi's Equation
3	Back Face Correction - Newman's Equation
4	Newman's Combined Front and Back Face Correction - Tension
5	Newman's Combined Front and Back Face Correction - Bending
6	Part-Thru Flaw Finite Width Correction
7	Thru-Thickness Flaw Finite Width Correction
8	Part-Thru Flaw Emanating From A Fastener Hole - Tension
9	Part-Thru Flaw Angular Correction
10	Back Face Correction For Crack At A Hole
11	Part-Thru Flaw Emanating From A Fastener Hole- Bearing
12	Correction for Double Part Thru Crack At A Hole
13	Thru-Thickness Flaw At A Hole - Tension
14	Thru-Thickness Flaw At A Hole- Bearing
15	Corner Crack Correction - LIU's EQ
16	Constant Multiplier (Input Variables) To Surface Or Depth
17	GKT - Exponential Correction
18-20	Input Tabular Correction
21	Edge Crack Correction (Tada)
22	Newman Finite Width - Part Through Flaw At A Hole

TABLE G-1 DESCRIPTION OF STANDARD GEOMETRY TYPES

ICASE Number	Specific Factors Combined - Table G-2	General Structural Arrangement Description
1	1,3,6	Part-Thru Surface Flaw (Constant Front Face Correction)
2	2,3,6	Part-Thru Surface Flaw (Equation Front Face Correction)
3	4,6	Part-Thru Surface Flaw (Newman-Tension)
4	5,6	Part-Thru Surface Flaw (Newman-Bending)
5	7	Thru Thickness Surface Flaw
6	1,8,9,10,12,22	Corner Flaw At A Hole (Tension)
7	1,9,10,11,12,22	Corner Flaw At A Hole (Bearing)
8	1,8,9,10,11,12,22	Corner Flaw At A Hole (Tension + Bearing)
9	7,13	Thru Thickness Flaw At A Hole (Tension)
10	7,14	Thru Thickness Flaw At A Hole (Bearing)
11	7,13,14	Thru Thickness Flaw At A Hole (Tension + Bearing)
12	6,15	Corner Flaw At An Edge
13	21	Thru-Thickness Flaw At An Edge
14	Combination of Any Input Values	Input Case (Part-Thru Flaw) (Does Not Transition)
15	Combination of Any Input Values	Input Case (Thru-Thickness Flaw)

Standard crack geometry types and stress intensity factors available are shown in Tables G-1 and G-2, respectively. The program accounts for the transition of a part-through crack to a through-the-thickness crack.

A superposition method [92,93] is used to determine the stress intensity factor for through-tension stress and for bolt hole bearing stress combinations for both part-through and through-the-thickness cracks in a fastener hole. Refer to subsection 5.4.6, Eq. 14 and Fig. 19 herein for further details.

Either a magnetic tape or cards can be used to input the load spectrum. Example output from the RXN crack growth computer program is shown in Table G-3. Refer to Ref. 67 for further details.

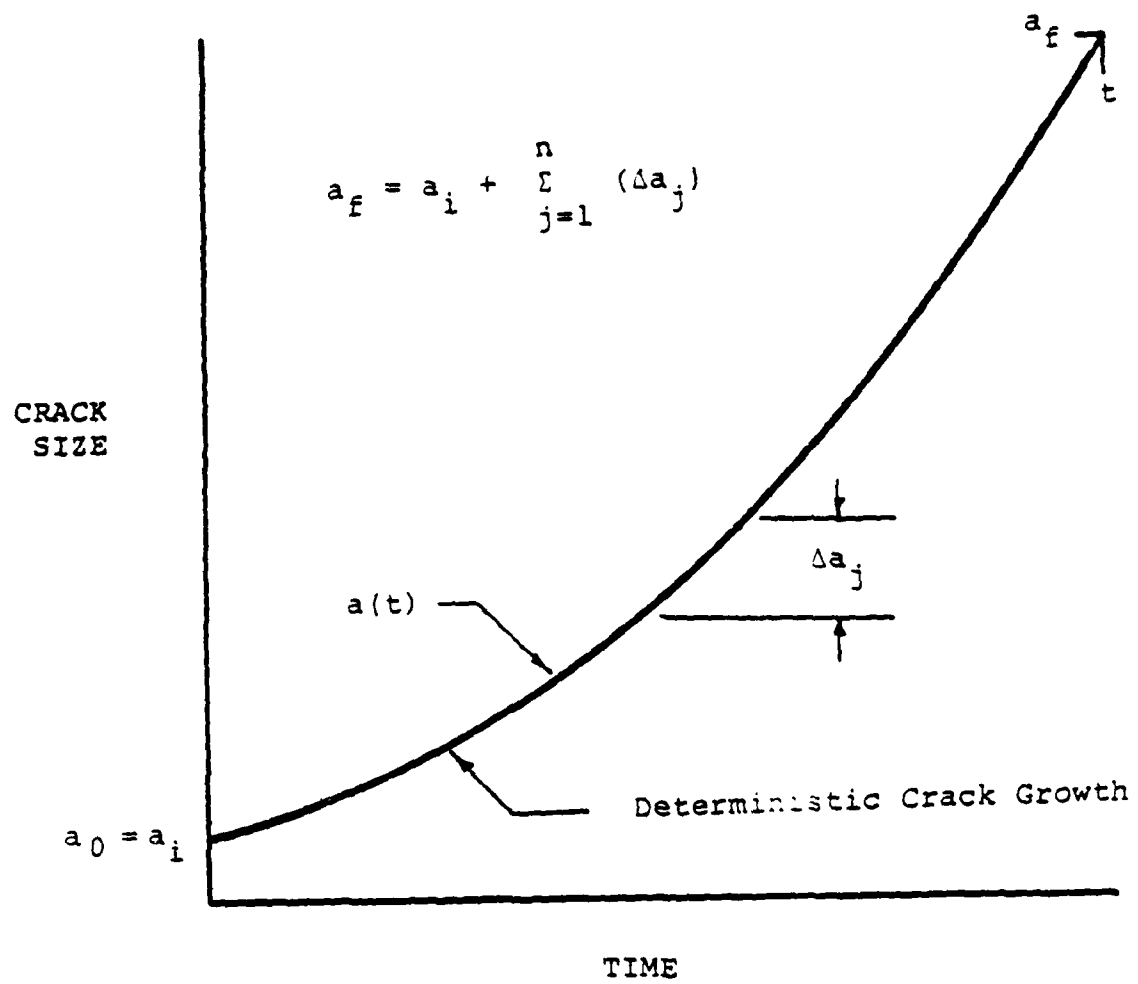


Fig. G-1 Deterministic Crack Growth Concept

## APPENDIX G

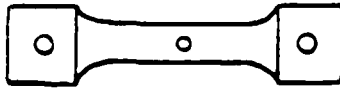
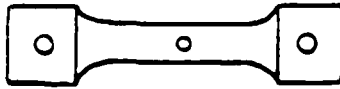
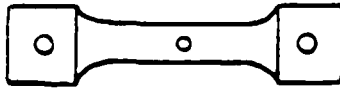
## DESCRIPTION OF ANALYTICAL CRACK GROWTH

## COMPUTER PROGRAM RXN

A general purpose analytical crack growth program, developed by General Dynamics, was used to make corrosion fatigue crack growth predictions for mechanically-fastened joints under this program (Ref. Subsection 5.7.3). This state-of-the-art crack growth computer program (RXN) has been used extensively at the General Dynamics/Fort Worth Division for durability and damage tolerance analyses [e.g. 64, 65]. A brief description of the RXN computer program and capabilities are given in this appendix and details are documented elsewhere [67].

RXN is a deterministic crack growth (Fig. G-1) program with several capabilities and user options. For example, the user has four retardation procedure options: (1) zero-retardation, (2) Wheeler retardation, (3) Modified Willenborg retardation and (4) Rockwell retardation (acceleration). The following options for computing the crack growth rate are available: (1) Paris, (2) Forman, (3) Modified Forman, (4) Walker- $K_{max}$ , (5) Interpolation of tabular input, (6) Walker- $\Delta K$  and (7) Rockwell-Chang.

Table F-13 Summary of Results for (Ave. Ni)<sub>Dry</sub> / (Ave. Ni)<sub>Wet</sub>  
Ratios for 7075-T7651 Aluminum

ENVIRONMENT	SPECIMEN TYPE	NO.	$\Delta\sigma$ (KSI)	$N_i$ NO. OF CYCLES TO INITIATION ( $a_o = 0.01"$ )	AVE $N_i$	FREQUENCY (Hz)	$\frac{(\text{AVE } N_i)_{\text{Dry}}}{(\text{AVE } N_i)_{\text{Wet}}}$
DRY AIR		A108	17	105000	103333	6	$\frac{1.28}{2.48} \rightarrow$
		A116	17	102000			
		A117	17	103000			
3.5% NaCl		A131	16.5	85000	81000		
		A132	16.5	83500			
		A133	16.5	74500			
DRY AIR		A105	20	57000	49833		
		A114	20	46000			
		A115	20	46500			
3.5% NaCl		A111	20	17500	20125		
		A112	20	23500			
		A113	20	16500			
		A124	20	23000			
DRY AIR		A1107	22.5	42000	42000		$\frac{2.33}{1.85} \rightarrow$
3.5% NaCl		A125	22.5	18000	18000		
DRY AIR		A102	25	25000	25000		
3.5% NaCl		A127	25	13500	13500		
DRY AIR		A101	18	120000	120000		
3.5% NaCl		A121	18	37000	37000		
DRY AIR		400	17	39000	44000		
		402	17	48000			
		403	17	35000			
3.5% NaCl		404	17	41000	34000		
		405	17	41000			
		406	17	20000			
DRY AIR		407	17	41000	33000		$\frac{1.29}{2.30} \rightarrow$
		408	17	25000			
3.5% NaCl		410	17	12000	14333		
		412	17	18000			
		413	17	13000			

Average ESF

$N = 7$   
 $\bar{X} = 2.11$   
 $(X) = 0.701$   
 C.O.V. = 33.2%

a fastener hole in a dry air and 3.5% NaCl environment, respectively.

Environmental scaling factors for comparable data sets are summarized in Table F-13. An average ESF of 2.11 was obtained for all the data sets combined in Table F-13 and the C.O.V. was 33.2%. The 95% confidence interval for the mean ESF ranged from 1.46 to 2.76. This is very interesting, because an average ESF of 2.08 and 95% confidence interval for the mean ESF ranged from 1.38 to 2.78 based on spectrum fatigue test results (see subsection 5.7.2.2).

air).

The basic objective of this section is to determine the average ESF and to estimate the 95% confidence interval using constant amplitude fatigue data. How does the resulting ESF based on CF crack initiation results compare with the ESF based on spectrum fatigue crack initiation and crack propagation results? The ESF determined herein was used to make TCI predictions for a 3.5% NaCl environment based on the predictions for a dry air environment (see subsection 5.7.2, case IV).

Considerable data have been acquired under this program for determining the effects of a 3.5% NaCl environment on crack initiation in fastener holes for 7075-T7651 aluminum (e.g., Ref. Vol. I and Vol. IV). Selected constant amplitude test results for dog-bone specimens with a center open hole for both dry air and 3.5% NaCl environments were used to determine the ESFs. The environmental scaling factors were determined using test results from Volumes I and IV for the same loading frequency and comparable stress levels. The environmental scaling factors were based on Eq. F-2,

$$ESF = \frac{(\text{Ave. } N_i)_{\text{dry}}}{(\text{Ave. } N_i)_{\text{wet}}} \quad (F-2)$$

where:  $(\text{Average } N_i)_{\text{dry}}$  and  $(\text{Average } N_i)_{\text{wet}}$  is the average number of cycles (or reversals) to initiate a 0.01" crack in

for three load spectra. These factors are based on the average scaling factor for the dry and 3.5% NaCl environments shown in Table F-10, the  $K_{\sigma}(LT)/K_{\sigma}(0)$  ratios of Table F-11 and Eq. 11. For example, the  $\bar{K}_t(LT)$  values in Table F-12 for baseline spectrum "A" were determined as follows. The average  $\bar{K}_t(0)$  for the open hole case, based on A-28/F/D (dry) and A-28/F/W (3.5% NaCl) data sets, is  $(3.21 + 3.02)/2 = 3.12$  (see Table F-12, top value in last column). Then, the  $\bar{K}_t(LT)$  values for the other bolt load transfer cases were determined using Eq. 11 as follows: (1) 20% LT;  $\bar{K}_t(LT = 0.2) = 3.12 \times 1.038 = 3.24$ , (2) 40% LT;  $\bar{K}_t(LT = 0.4) = 3.12 \times 1.066 = 3.32$  and (3) 100% LT;  $\bar{K}_t(LT = 1.0) = 3.12 \times 1.133 = 3.53$ .  $\bar{K}_t(LT)$  values for load spectra "B" and "C" were determined in a similar manner.

#### F.6 EVALUATION OF ENVIRONMENTAL SCALING FACTORS FOR CRACK INITIATION

Environmental scaling factors (ESF) based on constant amplitude fatigue test results from Volume I [22] are presented in this section. The ESFs are based on CF crack initiation results for 7075-T7651 Aluminum fatigue tests and two environments (i.e., dry air and 3.5% NaCl). If there is no significant synergistic effect between the mechanical-loading and environment, then it will be feasible to estimate the TICI for a wet environment (e.g., 3.5% NaCl) based on the TICI prediction for a baseline environment (dry

Table H-2 Load Summary for the NADC F-18  
Spectrum ("NADC")

<u>MAX LOAD %</u>	<u>MIN LOAD %</u>	<u>NO. CYCLE</u>
100.00	0.00	3
100.00	20.00	3
100.00	30.00	1
90.00	-20.00	1
90.00	0.00	10
90.00	10.00	1
90.00	20.00	7
90.00	30.00	1
80.00	-30.00	1
80.00	-10.00	4
80.00	0.00	15
80.00	10.00	16
80.00	20.00	20
80.00	30.00	5
70.00	-20.00	1
70.00	-10.00	4
70.00	0.00	51
70.00	10.00	43
70.00	20.00	46
70.00	30.00	17
70.00	40.00	1
60.00	-20.00	6
60.00	-10.00	20
60.00	0.00	139
60.00	10.00	127
60.00	20.00	91
60.00	30.00	6
50.00	-30.00	1
50.00	-20.00	5
50.00	-10.00	33
50.00	0.00	202
50.00	10.00	190
50.00	20.00	54
40.00	-20.00	2
40.00	-10.00	32
40.00	0.00	129
40.00	10.00	67
30.00	-20.00	6
30.00	-10.00	29
30.00	0.00	103

"A" so that the dog-bone specimens could be fatigue tested in load frames without special lateral support.

Two different load history simulations of the "NADC" load spectrum were used to investigate the possible effect of loading sequence. The two variations of the "NADC" spectrum were: (1) loads were randomized into a 300 hour hi-lo block (referred to as spectrum "B") and (2) loads were formatted into a 300 hour hi-lo block using the same format used to define the F-16 400 hour (hi-lo block) spectrum ("A"). A summary of the maximum and minimum percent loads versus number of load cycles per 300 flight hours for load spectra "B" and "C" is given in Tables H-3 and H-4, respectively. Due to the different load history simulation methods used, there are small variations in the actual load exceedances for load spectra "B", "C" and "NADC". For example, in Table H-5 load exceedances per 300 flight hours are shown for selected maximum load levels for the load spectra "B", "C" and "NADC".

For comparison purposes, the exceedances for load spectrum "A" were put on the same baseline as those for load spectra "B", "C" and "NADC". The exceedances for load spectrum "A" were estimated assuming two load points per loading cycle. Exceedances per 300 flight hours are shown in Table H-5 for the three load spectra considered in this program.

Table H-3 Load Summary for the F-18 300 Hour Spectrum ("B")

<u>MAX LOAD %</u>	<u>MIN LOAD %</u>	<u>NO. CYCLES</u>
100.00	0.00	2
100.00	10.00	1
100.00	20.00	3
100.00	30.00	1
89.90	-10.00	1
89.90	0.00	6
89.90	10.00	7
89.90	20.00	10
80.00	-30.00	1
80.00	-20.00	1
80.00	-10.00	2
80.00	0.00	21
80.00	10.00	14
80.00	20.00	13
80.00	30.00	5
70.00	-20.00	1
70.00	-10.00	11
70.00	0.00	52
70.00	10.00	43
70.00	20.00	41
70.00	30.00	11
70.00	40.00	1
60.00	-20.00	5
60.00	-10.00	16
60.00	0.00	151
60.00	10.00	143
60.00	20.00	68
60.00	30.00	8
50.00	-20.00	3
50.00	-10.00	15
50.00	0.00	270
50.00	10.00	139
50.00	20.00	54
50.00	30.00	1
40.00	-30.00	1
40.00	-20.00	2
40.00	-10.00	13
40.00	0.00	118
40.00	10.00	76
40.00	20.00	22
40.00	30.00	3
30.00	-20.00	1
30.00	-10.00	3
30.00	0.00	100
30.00	10.00	1
30.00	20.00	10
0.00	-20.00	7
0.00	-10.00	64

Table H-4 Load Summary for the F-18 300 Hour Spectrum ("C")

<u>MAX LOAD ‡</u>	<u>MIN LOAD ‡</u>	<u>NO. CYCLES</u>
100.00	0.00	5
100.00	20.00	8
90.00	-20.00	1
90.00	0.00	10
90.00	10.00	4
90.00	20.00	7
90.00	30.00	1
80.00	-30.00	1
80.00	-10.00	4
80.00	0.00	15
80.00	10.00	16
80.00	20.00	20
80.00	30.00	5
70.00	-20.00	1
70.00	-10.00	4
70.00	0.00	51
70.00	10.00	43
70.00	20.00	46
70.00	30.00	17
70.00	40.00	1
60.00	-20.00	6
60.00	-10.00	20
60.00	0.00	139
60.00	10.00	127
60.00	20.00	91
60.00	30.00	6
50.00	-30.00	1
50.00	-20.00	5
50.00	-10.00	33
50.00	0.00	202
50.00	10.00	190
50.00	20.00	54
40.00	-20.00	2
40.00	-10.00	32
40.00	0.00	129
40.00	10.00	67
30.00	-20.00	6
30.00	-10.00	29
30.00	0.00	103

Table H-5 Comparison of Exceedances per 300 Flight Hours for Selected % Maximum Load for Load Spectra "A", "B", "C" and NADC"

% Maximum Load	Exceedances/300 Flight Hours			
	"A"	"B"	"C"	"NADC"
91	4.4	7	13	7
81	16.4	31	36	27
71	44.5	88	97	88
61	264	248	260	251
51	1283	639	649	640
41	2831	1121	1134	1125
31	5542	1356	1364	1355
21	7037	1542	1502	1493

In Table H-5, note that spectrum "A" has fewer exceedances at the 91% maximum load level than either "B", "C" or "NADC". However, spectrum "A" has a larger number of load exceedances at the smaller % maximum load levels. For example, at the 21% maximum load level, load spectrum "A" has approximately five times as many load exceedances as the other spectra shown in Table H-5.

Since spectrum "A" has fewer numbers of peak load exceedances than the other spectra, this tends to minimize the retardation effect for this spectrum. Moreover, spectrum "A" has many more smaller load occurrences than either spectra "B" or "C". This further diminishes the retardation effect because the large number of smaller loads promotes crack growth through the plastic zone. As a result of the above, spectrum "A" is more severe than either spectra "B" (random) or "C" (hi-lo block). This observation is supported by the experimental results obtained.

Although spectrum "B" and "C" both satisfied the overall exceedance statistics for spectrum "NADC", spectrum "B" was clearly more severe than spectrum "C". Test results of this program clearly showed that loading sequence has an important effect on CF crack propagation. As a result of the different spectrum simulation methods used for spectra "B" and "C", spectrum "C" had a few more peak load occurrences than either spectrum "A" or "B". Overall, the exceedances for spectra "B" and "C" compared very well. It is concluded that

spectrum "B" is more severe than spectrum "C". Experimental results for CF crack propagation bear this out.

Strip chart traces of the load history for the F-16 400 hour (hi-lo block), F-18 300 hour (random) and F-18 300 hour (hi-lo block) spectra are shown in Figs. H-1, H-2 and H-3, respectively.

The maximum gross stress for all dog-bone specimen tests in Phase II was scaled to the "peak load" (i.e., overload) in each load spectra rather than the nominal maximum spectrum load. A baseline gross stress of 28 ksi was used for spectrum fatigue tests under Task 6 of Phase II.

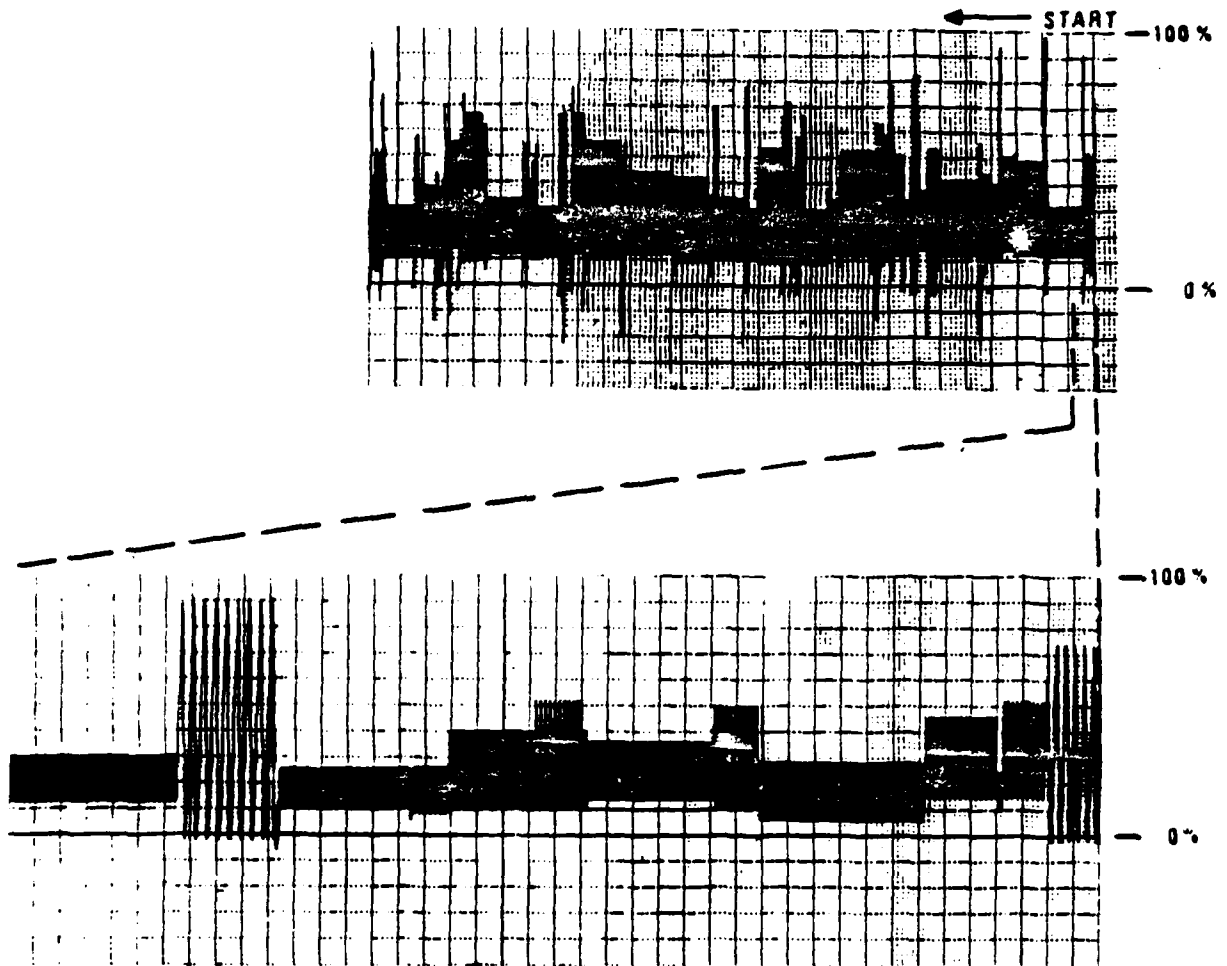


Fig. H-1 Samples of the Load History for the F-16 400 Hr. Spectrum

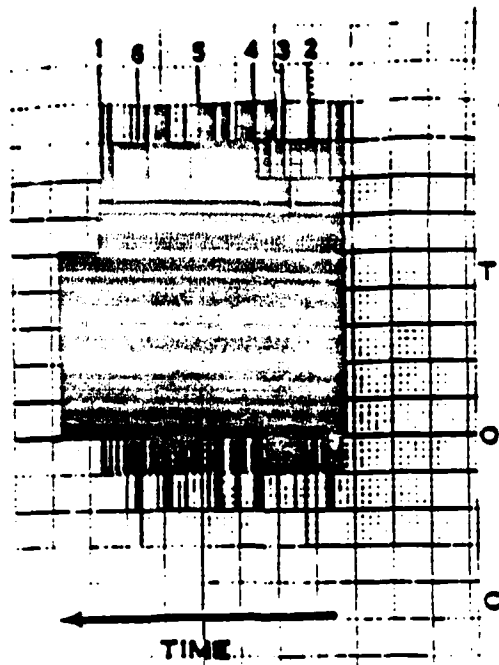


Fig. H-2 Strip Chart Trace of Load History for  
F-18 300 Hour (Random) Spectrum ("B")

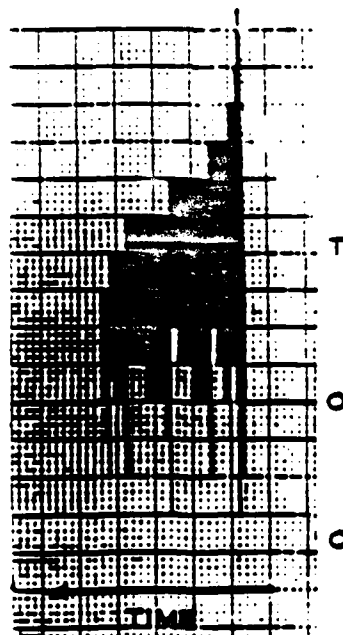


Fig. H-3 Strip Chart Trace of Load History for  
F-18 300 Hour (Block) Spectrum ("C")

NADC-83126-60-Vol. III

(This page intentionally left blank)

R E F E R E N C E S

1. R. J. Gran, et al, "Investigation and Analysis Development of Early Life Aircraft Structural Failures," Air Force Flight Dynamics Lab., AFFDL-TR-70-149, March 1971.
2. "F4 Fatigue and Damage Tolerance Assessment Program," McDonnell Aircraft Company, Report MDC A 2883, Vol. I and II, 28 June 1974.
3. C. F. Tiffany, "Durability and Damage Tolerance Assessments of United States Air Force Aircraft," Paper presented at AIAA Structural Durability and Damage Tolerance Workshop, Washington, D.C., April 6-7, 1978.
4. "Fatigue Strength Study Aimed at Improving Test Procedures," Aviation Week and Space Technology, April 6, 1979, p. 53.
5. B. J. Pendley, S. P. Henslee, and S. D. Manning, "Durability Methods Development, Volume III - Structural Durability Survey: State-of-the-Art Assessment," Air Force Flight Dynamics Lab., AFFDL-TR-79-3118, September 1979.
6. Y. H. Kim, S. M. Speaker, S. D. Manning, "Development of Fatigue and Crack Propagation Design and Analysis Methodology in a Corrosive Environment for Typical Mechanically-Fastened Joints; Volume II - State-of-the-Art Assessment," Naval Air Development Center, Report No. NADC-83126-60-Vol. II, March 1983.
7. SD-24K Volume 1, "General Specification for Design and Construction of Aircraft Weapon Systems;" Vol. 1 - Fixed Wing Aircraft, 13 June 1973.
8. MIL-A-8860(ASG), "Airplane Strength and Rigidity - General Specification for," 18 May 1960.
9. MIL-A-8861(ASG), "Airplane Strength and Rigidity - Flight Loads," 18 May 1960.
10. MIL-A-8863A, "Airplane Strength and Rigidity - Ground Loads for Navy Procured Airplanes," 12 July 1974.
11. MIL-A-8864, "Airplane Strength and Rigidity - Water and Handling Loads for Seaplanes," May 1960.
12. MIL-A-8865(ASG), "Airplane Strength and Rigidity - Miscellaneous Loads," 18 May 1960.

REFERENCES (Cont'd)

13. MIL-A-8866(ASG), "Airplane Strength and Rigidity - Reliability Requirements, Repeated Loads, and Fatigue," 18 May 1960.
14. MIL-A-8867(ASG), "Airplane Strength and Rigidity - Ground Tests," 18 May 1960.
15. MIL-A-8870, "Airplane Strength and Rigidity - Vibration, Flutter and Divergence."
16. R. J. H. Wanhill and J. J. DeLuccia, "An AGARD-Coordinated Corrosion Fatigue Cooperative Testing Programme," AGARD Report No. 695, February 1982.
17. "Corrosion Fatigue of Aircraft Materials," AGARD Report No. 659, October 1977.
18. L. R. Hall, R. W. Finger and W. F. Spurr, "Corrosion Fatigue Crack Growth in Aircraft Structural Materials," AFML-TR-73-204, September 1973.
19. R. J. H. Wanhill and J. J. DeLuccia, "Manual for the AGARD-Coordinated Corrosion Fatigue Cooperative Testing Programme (CFCTP)," NLR MP 79017 U, 1979.
20. C. Q. Bowles, "The Role of Environment, Frequency and Wave Shape During Fatigue Crack Growth in Aluminum Alloys," Dr. Thesis, Delft Univ. of Technology, Also Dept. of Aerospace Engineering, Report LR-270, May 1978.
21. R. J. H. Wanhill, "Environmental Effects on Fatigue of Aluminum and Titanium Alloys," NLR MP 77019 U, Paper 2 in AGARD Report No. 659, Corrosion Fatigue of Aircraft Materials, October 1977.
22. Y. H. Kim, R. P. Wei, D. E. Gordon, S. M. Speaker and S. D. Manning, "Development of Fatigue and Crack Propagation Design and Analysis Methodology in a Corrosive Environment for Typical Mechanically-Fastened Joints; Volume I - Phase I Documentation," Naval Air Development Center, Report No. NADC-83126-60-Vol. I, March 1983.
23. Song Chiou and R. P. Wei, "Corrosion Fatigue Cracking Response of Beta-Annealed Ti-6Al-4V Alloy in 3.5% NaCl Solution," Naval Air Development Center, Report No. NADC-83126-60-Vol. V, June 1984.

REFERENCES (Cont'd)

24. D. E. Gordon, S. B. Kirschner, S. D. Manning and R. P. Wei, "Development of Fatigue and Crack Propagation Design and Analysis Methodology in a Corrosive Environment for Typical Mechanically-Fastened Joints; Volume IV - Phase II Test and Fractographic Results," Naval Air Development Center, Report No. NADC-83126-60-Vol. IV, August 1984.
25. P. J. Noronha et al, "Fastener Hole Quality," Vol. I & II, Air Force Flight Dynamics Lab., AFFDL-TR-78-206, WPAFB, 1978.
26. S. M. Speaker et al, "Durability Methods Development, Volume VIII - Test and Fractography Data," Air Force Flight Dynamics Lab., AFFDL-TR-79-3118, November 1982.
27. R. P. Wei and G. W. Simmons, "Recent Progress in Understanding Environment Assisted Fatigue Crack Growth," Technical Report No. 8, Office of Naval Research Contract N00014-75-C-0543, NR 036-097, Jan. 1979.
28. M. R. Mitchell, "Fundamentals of Modern Fatigue Analysis for Design," in Fatigue and Microstructure, American Society for Metals, Metals Park, Ohio, 1978, pp. 385-437.
29. B. I. Sandor, Fundamentals of Cyclic Stress and Strain, the University of Wisconsin Press, 1972.
30. J. M. Stelle and T. C. T. Lam, "Improving the Accuracy of Fatigue Analysis," Machine Design, December 9, 1982, pp. 123-126.
31. L. F. Impellizzeri, "Cumulative Damage Analysis in Structural Fatigue," ASTM STP 462, 1970, pp. 40-68.
32. L. F. Impellizzeri, "Structural Fatigue Analysis and Testing for Fighter Aircraft," AGARD Specialist Meeting on Design Against Fatigue, AGARD-CP-141, Oct. 1973, pp. 3-1 to 3-12.
33. T. H. Topper, B. I. Sandor and J. D. Morrow, "Cumulative Fatigue Damage Under Cyclic Strain Control," Journal of Materials, JMLSA, Vol. 4, No. 1, March 1969, pp. 189-199.

REFERENCES (Cont'd)

34. R. W. Landgraf, F. D. Richards and N. R. La Pointe, "Fatigue Life Predictions for a Notched Member Under Complex Load Histories," in Fatigue Under Complex Loading, Vol. 6 of Advances in Engineering, R. M. Wetzels, Ed., Society of Automotive Engineers, Warrendale, PA, 1977.
35. D. Schutz and J. J. Gerharz, "Critical Remarks on the Validity of Fatigue Life Evaluation Methods Based on Local-Strain Behavior," ASTM STP 637, 1977, pp. 209-223.
36. D. F. Socie, "Fatigue Life Predictions Using Local Stress-Strain Concepts," SESA, Experimental Mechanics, Vol. 17, No. 2, 1977, pp. 50-56.
37. N. E. Dowling, W. R. Brose and W. K. Wilson, "Notched Member Fatigue Life Predictions by the Local Strain Approach," in Fatigue Under Complex Loading, Vol. 6 of Advances in Engineering, R. M. Wetzels, Ed., Society of Automotive Engineers, Warrendale, PA, 1977.
38. R. J. Mattos and F. V. Lawrence, "Estimation of the Fatigue Crack Initiation Life in Welds Using Low Cycle Fatigue Concepts," College of Engineering, Univ. of Illinois, Fracture Control Program, Report No. 19, Oct. 1975.
39. N. E. Dowling, "Crack Growth During Low-Cycle Fatigue of Smooth Axial Specimens," ASTM STP 637, 1977, pp. 97-121.
40. K. H. Donaldson, J. D. Morrow and D. F. Socie, "A Method for Real-Time Fatigue Damage Assessment," Proceedings of the 6th International Conference on Experimental Stress Analysis, Verein Deutscher Ingenieure, VDI-Berichte Nr. 313, 1978, pp. 843-848.
41. W. R. Brose, "Correlation of Smooth and Notched Body Stress Corrosion Crack Initiation," Fracture Mechanics: Fourteenth Symposium - Volume I: Theory and Analysis, ASTM STP 791, 1983, pp. I-463 to I-481.
42. D. F. Socie and P. Kurath, "Cycle Counting for Variable-Amplitude Crack Growth," Fracture Mechanics: Fourteenth Symposium - Volume II: Testing and Applications, ASTM STP 791, 1983, pp. II-19 to II-32.
43. N. E. Dowling, "Fatigue at Notches and the Local Strain and Fracture Mechanics Approaches," ASTM STP 677, 1979, pp. 247-273.

REFERENCES (Cont'd)

44. N. E. Dowling, "Fatigue Life Prediction for Complex Load Versus Time Histories," Trans. ASME, Vol. 105, July 1983, pp. 206-214.
45. P. H. Wirsching, "Computer Program for Local Strain Analysis - User Manual," Univ. of Arizona, Tucson, AZ, July 1982.
46. D. F. Socie and P. J. Artwohl, "Effect of Spectrum Editing on Fatigue Crack Initiation and Propagation in a Notched Member," ASTM STP 714, 1980, pp. 3-23.
47. J. R. Carroll, Jr., "Time Dependent Changes in Notch Stress/Notch Strain and Their Effects on Crack Initiation," ASTM STP 714, 1980, pp. 24-40.
48. H. Neuber, "Theory of Stress Concentration for Shear-Strained Prismatical Bodies with Arbitrary Nonlinear Stress-Strain Law," Journal of Applied Mechanics, Trans. ASME, Vol. 28, Dec. 1961, pp. 544-550.
49. T. H. Hopper, R. M. Wetzel and J. D. Morrow, "Neuber's Rule Applied to Fatigue of Notched Specimens," Journal of Materials, Vol. 4, No. 1, March 1969, pp. 200-209.
50. T. Seeger and P. Heuler, "Generalized Application of Neuber's Rule," Journal of Testing and Evaluation, JTEVA, Vol. 8, No. 4, July 1980, pp. 199-204.
51. J. R. Carroll, G. J. Gilbert and R. F. Wilkinson, "Investigation of Stress Strain History Modeling at Stress Risers," AFFDL-TR-76-150, June 1977.
52. H. G. Harris, I. Y. Ojalvo and R. E. Hooson, "Stress and Deflection Analysis of Mechanically Fastened Joints," Technical Report AFFDL-TR-70-49, May 1970.
53. B. L. Cornell and L. G. Darby, "Correlation of Analysis and Test Data to the Effect of Fastener Load Transfer on Fatigue," paper presented at the AIAA 6th Aircraft Design, Flight Test and Operations Meeting, Los Angeles, CA, August 12-14, 1974.

REFERENCES (Cont'd)

54. M. M. Frocht and H. N. Hill, "Stress-Concentration Factors Around a Central Circular Hole in a Plate Loaded Through Pin in the Hole," ASME Journal of Applied Mechanics, March 1940, pp. A-5 thru A-9.
55. H. T. Jessop, C. Snell and G. S. Holister, "Photoelastic Investigation on Plates with Single Interference-Fit Pins with Load Applied to Plate Only," Aeronautical Quarterly, Nov. 1956, pp. 297-314.
56. H. L. Cox, A. F. C. Brown, "Stresses Round Pins in Holes," Aeronautical Quarterly, Nov. 1964, pp. 357-372.
57. P. S. Theocaris, "The Stress Distribution in a Strip Loaded in Tension by Means of a Central Pin," ASME Journal of Applied Mechanics, March 1956, pp. 85-90.
58. "Stress Concentration Factors Load Pin in a Central Circular Hole in a Flat Bar," Engineering Sciences Data, Item No. 65004, London, U.K., September 1965.
59. "Stress Concentration Factors Axially Loaded Lugs with Clearance-Fit Pins," Engineering Science Data, Item No. 81006, London, U.K., April 1981.
60. R. D. Gregory, "Stress Concentration Around a Loaded Bolt Hole in an Axially Loaded Bar," Proc. Comb. Phil. Soc., No. 64, 1968, pp. 1215-1326.
61. W. Barrois, "Stresses and Displacements Due to Load Transfer by Fasteners in Structural Assemblies," Engineering Fracture Mechanics, Vol. 10, 1978, pp. 115-176.
62. C. Aubrey and J. L. McLean, "The Effect of Hole Clearance on the Fatigue Life of Aluminum Lugs," Canadian Aeronautics and Space Journal, June 1964, pp.
63. T. K. Moore, "The Influence of Hole Processing and Joint Variables on the Fatigue Life of Shear Joints," Ph.D. Dissertation, Ohio State University, 1977.
64. "F-16 Airframe Final Damage Tolerance Analysis," General Dynamics, Fort Worth Division, Report 16PR763, 3 September 1979.
65. "F-16 Airframe Final Durability Analysis," General Dynamics, Fort Worth Division, Report 16PR786, 3 September 1979.

REFERENCES (Cont'd)

66. S. D. Forness, "Fracture Mechanics Methodology Update," General Dynamics, Fort Worth Division, Report ERR-FW-2219 (Proprietary), December 1981.
67. S. D. Forness and J. B. Heckel, "User's Guide for Crack Growth Prediction Program - RXN," General Dynamics, Fort Worth Division, Report MRFF-82-003, 1982.
68. R. M. Engle, Jr. and J. A. Wead, "Cracks-PD, A Computer Program for Crack Growth Analysis Using the Tektronix 4051 Graphics System," Air Force Flight Dynamics Laboratory, Technical Memorandum AFFDL-TM-79-63-FBE, June 1979.
69. J. B. Chang, et al, "Improved Methods for Predicting Spectrum Loading Effects," Volume I - Technical Summary, Air Force Flight Dynamics Laboratory. AFWAL-TR-81-3092, November 1981.
70. J. F. Knott, Fundamentals of Fracture Mechanics, Halsted Press, John Wiley and Sons, New York, 1973.
71. R. W. Hertzberg, Deformation and Fracture Mechanics of Engineering Materials, John Wiley and Sons, New York, 1976.
72. S. T. Rolfe and J. M. Barsom, Fracture and Fatigue Control in Structures, Prentice-Hall, Inc., Englewood Cliffs, New Jersey, 1977.
73. A General Introduction to Fracture Mechanics, Mechanical Engineering Publications Limited, London, 1978.
74. H. O. Fuchs and R. I. Stephens, Metal Fatigue in Engineering, John Wiley and Sons, New York, 1980.
75. D. Broek, Elementary Engineering Fracture Mechanics, 3rd Ed., Martinus Nijhoff Publishers, The Hague, 1983.
76. S. D. Manning et al, "Durability Methods Development, Volume II - Phase II Documentation," Air Force Flight Dynamics Lab., AFFDL-TR-79-3118, Volume VII, Jan. 1984.
77. S. D. Manning and J. N. Yang, "USAF Durability Design Handbook: Guidelines for the Analysis and Design of Durable Aircraft Structures," Air Force Flight Dynamics Lab., AFWAL-TR-83-3027, Jan. 1984.

REFERENCES (Cont'd)

78. M. R. Spiegel, Theory and Problems of Statistics, Schaum Publishing Co., New York, 1961, pp. 241-268.
79. J. R. Benjamin and C. A. Cornell, Probability, Statistics, and Decision for Civil Engineers, McGraw-Hill Book Co., New York, 1970.
80. "Standard Test Methods for Constant-Amplitude Fatigue Crack Growth Rates Above  $10^{-8}$  m/Cycle," ASTM Standard E647-81, 1982 Annual Book of ASTM Standards, Part 10, Metals-Physical, Mechanical, Corrosion Testing, pp. 772-790.
81. J. F. Tavernelli and L. F. Coffin, Jr., "Experimental Support for Generalized Equation Predicting Low Cycle Fatigue," Trans. ASME, J. Basic Eng., Vol. 84, No. 4, Dec. 1962, p. 533.
82. S. S. Manson, discussion of Ref. 81, Trans. ASME, J. Basic Eng., Vol. 84, No. 4, Dec. 1962, p. 537 (referred to as Coffin-Manson relationship).
83. J. D. Morrow, in Fatigue Design Handbook, Section 3.2, SAE Advances in Engineering, Vol. 4, 1968, pp. 21-29.
84. S. S. Manson and G. R. Halford, "Practical Implementation of the Double Linear Damage Rule and Damage Curve Approach for Treating Cumulative Fatigue Damage," International Journal of Fracture, Vol. 17, 1981, 169-192 and R-35-R-42.
85. P. C. Paris, M. P. Gomez and W. E. Anderson, "A Rational Analytical Theory of Fatigue," The Trend In Engineering, Univ. of Washington, Vol. 13, No. 1, Jan. 1961, pp. 9.
86. P. C. Paris, "Fatigue - An Interdisciplinary Approach," Proceedings of the 10th Sagamore Conference, Syracuse Univ. Press, Syracuse, N.Y., 1964, pp. 107.
87. R. G. Forman, V. E. Kearney and R. M. Engle, "Numerical Analysis of Crack Propagation in a Cyclic-Loaded Structure," Journal of Basic Engineering, Vol. 89D, No. 3, 1967, pp. 459-464.
88. R. G. Forman and T. Hu., "Application of Fracture Mechanics on the Space Shuttle," Damage Tolerance of Metallic Structures: Analysis Methods and Applications, ASTM STP 842, 1984, pp. 108-133.

REFERENCES (Cont'd)

89. J. E. Collipriest, The Surface Crack: Physical Problems and Computational Solutions, J. L. Swedlow, Ed., American Society of Mechanical Engineers, N.Y., 1972, pp. 43-62.
90. K. Walker, "The Effect of Stress Ratio During Crack Propagation and Fatigue for 2024-T3 and 7075-T6 Aluminum," Effects of Environment and Complex Load History on Fatigue Life, ASTM STP 462, 1970, pp. 1-14.
91. R. Badaliane, "Application of Strain Energy Density Factor to Fatigue Crack Growth Analysis," Engineering Fracture Mechanics, Vol. 13, Pergamon Press, Ltd, 1980, pp. 657-666.
92. L. R. Hall, R. C. Shah and W. L. Engstrom, "Fracture and Fatigue Crack Growth Behavior of Surface Flaws and Flaws Originating at Fastener Holes," Volume I, AFFDL-TR-74-47, 1973.
93. J. P. Gallagher, F. J. Gressler and A. P. Berens, "USAF Damage Tolerant Design Handbook: Guidelines for the Analysis and Design of Damage Tolerant Aircraft Structures," AFWAL-TR-82-3073, May 1984.
94. W. Breyan, "Effects of Block Size, Stress Level, and Loading Sequence on Fatigue Characteristics of Aluminum-Alloy Box Beams," Effects of Environment and Complex Load History on Fatigue Life, ASTM STP 462, 1970, pp. 127-166.
95. G. H. Jacoby, "Comparison of Fatigue Lives Under Conventional Program Loading and Digital Random Loading," Effects of Environment and Complex Load History on Fatigue Life, ASTM STP 462, 1970, pp. 184-202.
96. O. E. Wheeler, "Spectrum Loading and Crack Growth," American Society for Mechanical Engineers Transactions, Journal of Basic Engineering, Vol. 94, March 1972, pp. 181-186.
97. J. Willenborg, R. M. Engle and H. A. Wood, "A Crack Growth Retardation Model Using an Effective Stress Concept," AFFDL-TR-71-1, Air Force Flight Dynamics Laboratory, Wright-Patterson Air Force Base, OH, Jan. 1971.

REFERENCES (Cont'd)

98. J. B. Chang, J. H. Stolpestad, M. Shinozuka and R. Vaicaitis, "Improved Methods for Predicting Spectrum Loading Effects - Phase I Report," AFFDL-TR-79-3036, Vol. 1, Air Force Flight Dynamics Laboratory, Wright-Patterson Air Force Base, OH, March 1978.
99. T. R. Porter, "Method of Analysis and Prediction of Variable Amplitude Fatigue Crack Growth," Engineering Fracture Mechanics, Vol. 4, No. 4, Dec. 1972, pp. 717-736.
100. T. D. Gray and J. P. Gallagher, "Predicting Fatigue Crack Retardation Following a Single Overload Using a Modified Wheeler Model," Mechanics of Crack Growth, ASTM STP 590, American Society of Testing and Materials, Philadelphia, 1976.
101. J. P. Gallagher and T. F. Hughes, "Influence of Yield Strength on Overload Affected Fatigue Crack Growth Behavior in 4340 Steel," AFFDL-TR-74-27, Air Force Flight Dynamics Laboratory, Wright-Patterson Air Force Base, OH, July 1974.
102. W. Elber, "The Significance of Fatigue Crack Closure," Damage Tolerance in Aircraft Structures, ASTM STP 486, American Society for Testing and Materials, Philadelphia, 1971, pp. 230-242.
103. P. D. Bell and M. Creager, "Crack Growth Analyses for Arbitrary Spectrum Loading," AFFDL-TR-74-129, Air Force Flight Dynamics Laboratory, Wright-Patterson Air Force Base, OH, 1974.
104. J. C. Newman, "A Finite Element Analysis of Fatigue Crack Closure," NASA TM X-72005, National Aeronautics and Space Administration, Hampton, VA, 1975.
105. H. D. Dill and C. R. Saff, "Spectrum Crack Growth Prediction Method Based on Crack Surface Displacement and Contact Analyses," Fatigue Crack Growth Under Spectrum Loads, ASTM STP 595, American Society for Testing and Materials, Philadelphia, 1976, pp. 306-319.

## REFERENCES (Cont'd)

106. H. D. Dill and C. R. Saff, "Analysis of Crack Growth Following Compressive High Loads Based on Crack Surface Displacement and Contact Stress Analyses," Cyclic Stress-Strain and Plastic Deformation Aspects of Fatigue Crack Growth, ASTM STP 637, American Society for Testing and Materials, Philadelphia, 1977, pp. 141-152.
107. M. F. Kanninen, C. Atkinson and C. E. Feddersen, "A Fatigue Crack Growth Analysis Method Based on a Simple Representation of Crack-Tip Plasticity," Cyclic Stress-Strain and Plastic Deformation Aspects of Fatigue Crack Growth, ASTM STP 637, American Society for Testing and Materials, Philadelphia, 1977, pp. 122-140.
108. W. Elder, "Equivalent Constant-Amplitude Concept for Crack Growth Under Spectrum Loading," Fatigue Crack Growth Under Spectrum Loads, ASTM STP 595, American Society for Testing and Materials, Philadelphia, 1976, pp. 236-250.
109. P. C. Paris, "Measurements and Analytical Models for Crack Closure in Fatigue," presented at Washington University, St. Louis, MO, 1976.
110. B. Budiansky and J. W. Hutchinson, "Analysis of Closure in Fatigue Crack Growth," Journal of Applied Mechanics, Vol. 45, No. 2, June 1978, pp. 267-276.
111. A. U. DeKoning, "A Simple Crack Closure Model for Prediction of Fatigue Crack Growth Rates Under Variable Amplitude Loading," NLF MP-80006U, National Aerospace Laboratory NLR, Amsterdam, Netherlands, Jan. 1980.
112. W. S. Johnson, "Multi-Parameter Yield Zone Model for Predicting Spectrum Crack Growth," Methods and Models for Predicting Fatigue Crack Growth Under Random Loading, ASTM STP 748, American Society for Testing and Materials, Philadelphia, 1981, pp. 85-102.
113. J. B. Chang, R. M. Hiyama and M. Szamossi, "Improved Methods for Predicting Spectrum Loading Effects," AFWAL-TR-81-3092, Air Force Flight Dynamics Laboratory, Wright-Patterson Air Force Base, OH, Vol. I, 1981.

## REFERENCES (Cont'd)

114. C. R. Saff, "Crack Growth Retardation and Acceleration Models," Damage Tolerance of Metallic Structures: Analysis Methods and Application, ASTM STP 842, 1984, pp. 36-49.
115. W. H. Bamford, "Implementing Corrosion-Fatigue Crack Growth Rate Data for Engineering Applications," Corrosion Fatigue: Mechanics, Metallurgy, Electrochemistry, and Engineering, ASTM STP 801, 1983, pp. 405-422.
116. T. T. Shih and R. P. Wei, "Influences of Chemical and Thermal Environments on Delay in a Ti-6Al-4V Alloy," in Fatigue Crack Growth Under Spectrum Loads, ASTM STP 595, American Society for Testing and Materials, 1976, pp. 113-124.
117. T. W. Weir, G. W. Simmons, R. G. Hart and R. P. Wei, "A Model for Surface Reaction and Transport Controlled Fatigue Crack Growth," Scripta Met., 14, 1980, pp. 357-364.
118. R. P. Wei and G. W. Simmons, "Surface Reactions and Fatigue Crack Growth," in FATIGUE: Environment and Temperature Effects, John J. Burke and Volker Weiss, eds., Sagamore Army Materials Research Conference Proceedings, Vol. 27, 1983, pp. 59-70.
119. R. P. Wei and P. S. Pao, "Mechanisms of Corrosion Fatigue in High Strength I/M and P/M Aluminum Alloys," Final Technical Report, Air Force Office of Scientific Research, F49620-81-K-0004, November, 1984.
120. R. P. Wei, P. S. Pao, R. G. Hart, T. W. Weir and G. W. Simmons, "Fracture Mechanics and Surface Chemistry Studies of Fatigue Crack Growth in An Alluminum Alloy," Met. Trans. A, 11A, January, 1980, pp. 151-158.
121. R. P. Wei, Gao, Ming and P. S. Pao, "The Role of Magnesium in CF and SCC of 7000 Series Aluminum Alloys," Scripta Met., 18(11), 1984, pp. 1195-1198.
122. J. B. Chang and R. M. Engle, "Improved Damage-Tolerance Analysis Methodology," J. Aircraft, Vol. 21, No. 9, Sept. 1984, pp. 722-730.

## REFERENCES (Cont'd)

123. J. T. Fong and N. E. Dowling, "Analysis of Fatigue Crack Growth Rate Data from Different Laboratories," Fatigue Crack Growth Measurement and Data Analysis, ASTM STP 738, 1981, pp. 171-193.
124. M. S. Miller and J. P. Gallagher, "An Analysis of Several Fatigue Crack Growth Rate (FCGR) Descriptions," Fatigue Crack Growth Measurement and Data Analysis, ASTM STP 738, 1981, pp. 205-251.
125. R. Mayle, "A Critical Study of Several Crack Growth Equations Which Model the Effect of Load Ratio," AFFDL-TM-FBR-73-154, Air Force Flight Dynamics Laboratory, Wright-Patterson AFB, Ohio, 1973.
126. P. C. Paris and F. Erdogan, "A Critical Analysis of Crack Propagation Laws," J. of Basic Engineering, Series D of the Trans. of ASME, Vol. 85, No. 3, 1963, pp. 528.
127. M. Katcher and M. Kaplan, "Effects of R-Factor and Crack Closure on Fatigue Crack Growth for Aluminum and Titanium Alloys," Fracture Toughness and Slow-Stable Cracking, ASTM STP 559, 1974, pp. 264-282.
128. S. W. Hopkins and C. A. Rau, Jr., "Prediction of Structural Crack Growth Behavior Under Fatigue Loading," Fatigue Crack Growth Measurements and Data Analysis, ASTM STP 738, 1981, pp. 255-270.
129. J. L. Rudd and R. M. Engle, Jr., "Crack Growth Behavior of Center-Cracked Panels Under Random Spectrum Loading," Methods and Models for Predicting Fatigue Crack Growth Under Random Loading, ASTM STP 748, 1981, pp. 103-114.
130. H. L. Ewalds, F. C. van Doorn and W. G. Sloof, "Influence of Environment and Specimen Thickness on Fatigue Crack Growth Data Correlation by Means of Elber-Type Equations," Corrosion Fatigue: Mechanics, Metallurgy, Electrochemistry, and Engineering, ASTM STP 801, 1983, pp. 115-134.
131. G. R. Chanani, "Investigation of Effects of Saltwater on Retardation Behavior of Aluminum Alloys," Corrosion-Fatigue Technology, ASTM STP 642, 1978, pp. 51-73.
132. H. D. Dill and C. R. Saff, "Environment-Load Interaction Effects on Crack Growth," AFFDL-TR-78-137, Nov. 1978.

133. "Standard Recommended Practice for Constant-Amplitude Low-Cycle Fatigue Testing" ASTM Standard E 606-80, 1984 Annual Book of ASTM Standards, Section 3, Vol. 03.01, pp. 653-670.

# DISTRIBUTION LIST

## Government Activities

### NAVY

	<u>No. of Copies</u>
NAVAIRSYSCOM (AIR-CCD4), 2 for retention, 3 for AIR-811B, 2 for AIR-530, AIR-5302, AIR-53021, AIR-530215.....	10
NAVAIRDEVCEN, Warminster, PA 18974 (3 for Code 8131).....	3
NAVAIRTESTCEN, Patuxent River, MD 20670 (Attn: Dr. J. Hoeg).....	1
NAVAIRENGCEN, Lakehurst, NJ 08733 (Attn: Mr. F. Sinatra, Neil Goodis).....	2
NAVAIREWORKFAC, NAS, Alameda, CA 94501.....	1
NAVAIREWORKFAC, MCAS, Cherry Point, NC 28533.....	1
NAVAIREWORKFAC, NAS, Jacksonville, FL 32212.....	1
NAVAIREWORKFAC, NAS, Norfolk, VA 23511 (Attn: Mr. Stokley).....	1
NAVAIREWORKFAC, NAS, North Island, San Diego, CA 92135.....	1
NAVAIREWORKFAC, NAS, Pensacola, FL 32508.....	1
Naval Weapons Center, China Lake, Ca 93555.....	1
NAVAVLOGCEN, Patuxent River, MD 20670.....	1
NAVPGSCHL, Monterey, CA 95940.....	1
NAVSEASYC, Crystal Mall 4, Rm. 109, Washington, DC 20360 (Attn: Mr. Vanderveldt).....	1
NAVSHIPANDCEN, Bethesda, MD 20034.....	1
NAVSHIPANDCEN, Annapolis, MD 21402.....	1
NOL, White Oak, MD 20910.....	1
NRL, Washington, DC 20375 (Attn: Mr. T. Crooker).....	1
NSWC, White Oak, MD 20910.....	1
ONR, Arlington, VA 22217 (Attn: Dr. Y. Rajapakse, Code 474).....	1

### FAA

	<u>No. of Copies</u>
FAA, Washington, DC 20591 (Attn: J. R. Soderquist).....	1
FAA, Technology Center, Atlantic City, NJ 08405 (Attn: Mr. D. Nesterok, ACT-330).....	1

### NASA

NASA, Langley Research Center, Hampton, VA 23365 (Attn: Mr. H. Hardrath).....	1
NASA, Washington, DC 20546 (Attn: Airframes Branch, FS-120).....	1
NASA, Lewis Research Center, Cleveland, OH 44135 (Attn: Technical Library).....	1
NASA, George C. Marshall Space Flight Center, Huntsville, AL 35812 (Attn: Technical Library).....	1

### USAF

AFWAL, WPAFB, OH 45433 (Attn: AFWAL/FIBE).....	1
(Attn: FIBEC).....	1
(Attn: FIBAA).....	1
(Attn: AFWAL/FIB).....	1
Ogden ALC, Hill AFB, UT 84055 (Attn: MANCC).....	1
Oklahoma City ALC, Tinker AFB, OK 73145 (Attn: MAQCP).....	1
Sacramento ALC, McClellan AFB, CA 95652 (Attn: MANE).....	1
San Antonio ALC, Kelly AFB, TX 78241 (Attn: MMETM).....	1
Warner Robbins ALC, Robins AFB, GA 30198 (Attn: MMSRD/Dr. T. Christian).....	1

### U. S. ARMY

Applied Technology Laboratory, USARTL (AVRADCOM), Fort Eustis, VA 23604 (Attn: H. Reddick).....	1
U. S. Army Materials and Mechanics Research Center (DRXMR-PL), Watertown, MA 02172.....	1
U. S. Army Research Office, Furham, NC 27701.....	1

### INFO SERVICES

DTIC, Cameron Station, Alexandria, VA 22314.....	12
MCIC, Battelle Columbus Laboratories, 505 King Avenue, Columbus, OH 43201.....	1
NTIS, U. S. Dept. of Commerce, Springfield, VA 22151.....	2

DISTRIBUTION LIST  
REPORT NO. NADC-83126-60  
AIRTASK NO. UF41400

NON-GOVERNMENT ACTIVITIES

	<u>No. of Copies</u>
ALCOA, ALCOA Labs, ALCOA Center, PA 15069 (Attn: Mr. J. G. Kaufman) .....	1
Batelle Columbus Labs, 505 King Avenue, Columbus, OH 43201 (Attn: Dr. B. Leis) .....	1
Boeing Commercial Airplane Co., P. O. Box 3707, Seattle, WA 98124 (Attn: Mr. T. Porter) .....	1
Douglas Aircraft Co., 3855 Lakewood Blvd., Long Beach, CA 90846 (Attn: Mr. Luce, Mail Code 7-21) .....	1
Drexel University, Phila., PA 19104 (Attn: Dr. Averbush) .....	1
Fairchild Industries, Hagerstown, MD 21740 (Attn: Tech Library)...	1
General Dynamics, Convair Division, San Diego, CA 92138 (Attn: Mr. G. Kruse) .....	1
General Dynamics Corporation, P. O. Box 748, Ft. Worth, TX 76101 (Attn: Dr. S. Manning) .....	1
Grumman Aerospace Corporation, South Oyster Bay Road, Bethpage, L.I., NY 11714 (Attn: Dr. H. Arman) (Attn: Dr. B. Leftheris) .....	1
(Attn: Dr. H. Eidenoff) .....	1
Lehigh University, Bethlehem, PA 18015 (Attn: Prof. G. C. Sih) .....	1
(Attn: Prof. R. P. Wei) .....	1
Lockheed-California Co., 2555 N. Hollywood Way, Burbank, CA 91520 (Attn: Mr. E. K. Walker) .....	1
Lockheed Georgia Co., Marietta, GA 30063 (Attn: Mr. T. Adams) .....	1
McDonnell Douglas Corporation, St. Louis, MO 63166 (Attn: Mr. L. Impellizeri) .....	1
(Attn: Dr. R. Pinkert) .....	1
Northrop Corporation, One Northrop Ave., Hawthorne, CA 90250 (ATTN: Mr. Alan Liu) .....	1
(Attn: Dr. M. Ratwani) .....	1
Rockwell International, Columbus, OH 43216 (Attn: Mr. F. Kaufman) .....	1
Rockwell International, Los Angeles, CA 90009 (Attn: Mr. J. Chang) .....	1
Rockwell International Science Center, 1049 Camino Dos Rios, Thousand Oaks, CA 91360 (Attn: Dr. F. Morris) .....	1
Rohr Corporation, Riverside, CA 92503 (Attn: Dr. F. Riel) .....	1
Sikorsky Aircraft, Stratford, CT 06622 .....	1
University of Dayton Research Institute, 300 College Park Ave., Dayton, OH 45469 (Attn: Dr. J. Gallagher) .....	1
University of Illinois, College of Engineering, Urbana, IL 61801 (Attn: Dept. of Mechanics and Industrial Eng., Profs. J. D. Morrow, D. F. Socie) .....	2
Vought Corporation, Dallas, TX 75265 (Attn: Dr. C. Dumisnil) .....	1
(Attn: Mt. T. Gray) .....	1
University of Pennsylvania, Dept. of Mechanical Engineering and Applied Mechanics, 111 Towne Bldg. D3, Phila., PA 19104 (Attn: Dr. Burgers) .....	1

**END**

**FILMED**

**11-85**

**DTIC**